The tumour suppressor protein LIMD1 is a novel regulator of HIF1 and the hypoxic response

Thomas M. Webb, BSc (Hons)

Thesis submitted to the University of Nottingham for the degree of Doctor of Philosophy, November 2009.

"I sleep better at night knowing that scientists can clone sheep."

— *Jeff Ayers.*

Acknowledgements

First and foremost, I would like to sincerely thank my supervisor Dr Tyson Sharp. I have learnt a lot from Tyson, in particular his passion for and dedication to science has been awe inspiring. I am grateful for Tyson's open office, which has graced my endless, often pointless questions over the years. The success of the project is hugely down to your enthusiasm and persistence and fingers crossed as a result this work is not heading for the journal of 'crapotology'! I am also indebted to Tyson for opening my eyes to science as an undergraduate, I certainly wouldn't be where I am today without his guidance.

Dr Thilo Hagen: Thank you for providing so many useful reagents and your initial feedback, which gave me such a great head start with this project.

Professor Greg Longmore, Dr YungFeng Feng and the rest of our collaborators from the Department of Cell Biology, Washington University School of Medicine, St. Louis. Thank you for providing the lentiviral knock down reagents and the mouse embryonic fibroblasts, of which are fantastic tools and have greatly enhanced my work.

Dr Rob Layfield, Dr Eleni Stylianou and Dr Ian Kerr, I would like to thank you for your support and help over the years and more importantly keeping me up to date with the School's gossip!

I would also like to thank the D45 crew, Dan, Pierre, Katherine, Mo, Nisha, Nektaria, Tom Vallim, James and Jo. Thanks for everything guys! In particular thank you Vicky for your generous help with the qRT-PCR. Thank you Dan, for putting up with my constant moaning in your unique, one might say sarcastic way. Pierre, I am also indebted to your 'it won't effect' attitude to science, which I am sure will always stay with me for better or for worse! Thank you to the project students which have passed through the lab in my time, including Foggy, Hayley, Claire, Ged and Charlotte.

Thanks to my ever-supportive parents for their guidance and care over the last few years. Furthermore, thank you for trying your hardest to take interest in my work which has often sounded like a foreign language to you both.

Thanks to all of my mates. In particular Stu, what can I say? Without you the last few years wouldn't have been the same. Fingers crossed our bachelor pad days of drinking jenga, me beating you at every computer game possible, including your favourite karaoke and nights out on the triple cranberries will continue.

I would like to dedicate this work to my girlfriend Suzanne, who has managed to find the love, patience and will power to support me throughout this whole process…..

Publications

Spendlove,I., Al-Attar,A., Watherstone,O., **Webb,T.M**., Ellis,I.O., Longmore,G.D., and Sharp,T.V. **(2008)**. *Differential subcellular localisation of the tumour suppressor protein LIMD1 in breast cancer correlates with patient survival.* ***Int J Cancer****. 15;123(10):2247-53.*

Sharp TV, Al-Attar A, Foxler DE, Ding L, de A Vallim TQ, Zhang Y, Nijmeh HS, **Webb TM**, Nicholson AG, Zhang Q, Kraja A, Spendlove I, Osborne J, Mardis E, Longmore GD. **(2008)** *The chromosome 3p21.3-encoded gene, LIMD1, is a critical tumor suppressor involved in human lung cancer development.* ***Proc Natl Acad Sci U S A****. 6;105(50):19932-7.*

Manuscripts in Preparation

Webb TM, James V, Hagen T, Feng Y, Ratcliffe PJ, Longmore GD and Sharp TV. *The Tumour Suppressor protein LIMD1 bridges the association between the Prolyl Hydroxylases and pVHL to repress HIF1 activity.*

Zhang Y, James V, Foxler DE, **Webb TM**, Self TJ, Chiu CY, de Moor CH, Feng Y, Morley S, Rana TM, Lagos D, Longmore GD, Bushell M and Sharp TV.
The LIM domain proteins, LIMD1, Ajuba and WTIP (LAW proteins) interact with Argonaute 2 and eIF4E and are components of the microRNA-mediated gene silencing pathway.

Abstracts

Webb TM, Hagen T, Feng Y, Longmore GD and Sharp TV. *The Tumor Suppressor Gene Product LIMD1 specifically binds the HIF-prolyl hydroxylases and pVHL and represses HIF mediated transcription.* Hypoxia and Angiogenesis, Keystone Symposium, Vancouver, Canada, 2008.

Webb TM, Hagen T, Feng Y, Longmore GD and Sharp TV. *The Tumor Suppressor Gene Product LIMD1 specifically binds the HIF-prolyl hydroxylases and pVHL and represses HIF mediated transcription.* National Cancer Research Institute, Birmingham, UK, 2008.

Webb TM, Hagen T, Feng Y, Longmore GD and Sharp TV. *The Tumour Suppressor Gene Product LIMD1 binds the HIF1-alpha Prolyl Hydroxylases 1, 2 and 3 and down regulates the hypoxic response in vivo.* Centre for Cell Biology and Biochemistry Symposia, Dynamic Structure and Function, University of Nottingham, UK, 2008.

Webb TM, Hagen T and Sharp TV. *The Tumour Suppressor Gene Product LIMD1 binds the HIF1-alpha Prolyl Hydroxylases 1, 2 and 3 and down regulates the hypoxic response in vivo.* Centre for Cell Biology and Biochemistry Symposia, Nuclear Structure and Function, University of Nottingham, UK, 2007.

Awards

Winner of the Biomedical Society Poster Prize, CBCB Nuclear Structure and Function Symposium, University of Nottingham, 2007 (awarded by Professor Peter Cook, University of Oxford).

Poster Prize winner, CBCB Dynamic Structure and Function Symposium, University of Nottingham, 2008 (awarded by Professor Kathryn Ayscough, University of Sheffield).

Winner of the University of Nottingham Novartis Postgraduate Prize, 2008.

Abbreviations

4EBP1	Eukaryotic initiation factor 4E-binding protein-1
AA	Amino acid
AHR	Mammalian aryl hydrocarbon receptor
AMP	Adenosine monophosphate
Ang-2	Angiopoietin 2
AOBS	Acousto-optical beam splitter
AOTF	Acousto-optic tuneable filter
Ang II	Angiotensin II
Ang-2	Angiopoietin 2
APS	Ammonium persulphate
ARD	Ankyrin repeat domains
ARD1	Arrest-deficient-1
ARNT	AHR nuclear translocator (HIF1β)
ATF-4	Activating transcription factor-4
bp	Base pairs
bHLH	Basic helix-loop-helix
BSA	Bovine serum albumin
C3CER1	Chromosome 3 common eliminated 1
CAD	C-terminal activation domain
CBP	Cyclic-AMP responsive element-binding protein
cDNA	complementary DNA
CH-1	Cysteine-histidine rich domain protein 1
ChIP	Chromatin immunoprecipitation
c-MET	mesenchymal-epithelial transition factor
CODD	C-terminal ODD
CRM1	Chromosome region maintenance 1
CRP-1	Cysteine-rich protein 1
CUL-2	Cullin 2

C-terminal	Carboxyl-terminal
CXCR4	C-X-C chemokine receptor 4
DAOCS	Deacetoxycephalosporin C synthase
DAPI	4',6-diamidino-2-phenylindole
DEAF-1	Deformed epidermal auto-regulatory factor **1**
DFO	Desferrioxamine
DMEM	Dulbecco's modified eagle's medium
DMOG	Dimethyloxallyl glycine
DMSO	Dimethyl sulfoxide
DNA	Deoxyribonucleic acid
dNTP	Deoxyribonucleic acid triphosphate
DSBH	Double-stranded β-helix motif
dsDNA	double-stranded DNA
EC	Endothelial cell
ECL	Enhanced chemiluminescence
ECM	Extra-cellular matrix
EDTA	Ethylenediaminetetraacetic acid
EGFP	Enhanced green fluorescent protein
Egl-9/EGLN	*C.elegans* egg laying 9
EMSA	Electrophoretic mobility shift assay
EMT	Epithelial mesenchymal transition
EPAS-1	Endothelial PAS domain protein 1 (HIF2α)
EPF	E2-endemic pemphigues foliaceus
EPO	Erythropoietin
ER	Endoplasmic reticulum
EVH1	Ena/Vasp Homology domain 1
FBS	Fetal bovine serum
FCS	Fetal calf serum
FH	Fumarate hydratase
FHIT	Fragile histidine triad gene
FIH-1	Factor inhibiting HIF-1

FKBP38	FK506 Binding Protein 38
GAPDH	Glyceraldehyde-3-phosphate dehydrogenase
GFP	Green fluorescent protein
Glut-1	Glucose transporter 1
Grb2	Growth factor receptor-bound protein 2
GRP	Glucose related protein
GSK3	Glycogen synthase kinase 3
GST	Glutathione S-Transferase
HA	Human influenza hemagglutinin
HAF	Hypoxia-associated factor
HBSS	Hanks' balanced salt solution
HDAC	Histone deacteylase
Hdm2	Human double minute 2
HEK 293	Human Embryonic Kidney 293 cells
HEK 293T	HEK 293 cells containing SV40 large T antigen
Hep3b	Human hepatoma cell line 3b
HIF	Hypoxia inducible factor
HLF	HIF1α-like factor (HIF2α)
HNSCC	Head and neck squamous cell carcinomas
HPLC	High performance liquid chromatography
HRE	Hypoxia response element
HRF	HIF related factor (HIF2α)
HRP	Horse radish peroxidase
Hsp90	Heat shock protein 90
IFA	Immunofluorescence assay
IκB	Inhibitors of κB
IKK	IκB kinase
ING4	Inhibitor of growth family member 4
IP	Immunoprecipitation
IPAS	Inhibitory PAS domain protein
IPTG	Isopropyl-beta-D-thiogalactopyranoside

IRES	Internal ribosome entry site
kbp	Kilo base pairs
kDa	Kilo Dalton
KLF2	Kruppel-like factor 2
K_m	Michaelis constant
LAW	LIMD1, Ajuba and WTIP
LB	Luria Broth
LC-MS/MS	Liquid chromatography-tandem mass spectrometry
LIMD1	LIM domains containing protein 1
LOH	Loss of heterozygousity
LOX	Lysyl oxidase
LPP	Lipoma preferred partner
mAb	Monoclonal antibody
MAGE-11	Melanoma antigen 11
MAP kinase	Mitogen activated protein kinase
MEF	Mouse embryonic fibroblasts
MOP-2	Member of the PAS family 2 (HIF2α)
Morg-1	Mitogen activated protein kinase organiser 1
mRNA	Messenger RNA
mTOR	Mammalian target of rapamycin
MUC1	Mucin 1
MYND	Myeloid, DEAF-1 zinc finger domain
N-terminal	Amino-terminal
NAD	N-terminal activation domain
NES	Nuclear export sequence
NFAT2	Nuclear factor of activated T cells 2
NF-κB	Nuclear factor kappa-light-chain-enhancer of activated B cells
NGF	Nerve growth factor
NIP3	E1B/Bcl-2 19kDa interacting protein 3 and pro-apoptotic protein

NLS	Nuclear localisation sequence
NMR	Nuclear magnetic resonance
NO	Nitric oxide
NODD	N-terminal ODD
NSCLC	Non-small cell lung cancer
ODD	Oxygen dependent degradation domain
ORP	Oxygen related protein
OS-9	Amplified in osteosarcomas 9
p300	Adenovirus E1A binding protein
PAS	Per-ARNT-AHR-Sim domain
PBS	Phosphate Buffered Saline
PCR	Polymerase chain reaction
PDGF	Platelet derived growth factor
PDK1	Pyruvate dehydrogenase kinase isozyme 1
PDM	Proline double-mutant
PER	*Drosophilla* Period protein
PFA	Paraformaldehyde
PHD	HIF-Prolyl hydroxylase
PI3K	Phosphoinositide 3-kinases or PI 3-kinases
PKC	Protein kinase C
PPIase	Peptidyl prolyl cis/trans isomerases
PRMT5	Protein arginine methyltransferase 5
PTEN	Phosphatase and tensin homologue
PVDF	Polyvinylidene Fluoride
pVHL	Von Hippel Lindau, generic term for both protein isoforms
qRT-PCR	Real-time quantitative reverse transcription PCR
RACK 1	Receptor of activated protein kinase 1
RB	Retinoblastoma protein
Rbx1	Ring-box protein 1
RCC4	Human renal cell carcinoma cell line

RNA	Ribonucleic acid
RNAi	RNA interference
ROS	Reactive oxygen species
RSUME	RWD-containing sumoylation enhancer
SAOS2	Sarcoma osteogenic cell line
SCID	Severe combined immunodeficient
SCF	Skp-1-Cdc53/Cullin F box complex
SDH	Succinate dehydrogenase
SDS-PAGE	Sodium dodecyl sulphate polyacrylamide gel electrophoresis
SENP1	SUMO1/sentrin specific peptidase 1
SH2/3	Sarcoma homology domains 2/3
ShRNA	small/short hairpin RNA
Siah	mammalian homolog of *Drosophilla* Seven in Absentia protein
SIP1	Smad interacting protein 1
SiRNA	small interfering RNA
SNP	Single nucleotide polymorphism
SSAT	Spermidine/spermidine-N^1-acetyltransferase
STAT3	Signal transducer and activator of transcription 3
TAE	Tris acetate EDTA
TB	Transformation Buffer
TCA	Tricarboxylic acid/Citric acid cycle
TEMED	N,N,N',N'-tetramethylethylenediamine
TNT	*In vitro* coupled transcription and translation
TPEN	*N,N,N',N'*-tetrakis[2-pyridylmethyl]ethylenediamine
TRAF6	TNF receptor associated factor 6
TriC	TCP-1 ring complex chaperone
TRIP6	Thyroid hormone receptor interactor 6
TSC2	Tumour suppressor complex 2
U2OS	Human Osteosarcoma cell line
UCP	Ubiquitin carrier protein
UTR	Untranslated region

VBC	VHL, elongin B-C protein complex
VDU2	VHL interacting de-ubiquitylating enzyme
VEGF	Vascular endothelial growth factor
VHL	Von Hippel Lindau
VO	Empty vector only
WT1	Wilms tumour 1
WTIP	Wilms tumour 1 interacting protein
Y2H	Yeast-2-Hybrid
YFP	Yellow fluorescent protein

Abstract

There are three prolyl hydroxylases (PHD1, 2 and 3) that regulate the hypoxia-inducible factors (HIFs), the master transcriptional regulators that respond to changes in intracellular O_2 tension. In high O_2 tension (normoxia) the PHDs hydroxylate HIFα subunits on 2 conserved proline residues inducing binding of the von-Hippel-Lindau (VHL) tumour suppressor, the recognition component of a multi-protein ubiquitin-ligase complex, initiating HIFα ubiquitylation and degradation by the 26S proteasome. However, it is not known whether PHDs and VHL act separately to exert their enzymatic activities on HIFα or as a multi-protein complex. In this thesis, data are presented that shows that the tumour suppressor protein LIMD1 acts as a molecular scaffold simultaneously binding the PHDs and pVHL into a *normoxi*c protein com*plex* (*normoxiplex*), increasing their physical proximity in order to enable efficient and rapid sequential modifications and thus degradation of HIF1α. Data are presented which indicates that increased LIMD1 expression down regulates HIF transcriptional activity, by promoting HIF1α degradation *via* the oxygen dependent degradation domain in a manner dependent on hydroxylase and 26S proteasome activities. However, degradation of this domain is not wholly dependent on the well characterised proline residues subject to hydroxylation, suggesting that LIMD1 may alter proline hydroxylation specificity or modulate HIF *via* a different mechanism. Furthermore, endogenous depletion of LIMD1 results in the converse, leading to HIF1α stabilisation and accumulation, enhancing HIF transcriptional activity. Moreover, Limd1$^{-/-}$ MEFs show increased HIF transcriptional activity. One mechanism by which this is achieved involves the binding of PHD2 within the N-terminal portion of LIMD1 while allowing concurrent binding of VHL to the C-terminal zinc-finger LIM domains. However, the LIMD1 mediated mechanism regulating HIF1α independently of proline residues 402 and 564 is still unclear. Finally, data are presented that show that the LIMD1 family member proteins Ajuba and WTIP all bind specifically to VHL but differentially to PHDs 1, 2 and 3 and thus these three LIM domain containing proteins represent a new group of hypoxic regulators.

CHAPTER 1: INTRODUCTION

1. Introduction

1.1 Identification and characterisation of the LIM domains containing 1 gene product

Interstitial gene deletions and loss of heterozygousity (LOH) of chromosome 3p have been identified in a diverse array of tumours including breast, cervix, bladder, renal and small cell lung carcinomas (Imreh et al., 1997). PCR marker analysis from tumour cell lines revealed a commonly eliminated segment at 3p21.3 referred to as the commonly eliminated region (C3CER1). This identification instigated the large scale sequencing of the 3p21.3 chromosomal region to map for genes with potential tumour suppressive functions. This led to the identification of a 5067bp cDNA containing an open reading frame found to encode a protein of 676 amino acids and a mass of 72.2 kDa, comprising three C terminal LIM domains. This gene was subsequently termed the LIM Domain containing 1 gene (*LIMD1*) and its mouse ortholog, *Limd1,* found encoded on mouse chromosome 9, of which shares 79.5% homology (Kiss et al., 1999)

1.2 LIM domain proteins

The LIM domain family of proteins are a diverse group of multi-functional proteins, incorporating either a single or multiple homologous zinc finger structure known as the LIM domain. The LIM domain was first isolated from three homeodomain containing proteins as a novel cysteine rich motif: C-X2-C-X17-19-H-X2-C-X2-C-X2-C-X7-11-(C)-X8-C, from the *Caenorhabditis elegans* gene lin-11 (Freyd et al., 1990) and mec-3 (Way and Chalfie, 1988) and rat isl-1 (Karlsson et al., 1990) and from which the acronym LIM is derived (for lin-11, isl-1, mec-3). The LIM domain proteins perform a spectrum of functions involved in cell identity, differentiation and growth control, *via* protein-protein associations involving the cysteine rich LIM homeodomain in addition to the interactions of other variable motifs

(Schmeichel and Beckerle, 1994; Kadrmas and Beckerle, 2004). LIM domains are zinc binding arrays of approximately fifty-five amino acids, whereby eight highly conserved cysteine or histidine residues coordinate two zinc atoms to form two tandemly repeated zinc fingers per LIM domain (Michelsen et al., 1993). These two zinc fingers exist as separate structural entities held together by hydrophobic interactions, elucidated by nuclear magnetic resonance (NMR) analysis of the LIM protein CRP-1 (Cysteine Rich Protein-1) (Michelsen et al., 1993).

The protein-protein interface binding repertoire of LIM domain containing proteins is achieved both by varying the number of LIM domains (from 1-5) and varying the non-LIM domain associations of the specific protein. Furthermore, a non-conserved amino acid sequence of X11-18 and X9-16 lies at the peak of each zinc finger binding sub-domain which confers addition functional specificity and thus diversity between the different LIM domains (Kadrmas and Beckerle, 2004). The extent of the LIM domain as a key cellular protein-protein interacting motif is indicated by the prevalence of LIM proteins in eukaryotic cells (135 different encoding sequences have been identified in 58 human genes) whereby LIM protein sequence occurrence is comparable with the well characterised Src-homology-2 (SH2) and SH3 domains (115 and 253 sequences respectively) (Pawson and Nash, 2003). Interestingly, the prevalence of LIM proteins in eukaryotes decreases with reduced organism complexity to the extent that LIM proteins are absent in prokaryotic organisms, which suggests their involvement in development in higher order organisms (Kadrmas and Beckerle, 2004). The structure of LIMD1 and the conserved sequence encoding the LIM domain are represented schematically in figure 1.2.

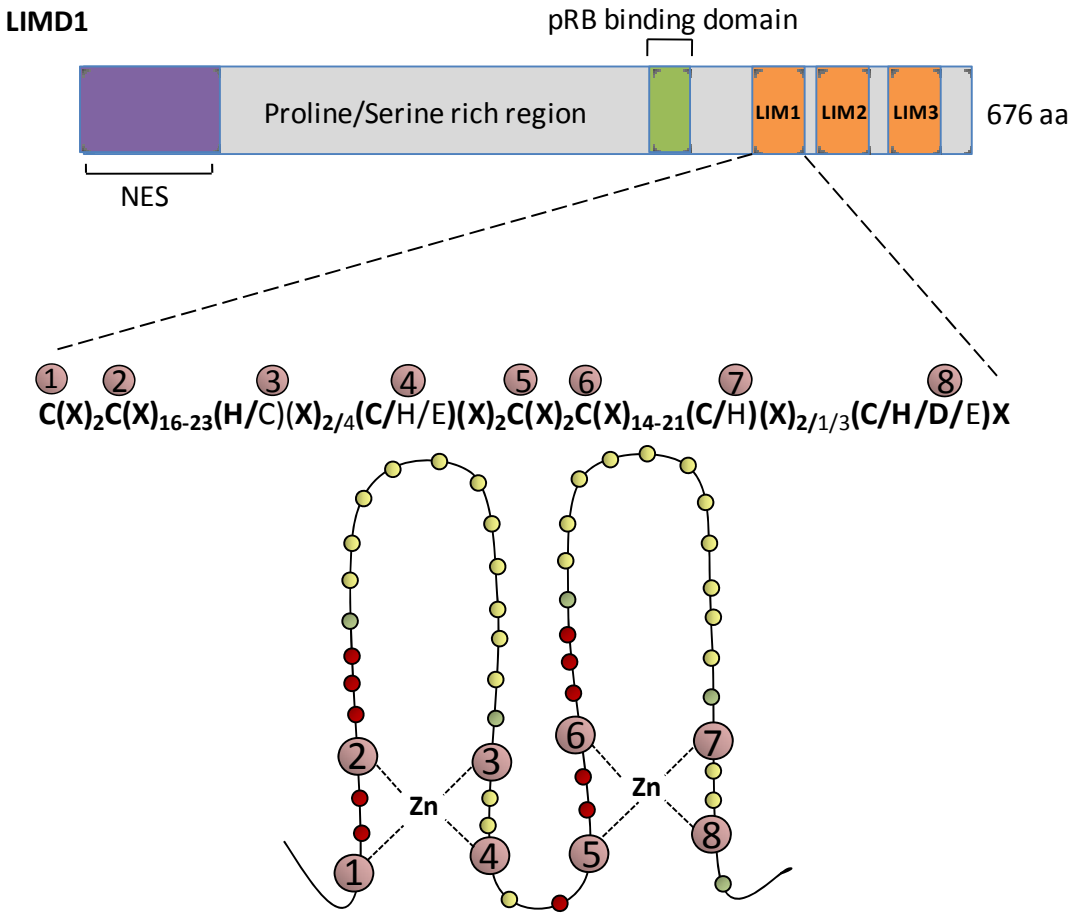

Figure 1.2 *Schematic representation of LIMD1 (676 amino acids) and the structure of the LIM domain.*

LIMD1 contains an N terminal nuclear export signal (NES) within residues 1-134, a retinoblastoma (pRB) binding interface within residues 404-442 and 3 C-terminal LIM domains preceded by a proline/serine rich region. The LIM domain comprises 2 tandem zinc finger structures, whereby 8 conserved cysteine and histidine residues coordinate 2 zinc atoms. [Modified from (Kadrmas and Beckerle, 2004; Michelsen et al., 1993)].

LIM domains are found in a multitude of proteins of cytoplasmic and nuclear localisation, in addition to proteins which translocate between both intracellular compartments (Zheng and Zhao, 2007; Kadrmas and Beckerle, 2004; Petit et al., 2000). One functional attribute which appears conserved upon most LIM proteins is the ability to interact with the actin cytoskeleton (Roof et al., 1997; Crawford et al., 1992). Coupled with the ability of many LIM proteins to shuttle into the nucleus, it is postulated that LIM proteins can associate with the actin cytoskeleton and focal adhesions and relay extracellular cues to the nucleus and the transcriptional machinery (Cattaruzza et al., 2004; Muller et al., 2002; Wang and Gilmore, 2003).

1.3 Zyxin Family of LIM proteins

LIM proteins are classified according to the sequence homologies of their LIM domains and their general structure (Dawid et al., 1998; Kadrmas and Beckerle, 2004). LIMD1 is categorised into Group 3 of LIM proteins due to the presence of C-terminal LIM domains associated with distinct N-terminal domains. All of the Group 3 LIM proteins are predominantly cytosolic with highly conserved LIM domains but divergent proline rich pre-LIM regions. Furthermore, within Group 3 of the LIM domain family of proteins, LIMD1 is categorised within a group of actin associated proteins named the Zyxin family of proteins also including Ajuba (Goyal et al., 1999), Trip6 (Yi and Beckerle, 1998), Zyxin (Crawford et al., 1992), LPP (Petit et al., 1996), WTIP (Srichai et al., 2004) and the more distantly related Migfilin (Tu et al., 2003). All of the Zyxin proteins comprise three highly conserved C-terminal LIM domains, associated with a non-conserved pre-LIM region containing additional non-catalytic domains.

Zyxin remains the best characterised of the family, located at focal adhesions *via* its proline rich N-terminal (Nix et al., 2001), whereby it regulates actin cytoskeleton dynamics, cell movement and signal transduction (Fradelizi et al., 2001). Within the Zyxin family of LIM proteins, a distinct structural and

functional separation lies between Zyxin, LPP and Trip6 and the LAW (LIMD1, Ajuba and WTIP) proteins, forming two sub-families, illustrated by their phylogenetic relationships in figure 1.3.

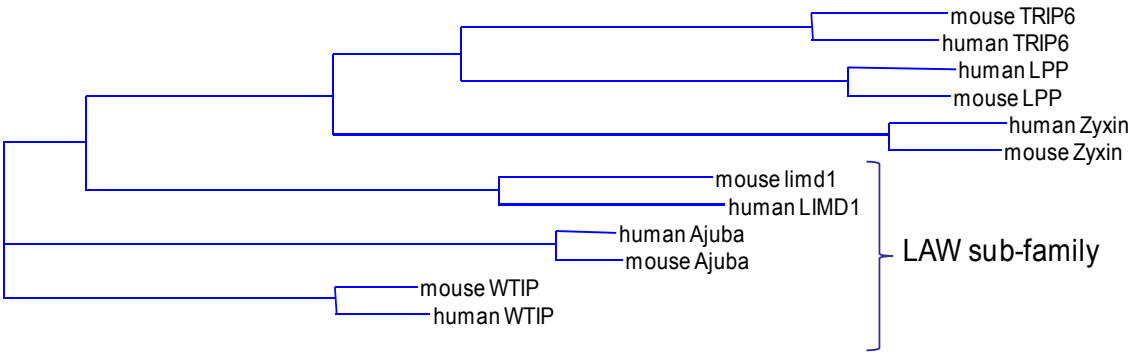

Figure 1.3 *Phylogenetic analysis of the Zyxin family proteins.*
The Zyxin family of LIM proteins comprises 7 proteins, namely Zyxin, TRIP6, LPP, LIMD1, Ajuba, WTIP and Migfillin (not shown), all of which contain 3 C-terminal LIM domains. Phylogenetic sequence analysis demonstrates the sub-categorisation of the Zyxin family into two further groups which share structural and functional homology, including the LIMD1, Ajuba and WTIP (LAW) sub-family.

As expected from their genetic homology, LPP (Lipoma-Prefered Partner) and Trip6 (Thyroid receptor-interacting protein 6) share similar functional attributes in cytoskeletal regulation as Zyxin. This is highlighted by the presence of multiple FPPPP binding motifs to recruit EVH1 (Ena/VASP homology domain 1) domains present in the actin regulatory proteins Ena/VASP, to the cell leading edge to influence actin assembly, which are not found in LIMD1 or Ajuba (Renfranz and Beckerle, 2002). Furthermore, LIMD1 and Ajuba lack α-actinin binding sites, present in the Zyxin sub-family (Li et al., 2003; Reinhard et al., 1999).

1.4 The LAW Sub-family of LIM proteins

To date, Ajuba is the best characterised of the LAW sub-family and displays both similar and distinct functions to the other Zyxin LIM proteins. Ajuba was initially identified as a binding partner of the adapter protein Grb2 (Growth factor receptor-bound protein 2), that couples signals from cell surface receptors to the activation of Ras and subsequently MAP kinase activation. Ajuba was demonstrated to interact with Grb2 SH3 domains *via* the pre-LIM region. Goyal et al demonstrated that Ajuba enhances MAP kinase activity to promote downstream *Xenopus* oocyte meiotic maturation in a Ras and Grb2 dependent manner (Goyal et al., 1999). One proposed functional trait distinguishing Ajuba from Zyxin is its cytoplasmic localisation and absence from focal adhesions (Goyal et al., 1999). However, there is disparity in this finding as more recent data reports the involvement of Ajuba in cytoskeletal regulation, modulating cell motility by recruitment of the adaptor protein p130Cas, to focal adhesions (Pratt et al., 2005). Ajuba null mice present impaired cell migration, believed to be due to defective p130Cas localisation to focal adhesions and the subsequent inability to activate Rac kinase (Pratt et al., 2005).

Kanungo et al demonstrated that Ajuba localises to sites of cell-cell adhesion with the ability to translocate into the nucleus dictated by a nuclear localisation sequence (NLS) within the LIM domains and shuttle out *via* a pre-LIM leucine-rich nuclear export sequence (NES) in a CRM1 (Chromosome region maintenance 1)-dependent manner (Kanungo et al., 2000). As cell-cell contact and adhesion to the extra-cellular matrix (ECM) regulate cell and tissue growth, it was postulated that Ajuba may relay extracellular cues to the nucleus influencing cell fate. This was demonstrated to be the case as ectopic expression of full length Ajuba increases proliferation, whilst an Ajuba LIM domain only construct that localises to the nucleus, spontaneously induced endodermal differentiation of P19 embryonal cells (Kanungo et al., 2000).

Recent data increasingly implicates the Ajuba sub-family of the Zyxin proteins with a role in transcriptional co-repression. LIMD1, Ajuba and WTIP all specifically interact with members of the Snail family transcriptional repressors *via* a conserved SNAG domain required for repressor complex assembly (Ayyanathan et al., 2007; Langer et al., 2008). The LAW proteins are believed to interact with Snail on endogenous E-cadherin promoters in the nucleus, serving as a platform for chromatin modifying factors such as the protein arginine methyltransferase 5 (PRMT5) (Hou et al., 2008) and histone deacetylases (HDAC) (Montoya-Durango et al., 2008) to repress E-cadherin expression. E-cadherin down regulation is a characteristic of epithelial mesenchymal transition (EMT), as cells repress epithelial gene expression and up-regulate mesenchymal genes to lose cell adherence and increase invasion (Thiery and Sleeman, 2006). Langer et al demonstrated that Ajuba mediated co-repression of E-cadherin, promotes EMT in *Xenopus*, driving processes such as neural crest development (Langer et al., 2008). As Ajuba has been demonstrated to interact with α-catenin and F-actin at cadherin-dependent cell-cell contacts, this provides a plausible mechanism whereby Ajuba may relay cues from cell-cell contacts to nuclear E-cadherin expression to regulate cell migration and developmental fates (Marie et al., 2003).

1.5 LIMD1 is a novel tumour suppressor

LIMD1 is encoded at chromosome 3p21.3, denoted the C3CER1 as it has been identified as one of the putative tumour suppressor regions by the elimination test; a test that identifies frequently deleted chromosome regions in microcell hybrid-derived SCID (Severe combined immunodeficient) tumours (Petursdottir et al., 2004; Kiss et al., 1999). Deletions in this 3p region are a common event in numerous solid malignancies including breast, gastric, colorectal, ovarian and renal (Petursdottir et al., 2004). Furthermore, LOH analysis of 576 tumours from 10 different tissue types, identified C3CER1 deletions in 83% of the tumours, exceeding the deletions in the well

characterised *VHL* (73%) and *FHIT* (Fragile histidine triad gene) (43%) regions of chromosome 3p (Petursdottir et al., 2004).

The tumour suppressive role of LIMD1 was first revealed in human lung carcinomas. Ectopic expression of LIMD1 was found to inhibit cell proliferation and repress colony formation in the non-small cell lung cancer (NSCLC) A549 cell line (Sharp et al., 2004). Viable A549 cells stably expressing HA-LIMD1 transduced by lentiviral technology were injected into the tail veins of athymic nude mice. HA-LIMD1 expression significantly reduced the incidence of lung metastases in comparison to transduction of the lentivirus only (Sharp et al., 2004). These *in vivo* and *in vitro* data concur with a reduction of LIMD1 protein levels in 75% of human squamous cell carcinomas and 79% of adenocarcinomas respectively, arising from a combination of gene deletion, LOH and epigenetic silencing (Sharp et al., 2008). Moreover, *Limd1*$^{-/-}$ mice predisposed to chemically-induced lung adenocarcinomas by administration of the carcinogen urethane, had an increased incidence of tumours compared to their wild type littermates (Sharp et al., 2008). *Limd1*$^{-/-}$ mice crossed with mice expressing a single copy of oncogenic *K-Ras*^{G12D} also had greatly increased tumour incidence which translated to an increased mortality over a 12-month period in comparison to the *K-Ras*^{G12D} mice (Sharp et al., 2008).

In head and neck squamous cell carcinomas (HNSCC) early LIMD1 alterations are also evident. In dysplastic lesions and HNSCC samples, LIMD1 showed high frequency promoter methylation, deletions and exhibited a reduction in mRNA expression (Ghosh et al., 2008).

In comparison to the loss of LIMD1 observed in human lung and HNSCC, analysis of LIMD1 in breast carcinomas revealed that differential sub-cellular localisation correlated with the tumour type and patient prognosis (Spendlove et al., 2008). LIMD1 is constantly shuttled between the nucleus and the cytoplasm *via* a CRM1-dependent nuclear export mechanism (Sharp et al., 2004). However, the equilibrium favours nuclear export as LIMD1 is predominantly localised in the cytoplasm, with approximately 14% of U2OS

cells expressing nuclear LIMD1 (Sharp et al., 2004). Down regulation of LIMD1 expression in the nucleus of neoplastic breast carcinoma cells as determined by immunohistochemistry, strongly correlated with poor patient prognosis, aggressive forms of breast carcinoma and increased tumour size (Spendlove et al., 2008). However, LIMD1 is rarely found in the nucleus but not in the cytoplasm. Therefore, the observed loss of nuclear LIMD1 may reflect a general loss of LIMD1 in the cytoplasm, therefore favouring the equilibrium for nuclear export. In this case, either loss of nuclear LIMD1 or reduction in LIMD1 protein levels correlates with poor prognosis. Both in lung and breast carcinomas, the expression level and localisation respectively, provide scope for the future therapeutic use of LIMD1 as a prognostic marker for early cancer development.

One elucidated mechanism of LIMD1-mediated tumour suppression is *via* interactions with the archetypal tumour suppressor retinoblastoma protein (pRB) (Sharp et al., 2004). LIMD1 directly binds pRB *via* residues 404-442 (Figure 1.2) and acts to co-repress E2F transcriptional activation of genes that facilitate G1/S phase transition, inhibiting cell proliferation which is fundamental in tumourigenesis. LIMD1 and pRB are believed to interact and regulate the transcriptional activation ability of the E2F family of transcription factors in a concentration dependent manner. This is in keeping with the previously reported role of the LAW proteins as transcriptional co-repressors (Ayyanathan et al., 2007; Langer et al., 2008; Hou et al., 2008; Montoya-Durango et al., 2008). Interestingly, mutation analysis led to the identification of a synonymous single nucleotide polymorphism (SNP) in the pRB interacting region of LIMD1 (1068T→C) in 7% of HSNCC samples (Ghosh et al., 2008). Furthermore, pRB is not directly lost in the development of every lung cancer, and therefore LIMD1 down regulation may induce a pRB loss of function to a similar effect as direct pRB loss (Wistuba et al., 2000).

As the LAW sub-family have conserved structural and functional attributes (Feng et al., 2007; Langer et al., 2008) it is plausible to hypothesise that Ajuba and WTIP may also have tumour suppressive functions. WTIP was first identified as an interacting protein for the zinc finger transcription factor

Wilms Tumour 1 (WT1) (Srichai et al., 2004). WT1 was originally identified as a tumour suppressor protein required for normal kidney nephrogenesis and podocyte differentiation, which was found inactivated in the development of Wilms tumours (or nephroblastomas) (Kreidberg et al., 1993). It has been proposed that WTIP acts in a scaffolding capacity within podocytes, visceral epithelial cells that form an essential component of the glomerular filtration barrier, to monitor the assembly of protein complexes regulating responses to slit diaphragm injury in order to modulate gene expression (Rico et al., 2005; Srichai et al., 2004). As WTIP interacts with the well characterised WT1 tumour suppressor, it is a possibility that WTIP may perform a conserved tumour suppressive function. In keeping with this hypothesis, Kanungo et al have demonstrated that expression of the Ajuba LIM domains inhibits cell growth in P19 embryonal cells (Kanungo et al., 2000). However, the LAW sub-family have also been reported to promote EMT, a pro-tumourigenic process resulting in increased metastasis and invasion, by repression of E-cadherin expression (Langer et al., 2008). Whether this represents the predominant LAW function is arguable and many factors need to be considered. These data apply within the context of the organism, in this case *Xenopus*, within which the research was performed. Furthermore, the LAW proteins (and particularly LIMD1) are principally localised in the cytoplasm (Sharp et al., 2004; Sharp et al., 2008), rather than in the nucleus where they may function to repress E-cadherin expression by interacting with the Snail family of transcriptional co-repressors, therefore, it is questionable whether this represents the predominant LAW function. As LIMD1 loss is observed in lung, head and neck carcinomas it appears that the overall phenotypic effect of LIMD1 is tumour suppressive. As to whether this translates to a conserved function of all the LAW proteins and how the dichotomic relationship between the involvement of LAW in EMT and tumour suppression lies, is yet to be fully understood.

Interestingly, LIMD1 deletion mutants absent of the pRB binding region still maintain a proportion of transcriptional repressive activity (Sharp et al., 2004). Furthermore, this is also the case in the $pRB^{-/-}$ human epithelial-like osteosarcoma SAOS2 (sarcoma osteogenic) cell line, whereby a degree of

LIMD1's tumour suppressive ability is maintained (Sharp et al., 2004). This suggests that LIMD1 may function as a tumour suppressor *via* pRB dependent and independent mechanisms. A yeast-2-hybrid screen (Y2H) was performed to identify novel LIMD1 interacting partners that may represent this pRB independent function. GAL4 DNA-binding domain LIMD1 amino acids 1-363 (denoted ∆364-676) was screened against a HeLa cDNA library and obtained a cDNA encoding full length prolyl hydroxylase 1 (PHD1) (Figure 1.5). PHD1 is one of three prolyl hydroxylases which target the hypoxia inducible factor (HIF) transcription factors for oxygen dependent degradation by the 26S proteasome, further elaborated in section 2. Data in this thesis confirms this interaction between LIMD1 and PHD1, in addition to the PHD2 and PHD3 isoforms and examines whether LIMD1 *via* this interaction modulates HIF activity.

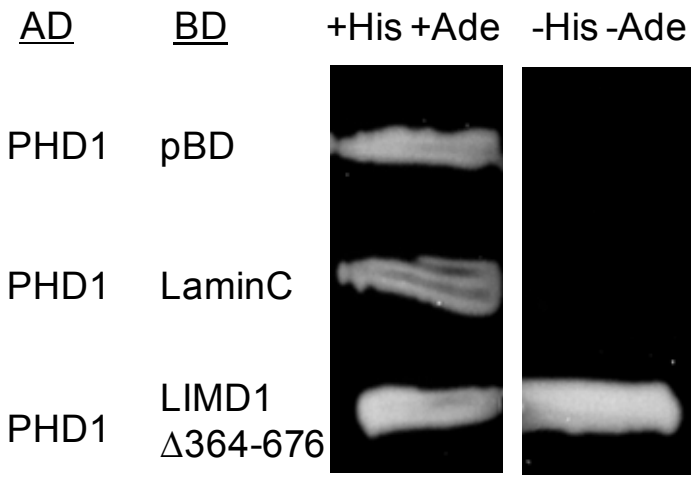

Figure 1.5 *LIMD1 interacts with PHD1 in a Y2H screen*

GAL4 DNA-binding domain (BD) LIMD1 (amino acids 1-363, i.e. ∆364-676) isolated a cDNA encoding full length PHD1 from a Y2H screen of a HeLa cDNA library. GAL4 BD-LIMD1 ∆364-676 and GAL4-activation domain (AD) -PHD1 were then co-transformed into the yeast strain PJ69-4a in addition to negative controls (PHD1 with pBD vector only and nuclear protein LaminC). Interaction was then assayed by prototrophy for histidine and adenine on medium lacking these amino acids.

1.6 HIF and the Intracellular Hypoxic Response

The precise concentration of cellular oxygen is essential in order to maintain intracellular bioenergetics and correct metabolic functioning. Therefore, responses to alterations in cellular oxygen tension are controlled by a tightly regulated oxygen sensing mechanism which couples oxygen levels to gene expression. In hypoxia, defined as a reduction in oxygen levels, the cellular response revolves around a signalling cascade mediated by a family of transcription factors termed the hypoxia inducible factors (HIFs). This section will provide an insight into the discovery, role and regulation of the HIFs and specifically the implications in cancer.

1.7 Early hypoxia biology research

The earliest research into hypoxia in tumour biology dates back to the early 20th century by Otto Warburg. Warburg observed that cancer cells experienced an 'injury of respiration' and a subsequent 'increase of fermentation' termed the Warburg effect (WARBURG, 1956). Warburg noted that cancer cells favoured anaerobic glycolysis independently of oxygen, postulating that chronic mitochondrial dysfunction could account for such a shift, following inducement of damage by treatment with carcinogenic x-rays. Warburg hypothesised that the increase in glycolysis is a major cause of cancer, a hypothesis which has more recently been superseded by the requirement for oncogene activation and down regulation of tumour suppressors, a process which most likely accounts for the Warburg effect itself rather than mitochondrial malfunction (Sherr, 2004).

Early indications of the presence of hypoxic tumour cells were observed by Thomlinson and Gray in 1955. From analysis of human lung tumour sections they noted a necrotic core surrounded by a region of viable cells adjacent to blood capillary vessels (THOMLINSON and GRAY, 1955). In multiple tumour types they consistently observed this band of viable cells of 170μm in width, approximately the calculated diffusion distance of O_2, suggesting this necrotic

region was due to insufficient O_2 supply as the tumour rapidly expands and distances from the vasculature. They proposed that an O_2 concentration gradient was present from the capillaries to the necrotic core and that on the edges of the necrotic region viable tumour cells existed.

The first molecular discovery in hypoxia biology came in the 1980's with the discovery of a number of genes stimulated by O_2 deprivation. These included the glucose-regulated proteins (GRPs) (Sciandra et al., 1984) and O_2-regulated proteins (ORPs) (Heacock and Sutherland, 1990). It was later found that an 80kDa ORP and a 78kDa GRP were in fact identical, suggesting that glucose and oxygen deprivation may induce the same cellular process. The nature of cellular O_2 sensing and how gene transcription was regulated in hypoxia were still to be elucidated. In 1991 a key link between hypoxia and gene transcription was identified by Semenza et al, by systematic characterisation of the oxygen regulated expression of the haematopoietic growth factor erythropoietin (EPO) gene. Semenza identified cis-acting DNA sequences approximately 120 base pairs 3' of the polyadenylation site of the human erythropoietin gene that enhanced EPO expression (Semenza et al., 1991; Pugh et al., 1991; Beck et al., 1991). EPO is the primary regulator of erythrocyte production and therefore tissue oxygen delivery. As EPO expression had been demonstrated to increase hundred-fold following hypoxic exposure (Schuster et al., 1989), this identified a hypoxia-inducible gene enhancer.

1.8 Identification and characterisation of the hypoxia inducible factors

In 1992, the trans-acting protein factor found able to regulate EPO gene expression was identified in Hep3B cells. Using a double stranded oligonucleotide probe encompassing key nucleotides in the EPO enhancer element, electrophoretic mobility shift assays (EMSA) were performed with Hep3B nuclear extracts exposed to normoxia and hypoxia (Semenza and Wang, 1992). This identified a hypoxia inducible nuclear factor, capable of binding to the EPO enhancer and promoting EPO expression in O_2

deprivation. This nuclear factor was designated hypoxia-inducible factor 1 (HIF1) and was further demonstrated to have a general role in the hypoxic activation of gene transcription in all mammalian cell lines tested, including both EPO and non-EPO producing cells (Wang and Semenza, 1993c). HIF1 induction by hypoxia was initially demonstrated to induce genes encoding glycolytic enzymes such as aldolase A and phosphoglycerate kinase 1, all of which were found to contain a homologous HIF1 binding site erythropoietin enhancer, termed a hypoxia response element (HRE) (Semenza et al., 1994). This HRE was restricted to a core motif of 5'-G/ACGTG-3', currently believed to be associated with 100-200 genes regulating a diverse array of cellular processes including erythropoiesis, angiogenesis, autophagy and energy metabolism (Figure 1.8.1) (Kaelin, Jr. and Ratcliffe, 2008).

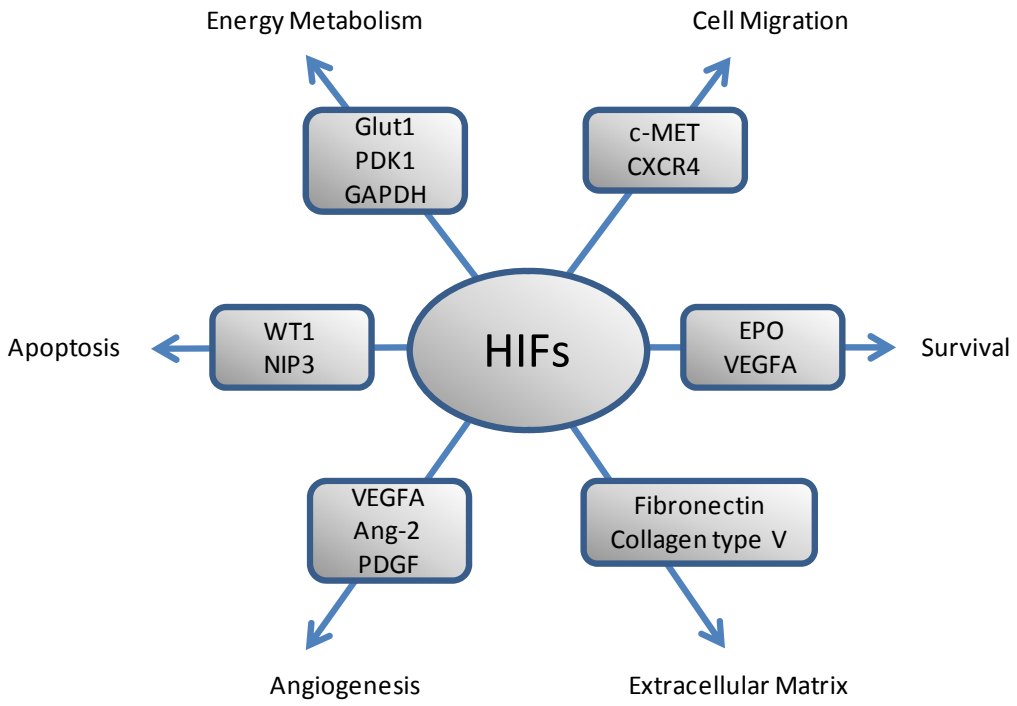

Figure 1.8.1 *Direct transcriptional targets of HIFs.*

A small subset of hypoxia response genes. Many of the protein products of these genes are involved in tumour progression. Glut1; glucose transporter 1 (Ebert et al., 1995), PDK1; pyruvate dehydrogenase kinase isozyme 1 (Kim et al., 2006), GAPDH; glyceraldehyde-3-phosphate dehydrogenase (Graven et al., 1999), c-MET; mesenchymal-epithelial transition factor (Pennacchietti et al., 2003), CXCR4; C-X-C chemokine receptor 4 (Schioppa et al., 2003), WT1; wilms tumour suppressor (Wagner et al., 2003), EPO; erythropoietin (Semenza and Wang, 1992), NIP3; E1B/Bcl-2 19kDa interacting protein 3 and pro-apoptotic protein (Bruick, 2000), VEGFA; vascular endothelial growth factor A (Levy et al., 1995), Ang-2; angiopoietin 2 (Oh et al., 1999), PDGF; platelet derived growth factor (Kourembanas et al., 1990).

Purification of HIF1 from Hep3B cells using DNA affinity chromatography, identified HIF1 as a heterodimer comprising of a 120kDa HIF1α and 91-94kDa HIF1β subunit (Wang and Semenza, 1995). Both HIF1α and HIF1β are basic-helix-loop-helix (bHLH)-PAS proteins, due to high sequence similarity to the *Drosophilla* proteins period (Per) and single-minded (Sim) and the mammalian aryl hydrocarbon receptor (AHR) and aryl hydrocarbon receptor nuclear translocator (ARNT) of which all contain 200-350 amino acids that constitute the PAS (Per-ARNT-AHR-Sim) domain (Wang et al., 1995). The oxygen sensitive regulation of HIF was found to be determined by a rapid redox dependent turnover of the HIF1α subunit under normoxic conditions and rapid stabilisation in hypoxic conditions (Huang et al., 1996). HIF1β, is found ubiquitously expressed independently of O_2 availability and is identical to the previously identified bHLH-PAS protein ARNT, which is reported to mediate biological and toxicological effects of xenobiotics in association with AHR (Hankinson, 1995).

HIF1α was found to be one of three closely related forms, each encoded by a distinct gene locus. HIF2α, previously termed HIF1α-like factor (HLF) (Ema et al., 1997), HIF-related factor (HRF) (Flamme et al., 1997), endothelial PAS domain protein 1 (EPAS-1) (Tian et al., 1997) and member of the PAS family 2 (MOP2) (Hogenesch et al., 1997), has the highest degree of functional and structural homology with HIF1α, with an amino acid sequence homology of 48% (O'Rourke et al., 1999). HIF3α or inhibitory PAS domain protein (IPAS) is less closely related to HIF1α and appears to demonstrate negative regulation of hypoxia dependent gene activation by forming transcriptional inactive heterodimers with HIF1α but not HIF1β (Makino et al., 2001). Due to the apparent general homology in HIF1α and HIF2α structure and function, they are commonly referred to as HIFα. The conserved structure of HIF1α, HIF2α and HIF1β are illustrated in figure 1.8.2.

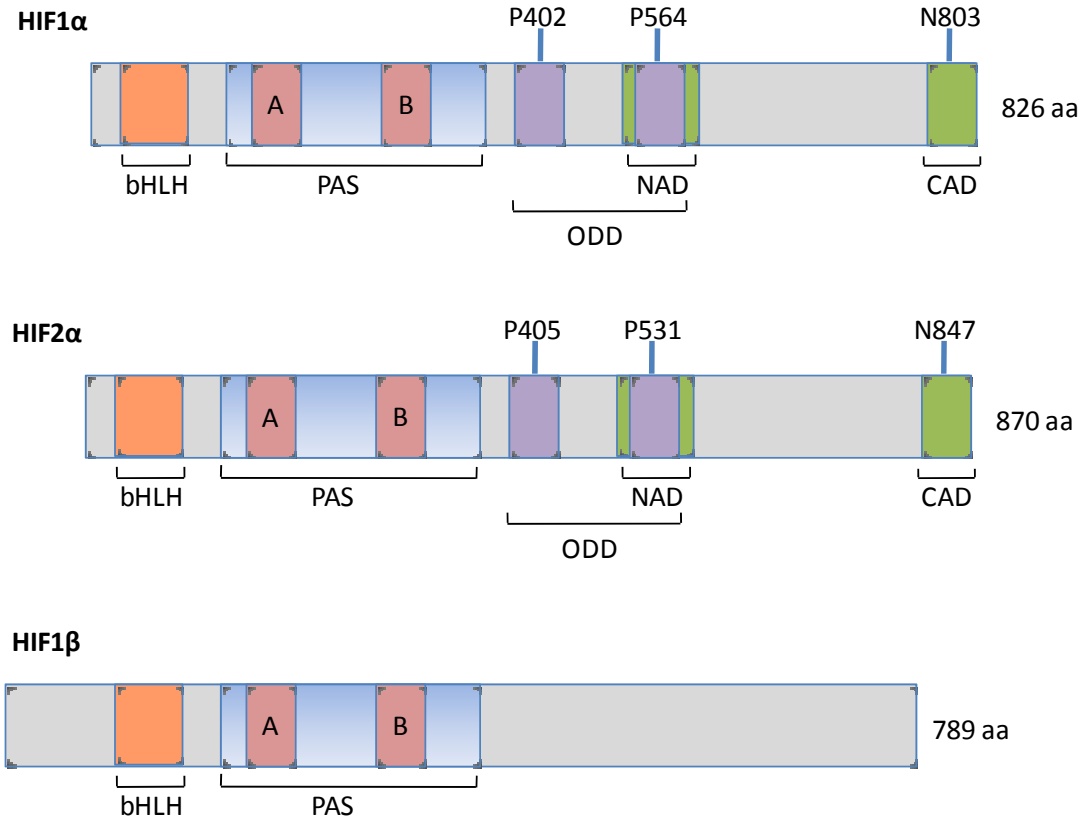

Figure 1.8.2 *Domain Structure of the hypoxia-inducible factors.*
HIFs comprise a basic helix-loop-helix (bHLH) domain required for DNA binding and two PAS domains of 100-120 amino acids which mediate HIF heterodimerisation. HIF1α and HIF2α contain an oxygen-dependent degradation domain (ODD) containing functionally important residues that convey oxygen responsiveness, proline 402 within an N-terminal (NODD) and 564 within a C-terminal oxygen-dependent degradation (CODD) sub-domain. HIF1α and HIF2α also contain two transactivation domains, an N-terminal activation domain (NAD) and a C-terminal activation domain (CAD) which interact with the transcriptional co-activator p300/CBP. [This figure is modified from (Schofield and Ratcliffe, 2004; Simon and Keith, 2008)].

HIF1α is expressed ubiquitously, whereas HIF2α and HIF3α exhibit more restricted tissue distributions. HIF2α expression is restricted to vascular endothelium, liver parenchyma, lung type II pneumocytes and kidney epithelial cells (Tian et al., 1997; Jain et al., 1998; Wiesener et al., 2003; Flamme et al., 1997), whereas HIF3α is found primarily expressed in the thymus, kidney, cerebellar Purkinje cells and corneal epithelium of the eye (Makino et al., 2001; Gu et al., 1998).

Under hypoxic conditions, stabilised HIFα translocates into the nucleus *via* a C-terminal nuclear localisation signal, where it heterodimerises with the stable constitutively nuclear protein HIF1β (Pollenz et al., 1994; Kallio et al., 1998). HIFα and HIF1β heterodimerisation occurs both *in vivo* and *in vitro* in the absence of DNA, mediated by the N-terminal PAS domains. DNA binding of the HIFα-HIF1β heterodimer is conferred by the bHLH domains which interact with HREs within target genes *via* both DNA strands in the major groove to activate expression of hypoxia response genes (Jiang et al., 1996; Wang and Semenza, 1993a).

HIF1α and HIF2α contain two transactivation domains in the C-terminal half of the protein, designated the N-terminal activation domain (NAD) and C-terminal activation domain (CAD), [HIF1α aa481-603 and aa776-826, (Jiang et al., 1997; Pugh et al., 1997)] [HIF2α aa450-571 and 824-876, (Ema et al., 1999)]. The CAD has been demonstrated to interact with the cysteine-histidine rich (CH-1) domain of the homologous transcriptional adaptor proteins adenovirus E1A-binding p300 (p300) and Cyclic-AMP responsive element-binding protein (CBP) inducing recruitment of the basal transcriptional machinery (Arany et al., 1996; Ema et al., 1999). The interaction of p300/CBP with HIF1α and HIF2α is also subject to oxygen sensitive regulation via hydroxylation of asparagine 803 (further discussed in section 1.12). HIF heterodimerisation, DNA binding and p300/CBP association are depicted diagrammatically in figure 1.8.3.

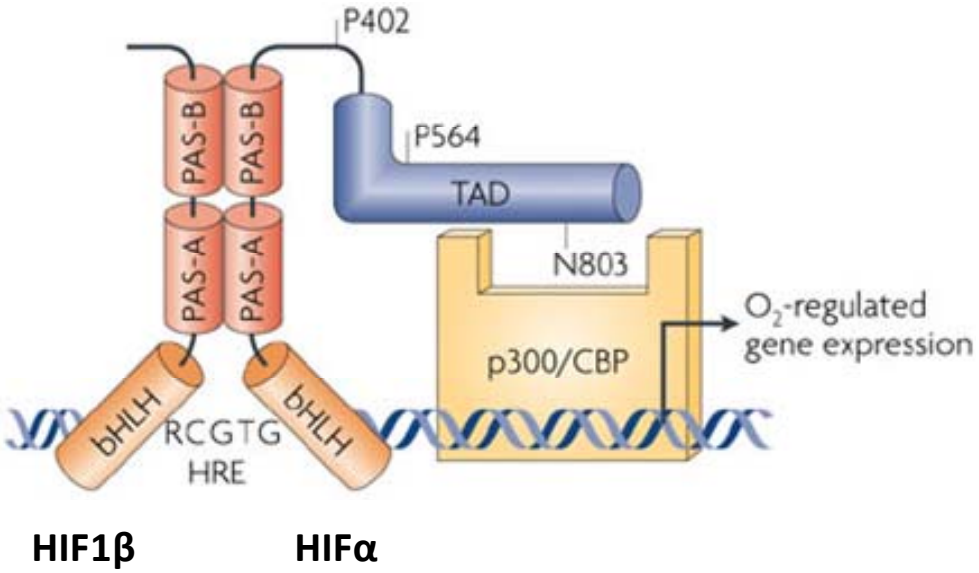

Figure 1.8.3 *Diagrammatic representation of HIF heterodimerisation and DNA binding properties.*

In hypoxic conditions HIFα translocates into the nucleus and heterodimerises with HIF1β mediated by the PAS domains, enabling the bHLH domains to bind to HRE elements of hypoxia response genes. The HIFα transactivation domain interacts with the p300/CBP transcriptional co-activator inducing recruitment of the basal transcriptional machinery to initiate gene expression. [Figure modified from (Simon and Keith, 2008)].

1.9 Oxygen dependent regulation of HIFα stability

Huang et al observed that HIFα had a rapid redox-dependent turnover in normoxia but became stabilised under hypoxic conditions (Huang et al., 1996). Furthermore, Huang et al demonstrated that HIFα mRNA was unaffected by changes in oxygen tension, hypothesising that the likely mechanism of regulation occurred at the post-transcriptional level, altering the rate of translation or rate of protein degradation (Wenger et al., 1997; Kallio et al., 1997). In 1997, Salceda et al elaborated on this hypothesis by demonstrating that HIFα was regulated in normoxia by the addition of a 76 amino acid polypeptide ubiquitin, which targeted the protein for degradation by the 26S proteasome, a multi-catalytic protease (Salceda and Caro, 1997). Mutation analysis of a Gal4-HIF1α fusion led to the identification of a ubiquitin-proteasome mediated, oxygen dependent degradation (ODD) domain between amino acids 401-603 (Huang et al., 1998). This domain conferred an extremely short normoxic half life of approximately 5 minutes to the full length protein and internal deletion of the ODD domain induced HIF stability, heterodimerisation and activation of HRE-luciferase reporter gene constructs (Huang et al., 1998).

1.10 Von-Hippel Lindau Tumour Suppressor

In 1999, Maxwell et al discovered a key link in the cellular oxygen sensing mechanism from observations of patients with von-Hippel Lindau (VHL) disease. VHL disease manifests in individuals with a germline mutation in the von-Hippel Lindau tumour suppressor. Somatic bi-allelic loss of the wild type *VHL* gene results in a striking up-regulation of angiogenesis and glucose metabolism, which consequently form highly vascularised tumours such as hemangioblastomas and renal clear cell carcinomas (Kaelin, Jr., 2002). Maxwell et al demonstrated that renal carcinoma cells absent of VHL, constitutively express HIFα and consequently multiple HIF response genes under normoxic conditions (Maxwell et al., 1999). Furthermore, Maxwell et al

showed that ectopic expression of VHL suppressed HRE-reporter activation and VHL re-introduction could restore normal hypoxic regulation of VHL inactive renal carcinoma cell lines. It was also revealed that VHL and HIFα interact and that VHL affects HIFα stability mediated *via* the ODD domain. However, the direct mechanism and link between VHL and HIFα ubiquitylation was still to be defined. This was achieved by Cockman et al in 2000 who demonstrated evidence that VHL regulates HIFα by promoting ubiquitylation as a component of a ubiquitin ligase complex (Cockman et al., 2000).

VHL mRNA encodes two protein isoforms of 24-30kDa and 19kDa, as a result of an internal translation initiation ATG at codon 54 (Iliopoulos et al., 1995; Iliopoulos et al., 1998). Therefore, the term pVHL is often used when generically referring to both isoforms.

VHL associates with elongin C (14kDa) and elongin B (18kDa), two regulatory subunits of the trimeric transcription elongation factor, elongin, to form a trimeric VBC complex (Duan et al., 1995; Kibel et al., 1995) . It was further demonstrated that this VBC complex could interact with the additional proteins Cullin-2 (CUL-2), a homolog of Cdc53 in *Saccharomyces cerevisiae (Pause et al., 1997)* and Rbx1, an evolutionarily conserved protein that contains a RING-H2 finger-like motif that interacts with the Cullin proteins (Kamura et al., 1999). Cdc53 is a known putative E3 ubiquitin ligase with defined functions in the degradation of cell cycle control proteins and therefore, led to the hypothesis that the VBC-CUL-2 complex could target transcription factors for proteolysis to regulate hypoxia dependent gene expression. This hypothesis was further elaborated by Lonergan et al who led to the proposal of a model based on homology with the SCF (Skp-1-Cdc53/Cullin-F-box) class of ubiquitin ligases (Lonergan et al., 1998). In addition to the homology between CUL-2 and Cdc53, elongin C shares homology with Skp-1 and elongin B sequence similarity to ubiquitin itself. This led to the conclusion that VHL as part of the VBC-CUL-2 complex forms an E3 ubiquitin ligase capable of targeting HIFα subunits for proteolytic

degradation in normoxic conditions. Structural homology of the VBC and SCF ubiquitin ligase complexes are depicted in figure 1.10.

The structure of the VBC complex was solved by Stebbins et al in 1999. Stebbins demonstrated that pVHL comprises an α-domain (aa 155-192) which associates with elongin C and a β-domain containing a seven stranded β-sandwich (aa 63-154) and an α-helix (aa193-204) (Stebbins et al., 1999). The β-domain of both VHL isoforms (aa 63-154) was demonstrated to be capable of directly interacting with HIFα residues 549-582 and inducing poly-ubiquitylation (Cockman et al., 2000; Ohh et al., 2000).

The functional importance of VHL's associations with elongin C and the HIFα subunit is emphasised by the fact that the majority of missense mutations that manifest into VHL disease, disrupt these interactions, thus providing a direct link between structure and function. VHL mutations can be classified into different types associated with the molecular defect and the resulting clinical manifestation (Kaelin, Jr., 2002). For example, the common type 2A mutations Y98H and Y112H within the VHL β-domain retain a significant residual ubiquitin ligase activity towards HIF1α *in vitro*, which translates to a low risk of renal cell carcinoma development (Knauth et al., 2006). However, type 2B mutations in the same residues, Y98N and Y112N, result in ablation of the interaction with HIF1α and therefore, VHL does not retain ubiquitin ligase activity, predisposing individuals to a high risk of renal cell carcinoma development (Knauth et al., 2006).

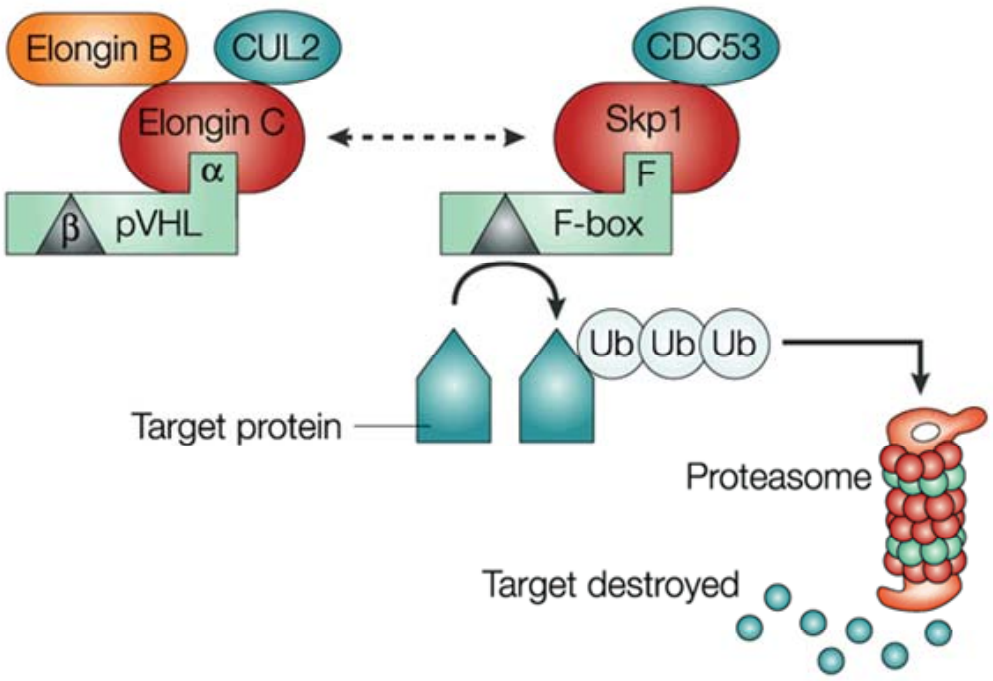

Figure 1.10 *VBC Ubiquitin ligase complex.*

VHL forms a VBC complex with elongin C, elongin B and cullin-2. This complex structurally and functionally resembles the SCF-like (Skp-1-Cdc53/Cullin-F-box) ubiquitin ligases. Ubiquitin ligases, in conjunction with E1 and E2 enzymes, target proteins (such as HIFα subunits) for poly-ubiquitylation, which labels them for degradation by the 26S Proteasome. VHL interacts with elongin C *via* three C-terminal helices within the VHL α-domain which resembles an F-box motif. VHL β-domain contains a substrate docking site capable of binding HIFα residues 549-582. [Figure adapted from (Kaelin, Jr., 2002)].

1.11 HIF regulation by proline hydroxylation

The precise oxygen sensing mechanism regulating the VHL-dependent degradation of the HIFα subunit was largely elucidated by the Ratcliffe, Kaelin and Lee groups in 2001. Previous evidence demonstrating the inhibition of HIFα degradation by the administration of iron chelators such as desferrioxamine and cobaltous ions suggested the involvement of an underlying oxygen-sensing ferroprotein (Wang and Semenza, 1993b; Goldberg et al., 1988).

Mass spectrometric analyses revealed oxidation of a conserved proline 564 residue within the ODD domain of the HIFα subunit. Synthetic production of a HIF peptide (556-574) incorporating a *trans*-4-hydroxy-*S*-proline residue was capable of out-competing the *in vitro* interaction of HIFα with pVHL confirming that the mechanism promoting HIFα ubiquitylation was dependent on the most common trans-4 proline hydroxylation by a HIFα-prolyl-4-hydroxylase (Jaakkola et al., 2001; Ivan et al., 2001; Yu et al., 2001).

It was subsequently identified that the HIF-prolyl hydroxylases comprised a family of 3 closely related enzymes encoded by individual genes (Epstein et al., 2001; Bruick and McKnight, 2001), who could preferentially hydroxylate two different, independent and non-redundant HIFα degradation domains, encompassing proline 402 and 564 in HIF1α (Masson et al., 2001). The HIF prolyl hydroxylase domain proteins are orthologues of the *Caenorhabditis elegans Egl-9* gene and are interchangeably referred to as PHD1, 2 and 3, or EGLN 2, 1 and 3 proteins respectively (Epstein et al., 2001). The PHDs are members of the 2-oxoglutarate-dependent dioxygenase family related to the procollagen prolyl hydroxylases, localised in the endoplasmic reticulum and whom are believed to modify collagen as it matures along the exocytotic pathway (Kivirikko and Pihlajaniemi, 1998). The PHDs are iron and oxygen dependent non-haem ferroproteins, that consistent with previous findings may be inhibited by iron chelation or iron substitution by cobaltous ions (Kivirikko and Myllyharju, 1998). The PHDs absolute requirement for oxygen as a co-substrate led to a direct link between oxygen availability and the

regulation of hypoxia inducible genes *via* HIFα stability. Proline substrate residues P402 and P564 of HIF1α, P405 and P531 of HIF2α and P491 of HIF3α, all align to a conserved hydroxylation LXXLAP motif (Ivan et al., 2001; Jaakkola et al., 2001).

The precise mechanism governing the selective recognition of HIFα *via* prolyl hydroxylation was further scrutinised by the Jones and Pavletich groups in 2002, who examined the crystal structure of the HIFα peptide (aa560-577) bound to the VBC complex. The HIFα CODD peptide binds *via* two distinct binding sites, amino acids 560-567 and 571-577, with pVHL residues 67-117 within the β-domain (Min et al., 2002; Hon et al., 2002). 560-567 represents the primary binding site, containing the hydroxyproline residue within the LAP motif, which is deeply buried within a hydrophobic core pocket containing 5 residues capable of hydrogen bonding with the hydroxyproline 564 residue. The pyrrolidine ring of the hydroxyproline makes multiple van der Waals contacts, whilst the 4-hydroxyl group forms hydrogen bonds with the N of histidine 115 and the OH group of serine 111. Without HIFα pro564 hydroxylation, binding would result in the energetically unfavourable desolvation of His 115 and Ser 111 and therefore, these residues are believed to act as key determinants in the strict selectivity for hydroxylation of pro564.

1.12 Asparaginyl hydroxylation regulates HIF transcriptional activity

As mentioned in section 1.8, in addition to prolyl hydroxylase mediated regulation of the HIFα ODD, transcriptional activation of the HIF C-terminal activation domain (CAD) is also negatively regulated by O_2, independently of HIFα stability by means of asparaginyl hydroxylation. Factor Inhibiting HIF-1 (FIH) (alternatively termed HIF asparaginyl hydroxylase) was identified as a HIFα interacting protein (Mahon et al., 2001), subsequently identified as an additional 2-oxoglutarate-dependent dioxygenase that worked in a similar Fe(II) and oxygen dependent manner as the PHD proteins to hydroxylate a conserved asparagine residue in the HIFα CAD (Lando et al., 2002; Hewitson et al., 2002). The oxygen dependent hydroxylation of HIF1α asparagine 803 (HIF2α asparagine 851) inhibits the association of HIF with co-activators such as p300/CBP, abrogating the recruitment of the transcriptional machinery and the expression of hypoxia inducible genes, illustrated in figure 1.12. It has further been demonstrated that hydroxylation occurs on the asparagine β-carbon which is part of an α-helix deeply buried within the molecular interface (McNeill et al., 2002; Freedman et al., 2002; Dames et al., 2002). It is hypothesised that the oxygen dependent hydroxylation may disrupt the hydrophobic interactions within the molecules and the α-helix, resulting in ablation of the interaction with the CH-1 domain of p300.

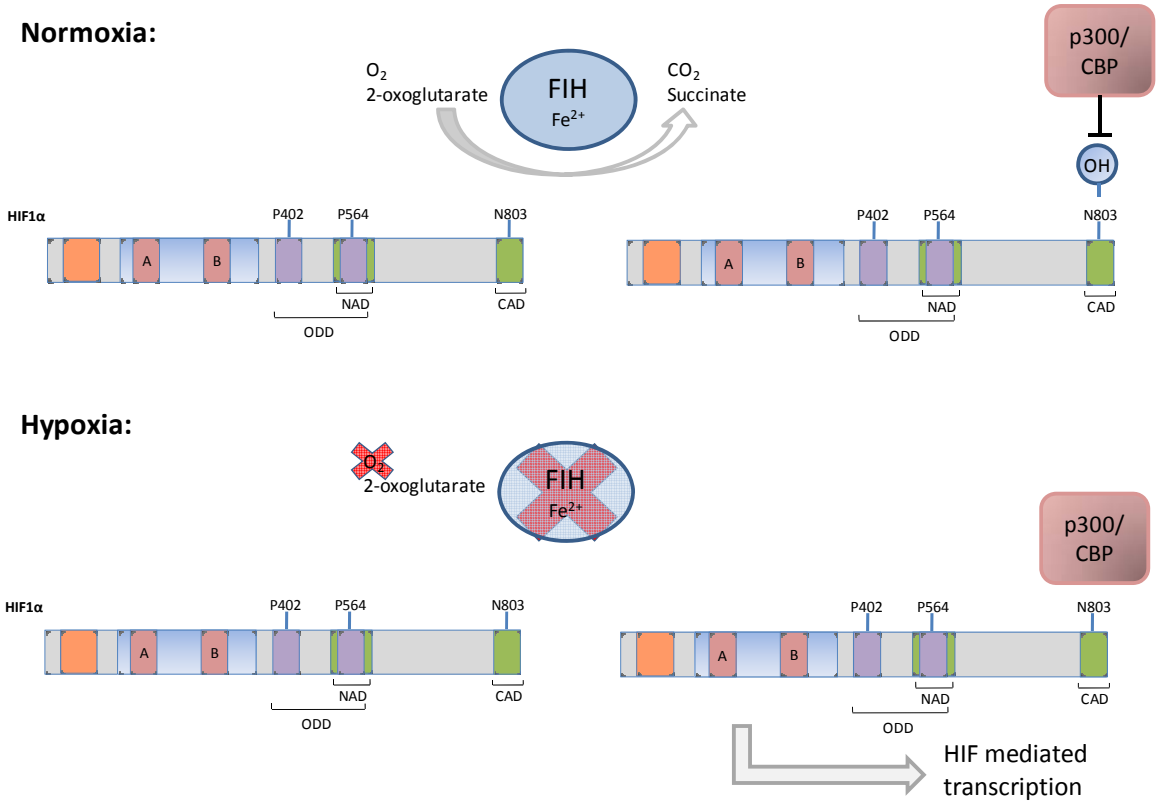

Figure 1.12 *HIFα CAD regulation by asparaginyl hydroxylation.*

Normoxic silencing of the CAD by FIH-1-mediated hydroxylation. In normoxia, FIH hydroxylates the target asparagine residue within the HIFα CAD using the co-substrates O_2 and 2-oxoglutarate. This hydroxylation precludes the association of the essential co-activators CBP/p300, repressing the transcriptional activity of the CAD. During hypoxia, when oxygen is limiting, FIH is unable to efficiently catalyse the hydroxylation of the CAD, enabling binding of CBP/p300 to the non-hydroxylated CAD and transactivation of target genes (Lisy and Peet, 2008)

The precise relationship between HIF hydroxylase activity and O_2 concentration has been deduced from a number of studies, indicating a finely tuned response to change in oxygen tension. *In vitro* derived K_m (Michaelis constant) values of the PHDs and FIH for oxygen (the concentration of oxygen that supports a half-maximal initial catalytic rate) using HIFα peptide substrates, indicate that the PHDs K_m were in the range of 230-250 μM whilst FIH has a higher affinity for O_2 with a K_m of 90 μM (Hirsila et al., 2003; Koivunen et al., 2004). This may propose a model whereby the PHDs lose catalytic activity in higher O_2 tensions than FIH, therefore generating a hypoxic window in which HIFα may accumulate but be largely transcriptionally inactive due to FIH mediated asparagine hydroxylation. However, it has been demonstrated that the second N terminal activation domain (NAD) can activate transcription and furthermore, certain HIF splice variants that lack the CAD can still activate the transcription of certain hypoxia inducible genes (Gothie et al., 2000). This may represent highly sensitive regulation of the transcription of specific hypoxia inducible genes in response to changes in oxygen tension. It has however, more recently been proposed that a more physiological K_m for the PHDs is approximately 100 μM (Koivunen et al., 2006; Ehrismann et al., 2007). As the typical tissue oxygen concentration is found to be 10-30 μM, significantly below the K_m for the HIF hydroxylases, enzyme activity is anticipated to be modulated by oxygen over the entire physiological range. Interestingly, HIF2α in comparison to HIF1α appears relatively resistant to FIH mediated inactivation, due to a conserved amino acid substitution of the HIF1α residue immediately downstream of the FIH substrate asparagine 803, alanine 804 to valine in all HIF2α orthologues (Bracken et al., 2006).

1.13 Structure and function of the 2-oxoglutarate-dependent dioxygenases

The PHD proteins are classified as 2-oxoglutarate-dependent dioxygenases due to their use of the citric-acid-cycle intermediate 2-oxoglutarate and due to the fact that they incorporate both oxygen atoms from molecular oxygen into their product. The first structural insight into 2-oxoglutarate-dependent dioxygenases came from X-ray crystallographic analysis of deacetoxycephalosporin C synthase (DAOCS), an enzyme involved in the biosynthesis of the β-lactam cephalosporin antibiotic (Valegard et al., 1998). In conjunction with the crystal structures of other 2-oxoglutarate-dependent dioxygenases, a core structure has been highlighted which can be applied to the PHD proteins due to sequence conservation and mutation analysis. A common catalytic structure comprises of eight core β-strands which form a double-stranded β-helix motif (DSBH) , commonly termed a 'jelly-roll' motif, illustrated in figure 1.13 (Schofield and Zhang, 1999).

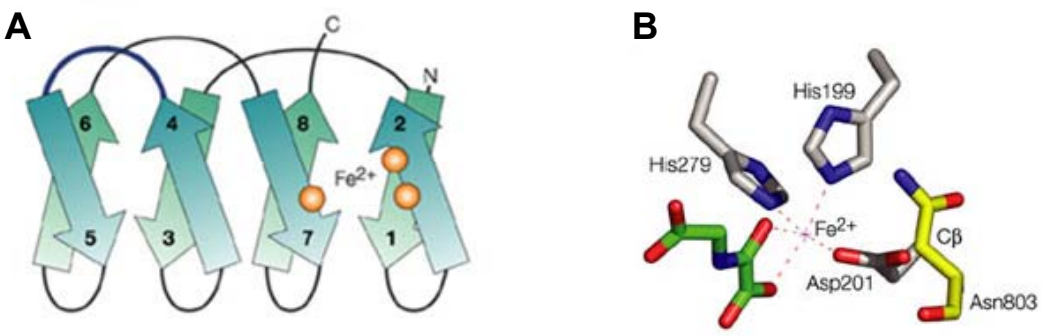

Figure 1.13 *Structure of the 2-oxoglutarate-dependent dioxygenases.*
(A) Schematic representation of the DSBH motif of the 2-oxoglutarate-dependent dioxygenases. Iron is coordinated by a two-histidine, one-carboxylate motif from 3 residues often contributed from the second or seventh β-strand of the DSBH motif. **(B)** Active site of FIH, whereby histidine 279 and 199, and a carboxylate motif from aspartic acid 201 coordinate iron. 2-oxoglutarate analogue N-oxalylglycine is present within the active site which is in contact with iron. FIH iron coordinating residue aspartic acid 201, brings the target asparagine 803 into the active site for hydroxylation *via* a hydrogen bond. [Modified from Schofield and Ratcliffe (Schofield and Ratcliffe, 2004)].

The fundamental mechanism of 2-oxoglutarate-dependent dioxygenases appears to be conserved, comprising the enzyme-Fe^{2+} complex initially binding 2-oxoglutarate, then its substrate and then oxygen. The DBSH motif critically provides the structural platform for the HIF hydroxylases to coordinate Fe^{2+} *via* a two-histidine, one-carboxylate motif from 3 residues often contributed from the second or seventh β-strand within the active site of the enzyme. Fe^{2+} in turn coordinates 2-oxoglutarate and molecular oxygen forming a reactive intermediate that drives the oxidative process. During catalysis, molecular oxygen is split, coupling one oxygen atom to the hydroxylation of HIFα and one to the oxidative decarboxylation of 2-oxoglutarate to succinate and CO_2 (Schofield and Zhang, 1999; Hegg and Que, Jr., 1997; Elkins et al., 2003). The availability of essential cofactors 2-oxoglutarate and Fe^{2+} in addition to oxygen, appear to be important determinants regulating the activity of the HIF hydroxylases, further discussed in section 1.18.

1.14 Structural differences between the PHDs

PHD1 and PHD2 have a similar domain organisation with a C-terminal catalytic domain (DBSH) and an N-terminal extension, (Figure 1.14). PHD3 shares the same conserved C-terminal catalytic domain but lacks the N-terminal extension (Bruick and McKnight, 2001; Epstein et al., 2001). The other most significant structural difference between the PHDs is the presence of the N-terminal myeloid, nervy and DEAF-1 (MYND)-type zinc finger domain only found in PHD2. It has been suggested that this domain performs an auto-inhibitory role down regulating PHD2 catalytic activity. Deletion of this domain or chelation of zinc using TPEN (*N,N,N',N'*-tetrakis [2-pyridylmethyl] ethylenediamine) has been demonstrated to increase the catalytic activity of PHD2 and destabilise HIFα *in vitro* and *in vivo* (Choi et al., 2005). The mechanism of inhibition still remains elusive, however it is not anticipated that the MYND domain inhibits by directly interacting with the

catalytic domain as no interaction can be detected by yeast-2-hybrid analysis (Choi et al., 2005).

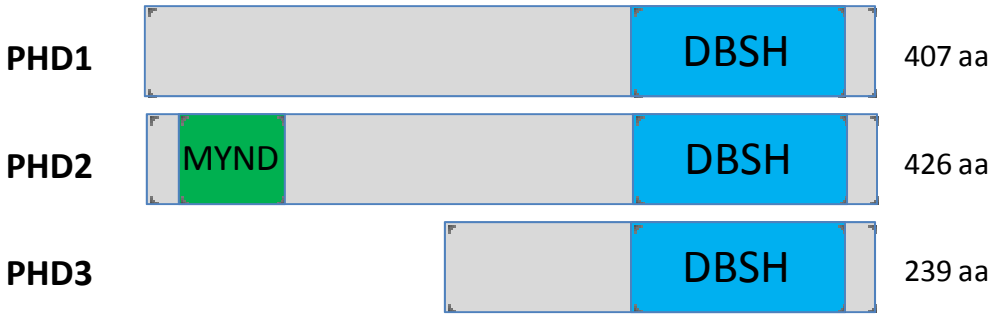

Figure 1.14 *Schematic representation of the PHDs.*
The three PHDs contain a conserved double-stranded β-helix motif (DBSH), incorporating the catalytic core of 2-oxoglutarate and Fe(II)-dependent dioxygenases. PHD2 contains an N terminal zinc finger domain unique within the PHD enzymes, known as a myeloid, nervy and DEAF-1 (MYND) domain which consists of a cluster of cysteine and histidine residues, arranged with an invariant spacing to form a zinc binding motif.

1.15 The multiple PHDs have differential functional attributes

Although flies and worms only contain the single PHD (EGLN) family member *Egl9*, higher metazoans contain three paralogous PHD genes. All three PHDs have a conserved catalytic domain and display the ability to hydroxylate HIFα *in vitro* (Bruick and McKnight, 2001; Epstein et al., 2001). However, it is increasingly apparent that the three PHDs have differential characteristics and individual functional niche.

All three genes are widely expressed, in particular PHD3 mRNA levels are elevated in the heart and PHD1 is exclusively expressed at high levels in the

testes (Lieb et al., 2002). PHD2 and PHD3 expression levels are elevated by hypoxia, which may represent a HIF-dependent auto-regulatory mechanism to limit HIFα induction in hypoxia or to accentuate the response to reoxygenation (Epstein et al., 2001; Berra et al., 2003). Conversely, PHD1 mRNA expression may be suppressed by hypoxia, which potentially suggests a fundamentally different role for PHD1 in the hypoxic response (Tian et al., 2006). Furthermore, ChIP (chromatin immunoprecipitation) analysis revealed that PHD1 promoter sequences are capable of interacting with ARNT1 (HIF1β) *in vivo* (Erez et al., 2004). Therefore, implicating a mechanism whereby HIF activation propagates its own stabilisation by inhibiting PHD1 expression.

GFP-tagged PHD proteins also appear to demonstrate distinct subcellular localisations. PHD1 has been demonstrated to be localised exclusively in the nucleus mediated by an importin-dependent mechanism, PHD2 in the cytoplasm and PHD3 in both the nucleus and the cytoplasm (Metzen et al., 2003a; Steinhoff et al., 2009) . However, recent publications have revealed that endogenous PHD2 can accumulate in the nucleus and shuttle between both intracellular compartments *via* CRM1-dependent nuclear export mediated by a NES (amino acids 6-20) and predicted NLS (amino acids 51-54 and 98-114) (Berchner-Pfannschmidt et al., 2008; Yasumoto et al., 2009). Whether the subcellular distribution of PHD2 alters HIFα turnover is unclear, as conflicting studies have shown that cytoplasmic PHD2 is required for HIFα ubiquitylation in RCC4 cells (Masson et al., 2001) but PHD activity of nuclear extracts is higher in human osteosarcoma cells (U2OS) (Berchner-Pfannschmidt et al., 2008).

1.16 Differential regulation of HIFα by the PHDs

The specific hydroxylase activity and contribution by each of the PHDs to the regulation of HIFα has been scrutinised. *In* vitro VHL capture assays, quantifying the amount of VHL interaction with a HIF1α minimal peptide incorporating proline 564, indicated an order of activity of PHD2 = 3 > 1 (Tuckerman et al., 2004). However, a different study demonstrated that PHD2 alone has the highest relative activity, which may be due to the abundance and widespread expression of PHD2, significant because the PHDs are non-equilibrium enzymes (*i.e.* they do not catalyse the reverse reaction) and due to the fact that oxygen K_m for each of the enzymes are equivalent (Appelhoff et al., 2004).

An alternative approach of assessing the individual roles of the three PHDs was performed by the Pouyssegur group in 2003, analysing HIF stabilisation following PHD silencing by short interfering RNAs. This study demonstrated that silencing of PHD2 was sufficient to stabilise HIF1α in normoxia and activate transcription, whilst PHD1 and PHD3 down regulation had no pronounced effect on HIF1α protein levels (Berra et al., 2003). This corroborated *in vitro* findings regarding PHD2 hydroxylase activity, establishing PHD2 as the critical oxygen sensor responsible for the regulation of steady-state HIFα during normoxia. Other reports have suggested that all three PHDs contribute to the regulation of both HIF1α and HIF2α, however there is a significant bias whereby PHD3 regulates HIF2α more substantially than HIF1α (Appelhoff et al., 2004).

In vivo data from $PHD^{-/-}$ mice substantiates the finding that PHD2 is the most critical of the prolyl hydroxylases. Takeda et al demonstrated that $PHD2^{-/-}$ mice are embryonically lethal due to heart and placental defects during development, whilst PHD1 and PHD3 null mice are viable and appear normal (Takeda et al., 2006). Moreover, more recent investigations show that conditional somatic inactivation of PHD2 in mice induces activation of a subset of HIF target genes including erythropoietin which manifested in

polycythemia (Takeda et al., 2008; Minamishima et al., 2008). Although, individual PHD1 and PHD3 null mice do not appear to develop any apparent abnormalities, double knock out mice ($PHD1^{-/-}$;$PHD3^{-/-}$) also manifest polycythemia. However, strikingly the polycythemic phenotype observed from the double knock out mice appears to arise in a different manner from the PHD2 null mice, *via* HIF2α activation and erythropoietin expression from the liver rather than from the kidney (Takeda et al., 2008). Recent metabolic analysis of $PHD1^{-/-}$ mice indicates reduced exercise tolerance and altered skeletal muscle metabolism arising from reduced glucose oxidation and enhanced glycolysis, which appears to be predominantly mediated by HIF2α activation (Aragones et al., 2008). Furthermore, examination of $PHD3^{-/-}$ mice imply a specific role for PHD3 in neuronal apoptosis, whereby PHD3 loss reduces apoptosis in the superior cervical ganglion indicating the requirement of functional PHD3 for the correct anatomical and physiological integrity of the sympathoadrenal system (Bishop et al., 2008).

1.17 Proline substrate specificity of the PHDs

An additional level of HIF regulation is exhibited by the PHDs who appear to demonstrate different substrate specificities for hydroxylation of the N-terminal and C-terminal proline residues within the ODD (proline 402 within the N-terminal ODD [NODD] and proline 564 within the C-terminal ODD [CODD] of HIF1α, Figure 1.8.2). Although only the hydroxylation of one of the proline residues is deemed to be sufficient for VHL binding and ubiquitylation, the presence of two proline substrate sites suggests a mechanism of differential regulation (Masson et al., 2001). PHD3 does not interact with or hydroxylate the NODD (Landazuri et al., 2006; Hirsila et al., 2003) whilst PHD1 displays less activity towards the NODD than the CODD relative to PHD2 (Hirsila et al., 2003). These differences may be accountable by non-conserved structures which may determine substrate specificity. As the catalytic domains are highly conserved (>80%) it is hypothesised that specificity is regulated by the binding affinity rather than the catalytic activity.

One plausible mechanism for distinguishing substrate preference may be due to a poorly conserved finger-like loop between β-strands 2 and 3, near the active site of the PHDs, distal to the iron centre (McDonough et al., 2006). Furthermore, swapping of this motif from PHD3 to PHD2 confers almost complete substrate specificity for the CODD (Flashman et al., 2008). An additional sequence, distinct from the catalytic site in the N-terminus of PHD2 (amino acids 236-252) has also been proposed as a poorly conserved region capable of determining substrate specificity (Villar et al., 2007). The physiological consequence of hydroxylase specificity has not been fully elucidated. However, one theory demonstrates that specificity for NODD or CODD is dependent on oxygen levels. In normoxia, the CODD appears to be more preferentially hydroxylated than the NODD and for efficient NODD hydroxylation, prior hydroxylation of the CODD is necessary (Chan et al., 2005). Furthermore, NODD hydroxylation appears more sensitive to oxygen than CODD hydroxylation under hypoxic conditions. These findings may represent a sensitive mechanism which closely controls HIFα stability in response to different levels of oxygenation.

1.18 Regulation of prolyl hydroxylase activity

As the PHDs execute such a finely tuned regulatory mechanism it is conceivable that they are subject to control by a number of interrelating factors in addition to O_2 tension, which regulate at the level of expression, stability and modulate their hydroxylase activity.

1.18.1 PHD stability

It has been demonstrated that the stability of the PHD proteins may be underpinned by the Siah (mammalian homologs of *Drosophila* Seven in Absentia) family of RING E3 ubiquitin ligases. PHD1, PHD3 and recently FIH have been revealed as substrates of Siah2 and Siah1a and were found to be targeted for proteasome-mediated degradation, which in turn determines HIF1α stability in hypoxia (Nakayama et al., 2004; Fukuba et al., 2008;

Fukuba et al., 2007). Furthermore, *Siah*$^{-/-}$ cells exhibit lower HIF1α protein levels than wild type cells during hypoxia (Nakayama et al., 2004). RNAi mediated suppression of PHD3 is sufficient to rescue hypoxic induced accumulation of HIF1α in Siah1a/2 double knock out mouse embryonic fibroblasts (Nakayama et al., 2004). Moreover, Siah2 activity appears to be elevated upon exposure to mild hypoxia which insinuates a mechanism whereby Siah regulates PHD1/3 stability within a range of oxygen tensions whereby the PHDs are still active. Interestingly, PHD2 does not appear to be regulated by the Siah E3 ubiquitin ligases, emphasising a structural difference which may account for PHD2's role as the predominant regulator of HIF1α levels in normoxia (Nakayama et al., 2004).

A recent publication demonstrates a mechanism whereby the FK506-binding protein 38 (FKBP38) may regulate PHD2 but not PHD1 or PHD3 stability by interacting with its unique MYND like zinc finger domain. FKBP38 has been revealed to regulate PHD2 stability in an isomerase (PPIase) independent manner, by inducing ubiquitin-independent proteasomal degradation of PHD2 (Barth et al., 2009; Barth et al., 2007).

PHD3 is also believed to be a substrate for the cytosolic chaperone TriC (TCP-1 ring complex). 50-60kDa subunits of the chaperone were co-purified with PHD3 but not PHD1 or PHD2, indicating an additional plausible mechanism regulating PHD3 stability (Masson et al., 2004).

A further level of control of PHD activity was revealed by the Gleadle group in 2006, who demonstrated that PHD1 exists as two species (PHD1p43 and p40), due to an alternative initiation AUG encoding amino acid 34. The shorter isoform PHD1p40 has equivalent catalytic activity but has a rapidly reduced half life of around 50 minutes compared with 100 minutes for the larger isoform. Although both isoforms appear to be regulated by Siah E3 ubiquitin ligases, the shorter PHD1 species demonstrates a preferential association with a stabilised RING finger domain mutant of Siah2, which may account for its reduced stability (Tian et al., 2006).

Interestingly, VHL activity is also subject to tight regulation at the level of protein stability. VHL has been reported to be ubiquitylated by the E2-endemic pemphigues foliaceus (EPF) ubiquitin carrier protein (UCP), resulting in HIF1α stabilisation (Jung et al., 2006). However an E3 ligase has yet to be identified.

1.18.2 Cofactor availability

The HIF hydroxylases have been demonstrated to be inhibited by numerous TCA (tricarboxylic acid) cycle intermediates, including citrate, isocitrate, succinate (Selak et al., 2005), fumarate (Isaacs et al., 2005), malate, oxaloacetate and pyruvate (Dalgard et al., 2004). The most consistent inhibitors of all three PHDs are succinate and pyruvate (Koivunen et al., 2007), which competitively inhibit hydroxylase activity by competing with 2-oxoglutarate as illustrated in figure 1.18 Genetic defects in the TCA cycle, notably defects that impair succinate dehydrogenase (Pollard et al., 2005; MacKenzie et al., 2007) and fumarate hydratase (Isaacs et al., 2005) activity have been demonstrated to elevate normoxic HIFα levels (‘pseudohypoxia’) due to impaired PHD activity, predisposing individuals to development of highly vascularised tumours including parangliomas (rare benign neoplasms of the abdomen, thorax, head and neck regions) and phaeochromocytomas (neuroendocrine tumours of the medulla of the adrenal glands that originate from chromaffin cells) .

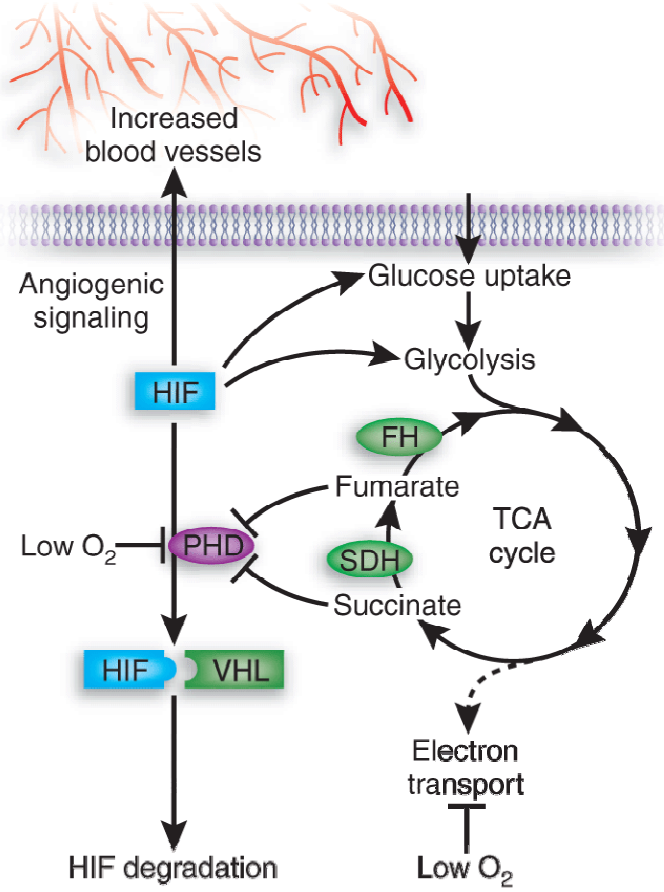

Figure 1.18 *Modulation of HIF signalling via TCA cycle intermediates.*
Loss of function mutations in succinate dehydrogenase and fumarate dehydratase lead to increased levels of the metabolites succinate and fumarate. These metabolites in turn competitively inhibit PHD hydroxylation of HIFα subunits by inhibiting the oxidative decarboxylation of 2-oxoglutarate to succinate. This results in elevated HIF levels and associated changes in gene expression leading to increased angiogenesis, which contributes to tumour development. [Modified from Esteban *et al* (Esteban and Maxwell, 2005)].

1.18.3 Iron and Ascorbate

The requirement for Fe(II) is well demonstrated by the classical characteristics of HIF induction by treatment with iron chelators such as desferrioxamine (DFO) or divalent cations capable of replacing Fe(II) in the active site of the hydroxylase. The HIF hydroxylases can also be stimulated *in vitro* by the addition of Fe(II) and also ascorbate (an ion of vitamin C) (Kivirikko and Myllyharju, 1998). The precise role of ascorbate has yet to be fully elucidated, however, it is hypothesised that it may be involved in the reduction of Fe(III) to Fe(II) increasing the availability for the active site of the hydroxylase. Several lines of evidence also indicate that rapidly growing cancers are often associated with a cellular iron deficiency in the tumour mass (Le and Richardson, 2002). Furthermore, in cultured cells with activated oncogenic pathways, HIFα can accumulate under well oxygenated conditions (Chan et al., 2002). Addition of iron or ascorbate to these cells down regulates HIFα, posing the possibility that iron or ascorbate may be fundamental limiting factors (Knowles et al., 2003). An additional mechanism regulating HIF2α but not HIF1α may also confer iron responsiveness. HIF2α contains an iron response element in its 5'UTR, which has been proposed to restrict its expression during iron deficiency. As erythropoietin production is believed to be predominantly responsive to HIF2α, iron dependent expression is postulated to prevent unproductive erythropoietic drive in the absence of iron for haemoglobin (Sanchez et al., 2007).

1.18.4 Free radicals; Reactive Oxygen Species (ROS) and Nitric Oxide (NO)

Reactive oxygen species include oxygen ions, free radicals and peroxides which are highly reactive ions due to the presence of unpaired valence shell electrons. One reported mechanism of ROS production is within intracellular organelles such as mitochondria, whereby during oxidative phosphorylation along the electron transport chain, oxygen is prematurely reduced to give the superoxide radical $\cdot O^{2-}$, which at physiological pH exists as hydrogen peroxide (H_2O_2). It is increasingly apparent that ROS can affect the rate of HIFα hydroxylation. Addition of exogenous H_2O_2 to cells under normoxic conditions stabilises HIFα protein levels, indicating that ROS inhibit HIFα hydroxylation (Chandel et al., 2000). One hypothesis suggests that ROS reduce the availability of the cofactor Fe(II) required for PHD mediated HIF hydroxylation in cells absent of the transcription factor JunD, shown to protect cells from oxidative stress (Gerald et al., 2004). Furthermore, ROS levels have been demonstrated to increase in hypoxic conditions, thus PHD activity may be subject to regulation by limiting O_2 levels and Fe(II) availability due to the action of ROS (Chandel et al., 1998).

The G-protein-coupled receptor agonist angiotensin II (Ang II) has been shown to link the role of ROS with the requirement for ascorbate, by potently inducing HIF1 in vascular smooth muscle cells. Ang II has been demonstrated to regulate HIF1α stability by the increased generation of H_2O_2 and a subsequent reduction of ascorbate, resulting in a reduction in PHD activity and HIF1α stabilisation (Page et al., 2008).

The free radical nitric oxide (NO) has also been demonstrated to modulate HIFα stabilisation by mitochondrial dependent and independent mechanisms (Mateo et al., 2003). NO is biosynthesised from arginine and oxygen by nitric oxide synthase and acts as an important signalling molecule that performs a variety of biological processes. One mitochondrial independent mechanism of NO mediated HIF stabilisation may be due to S-nitrosation, the post-

translational modification of HIFα cysteine thiol groups by interaction with NO, which has been demonstrated to impair HIFα-VHL binding and ubiquitylation (Metzen et al., 2003b). Alternatively, similarly to the reported effect of ROS, inhibition of the PHD enzymes may arise due to the reactive free radical nature of NO, interacting with and reducing the availability of Fe(II), thus impeding the ability of the PHDs to blunt HIF stabilisation (Gerald et al., 2004). NO has also been demonstrated to promote HIFα degradation, *via* inhibition of cytochrome c-oxidase (complex IV) of the mitochondrial electron transport chain. It is hypothesised that NO mediated inhibition of mitochondrial respiration may redistribute oxygen towards other oxygen-dependent systems, thus reactivating PHD activity (Hagen et al., 2003).

1.18.5 Interacting Proteins

To date the number of reported PHD interacting proteins has been fairly limited, divided into those that appear to regulate PHD stability (as described in section 1.18.1) and those that modulate hydroxylase activity.

OS-9 (amplified in osteosarcoma), is a ubiquitously expressed protein previously implicated in the transport of proteins from the ER to the golgi, which has been reported to promote HIFα hydroxylation. OS-9 is reported to directly bind HIF1α, PHD2 and PHD3, whereby it is hypothesised to augment the interaction between the PHDs and HIF1α within a ternary complex, promoting HIF1α hydroxylation and degradation, thus inhibiting HIF mediated transcription (Baek et al., 2005). However, the finding that OS-9 is found over expressed in osteosarcomas appears contradictory to the role of OS-9 as a negative regulator of HIFα, as it is well documented that HIFα levels increase in the majority of human cancers including osteosarcomas (Yang et al., 2007). Another protein reported to enhance PHD hydroxylase activity is Morg-1 (Mitogen-activated protein kinase organiser 1) *via* interacting with PHD3 (Hopfer et al., 2006). Morg-1 expression represses HIF transcriptional activity and RNA silencing causes de-repression. The precise mechanism of

Morg-1 action is yet to be elucidated, however, it is postulated that Morg-1 acts as a molecular scaffold acting to enhance PHD3 activity. The oncoprotein Mucin 1 (MUC1), found over expressed in most human carcinomas is also reported to regulate PHD3 (Yin et al., 2007). Yin et al have demonstrated that MUC1 acts to block and prevent hypoxia-induced increase in ROS, increase PHD3 expression and potentiate PHD mediated HIF1α suppression. Furthermore, MUC1 expression is reportedly increased by hypoxia in a human lung adenocarcinoma cell line (Mikami et al., 2009). The dichotomy of this oncogene inducing a reduction in HIF activity, still requires elucidation.

The tumour suppressor protein, inhibitor of growth family member 4 (ING4), has been demonstrated to directly interact with PHD2 (Ozer et al., 2005). ING4 has previously been implicated as a repressor of angiogenesis and tumour growth through association with NF-κB (Nuclear factor kappa-light-chain-enhancer of activated B cells). However, ING4 may also inhibit tumour growth by suppressing HIF target gene expression in hypoxia. Interestingly, it is believed that *via* association with PHD2, ING4 is recruited to HIF in hypoxia, to act as an adapter protein to recruit transcriptional repressors, independent of PHD hydroxylase activity (Ozer et al., 2005). There is however, already a precedent for a hydroxylase independent role for PHD2 in regulating HIF transcriptional activity. It has been demonstrated that over expression of a hydroxylase-deficient PHD2 mutant impaired the stimulating effect of hypoxia on the proliferation of cultured endothelial cells, without altering the abundance of HIF1α (Takeda and Fong, 2007). Furthermore, this is corroborated by another study which demonstrated that forced PHD2 expression in a VHL-deficient cell line also reduced HIF transcriptional activity without modulating its stability (To and Huang, 2005). These data introduce a further level of fine tuning in the control of HIF activity.

Only one protein interaction is presently reported to directly attenuate PHD activity. MAGE-11 (Melanoma antigen-11) suppresses PHD2 activity without affecting protein levels, which is accompanied by stabilisation of endogenous HIF1α protein (Aprelikova et al., 2009). Mage-11 is one of a family of twelve

cancer-testis antigens expressed only in the testis and placenta. Due to the restricted expression pattern, MAGE-11 may represent a suitable therapeutic target to down regulate HIF in the future.

1.19 PHD functions independent of HIFα

The role of the HIF hydroxylases, in particular PHD1 and PHD3, in HIF-independent functions is an area under current investigation. PHD3, but not the other PHDs can induce neuronal apoptosis, in sympathetic neuronal precursor cells. PHD3 promotes c-Jun-dependent apoptosis during normal development as nerve growth factor (NGF) becomes limiting (Lee et al., 2005). PHD3 induced apoptosis requires PHD3 catalytic activity and is not recovered by production of stabilised HIF1α or HIF2α, suggesting a non-HIF target. Furthermore, $PHD3^{-/-}$ mice exhibit reduced apoptosis in superior cervical ganglion neurons, whilst the sympathoadrenal system appeared hypofunctional, reducing target tissue innervation (Bishop et al., 2008). This data implicates PHD3 in neuronal cell survival but also the anatomical and physiological integrity of the sympathoadrenal system. Apoptosis induction by PHD3 is not restricted to neuronal cells, as forced PHD3 expression induces aggresome formation and apoptosis induction in normoxia in HeLa cells (Rantanen et al., 2008). Interestingly, this phenotype required PHD3 hydroxylase activity and was only observed in normoxia, suggesting PHD3 acts to regulate protein aggregation in response to oxygen availability.

Additionally, PHD3 has been shown to regulate the stability of activating transcription factor-4 (ATF-4) and myogenin. ATF-4 is induced under anoxia (a total decrease in O_2 levels), mediates the endoplasmic reticulum (ER) stress response and is a critical regulator of cell fate. PHD3 is reported to interact and induce ATF-4 degradation *via* an oxygen dependent degradation domain in a prolyl hydroxylase dependent, but VHL independent mechanism (Koditz et al., 2007). Conversely, PHD3 interacts with and stabilises myogenin, a MyoD family bHLH transcription factor, which plays a role in

skeletal muscle differentiation (Fu et al., 2007). However, VHL association with myogenin has the opposite effect, acting to destabilise myogenin *via* the ubiquitin-proteasomal system. Therefore, it is postulated that the PHD3 interaction may prevent myogenin degradation by inhibiting its association with VHL (Fu et al., 2007).

PHD1 has also been demonstrated to perform non-HIF functions *via* modulation of NF-κB activity. The transcription factor NF-κB is activated by hypoxia, particularly during cancer progression, promoting tumour survival and growth by increasing the expression of genes that inhibit apoptosis and growth arrest. NF-κB is regulated by inhibitors of κB (IκB), a family of proteins containing ankyrin repeat domains (ARD), which act to mask NF-κB NLS, preventing translocation into the nucleus (Yamamoto and Gaynor, 2004). This inhibition is overcome by signal induced degradation of the IκB, mediated by phosphorylation by IκB kinase (IKK). Cummins et al confirmed that hypoxia induces NF-κB by phosphorylation-dependent degradation of IκBα, by increasing the pool and activation of the IKKβ subunit (Cummins et al., 2006). However, IKKβ undergoes negative regulation by PHD1, mediated by a proline residue within a conserved LXXLAP consensus motif for prolyl hydroxylation. PHD1 over expression decreases NF-κB activity, by inhibition of IKKβ and stabilisation of IκB (Cummins et al., 2006). As PHD1 expression is reduced in hypoxia, this is a plausible explanation for the observed increase in hypoxic NF-κB activity. Interestingly, to date no non-HIF substrates have been confirmed to be hydroxylated by either PHD1 or PHD3.

ARD-containing proteins have also been identified as alternative FIH substrates, including several IκB (Cockman et al., 2006) and notch receptor family members (Coleman et al., 2007). As the human proteome contains 200-300 ARD-containing proteins, of which the FIH target asparagine residue forms part of the ankyrin consensus, it is believed that many of these proteins will be hydroxylated (Cockman et al., 2009). The functional significance of ankyrin hydroxylation is currently still unclear. It has been demonstrated that ankyrin hydroxylation may stabilise the ankyrin fold (Kelly et al., 2009; Hardy et al., 2009). Furthermore, measurements indicate that FIH may interact with

ARDs with a higher affinity and have a lower oxygen K_m for hydroxylation than for HIF1α (Wilkins et al., 2009). This suggests a mechanism whereby ARDs may compete with HIF1α for FIH hydroxylation and whereby the cellular pool of ARDs may restrict HIF1α asparaginyl hydroxylation (Zheng et al., 2008).

1.20 PHD/VHL-independent HIF1α degradation mechanisms

Novel mechanisms of HIF1α stabilisation and/or degradation, which act in an alternative fashion to the well characterised targeting of HIF1α for proteasomal degradation by hydroxylation and ubiquitylation, are rapidly emerging [Figure 1.20 and for review (Yee et al., 2008)]. These mechanisms occur *via* novel HIF1α interacting proteins and/or post-translational modifications which act as stimuli for HIF1α stabilisation or degradation.

Numerous post-translational modifications have been reported to promote HIF1α degradation, including phosphorylation, sumoylation and acetylation. HIF1α lysine 532 acetylation by arrest-defective-1 (ARD1) *N*-acetyltransferase, has been reported to facilitate recognition by VHL (Jeong et al., 2002), although there is some disparity in this finding as more recent research have disputed that ARD1 modulates HIF1α stability (Arnesen et al., 2005; Bilton et al., 2005). The ability of VHL to interact with HIF1α is blocked by signal transducer and activator of transcription 3 (STAT3) (Jung et al., 2008) and c-Jun, which interact with HIF1α masking the sites for ubiquitylation and consequently inhibiting degradation (Yu et al., 2009). STAT3 has also been demonstrated to positively modulate HIF activity at the transcriptional level, by interacting with HIF1 at VEGF promoters to enhance expression (Gray et al., 2005). VHL function is further regulated by spermidine/spermidine-N^1-acetyltransferase 2 (SSAT2) demonstrated to stabilise the interaction between VHL and elongin C (Baek et al., 2007a). Another SSAT protein, SSAT1, also promotes HIF1α degradation, but through an entirely different mechanism, in an oxygen-independent fashion.

SSAT1 stabilises the RACK1-HIF1α interaction dependent on SSAT acetyltransferase activity (Baek et al., 2007b). Receptor of activated protein kinase C (RACK1) competes for binding with HIF1α amino terminal PAS-A with the molecular chaperone 90 kDa heat shock protein (HSP90) (Liu et al., 2007). RACK1 recruits elongin C and other components of the VBC complex to HIF1α, leading to ubiquitylation and degradation, stimulated by HSP90 inhibition, in a manner similar to but independent of VHL (Liu et al., 2007). RACK1 mediated HIF1α degradation is prevented by the septin family member GTP-binding cytoskeletal protein, SEPT9_v1, which has been reported to blockade the RACK1-HIF1α interaction (Amir et al., 2009). Furthermore, Kruppel-like factor 2 (KLF2), a protein found to potently inhibit angiogenesis, was identified to disrupt HIF1α interaction with HSP90, resulting in HIF1α depletion by allowing RACK1 facilitated degradation or by impairing HIF1α folding and maturation (Kawanami et al., 2009).

Phosphorylation as a stimulus for HIF1α degradation has also been reported, however, its role in HIF regulation remains controversial. Over expression of glycogen synthase kinase 3 (GSK3), inactivated by the upstream Phosphoinositide 3-kinase (PI3K) signalling cascade, results in PHD- and VHL-independent HIF1α ubiquitylation and proteasomal degradation *via* GSK3 mediated HIF1α phosphorylation (Flugel et al., 2007). Conversely, sphingosine kinase 1 (Sphk1), an oncogenic lipid kinase which has been shown to be stimulated in hypoxia and mediated by the Akt/GSK3 signalling pathway, acts to prevent VHL-dependent HIF1α degradation (Ader et al., 2008). Candidate E3-ubiquitin ligases for the VHL-independent HIF1α degradation, such as that promoted by phosphorylation, have been described. Non-VHL VBC complex E3 ubiquitin-ligases reported to regulate HIF1α include human double minute 2 (Hdm2) which induces p53 degradation (Ravi et al., 2000) and hypoxia-associated factor (HAF) which ubiquitylates HIF1α but not HIF2α, promoting proteasomal degradation, independent of oxygen tension (Koh et al., 2008). Regulation of ubiquitylation of HIF1α is also achieved by de-ubiquitylation by the VHL interacting de-ubiquitylating enzyme (VDU2), which acts in a VHL-dependent manner to salvage ubiquitylated HIF1α from degradation (Li et al., 2005). Interestingly,

VDU2 can be ubiquitylated by VHL and degraded itself (Li et al., 2002b). Furthermore, VDU2 interacts with VHL *via* the same region as HIF1α, of which commonly harbours mutations in VHL disease patients (Li et al., 2002a). However, the precise interplay between VHL, VDU2 and HIF1α in cancer development remains to be determined.

Interestingly, human renal HK-2 cells treated with 15-deoxy-delta(12,14)-prostaglandin-J(2), accumulate HIF1α in lysosomes, demonstrating the possibility of a novel proteasome-independent lysosomal-mediated degradation mechanism (Olmos et al., 2009).

One notable modification is the addition of a ubiquitin-like protein, the small ubiquitin-related modifier-1 (SUMO-1). Human SUMO-1 is a 101 amino acid polypeptide which shares 18% sequence homology with ubiquitin (Muller et al., 2001). The involvement of sumoylation in HIF regulation was first identified in 2004 when Shao et al observed an increase in SUMO-1 mRNA and protein levels in response to hypoxia and further demonstrated that following exposure to hypoxia SUMO-1 interacted with HIF1α in heart and brain tissue (Shao et al., 2004). However, whether HIF sumoylation promotes its stabilisation or degradation remains unclear. Bae et al demonstrated that the interaction between SUMO-1 and HIF1α was as a result of the covalent attachment of SUMO-1 (sumoylation) within the ODD at residues Lys^{391} and Lys^{477}. Furthermore, Bae et al showed that ectopic SUMO-1 expression stabilises HIF1α protein, the converse effect to ODD ubiquitylation (Bae et al., 2004). Identification of the RWD-containing sumoylation enhancer (RSUME) further implies a role of sumoylation in HIF1α stabilisation (Carbia-Nagashima et al., 2007). RSUME interacts with the SUMO E2 conjugating enzyme Ubc9, increasing the non-covalent interaction of SUMO-1 to Ubc9, inducing SUMO-1 polymerisation and activation for conjugation to substrate lysine side chains. siRNA mediated knock down of endogenous RSUME diminished HIF1α sumoylation and resulted in the inhibition of endogenous HIF1α stabilisation in hypoxia.

In contrast to previous research, Berta et al and Cheng et al proposed the role of sumoylation as a negative regulator of HIF function in 2007. Berta et al confirmed that HIF1α lysine residues 391 and 477 within the ODD are subject to sumoylation. By implementing siRNA targeted to endogenous HIF1α and re-introducing an siRNA resistant HIF1α construct with mutated lysine 391 and 477, Berta et al demonstrated that SUMO-deficient HIF1α has an identical half life to the wild type form, contradicting previous studies (Berta et al., 2007). However, they elucidate that the consequence of sumoylation is a reduction of HIF transcriptional activity, as a 1.4-1.7 fold increase was observed by the SUMO-deficient HIF1α construct.

More recent evidence corroborates findings that sumoylation plays a role in promoting HIF1α degradation. Hypoxia inducible sumoylation of HIF1α, can promote hydroxyproline-independent binding of the VHL VBC complex to HIF1α *via* sumoylation of lysine 391 and 477, leading to VHL mediated ubiquitylation and degradation by the proteasome (Cheng et al., 2007). Similarly to regulation of de-ubiquitylation enzymes, acting to salvage HIF1α from degradation, a nuclear SUMO protease SUMO1/sentrin specific peptidase 1 (SENP1) has been demonstrated to de-conjugate sumoylated HIF1α, enabling its escape from degradation. The physiological role of SENP1 in HIF regulation is substantiated by the finding that $SENP1^{-/-}$ mice embryos exhibit fetal anaemia, due to deficient erythropoietin production (Cheng et al., 2007) This PHD-independent VHL-dependent mechanism is a plausible mechanism to explain the finding of Andre et al, who demonstrated that HIF1α was sensitive to proline 402 and 564 independent degradation and notably a proline double mutant construct was only stabilised within short periods of hypoxic exposure (1-2 hours) (Andre and Pereira, 2008).

These novel mechanisms of regulation may be required in order to cope with the physiological complexity of hypoxia. Alternatively, these mechanisms may provide a system which enables the control of HIF activity not only by O_2 tension but from other cellular stimuli which may necessitate the activity of HIF in promoting cell survival and proliferation.

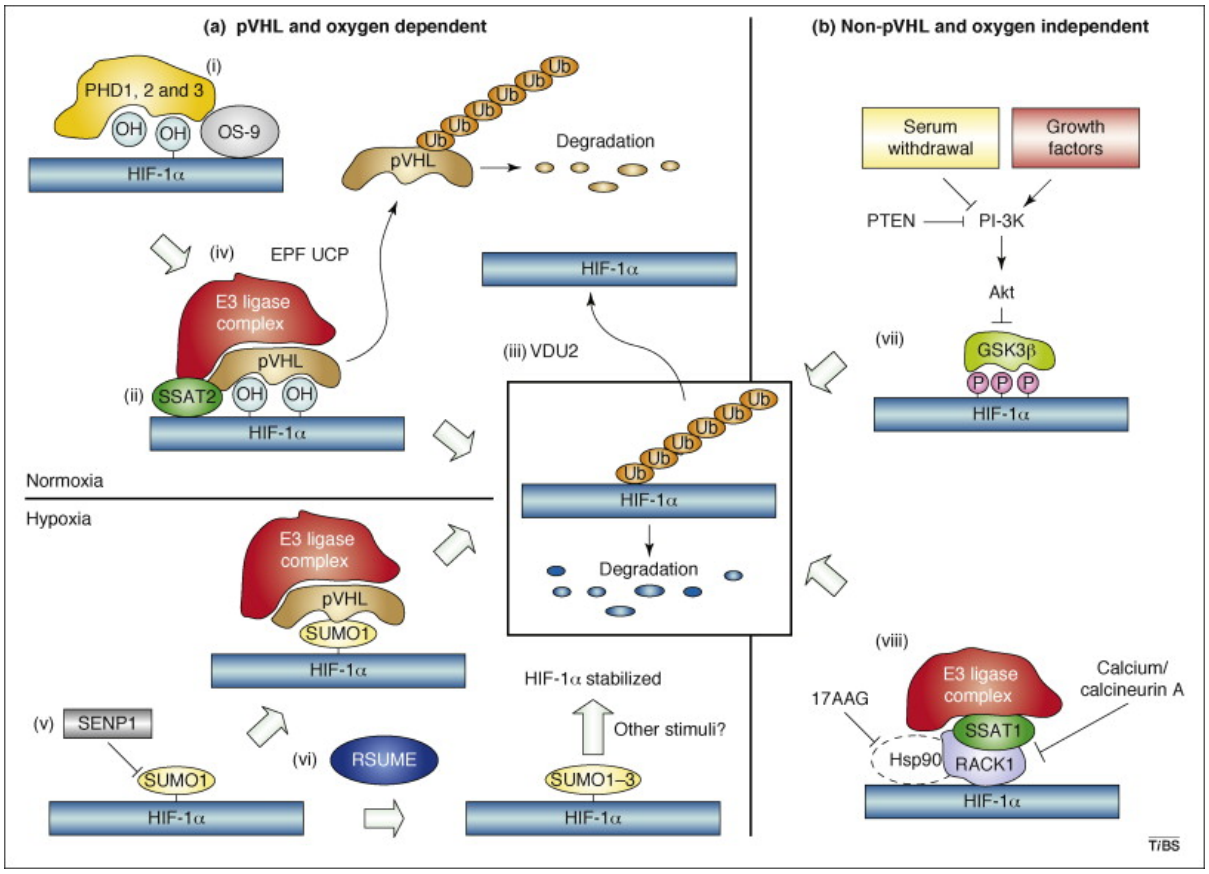

Figure 1.20 *Diverse pathways involved in the regulation of HIFα stability.*
HIF1α is subject to both VHL and O_2 dependent **(a)** and independent **(b)** degradation mechanisms. **(a)** The well characterised normoxic hydroxylation and ubiquitylation of HIF1α by the PHDs and VHL is facilitated by binding of OS-9 **(i)** which scaffolds PHD2 and 3 with HIF1α, whilst SSAT2 stabilises VHL and elongin C interaction **(ii)**. Ubiquitylated-HIF1α can be salvaged from degradation by de-ubiquitylation by VDU2 **(iii)**. Furthermore, VHL is regulated by EPF UCP E2 ubiquitylating enzyme which targets VHL for degradation **(iv)**. In hypoxia, HIF1α can be sumoylated targeting it for VHL mediated degradation. This can be reversed by SENP1 de-sumoylation leading to HIF1α destabilisation **(v)**. Conversely, RSUME has been reported to stabilise HIF1α by sumoylation **(vi)**. **(b)** O_2 and VHL independent mechanisms include GSK3 phosphorylation, regulated by the PI3K pathway **(vii)** and RACK1 recruitment of the E3 ligase complex **(viii)** which can be promoted by Hsp90 inhibition or inhibited by calcineurin A which prevents RACK1 dimerisation. [Adapted from (Yee et al., 2008)]

1.21 HIFs, hypoxia and cancer

Solid tumours often contain hypoxic regions either due to their chaotic architecture of blood vessels and altered tumour blood rheology, from their increased metabolic activity and/or from expansion from their existing blood supply. Subsequently, from analysis of human cancer biopsy samples and experimental animal models it is increasingly clear that both HIF1α and HIF2α are commonly increased in a variety of tumours and thus play a crucial role in cancer progression. This section describes specific pathways that contribute to aberrant HIF signalling, HIF induced pro-tumourigenic processes and the therapeutic implications [for review (Kaelin, Jr. and Ratcliffe, 2008; Bertout et al., 2008; Rankin and Giaccia, 2008; Pouyssegur et al., 2006)].

1.21.1 HIF overexpresson in cancer

HIFα is found over expressed in a broad range of human malignancies and is associated with poor patient survival. HIF1α accumulation has been associated with a range of tumours including cervical, breast, ovarian, endometrial, pancreatic, bladder, head and neck, colorectal and osteosarcomas (Talks et al., 2000). HIF2α expression correlates with poor patient prognosis in NSCLC, hepatocellular, melanoma and neuroblastomas (Talks et al., 2000). Interestingly, HIF1α expression gradually decreases in patients with VHL disease such as renal cell carcinomas (RCC), whereas HIF2α levels increase (Raval et al., 2005; Sowter et al., 2003). In fact, the effect of HIF1α on RCC tumour xenografts was shown to retard cancer growth suggesting that the effect of HIF is dependent on the tumour type and context (Raval et al., 2005). However, collectively these findings highlight that HIF activation and accumulation is a common event in cancer, either as a marker or a cause of malignant cell behaviour.

1.21.2 HIF activation in cancer

HIF can be activated in tumours in normoxic conditions by genetic alterations in the oxygen-signalling pathway and/or cellular signal transduction pathways involving the mammalian target of rapamycin (mTOR) and PI3K. The most prevalent genetic alterations in the oxygen signalling pathway are *VHL* germ-line mutations, which manifest in VHL disease, whereby VHL inactivation results in normoxic HIF stabilisation and constitutive hypoxic gene expression (Maxwell et al., 1999). This predisposes patients to the development of highly vascularised tumours, as a result of HIF induced VEGF expression, including hemangioblastomas, renal cell carcinomas and pheochromocytomas (Gnarra et al., 1994; Sprenger et al., 2001).

mTOR is a serine/threonine kinase which orchestrates protein synthesis, promoting protein translation by phosphorylation of a series of substrates involved in protein translation including eukaryotic initiation factor 4E-binding protein-1 (4EBP1) (Guertin and Sabatini, 2005). Cancer associated inactivating mutations in mTOR negative regulators including *PTEN* (phosphatase and tensin homologue), which regulates upstream PI3K activity, and *TSC2* (tumour suppressor complex), lead to activation of GTP-Rheb which in turn activates mTOR, promoting HIF1α transcription and translation (Brugarolas et al., 2004). Other cellular oncogenes have also been reported to induce HIF accumulation by stabilising HIF1α in normoxic conditions. Transfection of RasV12, v-Src and Akt rapidly augment HIFs transactivation ability of a HRE-luciferase reporter (Chan et al., 2002). Levels of non-hydroxylated HIF1α are detected suggesting that activated oncogenes inhibit proline hydroxylation. Ras activation increases intracellular ROS production, which is reported to inhibit prolyl hydroxylase activity (as described in section 1.18.4) and therefore this may account for increased HIF activity (Gerald et al., 2004). This indicates a direct link between oncogenic activity, HIF1α and tumour progression in normoxia.

1.21.3 HIF functions in cancer

HIF promotes a number of alterations in cell physiology that contribute to the hallmarks of cancer; increasing proliferation, angiogenesis, invasion and metastasis (Hanahan and Weinberg, 2000).

1.21.3.1 Angiogenesis

Angiogenesis, the formation of new blood vessels upon a point whereby the tissues demand for oxygen and nutrients exceeds the ability of the existing vasculature and neovascularisation, the formation of functional microvascular networks with red blood cell perfusion are critical in tumour formation (Carmeliet and Jain, 2000). In many solid tumours, rapid cellular expansion distances cells from the existing vasculature, resulting in reduced oxygen and nutrient supply to tumour cells more than 100μm away from a blood vessel, a phenomena initially observed by Thomlinson and Gray in 1955. Consequently hypoxia induced accumulation of HIFα leads to expression of a range of hypoxia inducible genes which enable tumour cells to promote angiogenesis.

Two key angiogenic factors which may be up-regulated by HIFs are the receptor ligands vascular endothelial growth factor (VEGF-A) (Ferrara et al., 2003) and the endothelial specific angiopoietin 2 (Ang-2) (Maisonpierre et al., 1997). VEGF-A contains a functional HRE and is induced and secreted in hypoxia, guiding sprouting neo-blood vessels into oxygen depleted regions of the tumour mass *via* a graded VEGF-A distribution (Hellstrom et al., 2007). VEGF-A expression is coupled with Ang-2 expression, which permits blood vessel remodelling by inhibition of the closely related Angiopoietin 1. Angiopoietin 1 induces blood capillary maturation, *via* activation of the NOTCH pathway, rendering the vessels quiescent and unable to respond to VEGF-A. Angiopoietin 2 acts as an Angiopoietin 1 antagonist, preventing the ligand binding to its receptor thus preventing the concomitant maturation of blood vessels (Yancopoulos et al., 2000). Although Ang-2 is hypoxia

inducible it is uncertain whether it contains a functional HRE. However, it is possible that Ang-2 contains either an un-identified HRE or may be indirectly induced by transcription factors which themselves are HIF induced (Fong, 2009).

Recent research has analysed the role of the PHDs in angiogenesis. Inactivation of PHD2 stimulates angiogenesis (Milkiewicz et al., 2004; Takeda et al., 2007); however, recent data also implicates PHD2 in morphogenesis of blood vessel endothelial cell (EC) lining. Morphogenesis of EC lining is often aberrant ('non-productive angiogenesis') in tumours as a result of excessive release of hypoxia induced angiogenic cytokines, resulting in malshaped endothelial lining of tumour blood vessels which limits oxygen supply (Jain, 2005). Reduced oxygen supply has implications in the ability of radio therapeutic and chemotherapeutic approaches to treat cancer. These areas of lowered oxygenation convey reduced sensitivity to both radiation therapy which requires O_2 to form cytotoxic DNA breaks and chemotherapy which insists on proliferating cells for cytotoxicity (Graeber et al., 1996). Therefore, hypoxia augments malignant progression whilst reducing responsiveness to therapeutic measures. Interestingly, implanting tumours in haplodeficient $PHD2^{+/-}$ mice normalised the endothelial lining and promoted vessel maturation (Mazzone et al., 2009). This vessel normalisation tightened the endothelial barrier improving tumour oxygenation resulting in down regulation of hypoxia induced metastatic genes suppressing tumour invasion (Mazzone et al., 2009). Therefore, rather than increasing HIF induced pro-tumourigenic gene expression, the predominant result of decreased PHD activity in hypoxic conditions appears to aid tumour suppression, thus providing alternative therapeutic opportunities.

1.21.3.2 Metastasis

Metastasis, the process by which cancer spreads from the place at which it first arose as a primary tumour to distant locations in the body, is a critical step in tumour pathogenesis, involving tumour cell invasion, intravasation,

extravasation and proliferation. HIF activation can promote tumour metastasis through the regulation of key factors including E-cadherin and lysyl oxidase (LOX). E-cadherin, is a cellular adhesion molecule that represses cell growth *via* interactions with β-catenin. VHL inactivation in renal cell carcinomas and the subsequent HIF activation has been demonstrated to repress E-cadherin by up-regulating E-cadherin specific repressors Snail and Smad interacting protein 1 (SIP1) (Evans et al., 2007). HIF has also been shown to directly increase LOX expression, an amine oxidase, responsible for invasive properties of hypoxic tumour cells *via* focal adhesion kinase activity and cell to matrix adhesion (Erler et al., 2006). To this effect LOX inhibition results in elimination of metastasis in mice with orthotopically grown breast cancer tumours.

1.21.3.3 Metabolism and Proliferation

Observations of a metabolic shift from oxidative to glycolytic pathways in tumour cells ('Warburg effect') date back to over 70 years ago and it is well established that HIF directly promotes glycolytic metabolism by inducing expression of genes including glucose transporters and glycolytic enzymes (Semenza, 2007). However, HIF1 is also reported to promote glycolysis by negatively regulating mitochondrial biogenesis and mitochondrial oxygen consumption, demonstrated in VHL deficient RCC cells. This is mediated by inhibition of the transcription factor c-Myc *via* two mechanisms, by HIF1 induced transcriptional activation of the c-Myc inhibitor MXI-1 and by promoting c-Myc proteasomal degradation (Zhang et al., 2007). However, c-Myc activity is predominantly responsible for inducing the expression of genes involved in the pro-tumourigenic promotion of cell cycle proliferation, for example activating the expression of the cyclin proteins (Arabi et al., 2005). Fascinatingly, HIF2 unlike HIF1 promotes c-Myc activation of cyclin D2 and repression of cyclin kinase inhibitor p27 in RCC cells, augmenting proliferation (Gordan et al., 2007). The mechanism by which HIF1 and HIF2 discriminate between c-Myc repression and activation respectively, remains unclear, but contributes to increased cancer metabolism and proliferation.

1.21.3.4 Therapeutic Implications

These observations suggest that drugs that inhibit HIF or its critical downstream target genes may be advantageous in treating cancers. Numerous drugs targeting HIF have been reported including mTOR, HSP90 and HDAC inhibitors (Kaelin, Jr., 2007). As previously mentioned (section 1.18.3) ascorbate administration in culture can enhance PHD activity to down regulate HIFα in tumour cells which could be exploited therapeutically (Knowles et al., 2003). However to date, inhibiting transcription factor function with drugs has been difficult. Drugs that inhibit HIF target gene VEGF or its receptor (sorafenib and sunitinib), have been approved which demonstrate activity in patients with advanced kidney cancer.

Alternatively, patients with anaemic and ischemic diseases, which result from inadequate tissue oxygenation, may benefit from stabilisation of HIFα to promote oxygen delivery. Numerous PHD inhibitors have been developed which act to stabilise HIFα, many of which are in clinical trials for treatment of ischemic diseases. However, whether chronic PHD inhibition for the treatment of ischemic diseases would promote tumour growth from stabilised HIFα is unknown. Initial tests from patients with familial erythrocytosis caused by a hypomorphic *PHD2* mutation, indicate that this is not the case, as the level of HIF activity required for tumourigenesis exceed that required to promote processes such as erythropoiesis in anaemic/ischemic disorders (Percy et al., 2006). Treating such diseases without promoting tumour growth by inhibiting PHD activity will require careful strategic planning.

1.22 Aims and Objectives

Recent data has indicated that LIMD1 is a novel tumour suppressor, which suppresses growth by co-repressing transcription of the E2F family of transcription factors with pRB. However, it has been demonstrated that deletion of the pRB binding interface within LIMD1 and expression of LIMD1 in a $pRB^{-/-}$ cell line did not completely attenuate LIMD1 mediated tumour suppressive activity. Therefore, this led to the hypothesis that LIMD1 may perform multiple tumour suppressive functions. A Y2H screen of a HeLa cDNA library indicated that LIMD1 amino acids 1-363 interacted with PHD1, one of three critical oxygen sensing prolyl hydroxylases, responsible for the oxygen dependent targeting of HIFα for proteasomal degradation. HIF and its regulatory proteins have emerged as major therapeutic targets as HIF is responsible for the transcription of over 100 HRE containing genes, of which many of these gene products promote pro-tumourigenic events, including angiogenesis and metastasis. Therefore, at the start of this project, in keeping with the previously established tumour suppressive function of LIMD1 as a transcriptional repressor, it was hypothesised that LIMD1 may negatively regulate HIF activated transcription, by enhancing the activity of the PHDs. As LIMD1 and its family members Ajuba and WTIP share a high degree of structural and functional homology, it was investigated whether these LAW proteins represent a new family of hypoxic modulators, adding a further additional level of control to HIF regulation.

Specifically, whether the observed interaction between LIMD1 and PHD1, identified from the Y2H screen, represented a conserved interaction between both LIMD1 family members (LAW) and all three PHD isoforms *in vitro* and *in vivo* was examined. As LIMD1 contains no intrinsic enzymatic activity and LIM proteins have been reported to often function as adaptor proteins, whether LIMD1 may regulate HIF in a similar way by scaffolding PHD activity with other components involved in promoting HIFα degradation was also investigated. To confirm that LIMD1 may promote HIFα degradation, the effect of LIMD1 ectopic expression on the stability of the ODD domain of HIF1α was analysed and whether this also led to repression of HIF driven

transcription using a HRE-luciferase reporter system was also examined. Additionally, it was addressed whether effects observed by ectopic LIMD1 expression also translated to the same function as endogenous LIMD1. Therefore, the effects of LIMD1 depletion by RNAi and in *Limd1*$^{-/-}$ derived mouse embryonic fibroblasts (MEFs), on HIFα protein levels, HIF transcriptional activity and the effects on downstream HIF gene expression were also examined.

CHAPTER 2: MATERIALS AND METHODS

2. Materials and Methods

2.1 Media and Antibiotics

2.1.1 Media

2.1.1.1 Bacterial Growth Media

Luria Broth (LB): 2.5% (w/v) LB was dissolved in distilled water and autoclaved for 20 minutes at 121°c. After cooling, the appropriate dilution of antibiotic was added. (L3522-1KG, Sigma-Aldrich, Saint Louis, USA)

LB-Agar: 3.5% (w/v) LB-Agar was dissolved in distilled water and autoclaved. After cooling, the appropriate dilution of antibiotic was added and the media was then poured into sterile plates. Plates were left to set at room temperature and then stored at 4°c for use within 4 weeks. (L2897-1KG, Sigma-Aldrich, Saint Louis, USA)

2.1.1.2 Cell Culture Media

Dulbecco's Modified Eagle's Medium (DMEM): 4500mg/Lglucose, 2mM L-glutamine and 100mg/L sodium pyruvate. DMEM was supplemented with 10% (v/v) Foetal calf serum (FCS) and 1% (v/v) penicillin/streptomycin. Media was stored at 4˚c. (D6429, Sigma-Aldrich, Saint Louis, USA)

Opti-MEM®: Opti-MEM® media was aliquoted and stored at 4°c. (31985, GIBCO, N.Y. USA)

1x Trypsin/EDTA Solution: 0.5g/100ml porcine trypsin, 0.2g/100ml EDTA, 4Na per litre of Hanks' Balanced Salt Solution (HBSS) and phenol red. Trypsin/EDTA was kept at -30°c for long term storage and stored at 4˚c whilst in use. Trypsin/EDTA was warmed to 37°c in a water bath prior to use. (T3924, Sigma-Aldrich, Saint Louis, USA)

Fetal Bovine Serum (FBS): FBS was divided into 50ml aliquots and stored at -20˚C. Prior to use FBS was thawed at 37°c and then added to cell growth medium [10% (v/v) FBS/Medium] within a cell culture fume hood. (F9665, Sigma-Aldrich, Saint Louis, USA)

2.1.2 Antibiotics

Ampicillin: Ampicillin stock solutions were prepared by dissolving ampicillin sodium salt in distilled water to a concentration of 100mg/ml. The solution was then filter sterilised using a disposable 0.2µm filter and stored at -20°c. Ampicillin was typically used at a working concentration of 100µg/ml. (A2804-50mg, Sigma-Aldrich, Saint Louis, USA)

Kanamycin: Kanamycin stock solutions were prepared by dissolving Kanamycin monosulphate in distilled water to a concentration of 30mg/ml. The solution was then filter sterilised using a disposable 0.2µm filter and stored at -20°c. Kanamycin was typically used at a working concentration of 30µg/ml. Kanamycin is light sensitive and therefore was stored and utilised in a lightproof environment. (K1637-1G, Sigma-Aldrich, Saint Louis, USA)

Puromycin: Puromycin stock solution of 100mg/ml concentration was stored at -20˚C. Puromycin was used at a final concentration of 3µg/ml. (ant-pr-1, InvivoGen, California, USA)

G418/Geneticin: G418 stock solution of 50mg/ml in PBS was prepared in sterile cell culture conditions and was stored at -20˚C. Puromycin was used at a final concentration of 500µg/ml. (G0175, Melford, Suffolk, UK)

Penicillin/Streptomycin: Containing 10,000 units of Penicillin and 10mg/ml Streptomycin in 0.9% NaCl. Penicillin/Streptomycin solution was kept at -30°c for long term storage and stored at 4˚c whilst in use. Penicillin/Streptomycin was routinely used at 1% (v/v) in growth medium (P0781, Sigma-Aldrich, Saint Louis, USA)

2.2 Buffers and Solutions

2.2.1 Bacteriological Buffers and Solutions

Transformation Buffer (TB): 55mM $MnCl_2$, 15mM $CaCl_2$, 250mM KCl and 10mM PIPES pH 6.7 were mixed with HPLC water. The solution was then filter sterilised using a disposable 0.2µm filter and stored at -20°c.

2.2.2 DNA Buffers

1 x Tris-Acetate EDTA (TAE): 40mM Tris-acetate and 2mm EDTA pH 8.0 were dissolved in distilled water and stored at room temperature.

10 x Agarose Gel Sample Buffer: 0.25% (w/v) Bromophenol Blue and 30% (v/v) glycerol were dissolved in distilled water and stored at room temperature.

2.2.3 Cell Lysis Buffers

RIPA: 150mM NaCl, 1%(v/v) IGEPAL-630, 0.5% (w/v) sodium deoxycholate, 0.1% (w/v) SDS and 50mM Tris pH 8, were dissolved in distilled water and stored at 4°c for use within 4 weeks.

Low Salt: 1%(v/v) IGEPAL-630 and 50mM Tris pH 8 were dissolved in distilled water and stored at 4°c for use within 4 weeks.

Nonidet P-40 (NP40/IGEPAL-630): 150mM NaCl, 1%(v/v) IGEPAL-630 and 50mM Tris pH 8, were dissolved in distilled water and stored at 4°c for use within 4 weeks.

High Salt: 500mM NaCl, 1% (v/v) IGEPAL-630 and 50mM Tris pH8, were dissolved in distilled water and stored at 4°c for use within 4 weeks.

Protease Inhibitors: One Complete™ Protease Inhibitor or Complete™ EDTA free Protease Inhibitor Cocktail tablet (Roche, Mannheim, Germany) was dissolved in either 25ml or 50ml of lysis buffer depending on the desired degree of protease inhibition required. Solutions were stored at 4°c for 2 weeks.

Phosphatase Inhibitors: One PhosSTOP™ Phosphatase Inhibitor Cocktail tablet (Roche, Mannheim, Germany) was added to 10ml of lysis buffer and stored at 4°c for 2 weeks.

MG-132 Proteasome Inhibitor: MG-132 [Z-Leu-Leu-Leu-CHO] (PI102-0005, Biomol International, Enzo Life Sciences Ltd, UK). MG-132 is a potent, cell permeable inhibitor of the proteasome. MG-132 stock solution was prepared by dissolving in sterile DMSO (Dimethyl Sulfoxide, D2438, Sigma-Aldrich) in a tissue culture hood to a final concentration of 10mM. The stock solution was stored at -80°c and used within 2 months at a working concentration between 10-50μM.

2.2.4 Solutions for Sodium Dodecyl Sulphate-Polyacrylamide Gel Electrophoresis (SDS-PAGE) and Immunoblotting

5 x SDS-PAGE Sample buffer: 250mM Tris-HCl pH 6.8, 50% (v/v) Glycerol, 5%(w/v) SDS, 0.05%(w/v) Bromophenol Blue and 5%(v/v) β-Mercaptoethanol were dissolved in distilled water in a fume hood. The solution was aliquoted and stored at -30°c.

Phosphate Buffer Saline (PBS): Premixed 10x PBS (11666789001, Roche Diagnostics GmbH, Mannheim, Germany, [2.5mM KH_2PO_4, 25mM Na_2HPO_4, 0.34 M NaCl, 6.75mM KCl, pH 7.4]) was diluted 10 fold in distilled water and stored at room temperature.

PBS-Tween: 0.05%(v/v) Tween®20 (P2287-500ml, Sigma-Aldrich, Saint Louis, USA) was mixed in 1 x PBS and stored at room temperature.

Resolving Gel Buffer: A typical 10% acrylamide gel comprised 1.9ml of H2O, 1.7ml of 30% (w/v) Acrylamide solution (37.5:1 Acrylamide:Bis-acrylamide, Severn Biotech Ltd, UK), 1.3ml of 1.5M Tris pH8.8 and 50µl of 10% (w/v) SDS. To polymerise the acrylamide, 50µl of 10% (w/v) Ammonium Persulphate Solution (APS) and 2µl of N,N,N',N'-tetramethylethylenediamine (TEMED) were added immediately before pouring.

Stacking Gel Buffer: 5% acrylamide stacking gel solution contained 1.4ml of H2O, 330µl of 30% acrylamide solution, 250µl of 1.0M Tris pH 6.8 and 20µl of 10%(w/v) SDS per gel and was polymerised by the addition of 20µl of 10% (w/v) APS and 2µl of TEMED.

SDS-PAGE Running Buffer: 250mM Tris, 2M Glycine and 10% (w/v) SDS were dissolved in distilled water. The solution was stored at room temperature and used within 8 weeks.

Transfer Buffer: 10x Tris-Glycine transfer buffer solution (250mM Tris-HCl pH 7.5, 2M glycine, [93015, Fluka, Sigma-Aldrich, UK]) was diluted 10 fold in distilled water and 10% (v/v) methanol was added. The buffer was stored at 4°c.

Blocking Solution: 5%(w/v) Marvel dried skimmed milk powder was dissolved in 1 x PBS-Tween [0.05% (v/v) Tween 20]. Blocking solution was stored at 4°c overnight and made fresh for each experiment.

Coomassie Blue Protein Stain: 0.12% [w/v] Coomassie Brilliant Blue R was dissolved into a 50% [v/v] Methanol, 20% [v/v] Glacial Acetic Acid solution. The solution was then filtered through filter paper and then stored at room temperature.

Coomassie Blue De-staining solution: 10% (v/v) Methanol and 10% (v/v) Glacial Acetic Acid were mixed with distilled water and stored at room temperature.

Ponceau S Protein Stain: 0.1% [w/v] Ponceau S was dissolved into a 10% [v/v] Glacial Acetic Acid solution and stored at room temperature.

2.2.5 Indirect Immunofluorescence Assay (IFA) Solutions

Paraformaldehyde (PFA): Stock PFA was prepared by dissolving 20% (w/v) paraformaldehyde in 1 x PBS and was heated to 50°c on a heated plate within a fume hood until the solution became clear. pH was adjusted to 7.5 using 1M HCl. 20% (w/v) PFA/PBS was then further diluted in 1 x PBS to a final working concentration of 4% (v/v).

Permeabilisation Solution: 0.05% (v/v) Triton X-100 was mixed with distilled water and stored at room temperature.

Blocking Solution: 3% (w/v) BSA, 1mM $MgCl_2$ and 1mM $CaCl_2$ were added to 1 x PBS. The blocking solution was stored on ice and made fresh for each IFA experiment.

Washing Solution: The blocking solution was diluted 10 fold in 1 x PBS with an additional 1mM $MgCl_2$ and 1mM $CaCl_2$, (to a final concentration of 0.3% [w/v] BSA, 1mM $MgCl_2$, 1mM $CaCl_2$). The washing solution was stored on ice and made fresh for each IFA experiment.

Mounting Media: Vectashield Mounting Medium with DAPI (Vector Laboratories Inc. CA, USA), stored at 4°c in the dark.

2.2.6 Dual-Luciferase Reporter Assay Solutions

Dual-Luciferase Reporter Assay System: This kit compises of 5x Passive Lysis Buffer, a Luciferase Assay Buffer and Stop & Glo® Reagent. Components were stored at -30°c and thawed for use at room temperature. (E1960, Promega, Madison,USA).

Passive Lysis Buffer: 5 x Passive lysis buffer, stored at -30°c was thawed at room temperature and diluted to 1x with distilled water. Once used passive lysis buffer was stable for 6 hours at room temperature.

2.2.7 Lentiviral Reagents

Protamine Sulphate: A stock solution of protamine sulphate was prepared by dissolving salmon protamine sulphate salt in HPLC grade water to a concentration of 10mg/ml. The stock solution was diluted to a final working concentration in growth media of 10µg/ml. Protamine sulphate was utilised to enhance gene transfer by viral vectors. Store at -20˚C. (P3369, Sigma-Aldrich, Saint Louis, USA)

Methods

2.3 Bacterial Culture methods

2.3.1 Preparation of Chemically-Competent Cells

100ml of LB was inoculated with 100µl of a 10ml overnight culture of bacterial cells (*DH5α*). The cells were grown overnight at 20-22°c with vigorous shaking (200-220rpm) until an OD_{600} of 0.45-0.65 was reached monitored by spectrophotometric analysis. The cells were then chilled on ice for 15 minutes and then pelleted by centrifugation at 3500rpm at 4°c for 15 minutes. The supernatant was discarded and the bacterial pellet was re-suspended in 10ml of filter sterilised (0.2µm) transformation buffer (TB). Cells were chilled on ice for 10 minutes and then re-centrifuged at 3500rpm. The pellet was re-suspended in 2ml TB-DMSO (7% [v/v] DMSO in TB) and placed on ice for 10 minutes. Cells were aliquoted into eppendorf tubes and frozen immediately in liquid nitrogen before storing at -80°c.

2.3.2 Transformation of Chemically Competent Cells

50µl aliquots of chemically competent *DH5α* bacteria (section 2.3.1) were removed from -80°c and thawed on ice. 5µl of ligated DNA or 10ng of plasmid DNA was added to the cell suspension and gently agitated to mix before incubation on ice for 30 minutes. The cells were then heat shocked at 42°c in a water bath for 90 seconds and then returned to ice for 5 minutes. 1ml of Luria Broth (LB) was added to the cells which were then incubated at 37°c with shaking at 200-220 rpm for 1 hour. 200µl and 800µl of cell suspension was then plated onto LB-agar plates containing plasmid-selective antibiotic and incubated at 37°c overnight. Positive colonies were picked from plates using a sterile autoclaved 200µl pipette tip and inoculated into a 10ml LB culture containing the vector appropriate antibiotic.

2.3.3 Propagation of Bacteria

Typically 10ml or 50ml of LB containing plasmid-selective antibiotic was inoculated with a single bacterial colony picked from an LB-agar plate containing plasmid-selective antibiotic and grown with agitation at 37°c overnight. The cultures were then centrifuged at 4000rpm for 10 minutes to pellet the bacteria and the supernatant was discarded.

2.4 Nucleic Acid Techniques

2.4.1 Plasmid DNA Extraction from Bacteria

Plasmid DNA from 10ml cultures was isolated using a modified alkaline-SDS lysis procedure (GenElute™ Plasmid Miniprep, Sigma-Aldrich, MO, USA-Aldrich, UK). Harvested cells (2.3.3) were re-suspended in 200µl of re-suspension solution containing RNase A by vortexing and were then transferred to a clean 1.5ml Eppendorf tube. Cells were lysed by the addition of 200µl of the lysis solution, gently mixed by inversion until the mixture became clear and viscous and incubated for 5 minutes. The cell debris was precipitated by addition of 350µl of the neutralisation/binding solution. Cells were gently inverted and then centrifuged at 13000 rpm for 10 minutes to pellet cell debris, proteins, lipids, SDS and chromosomal DNA. The GenElute™ Miniprep binding column was placed into a microcentrifuge tube and 500µl of Column Preparation solution was added to enhance binding of plasmid DNA to the silica membrane within the column. The column was centrifuged at 13000rpm for 1 minute and the flow-through solution discarded. The cleared bacterial lysate was transferred into the column and centrifuged at 13000rpm to enable binding of the plasmid DNA. Additional bacterial contaminants and residual salt were removed by the addition of 500µl of the Optional Wash Solution and 750µl of the Wash Solution, which were centrifuged and the through-flow discarded after each wash. The column was centrifuged an additional time to ensure the removal of any remaining wash solution. The column was transferred to a new microcentrifuge tube and eluted by the addition of 100µl of HPLC grade

water. The column was centrifuged at 13000 rpm for 1 minute and the eluate containing the plasmid DNA was stored at -20°c for further use.

For larger DNA yields, plasmid DNA was isolated from 50ml cultures using QIAGEN Plasmid Midi kits (12143, QIAGEN, Maryland, USA). Bacterial cells were harvested by centrifugation in 50ml poly-sulphonate centrifuge tubes at 6000g for 15 minutes at 4°c. The bacterial pellet was re-suspended by vortexing in 4ml of Buffer P1 (50mM Tris-Cl pH 8.0, 10mM EDTA, 100µg/ml RNase A). The cells were lysed by the addition of 4ml of Buffer P2 (200mM NaOH, 1% w/v SDS). The cell suspension was gently inverted to mix and incubated at room temperature for 5 minutes. 4ml of ice-cold Buffer P3 (3.0M potassium acetate pH 5.5) was added to the lysate to precipitate genomic DNA, proteins and cell debris. The lysate was incubated on ice for 15 minutes, prior to centrifugation at 20000g for 30 minutes at 4°c to pellet the cell debris. The supernatant was further centrifuged at 20000g for 15 minutes at 4°c to entirely remove suspended material for subsequent steps. A QIAGEN-tip 100 was equilibrated by applying 4ml of Buffer QBT (750mM NaCl, 50Mm MOPS pH 7.0, 15% [v/v] isopropanol, 0.15% [v/v] Triton X-100). The supernatant was then transferred to the QIAGEN-tip and allowed to pass through the resin by gravity flow. The DNA bound to the QIAGEN-tip resin was then washed twice with 10ml of Buffer QC (1.0M NaCl, 50mM Tris-Cl pH 7.0, 15% [v/v] isopropanol) and then eluted into a polysulphonate centrifuge tube with 5ml of Buffer QF (1.25M NaCl, 50mM Tris-Cl pH 8.5, 15% [v/v] isopropanol). DNA was precipitated by adding 3.5ml of room temperature isopropanol, the eluate was mixed and immediately centrifuged at 15000g for 30 minutes at 4°c. The supernatant was carefully decanted and discarded, and the DNA pellet was washed with 2ml of 70% (v/v) ethanol. The eluate was centrifuged at 15000g for 10 minutes. The supernatant was discarded and the DNA pellet left to air dry for 10 minutes. The DNA was carefully re-suspended in 500µl of HPLC grade water and stored at -20°c for further use.

2.4.2 Determination of DNA concentration

dsDNA concentration was determined using a NanoDrop® ND-1000 spectrophotometer (NanoDrop Technologies, Inc. Wilmington USA). The upper and lower pedestals of the NanoDrop® were wiped cleaned with 100% (v/v) ethanol and nuclease free water prior to use. The NanoDrop® was initialised and then blanked to zero by the addition of 1.5µl of water. 1.5µl of DNA was then pipetted onto the lower pedestal and the concentration derived from the absorbance at 260nm (the maximum light absorption of nucleic acids). Protein absorbs light at 280nm, therefore the DNA/RNA purity can be determined by the ratio of OD_{260}:$OD_{280.}$ Ratio values less than 1.8/2.0 indicate protein or phenol contamination of the sample. The DNA concentration was measured twice and the average value was recorded.

2.4.3 DNA sequencing

All DNA sequencing was carried out by the Bipolymer Analysis and Synthesis Unit (School of Biomedical Sciences, University of Nottingham) using a 3130 ABI PRISM Genetic Analyser.

2.4.4 Restriction Endonuclease Digestion of DNA

All DNA was digested using appropriate restriction enzymes (Promega, WI, USA) in the recommended compatible reaction buffer (ensured by utilising the online Promega Restriction Enzyme Resource). Digestions contained 10 units of each restriction enzyme, 1x Bovine Serum Albumin (R396D, Promega, WI, USA), 1x reaction buffer and 0.2-1.5µg of DNA depending on whether the digestion is for analytical or preparative use. HPLC grade water was then added, typically to a final volume of 30µl. Restriction digests were performed at 37°c in a water bath for 1 hour. Restriction digests were terminated by the addition of 10x Agarose Gel Sample Buffer prior to DNA fragment isolation by agarose gel electrophoresis.

2.4.5 Agarose Gel Electrophoresis of DNA

All electrophoresis of nucleic acids was performed using horizontal agarose gel electrophoresis equipment run with a constant voltage of 5V per cm between the electrodes. Agarose gels were typically prepared by melting 0.7-2% (w/v) agarose in 1x TAE buffer, dependent on the size of the DNA fragment and the required resolution. The agarose gel was then left to cool and Ethidium Bromide added at a concentration of 0.5µg/ml. Smartladder (200bp-10kb, MW-1700-10, Eurogentec, Belgium) DNA ladder was used in order to estimate the size and approximate concentration of the DNA fragment. DNA gels were visualised by UV trans-illumination and a digital photograph was taken using a GENEgenius Bioimaging system (Syngene, Synoptics Ltd, Cambridge, UK) and GeneSnap software (Syngene).

2.4.6 Extraction and Purification of DNA from Agarose

The desired DNA bands to be purified were excised from the agarose gel using a sterile scalpel blade under UV trans-illumination. The DNA was extracted from the agarose gel using the GenElute™ Gel Extraction Kit (Sigma-Aldrich, MO, USA-Aldrich, UK). The excised gel was placed in an Eppendorf tube and the weight of the gel measured. Gel Solubilisation Solution was added (300µl for every 100mg) and the gel was heated in a water bath at 50°c for 10 minutes to dissolve the gel. 1 gel volume of 100% (v/v) isopropanol was added to the dissolved gel and mixed until homogenous. The solution was then transferred into a GenElute™ Binding Column G, previously washed with 500µl of Column Preparation Solution, and centrifuged at 13000rpm for 1 minute. The flow-through was discarded and 700µl of Wash Solution Concentrate G added, centrifuged again and the eluate discarded. The column was then left to air dry for 5 minutes to remove additional ethanol. The column was transferred to a new microcentrifuge tube and eluted with 50µl of HPLC water.

2.4.7 Ligation of Restriction Enzyme Digested DNA Fragment into a Linearised Vector

All ligations performed were sticky-end ligations whereby DNA insert fragment and linearised plasmid vectors contained complementary DNA overhangs. Insert and vector DNA fragments were generated by restriction endonuclease digestion (section 2.4.4) and were then purified and isolated by agarose gel electrophoresis (section 2.4.5 and 2.4.6). Restriction endonuclease digestion of both the insert and vector using two specific endonucleases allowed the orientation specific ligation of the DNA insert and plasmid vector. All ligation reactions were set up with DNA insert: plasmid vector ratios of 1:1. 3:1 and 5:1 using 25-50ng of vector: The following calculation was used to calculate the appropriate ratio:

$$\frac{\text{ng vector} \times \text{insert size (Kb)}}{\text{vector size (Kb)}} \times \text{ratio} \frac{\text{insert}}{\text{vector}} = \text{ng insert}$$

Ligation reactions were typically performed in a total volume of 20µl, containing the appropriate amount of DNA insert and plasmid vector, 2µl of T4 DNA ligase (M1801, 6U/µl, Promega, WI, USA) and 2µl of 10x T4 DNA ligase buffer. Reactions were performed alongside a control reaction containing no DNA insert, in order to estimate the degree of re-annealment of the plasmid vector. Reactions were performed at 16°c overnight. 5µl of the ligation reaction mixture was then transformed into chemically competent bacteria (section 2.3.2).

2.5 Polymerase Chain Reaction (PCR)

2.5.1 Nucleic Acid Amplification by PCR

Nucleic acid amplification was performed using PCR employing either the Expand High Fidelity PCR System comprising Taq DNA polymerase activity (3U/µl, 11 732 641 001, Roche, Mannheim, Germany) or PFU polymerase activity (3.5U/µl, M774A, Promega, WI, USA). Reaction volumes were set up

in a final volume of 25µl containing 3U of Polymerase enzyme, 1 x PCR buffer, 1µl of deoxynucleotide mix (11 581 295 001, Roche, Mannheim, Germany) equating to a final concentration of 200µM of each dNTP and 0.6µM of each specific forward and reverse primer. PCR was performed using a HYBAID PCR Authorised Thermal Cycler (HBSP05220, HYBAID Ltd, UK) using the following programme:

Initial denaturation	5 min at 95˚c	
Denaturation	1 min at 95˚c	35 Cycles
Primer annealing	1 min at 50˚c	
DNA amplification	1 min at 72˚c	
Final extension	2 min at 72˚c	

All PCR reactions were held at 4°c once complete and PCR products were verified by agarose gel electrophoresis (section 2.4.5) and purified using the GenElute™ Gel Extraction Kit (Sigma-Aldrich, MO, USA-Aldrich, UK) (section 2.4.6).

2.5.2 PCR Amplification of GC-RICH DNA templates

For amplification of difficult GC rich templates, the GC-RICH PCR System (12 140 306 001, Roche, Mannheim, Germany) was employed. The reaction was set up as for a standard PCR reaction using 2U of GC-RICH PCR System enzyme mix, 1 x GC-RICH PCR reaction buffer with DMSO and 1M of GC-RICH resolution solution in a final volume of 50µl. GC melt PCR was performed using the following PCR parameters:

Initial denaturation	1 min at 95˚c	
Denaturation	30 sec at 94˚c	
Primer annealing	1 min at 50˚c	30 Cycles
DNA amplification	3 min at 68˚c	
Final extension	3 min at 68˚c	

2.5.3 TA Cloning of PCR Products

TA cloning® was used to quickly and efficiently clone purified PCR products into the pcDNA4/HisMax©-TOPO® plasmid vector using the pcDNA4/HisMax©-TOPO® TA Expression Kit (K864-20, Invitrogen, Carlsbad, USA). The PCR product is integrated within the linearised plasmid vector supplied with single 5' thymidine overhangs. PCR products amplified by Taq polymerase contain a 3' single deoxyadenosine due to the non-template dependent terminal transferase activity of the polymerase therefore allowing efficient insertion into the linearised pcDNA4/HisMax©-Topo® plasmid vector. Furthermore, the pcDNA4/HisMax©-Topo® vector is supplied with topoisomerase I from the *Vaccinia* virus covalently attached. The topoisomerase binds *via* tyrosine-274 after a specific 5'-CCCTT and cleaves the phosphodiester backbone of the vector. This phosphor-tyrosyl bond can then be attacked by the 5'hydroxyl of the original cleaved strand, reversing the reaction and forming a phosphodiester bond with the insert PCR product.

TA cloning reactions were performed in a final volume of 5µl, containing 0.5-4µl of fresh purified PCR product, 1µl of salt solution and 0.5µl of TOPO® vector. The reaction mixture was gently mixed and incubated at room temperature for 30 minutes. 2µl of the reaction mixture was then transformed into chemically competent cells (section 2.3.2). Reactions were performed in parallel to a vector only control, providing an estimation of vector re-annealment.

2.5.4 RNA extraction and Real-time quantitative reverse transcription PCR

RNA was extracted from U2OS cells, seeded into a 24 well plate at a density of 4 x 10^4 and transfected with siRNA targeting LIMD1 or a non-specific scrambled control, using the RNAqueous micro kit (Ambion). RNA was extracted immediately with disruption with 100µl of lysis solution containing guanidinium thiocyanate which rapidly inactivates ribonucleases. 50µl of

100% (v/v) ethanol was added to the lysate and the lysate loaded onto a silica-based filter that selectively binds RNA. The filter was washed with 180µl of wash solution 1 and then twice with 180µl of wash solution 2/3. The RNA was then eluted in 10µl of elution solution preheated to 75°c. RNA (1µg) pre-treated with DNase I (Invitrogen) was then reverse transcribed using oligo-dT primers and High Fidelity Reverse Transcriptase (Roche). To quantify the mRNA levels of HIF1α, BNIP3, VEGF, LIMD1 and β-tubulin quantitative real-time PCR was conducted using 1XTaqMan Power SYBR green Mastermix (Applied Biosystems), 0.4mM forward and reverse primers, 2.5µl cDNA and dH_2O to a final volume of 25µl, reactions were run on an ABI7000 instrument (Applied Biosystems).

qRT-PCR primers:

BNIP3 (5'-3'):
Forward: ATGTCGTCCCACCTAGTCGAG
Reverse: CTCCACCCAGGAACTGTTGAG

VEGF (5'-3'):
Forward: ACCTCCACCATGCCAAGTG
Reverse: TCTGATTGGATGGCAGTAG

HIF1α (5'-3'):
Forward: CCAGTTACGTTCCTTCGATCAGT
Reverse: TTTGAGGACTTGCGCTTTCA

LIMD1 (5'-3'):
Forward: TGGGGAACCTCTACCATGAC
Reverse: CACAAAACACTTTGCCGTTG

β-Tubulin (5'-3'):
Forward: ATACCTTGAGGCGAGCAAAA
Reverse: CTGATCACCTCCCAGAACTTG

The data was normalised to the housekeeping gene β-tubulin and relative quantification was determined by the comparative Ct method ($2^{-[delta][delta]Ct}$). (RNA extractions and qRT-PCR experiments were performed in collaboration with Dr Victoria James, School of Biomedical Sciences, University of Nottingham.)

2.6 Cell Culture Methods

2.6.1 Cell Maintenance and Passaging of Cells in Monolayer Culture

Adherent human cell lines (U2OS, HeLa, HEK 293, HEK 293T) were maintained in monolayer culture, typically in 75cm^2 flasks. Cells were cultured in Dulbecco's modified Eagles medium supplemented with 10% (v/v) Foetal calf serum (FCS) and 1% (v/v) penicillin/streptomycin and incubated at 37°c with 5% CO_2. Cells were maintained at 80% confluency *via* trypsinization with (1x) Trypsin and EDTA.

Cells were inspected using an inverted light microscope. Cells were passaged by trypsinization when cells reached 80% confluency. Medium was removed by aspiration and the cells washed with 10ml of 1 X sterile PBS. Cells were detached by addition of 2.5ml of 1x trypsin-EDTA and incubated at 37°c for 5 minutes. Each plate was then gently tapped to aid the detachment of cells and observed using a light microscope. Trypsin-EDTA was then neutralised by addition of 7.5ml of DMEM growth medium and cells were harvested by centrifugation at 1500rpm for 5 minutes. The remaining supernatant was aspirated off and the cells were then re-suspended in an appropriate volume of growth medium. Cells were then transferred into a new 75cm^2 flask typically at a 1:3 to 1:10 dilution. 10ml of growth medium was added to the flask, cells were dispersed evenly by gentle shaking and returned to incubate at 37°c.

2.6.2 Cell Freezing

Cells were trypsinised and harvested by centrifugation (section 2.6.1) and then re-suspended in 10ml of cold PBS. Cells were pelleted by centrifugation at 1500rpm for 5 minutes and the supernatant removed by aspiration. Cells were re-suspended in 1ml of freezing media (90% (v/v) FCS, 10% (v/v) dimethyl sulfoxide [DMSO]) and transferred into cryovials. Cells were then immediately stored at -80°c overnight and then transferred into liquid nitrogen (-196°c) for long term storage.

2.6.3 Cell Counting Using a Haemocytometer

Cells were counted utilising an Improved Neubauer Haemocytometer (AC1000, Hawksley & Sons Ltd, Lancing, UK) to ensure reliable and consistent seeding of cells. Following trypsinization, cells were re-suspended evenly by pipetting up and down 5 times. With the coverslip in place, 10µl of the cell suspension was transferred to both chambers of the haemocytometer. Cells were counted using an inverted light microscope, counting all cells in the large 1mm corner squares. Typically at least 100 cells were counted, including cells touching the upper and left border but not the right or lower borders. Each large square represents a total volume of $0.1mm^3$ or 10^{-4} cm^3 and as $1cm^3$ is approximately 1ml, the subsequent formula was used to determine the cell number per ml:

Cells/ml = (Average count) x 10^4
Total cells = (Cells/ml) x (original volume)

2.6.4 Hypoxic Treatment

Cells were exposed to hypoxia for 4-72 hours at 37°c and 1% O_2 maintained using a ProOx 110 (BioSpherix Ltd, New York, USA) controller and chamber. Following hypoxic treatment cells were rapidly lysed to prevent reoxygenation.

2.7 Nucleic Acid Transfection of Monolayer Cells in Culture

2.7.1 GeneJuice® Transfection

24 hours prior to transient transfection the desired cell lines were seeded into 6 well plates at a density of 1 x 10^5 corresponding to approximately 50% confluency. For each 6 well, 3µl of GeneJuice® (70967-6, Novagen®, Darmstadt, Germany) was directly added to 100µl of Opti-MEM® media into a sterile eppendorf tube. The solution was thoroughly agitated to mix and incubated at room temperature for 5 minutes. 1µg of DNA was added directly to the solution and incubated at room temperature for 30 minutes to enable the formation of a GeneJuice®-DNA complex. The reagent-DNA mixture was then added drop-wise to the cells in complete growth medium. The 6 well plate was gently rocked to ensure even distribution of the mixture. The cells were then incubated for 12-72 hours at 37°c and 5% CO_2 prior to harvesting of cells for analysis. GeneJuice® was used for transfection of a variety of different size cell culture dishes, where the volume of GeneJuice® was maintained 3 times the volume of the DNA mass used (3µl :1µg).

2.7.2 DharmaFECT® siRNA Transfection

Cells were seeded into 12 well plates at a density of 5 x 10^4 and incubated in 1ml of complete growth medium for 24 hours. siRNA was re-suspended in 1 x siRNA buffer (Thermo Scientific Dharmacon®, Lafayette, USA) to a final concentration of 20µM. siRNA was typically used at 20nM, so in a total volume of 1ml per 12 well, 1µl of stock solution was used. Solution A was prepared by mixing 1µl of siRNA stock solution with 99µl of Opti-MEM® by pipetting, in a sterile microcentrifuge tube and incubated at room temperature for 5 minutes. Solution A was then mixed by pipetting with solution B comprising 1µl of DharmaFECT® Duo Transfection reagent (T-2010-03, Thermo Scientific Dharmacon®, Lafayette, USA) and 99µl of Opti-MEM®, and incubated for 20 minutes at room temperature. Growth medium was aspirated off of the cells and cells were washed with 2ml of 1 x PBS. 800µl of complete growth medium was added onto the cells prior to the addition of

200µl of the siRNA-reagent mixture. Cells were incubated for 24-72 hours at 37°c and 5% CO_2 before harvesting and analysis.

2.8 Stable LIMD1 knock down cell line production by the Lentiviral shRNA system

Lentiviral vectors have the ability to integrate into the host cell DNA irreversibly and therefore, are suitable vectors for permanent genetic modification of cells. Stable LIMD1 knock down cell lines were produced by utilizing lentiviral-mediated gene transfer by simultaneously transfecting three plasmids; the pHR'-CMV-8.2ΔR (packaging), pCMV–VSV-G (envelope) and the pFLRu derived plasmid encoding short hairpin RNA's (shRNA) targeting LIMD1 mRNA (Figure 2.8.1 and vector appendix for plasmid information).

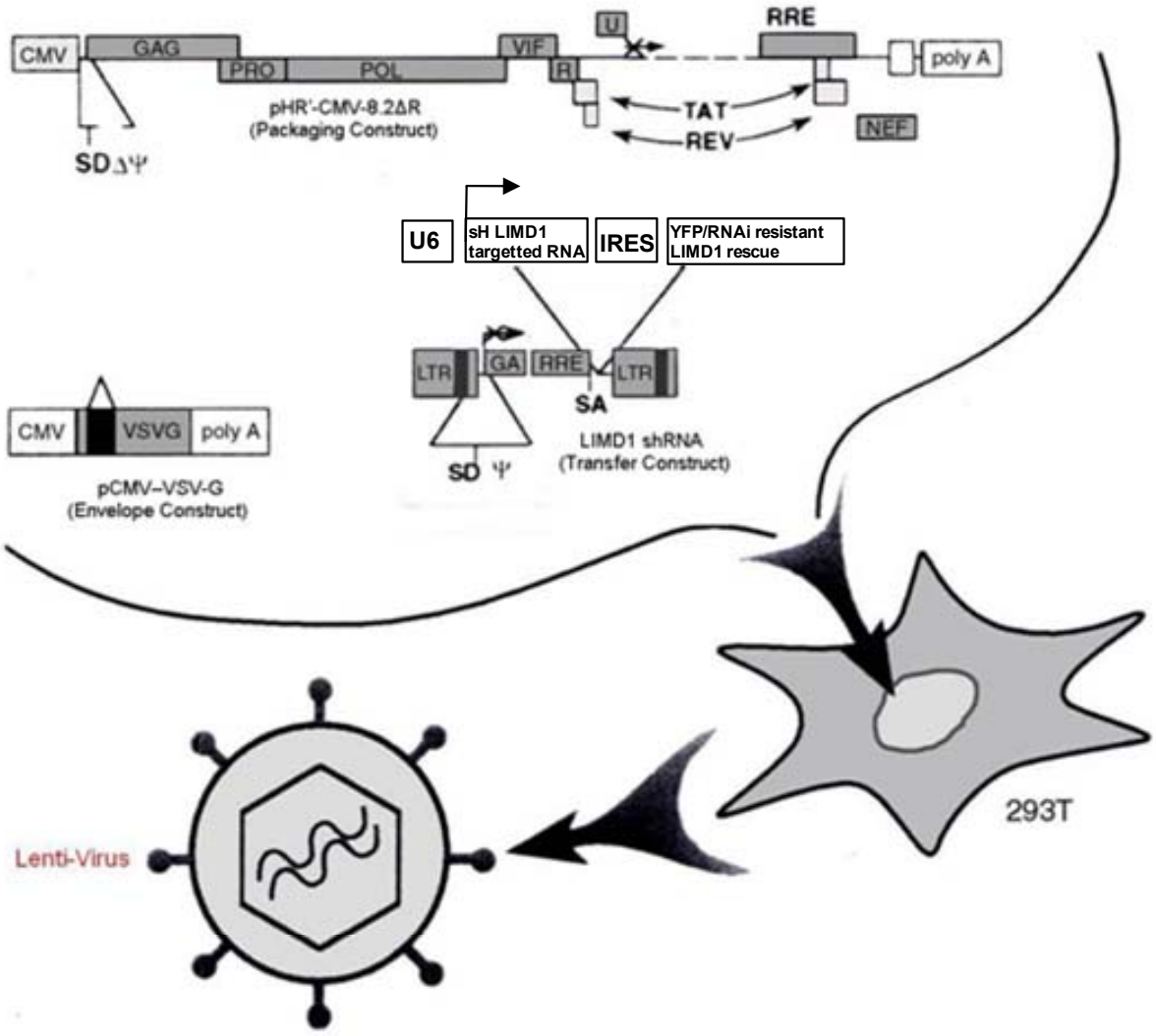

Figure 2.8.1 *Schematic Representation of Lentiviral mediated genetic modification.*

Lentivirus is produced by the transient co- transfection of HEK 293T cells with an envelop construct and packaging construct for viral generation and a transfer construct containing shRNA targeted for LIMD1 mRNA. Lentivirus was then collected and used to infect target cell lines to generate desired stable cell lines.

For lentivirus production, these three plasmids were co-transfected into the packaging HEK 293T cell line. HEK 293T cells were seeded into 10cm dishes at a density of $3x10^6$. 20 minutes prior to transfection, cells were washed with room temperature 1 x PBS and 7.5ml of media was replaced. The three plasmids were mixed prior to transfection in a 0.5ml microcentrifuge tube containing 5µg of the pFLRu derived plasmid, 4.4µg of the pHR'8.2ΔR plasmid and 0.6µg of the pCMV-VSV-G plasmid. The HEK 293T cells were then transfected with the plasmid DNA mixture using GeneJuice® (as described in 2.7.1). 24 hours later an additional 7.5ml of complete growth media was added to the cells to a total of 15ml. The transfected cells were allowed to culture for another 24 hours to accumulate virus. The efficiency of HEK 293T transfection and lentiviral production was monitored *via* visualisation of an IRES-YFP (Internal Ribosome Entry Site – Yellow Fluorescent Protein) construct (replaced with an RNAi resistant LIMD1 rescue in one of the constructs) by fluorescent microscopy. The supernatant containing virus was then removed, filtered using a 0.45µm filter and then stored at -80°c.

Target cell lines were seeded in 10cm dishes at a density of $4x10^6$ and cultured until they were 80% confluent. Cells were then washed in room temperature 1 x PBS and then 5ml of filtered lentivirus and 5ml of complete growth medium were added to the cells (10ml total volume). 24 hours following the initial viral transduction, cells were 'super-infected' by removing 5ml of medium from the cells which was replaced by another 5ml of virus. Viral transduction was supplemented with protamine sulphate (Sigma-Aldrich, MO, USA) added to the viral stock to the final concentration of 10µg/ml, to enhance the efficiency of lentiviral infection. 24 hours following the second transduction the media was replaced with complete growth medium containing puromycin to a final concentration of 3µg/ml to select for the transduced cells. Cells were cultured with medium containing puromycin for 10 days to ensure survival of only lentiviral transduced cells. Viral transduction was then evaluated by visualisation of the IRES-YFP construct by fluorescent microscopy and SDS-PAGE and immunoblotting of cell lysates to evaluate levels of protein knock down (Figure 2.8.2). Lentiviral transduced

cell lines were then cultured at 37°c in complete growth media and a proportion frozen in freezing media and stored at -196°c in liquid nitrogen (section 2.6.2) for future use.

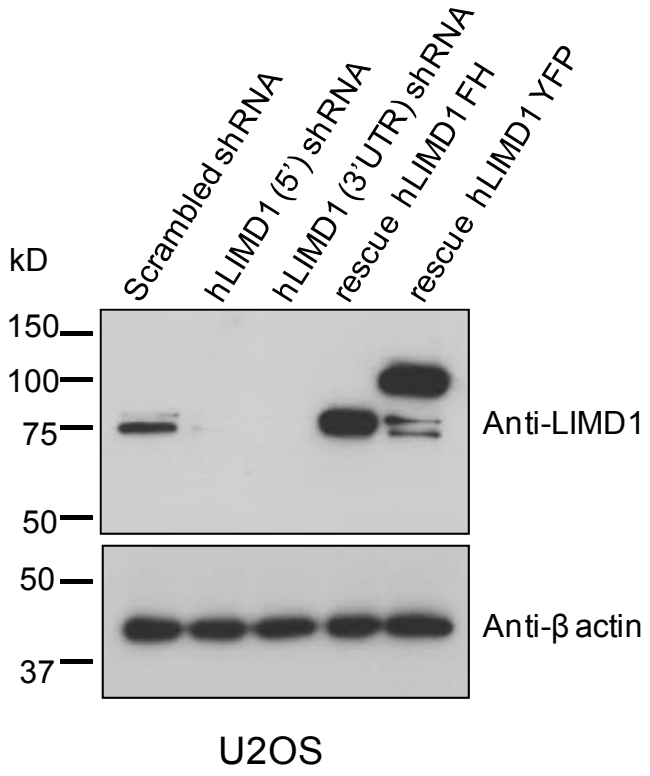

Figure 2.8.2 *Western blot confirmation of lentiviral mediated LIMD1 knock down.*

U2OS cells stably expressing LIMD1 shRNA express reduced LIMD1 in comparison with the scrambled shRNA control. Rescue RNAi resistant LIMD1, expressed on top of a LIMD1 shRNA background, rescues expression with a Flag-His or YFP tag. Anti-β actin immunoblot was used as a protein loading control.

2.9 Standard Protein Techniques

2.9.1 SDS-PAGE

Protein samples were typically resolved on 8-12% SDS-PAGE gels (8cm x 7.3cm x 0.75mm) using the Mini-PROTEAN® 3 system (Bio-Rad Laboratories UK). Per gel, the 10% acrylamide solution contained 1.9ml of H_2O, 1.7ml of 30% (w/v) Acrylamide solution (37.5:1 Acrylamide:Bis-acrylamide, Severn Biotech Ltd, UK), 1.3ml of 1.5M Tris pH8.8 and 50µl of 10% (w/v) SDS. To polymerise the acrylamide, 50µl of 10% (w/v) Ammonium Persulphate Solution (APS) and 2µl of N,N,N',N'-tetramethylethylenediamine (TEMED) were added, vortexed to mix and the gel was poured immediately. Gels were overlaid with ethanol to ensure an even surface and allowed to set for 30 minutes. The 5% stacking gel solution contained 1.4ml of H_2O, 330µl of 30% acrylamide solution, 250µl of 1.0M Tris pH 6.8 and 20µl of 10% (w/v) SDS and was polymerised by the addition of 20µl of 10% (w/v) APS and 2µl of TEMED. Either 10 or 15 well combs were inserted and the stacking gel allowed to set for 30 minutes before the gel was placed into the mini electrophoresis tank within the clamped electrode assembly apparatus. The tank was then filled with electrode buffer and the comb removed.

Proteins were prepared by lysis in 5 x Sample Buffer and heated at 95°c for 5 minutes. Samples were then loaded into each well using a 250µl gel loading pipette tip. 5µl of All Blue Precision Plus Protein™ Standards (Bio-Rad laboratories, UK) were loaded as a protein size marker. Gels were run at a constant 100 volts.

2.9.2 Immunoblot detection of Protein

Resolved proteins were transferred following SDS-PAGE onto Polyvinylidene Fluoride (PVDF) membrane (Roche Diagnostics, USA). PVDF membranes were equilibrated in 100ml of Methanol, 100ml of 50% (v/v) Methanol, 100ml of H_2O and 100ml of Tris-glycine Transfer Buffer (25Mm Tris-HCl pH 8.3, 200mM Glycine, 10% Methanol [Fluka, Sigma-Aldrich, UK]) for 5 minutes each with gently rocking. Proteins were transferred using a Trans-Blot Semi-

Dry Electrophoretic Transfer Cell (Bio-Rad Laboratories, UK) at a constant voltage of 20V for approximately 90 minutes. The membranes were then incubated in Blocking Solution (5% [w/v] Marvel in PBS-Tween [0.05% (v/v) Tween 20]) for 1 hour at room temperature with gentle rotation. The membrane was then incubated in 5ml of primary antibody diluted 1:500-1:5000 (primary antibody appendix) in Blocking Solution at 4°c overnight with gentle agitation. The membrane was then washed 3 times in PBS-Tween solution for 20 minutes per wash with agitation. Membranes were then probed with secondary antibody (Horseradish Peroxidase [HRP] conjugated Goat anti-mouse or Goat anti-rabbit, Dako, Denmark) at a concentration of 1:5000 in Blocking solution, for 1 hour at room temperature. The membrane was then washed 3 further times with PBS-Tween. The membrane was then placed face up on cling film and incubated with Enhanced Chemiluminescence Reagent (ECL) Western Blotting Detection System (Amersham™, GE Healthcare, UK) for 5 minutes at room temperature to initiate a HRP-catalysed luminescent reaction. Excess ECL was poured away and the membrane placed in an autoradiography cassette. Under red light ECL Hyperfilm (Amersham™) was exposed to the membrane for 10 seconds to 1 hour dependent on the strength of the expected signal. The film was then hand developed in PQ Universal Paper Developer (Ilford, UK) and fixed in 2000RT fixer (Ilford) before being rinsed in water and allowed to air dry.

2.9.3 Ponceau S Staining of Protein immobilised onto PVDF membrane

Ponceau S solution (0.1% [w/v] Ponceau S, 10% [v/v] Glacial Acetic Acid) was utilised to determine the resolution of electrophoresis and the efficiency of protein transfer onto the PVDF membrane. Membranes were immersed in Ponceau S solution for 2 minutes and then the solution was discarded. The membrane was washed with distilled water until protein bands were visible by pink staining.

2.9.4 Antibody Stripping and Re-probing of PVDF Membrane

Membranes were stripped in Antibody Stripping Buffer (Gene Bio-Application LTD, Israel) with agitation for 15 minutes at room temperature to remove both annealed primary and secondary antibodies. The membrane was then washed 5 times with 5ml of distilled water to remove the remaining buffer. Membranes were then re-blocked with Blocking Solution and re-probed with primary and secondary antibodies (section 2.9.2).

2.9.5 Coomassie Blue Protein Staining

Coomassie Blue Stain (50% [v/v] Methanol, 20% [v/v] Glacial Acetic Acid and 0.12% [w/v] Coomassie Brilliant Blue R) was used to visualise proteins resolved by SDS-PAGE. SDS-PAGE acrylamide gels were incubated for 1 hour in Coomassie Blue Stain and then de-stained in destaining solution (10% [v/v] Methanol, 10% [v/v] Glacial Acetic Acid) overnight.

2.10 Protein-Protein Interaction Assays

2.10.1 Immunoprecipitation (IP)

Immunoprecipitations were performed to analyse the specific *in vivo* protein-protein interactions of a desired antigen within a cell lysate. Prior to harvesting of cells the IP antibody-IP matrix complex was formed. 40µl of suspended (25% [v/v]) IP matrix (For immunoprecipitation of antibodies raised in mice sc45042, raised in rabbit sc-45043, Santa Cruz Biotech, CA, USA) was incubated with 1-5µg of IP antibody in 1ml of 1 x PBS and rotated for 4 hours at 4°c. 1 x 10^6 adherent cells were plated in 10cm^2 dishes and transfected using GeneJuice® transfection reagent (section 2.7.1). 48 hours post-transfection, the cells were washed three times with ice-cold PBS and lysed by the addition of 750µl RIPA buffer (150 mM NaCl, 1% [v/v] IGEPAL-630, 0.5% [w/v] sodium deoxycholate, 0.1% [w/v] SDS, 50mM Tris, pH 8) and cell scraping. Lysis was allowed to continue with vertical rotation for 30 minutes at 4°c. The cell debris was then pelleted by centrifugation at 13,000 rpm for 10 minutes. To reduce non-specific co-immunoprecipitation lysates

were pre-cleared before addition of the antibody using a slurry of 15µl of protein G agarose (P4691, Sigma-Aldrich, MO, USA) and 15µl of IgG sepharose™ (17-0969-01 GE healthcare, Uppsala, Sweden). In order to remove residual preservative ethanol, the protein G:IgG slurry was washed twice with 1ml of ice cold PBS and centrifuged at 2000 rpm for 1 minute prior to incubation with the lysates for 1 hour at 4°c with rotation. The lysates were then centrifuged to pellet the beads and the supernatant containing the cleared lysate retained. The IP antibody-IP matrix complex was washed twice by the addition of 1ml of 1 x PBS and centrifugation at 2000 rpm for 1 minute, to remove any free unbound antibody. 50µl of the cleared cell lysate was aliquoted as an input and the remaining lysate added to the IP antibody-IP matrix complex and incubated with rotation overnight at 4°c. The beads were then centrifuged at 2000 rpm for 1 minute and the supernatant discarded. 1ml of lysis buffer was added and the beads washed for 5 minutes with rotation at 4°c. This wash was then repeated a further 2 times and then finally by the addition of 1ml of 1 x PBS. Following washing the remaining PBS was carefully removed by pipetting avoiding the removal of any of the beads. The beads were re-suspended in 40µl of 5 x SDS-PAGE sample buffer and heated at 95°c for 5 minutes before analysis by SDS-PAGE and immunoblotting (section 2.9.1 and 2.9.2).

2.10.2 Endogenous Immunoprecipitation

An IP antibody-IP matrix complex was formed (section 2.10.1) by the addition of 5µg of IP antibody and 80µl of IP matrix in 1ml of 1 x PBS. An 80% confluent 225cm^2 flask of the desired cell line (U2OS, HEK-293) was lysed in 4ml of RIPA buffer containing Complete™ Protease Inhibitor Cocktail (Roche, Mannheim, Germany) and PhosSTOP™ Phosphatase Inhibitor Cocktail (Roche, Mannheim, Germany). Lysis was allowed to continue with rotation for 30 minutes at 4°c and cell debris was pelleted by centrifugation at 3,400 rpm for 10 minutes. 50µl inputs were taken and the lysates added to the washed IP antibody-IP matrix complex and incubated overnight at 4°c

with rotation. The beads were washed (as in section) with 4ml of lysis buffer and then finally re-suspended in 40µl of 5 x SDS-PAGE sample buffer.

2.10.3 Nickel Affinity Capture of His-tagged proteins

Nickel affinity capture of poly-His tagged proteins was employed as an assay to confirm protein-protein interactions in the absence of the heavy and light chains of antibodies encountered when immunoprecipitating. 48 hours post-transfection; cells were washed three times with ice-cold PBS and lysed by scraping in 750µl of RIPA buffer plus 10-20mM of imidazole (from a 2M Imidazole stock, pH7.4, 56750, Fluka Chemika, Sigma-Aldrich, Switzerland). Imidazole is an organic compound which comprises the same aromatic heterocyclic ring as histidine and therefore acts to out-compete weak nickel binding proteins to prevent non-specific binding of His rich proteins to the Nickel affinity gel. RIPA buffer also contained Complete™ EDTA free Protease Inhibitors (1 tablet per 50ml of lysis buffer, 04 693 132 001, Roche, Mannheim, Germany). It is essential that the protease inhibitors used are EDTA free to ensure that Ni^{2+} ions are not chelated. Lysis was allowed to continue with vertical rotation for 30 minutes at 4°c prior to centrifugation at 13,000 rpm for 5 minutes. The supernatant was then pre-cleared with 20µl of Protein G agarose (P4691, Sigma-Aldrich, MO, USA) prepared by washing twice in PBS, for 1 hour at 4°c. Lysates were separated from the protein G agarose by centrifugation at 2000 rpm and 50µl inputs aliquoted. Ezview™ Red HIS-Select HC Nickel Affinity Gel (E-3528, Sigma-Aldrich, MO, USA) was prepared by washing twice in RIPA. Cleared lysates were then added to the washed Nickel Affinity beads to capture His-LIMD1 and was incubated with rotation overnight at 4°c.

To remove non-specific and weakly bound proteins, the supernatant was removed and replaced with 1ml of cold RIPA containing 10-20mM of imidazole and rotated for 5 minutes. The beads were centrifuged at 2000 rpm and the supernatant discarded. This wash was repeated twice and then once additionally with cold 1 x PBS. Bound proteins were eluted from the Nickel

beads by the addition of 5 x SDS sample buffer and heated at 95°c prior to analysis by immunoblotting.

2.10.4 Glutathione S-Transferase (GST) Gene Fusion System for Detection of Protein-Protein Interactions

The Glutathione S-Transferase (GST) gene fusion system (Amersham Biosciences, GE Healthcare, Buckinghamshire, UK) enables the high level expression of native active gene fusions to the *Schistosoma japonicum* GST gene. GST fusions can then be purified from bacterial lysates using affinity chromatography by glutathione immobilised as glutathione sepharose. The GST gene fusion system was employed as a versatile system to detect protein-protein interactions between GST tagged proteins expressed in bacteria with mammalian cell lysates.

2.10.4.1 Expression of Recombinant GST Fusion Proteins in Bacteria

cDNA encoded within the pGEX 4T-1 plasmid (27-4580-01, Amersham Biosciences, GE Healthcare, Buckinghamshire, UK) was transformed into the chemically competent *E.coli* strain BL21(DE3), suitable for propagation and efficient protein expression (section 2.3.2), with ampicillin selection (100µg/ml). A single colony was picked and inoculated a 10ml LB/Ampicillin culture (100µg/ml Ampicillin) grown overnight at 37°c with shaking at 220 rpm. The culture was then scaled up into a 50ml LB/Ampicillin culture at a ratio of 50:1 and incubated for a further 3 hours at 37°c with shaking. The pGEX 4T-1 plasmid contains an isopropyl-beta-D-thiogalactopyranoside (IPTG) inducible promoter to induce high level expression of the desired GST fusion protein. 200µm IPTG was administered to the culture, which was grown for a further 3 hours at 37°c with gentle shaking. The cells were then collected by centrifugation at 4000 rpm for 15 minutes. The supernatant was discarded and the cells freeze/thawed overnight at -30°c to aid lysis. The cells were then thoroughly re-suspended in 1ml of 1 x PBS. The cells were maintained on ice and lysed by sonication. Cells were exposed to 5 x 15

second bursts at the highest intensity, with 15 second intervals between each burst. The lysates were then centrifuged at 13,000 rpm for 10 minutes to pellet the insoluble cell debris. The supernatant was retained and stored at -20°c for future use.

2.10.4.2 Purification of Recombinant GST Fusion Proteins from Bacterial Lysates

GST fusion proteins can be purified from bacterial lysates due to the high affinity of the GST moiety for glutathione. Glutathione immobilised on sepharose (Glutathione Sepharose™ 4B, 17-0756-01, Amersham Biosciences, GE Healthcare, Buckinghamshire, UK) was stored at 4°c preserved in a 20% (v/v) ethanol solution. Prior to use the Glutathione Sepharose™ 4B was washed twice with 1ml of 1 x PBS to remove the ethanol solution. The appropriate amount of the bacterial lysate expressing the GST fusion alone (as a control) and the GST-tagged protein of interest was added to 30µl of washed glutathione sepharose and incubated in a total volume of 1ml, made up by 1 x PBS, for 20 minutes with rotation at 4°c. The beads were collected by centrifugation at 2000rpm for 1 minute and the supernatant containing the bacterial lysate was discarded. In order to remove proteins non-specifically bound to the Glutathione Sepharose™ 4B, the beads were washed twice with 1ml of RIPA buffer for 5 minutes followed by collection by centrifugation at 2000rpm. The GST fusion proteins may then be eluted from the Glutathione Sepharose™ 4B beads in denaturing conditions by the addition of 30µl of 5x SDS-PAGE sample buffer. Samples were then analysed by SDS-PAGE (section 2.9.1) and acrylamide gels were then coomassie stained (section 2.9.5) to quantify the GST fusion protein expression and purification.

2.10.4.3 GST fusion – Protein Interaction Assays

GST fusions immobilised onto Glutathione Sepharose™ 4B were then subjected to prey interacting proteins from human cell lysates or proteins expressed *in vitro* in Rabbit Reticulocyte lysate. The GST fusion proteins immobilised onto Glutathione Sepharose™ 4B beads were then blocked by incubation in 1ml of 5% (w/v) BSA in 1 x PBS for 1 hour at 4°c with rotation. This blocking step minimalises the amount of non-specific binding of the prey protein to the GST fusion, to the beads or to the eppendorf tube. The beads were pelleted by centrifugation at 2000 rpm for 1 minute and the blocking solution removed. The beads were then incubated with the prey protein, either expressed *in vitro* (prepared as described in section 2.10.4.4) or as human cell lysate overnight at 4°c with rotation. For *in vitro* transcribed and translated [^{35}S]-methionine labelled proteins, 1-20µl of the reaction mixture was added to the beads in 1ml of 5% (w/v) BSA in 1 x PBS. Human cell lysates were prepared as for immunoprecipitations (described in section 2.10.1), lysed in 500µl of cold RIPA, and incubated with the glutathione immobilised GST fusions in an additional 500µl of 10% (w/v) BSA in 1 x PBS, so that the final concentration of BSA is maintained at 5%. Prior to incubation of the prey protein to the beads, an appropriate input was aliquoted in order to evaluate the degree of protein interaction achieved by the assay.

Following overnight incubation, the beads were pelleted by centrifugation at 2000rpm for 1 minute and the supernatant discarded. The beads were washed 3 times for 5 minutes in 1ml of the incubation buffer (RIPA or PBS). The GST fusion proteins were eluted by re-suspension in 30µl of 5 x SDS sample buffer. The proteins were then resolved by SDS-PAGE and then stained using coomassie blue stain (section 2.9.5). Experiments utilising proteins expressed *in vitro* in rabbit reticulocytes, were analysed for protein interaction by drying of the polyacrylamide gel and then autoradiography to detect the [^{35}S]-methionine label of the prey protein (section 2.10.4.5). For interaction assays using human cell lysates, the eluate was resolved by SDS-

PAGE and then analysed by immunoblot for the presence of the interacting protein.

2.10.4.4. *In Vitro* Transcription and Translation

To evaluate whether a protein-protein interaction is direct in its nature, rather than indirect *via* an additional protein, GST fusion proteins were subjected to proteins expressed *in vitro* in rabbit Reticulocyte lysate. As Rabbit reticulocytes have minimal cellular proteins except those required for globin production, an indication regarding the nature of the protein-protein interaction can be deduced. The TNT® Coupled Reticulocyte Lysate System (Promega, WI, USA) was utilised to generate radio-labelled prey protein. The components of the system were removed from storage at -80°c. The TNT® T7 RNA polymerase was immediately placed on ice whilst the TNT® Reticulocyte lysate was thawed by hand and the other components were thawed at room temperature before incubation on ice. The following components for a standard TNT® lysate reaction were then assembled in a 0.5ml eppendorf tube on ice:

Component	Volume (µl)
TNT® Rabbit Reticulocyte Lysate	27.5
TNT® Reaction Buffer	2
TNT® T7 RNA Polymerase	1
Amino Acid Mixture, Minus Methionine, 1mM	1
[^{35}S] methionine (Ci/mmol)	2
RNasin® Ribonuclease Inhibitor (40U/µl)	1
DNA template (0.5µg/µl)	2
HPLC grade H2O to a final volume of	50

The reaction mixture was then mixed by vortexing and then incubated at 30°c for 90 minutes. The translation product was then either immediately used (section 2.10.4.3) or stored at -30°c for future use.

2.10.4.5 Gel drying and Auto-Radiography

Coomassie Blue stained SDS-PAGE acrylamide gels were placed onto Whatman filter paper and overlaid with cling film. Gels were then dried using a BioRad Gel Dryer (model 583) for 2 hours. The cling film was then removed and the gels placed into a developing cassette. Under red light ECL Hyperfilm (Amersham™) was exposed to the gel and then incubated for 24-72 hours at -80°c. The cassette was then allowed to thaw and the film was then hand developed.

2.11 Dual-Luciferase® Reporter Assay

The Dual-Luciferase® Reporter Assay System (E1960, Promega, WI, USA) was used to simultaneously measure the activity of two individual reporter enzymes (firefly [*Photinus pyralis*] and *Renilla* [*Renilla reniformis*]) sequentially within a single system. As Firefly and R*enilla* luciferases have distinct evolutionary origins their enzyme structures and substrate requirements are different. Firefly luciferase uses luciferin in the presence of oxygen, ATP and magnesium to produce light, while *Renilla* luciferase requires only coelenterazine and oxygen. Firefly luciferase produces a greenish yellow light in the 550–570nm range. *Renilla* luciferase produces a blue light of 480nm. Therefore, these enzymes can be used in dual-reporter assays due to their differences in substrate requirements and light output.

Cells were seeded at 5 x 10^4 into 12 well tissue culture plates and were transfected as described in section 2.7.1, with 50ng of the pGL3-HRE Firefly luciferase encoding reporter plasmid and 5ng of the Thymidine Kinase (TK)-*Renilla* constitutive control reporter plasmid per well (10:1 Firefly to *Renilla* ratio). 24 hours post-transfection cells were washed once with room temperature 1 x PBS and then lysed in 200µl of 1 x Passive Lysis Buffer (from 5x Passive Lysis Buffer Stock, diluted with distilled water). Cells were then lysed by agitation for 15 minutes and then transferred into 1.5ml eppendorf tubes. Lysates were then freeze-thawed and then centrifuged at 13,000 rpm at 4°c for 2 minutes to pellet insoluble cell debris. 20µl of the

supernatant was then loaded onto a 96 well plate for analysis. The Firefly activity was first measured by administration of 80µl per well of the Luciferase Assay Buffer-Substrate Solution (prepared by addition of 1 vial of lyophilized Luciferase Assay Substrate to 10ml of the Luciferase Assay Buffer II). The samples were then processed by a TopCount NXT™ Microplate Scintillation and Luminescence Counter (C384V00, Packard, Perkin Elmer, USA) after a 5-minute delay to reduce background luminescence. 80µl of the Stop & Glo® Buffer-Substrate Solution (prepared by addition of 200µl of Stop & Glo® substrate to 10ml of the Stop & Glo® buffer) was then added which quenches the Firefly Luciferase reaction while simultaneously activating the luminescent reaction of the control *Renilla* Luciferase. Data was then analysed using TopCount NXT™ Software Version 1.05 and Microsoft® Office 2002 Excel Software.

2.12 Indirect Immunofluorescence Assay (IFA)

Cells were seeded onto square glass cover slips within a 35mm well. Cover slips were stored in 100% (v/v) ethanol to ensure sterility. Cover slips were placed into the 35mm well and washed once with 1 x PBS to remove residual ethanol. 2×10^5 cells were seeded per well and incubated for 24 hours prior to transfection.

48 hours following transfection the medium was removed and the cells were washed 3 times with ice-cold 1 x PBS. The cells were then fixed in cold 4% (v/v) Paraformaldehyde in PBS at room temperature for 5 minutes. The cells were washed 5 times with cold 1 x PBS and then permeabilised with 0.05% (v/v) Triton X-100 in PBS at room temperature with gentle agitation. Cells were washed a further 3 times with PBS and then incubated in blocking buffer (3% [w/v] BSA, 1mM $MgCl_2$, 1mM $CaCl_2$ in 1 x PBS) for 1 hour at room temperature with gentle shaking. The blocking buffer was then removed and the cells were washed 3 times in washing solution (0.3% [w/v] BSA, 1mM $MgCl_2$, 1mM $CaCl_2$ in 1 x PBS). The cells were then incubated with primary

antibody diluted in washing buffer to the appropriate working concentration typically 1:200 to 1:1000 at room temperature for 1 hour with gentle agitation. The primary antibody was then removed and the cells washed 3 times with washing buffer. The appropriate complementary Alexafluor® (Invitrogen, Oregon, USA) dye conjugated secondary antibody (antibody appendix) was then added to the cells diluted 1:1000 in washing buffer and incubated for 1 hour at room temperature with gentle agitation. Cells were washed a final 2 times in washing buffer and once in 1 x PBS prior to mounting of the cover slips onto glass slides. A drop of Vectashield Mounting Medium with DAPI (Vector Laboratories Inc. CA, USA) was added onto the slide prior to mounting to enhance and retain fluorescence and enable visualisation of DNA. Slides were then stored at 4°c prior to analysis.

2.13 Confocal Microscopy and Imaging Analysis

Confocal microscopy was performed 48 hours post-transfection of the desired cell line, using a Leica TCS-SP2 Spectral Confocal & Multiphoton System (D69120, Leica Microsystems Heidelberg, Germany). The Leica Confocal system comprises a confocal imaging spectrophotometer system attached to a Leica DMIRE inverted fluorescence microscope, equipped with an argon laser, two HeNe lasers, an acousto-optic tuneable filter (AOTF) to attenuate individual visible laser lines and a tuneable acousto-optical beam splitter (AOBS).

The slides were visualized using Leica Confocal Software (Version 2.61 Build 1537) whereby a 63x/20x 1.32 oil-immersion objective was employed; the number of frames to average was defined at 20 and the number of xy- or xz-sections was selected at 1. Illumination of the objective lens was set to Beam expand 6; the diameter of detection pinhole was set to Airy 1(≈115µm); the Photomultiplier Tube 1 (PMT1) was set as Smart Gain and the Photomultiplier Tube 2 (PMT2) was set as Smart Offset.

For Multi-Channel Confocal Microscopy, sequential scan mode was selected and the scanning mode was selected as between frames. Laser type and excitation line selection for suitable fluorescent dyes are listed as in Table 2.3

Laser	Excitation lines	Suitable fluorescent dyes
Diode 20mW	**405nm**	Alexa 405, DAPI, Hoechst
Ar 100mW	**458nm**	Alexa 458, ECFP
	476nm	EGFP
	488nm	Alexa 488, FITC, EGFP
	514nm	Alexa 514, EYFP, mBanana
HeNe 1.5mW	**543nm**	Alexa 568, TRITC, mTan
HeNe 10mW	**633nm**	mTan, mChe, AsRed

Table 2.3 *Fluorescent dyes and their excitation lines used in confocal microscopy.*

CHAPTER 3: RESULTS

LIMD1, PHD and VHL interactions and binding interfaces

3. LIMD1, PHD and VHL interactions and binding interfaces

3.1 LIMD1 interacts with the Prolyl Hydroxylases 1, 2 and 3 *in vivo*

Preliminary Yeast-2-Hybrid data indicated that LIMD1 interacted with PHD1 (Figure 1.5). Therefore, the ability of LIMD1 to interact *in* vivo with PHD1 and additionally PHD2 and PHD3 whom share functional and structural homology was examined (Epstein et al., 2001). Co-immunoprecipitations were employed to investigate this hypothesis using the LIMD1 specific monoclonal antibody to immunoprecipitate exogenously expressed Xpress-tagged LIMD1 with exogenous PHDs in U2OS cells (Figure 3.1.1 and 3.1.1.2).

3.1.1 Optimisation of co-immunoprecipitations

The conditions within which protein-protein interactions take place are highly specific and are sensitive to salt and detergent concentrations within the lysis buffer. Therefore lysis and binding conditions for co-immunoprecipitation reactions were optimised using low to high salt buffers (50-500mM Tris) in the absence and presence of detergents such as IGEPAL-130. Optimisations were initially performed whilst attempting to co-immunoprecipitate LIMD1 with PHD1, which exhibited an interaction in all lysis conditions (data not shown). Low stringency lysis buffers such as PBS absent of detergents, demonstrated a high degree of interaction, including lower molecular weight proteins, presumably PHD1 degradation products. Higher stringency lysis buffers such as RIPA maintained a more specific interaction of full length PHD1 (Figure 3.1.1). As RIPA has the greatest ability to disrupt cells and therefore, the greatest protein recovery, it was selected as the condition to perform future co-immunoprecipitation reactions.

The ability to detect the PHDs following co-IP reactions proved problematic due to the molecular weights of PHD1 (44-47kDa), PHD2 (46kDa) and PHD3 (27kDa) due to cross-reactivity of the heavy and light chains of the antibody

used for immunoprecipitations with the antibodies used to immunoblot to confirm the protein interaction. The amount of antibody used for immunoprecipitations (2.5-5µg) caused smearing of protein during immunoblotting which impaired the ability to clearly detect the presence of the PHD proteins (Figure 3.1.1).

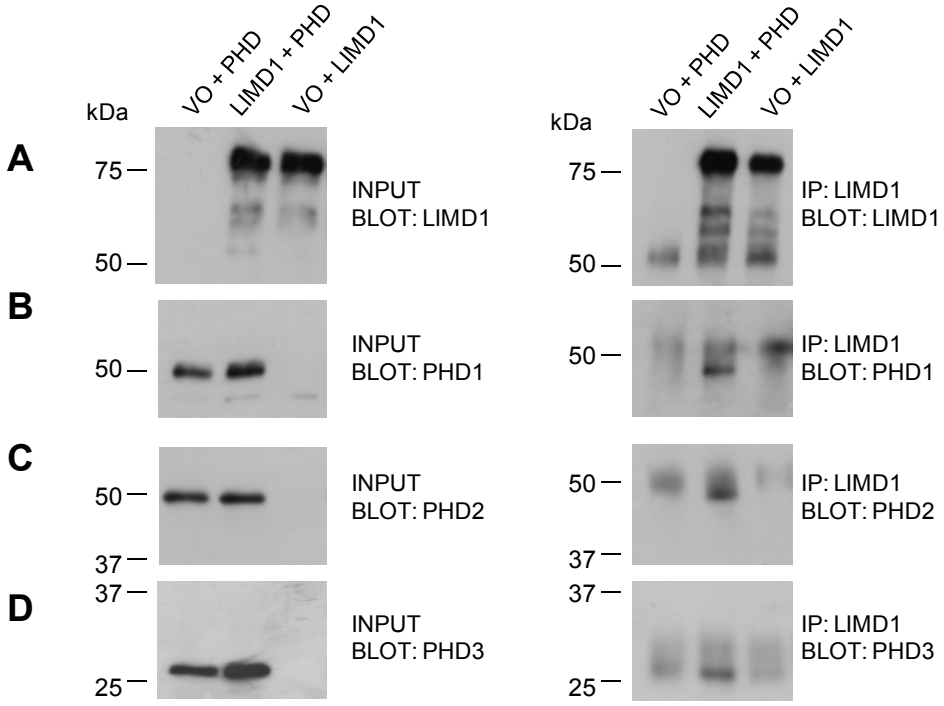

Figure 3.1.1 *Optimisation of LIMD1 co-immunoprecipitations with PHD1-3.*
(A) Xpress-tagged LIMD1 expressed in U2OS cells, was immunoprecipitated using 2.5µg of LIMD1 mAb and 30µl of protein G agarose. 2% inputs were taken prior to addition of antibody (left side of panels). Representative blot indicates LIMD1 immunoprecipitation (right right side of panels). **(B/C/D)** PHD1, PHD2 and PHD3 were individually co-transfected with LIMD1 or vector only control (left side of panels). All three PHDs specifically interact with LIMD1.

The co-IP experiments were optimised by eluting proteins from the antibody-bead complex utilising a more concentrated SDS sample buffer (5 x sample buffer rather than 2 x laemlli sample buffer) which improved protein denaturation and resolution by SDS-PAGE. Furthermore, rather than complexing the IP antibody with protein G (Sigma P4691) the Santa Cruz IP kit (ExactaCruz™ E: sc-45042) was used. This greatly reduced the degree of antibody cross reactivity, enabling a clear detection of PHD1 co-immunoprecipitation with LIMD1 (Figure 3.1.1.2).

Co-immunoprecipitations confirmed that LIMD1 interacted *in vivo* with all three PHDs when immunoprecipitated with a LIMD1 mAb, (Figure 3.1.1.2). To our knowledge, this is the first identified protein (excluding HIFα) to interact with all three PHD proteins. In addition, the ability of LIMD1 to interact with an EGFP-HA-tagged FIH construct was also examined. FIH also exhibited specific binding to LIMD1 *in vivo*. However, FIH co-immunoprecipitated with LIMD1 to a lesser extent relative to PHD1, 2 and 3 in comparison with their respective inputs and could only be determined by a longer film exposure (Figure 3.1.1.2). To control for specificity of interactions, co-immunoprecipitations were performed with LIMD1 and prey proteins alone with the representative vector only control and in the presence of both LIMD1 and PHD/FIH. Interactions were only observed in the presence of both LIMD1 and PHD/FIH (Figure 3.1.1.2)

As all three PHD proteins specifically interacted with full length LIMD1 this is indicative that LIMD1 may bind to this family of dioxygenases *via* their shared C-terminal catalytic oxygenase/hydroxylase domain. As FIH does not bind to the same extent this may be indicative of an indirect protein-protein interaction. Alternatively, LIMD1 may interact with FIH with a much lower affinity.

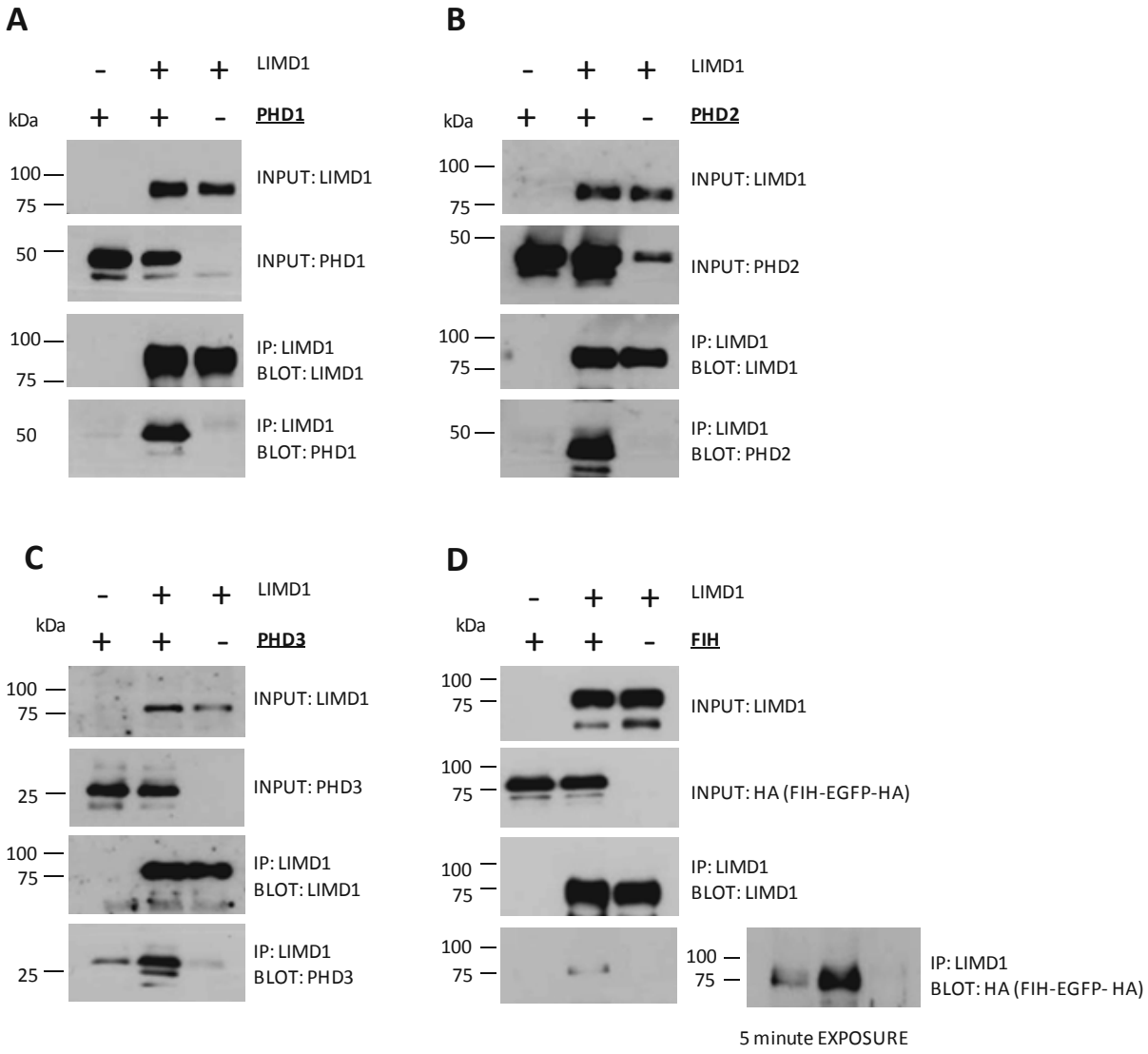

Figure 3.1.1.2 *LIMD1 co-immunoprecipitations in vivo with PHD1-3.*

Xpress-tagged LIMD1 was co-transfected with PHD1-3 and EGFP-HA-tagged FIH in U2OS cells. LIMD1 was immunoprecipitated using 2.5µg of LIMD1 mAb using the Santa Cruz IP Kit. **(A)** PHD1, **(B)** PHD2, **(C)** PHD3, and **(D)** FIH all co-immunoprecipitated with a LIMD1 mAb, only in the presence of LIMD1 highlighting the specificity of the interaction. FIH interacts with LIMD1 to a lesser extent, demonstrated by a longer exposure time of the film to the ECL reagent. 2% inputs loaded indicate protein levels prior to addition of the IP antibody.

3.1.2 Nickel-Histidine capture assays confirm LIMD1-PHD2 interaction

Nickel bead pulldown assays were employed as an approach to further confirm LIMD1's interaction with PHD2. Utilisation of this technique allows analysis of interacting partners *via* immunoblotting in the absence of the light and heavy chains of antibodies used when performing co-immunoprecipitations. pcDNA4-His/Max-Topo LIMD1 incorporates an N-terminal hexa-His tag which confers a high affinity to bind nickel conjugated to beads. However, endogenous histidine containing proteins or the substrate for the binding assay may also bind to the beads undesirably. Therefore, addition of the organic compound imidazole which comprises the same aromatic heterocyclic ring as histidine, acts to out compete weak nickel binding proteins. The amount of imidazole added to the lysis buffer and subsequent wash buffers was optimised from 10mM to 30mM, with hexa-His LIMD1 as the binding substrate, (Figure 3.1.2). Using 10mM imidazole, PHD2 was pulled down in both the presence of the vector only control and hexa-His LIMD1. However, increasing the imidazole concentration to 15-30mM imidazole resulted in only the specific capture of PHD2 in the presence of hexa-His LIMD1 immobilisation by the nickel beads (Figure 3.1.2). The results of this assay further corroborate the specificity of the LIMD1-PHD2 interaction.

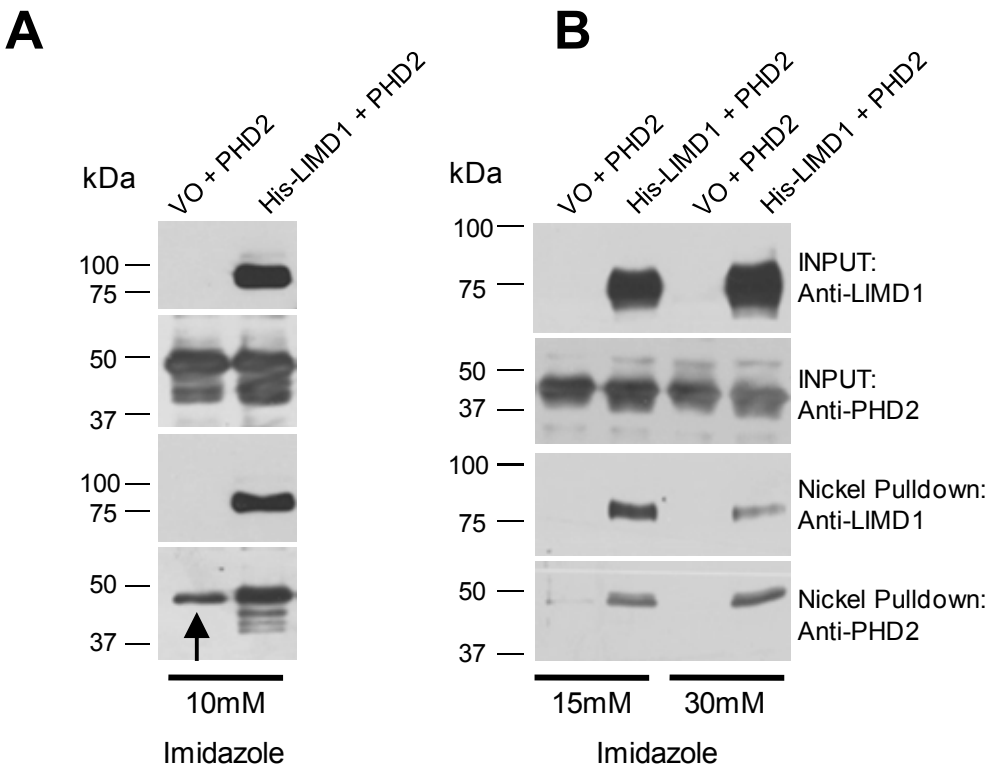

Figure 3.1.2 *PHD2 interacts with LIMD1 captured by nickel-histidine capture assays.*

pcDNA4-His/Max-Topo Vector only and hexa-His LIMD1 were co-transfected with PHD2 into U2OS cells. Lysates were incubated with nickel beads in the presence of imidazole. Imidazole concentration was optimised from 10mM **(A)** to 30mM **(B)**. At 10mM imidazole PHD2 non-specifically bound to the nickel beads (arrow, A). At 15 and 30mM imidazole, PHD2 specifically interacted with hexa-His LIMD1. 2% inputs indicate protein levels prior to nickel bead capture.

3.1.3 LIMD1 interacts with endogenous PHD2 *in vivo*

To detect if *in vivo* co-IPs of ectopically expressed LIMD1 and PHD2 were physiologically relevant, endogenous co-IPs of LIMD1 and PHD2 were performed. Focus was directed towards whether LIMD1 could co-IP endogenous PHD2, as it is believed that PHD2 exhibits the predominant HIF hydroxylase activity *in vivo* (Berra et al., 2003). Endogenous co-immunoprecipitations were performed using complete protease and phosphatase inhibitors. PHD2 was immunoprecipitated using a rabbit polyclonal antibody. PHD2 was chosen rather than LIMD1 for immunoprecipitation as cross reactivity of the rabbit PHD2 antibody with the heavy chain of the IP antibody during immunoblot, impairs the ability to clearly detect the presence of PHD2. As LIMD1 is 72kDa in molecular weight and detected by an antibody raised in mouse, it resolves further from the heavy chain and does not cross react with the IP antibody raised in rabbit, therefore, it was easier to evaluate whether endogenous LIMD1 interacts *in vivo* with PHD2. An isotype control rabbit polyclonal Ab (anti- hemagglutinin [HA], Sigma H6908) was used as a negative control, to ensure for specificity of the interaction of LIMD1 with PHD2. Increased amounts of LIMD1 co-immunoprecipitated with PHD2 than with the isotype control antibody (Figure 3.1.3). This demonstrated that endogenous LIMD1 and PHD2 bind *in vivo*, indicating a physiologically relevant interaction. Furthermore, this highlights the validity of the binding assays previously performed with ectopically expressed proteins.

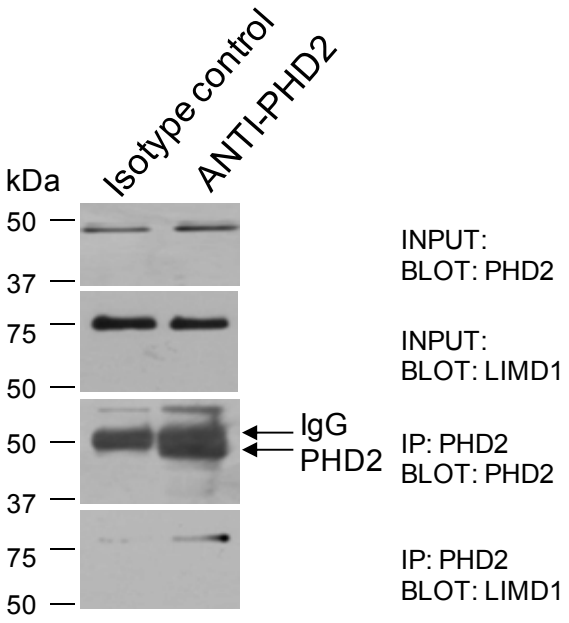

Figure 3.1.3 *Endogenous LIMD1 interacts with endogenous PHD2 in vivo.* U2OS cells were lysed with RIPA buffer and PHD2 immunoprecipitated using 5µg of rabbit polyclonal anti-PHD2. PHD2 immunoprecipitated by the antibody is indicated by arrows, and runs just below the IP antibody heavy chain. Endogenous LIMD1 interacted with endogenous-PHD2 but did not co-IP with the HA isotype control antibody. 2% inputs loaded indicate protein levels prior to addition of the IP antibody.

3.1.4 LIMD1 interacts with PHD1, 2 and 3 *in vitro*

To further verify that LIMD1 interacts with the PHDs, binding assays were performed with GST-LIMD1 fusion proteins and [^{35}S]-methionine labelled PHDs expressed in rabbit reticulocyte lysates *in vitro*. To maximise globin production, rabbit reticulocyte lysates contain minimal cellular proteins except for proteins involved in the transcriptional and translational machinery. Therefore, reticulocyte lysates provide a model environment to indicate whether the nature of a protein-protein interaction may be direct or indirect *via* an additional protein or macromolecule.

GST-LIMD1 and a GST vector only control, propagated in *E.coli* and induced by IPTG administration were immobilised onto glutathione sepharose beads prior to incubation with reticulocyte lysate containing the radiolabelled PHD protein. The beads were pre-blocked and binding assays performed in 5% (w/v) BSA in 1 x PBS to increase specificity and prevent non-specific binding of the radiolabelled protein to the GST fusion protein, the glutathione sepharose or the microcentrifuge tube. To further ensure specificity of the interaction, an excess of the GST vector only protein was used in the assay, demonstrated by a representative coomassie stained acrylamide gel (Figure 3.1.4).

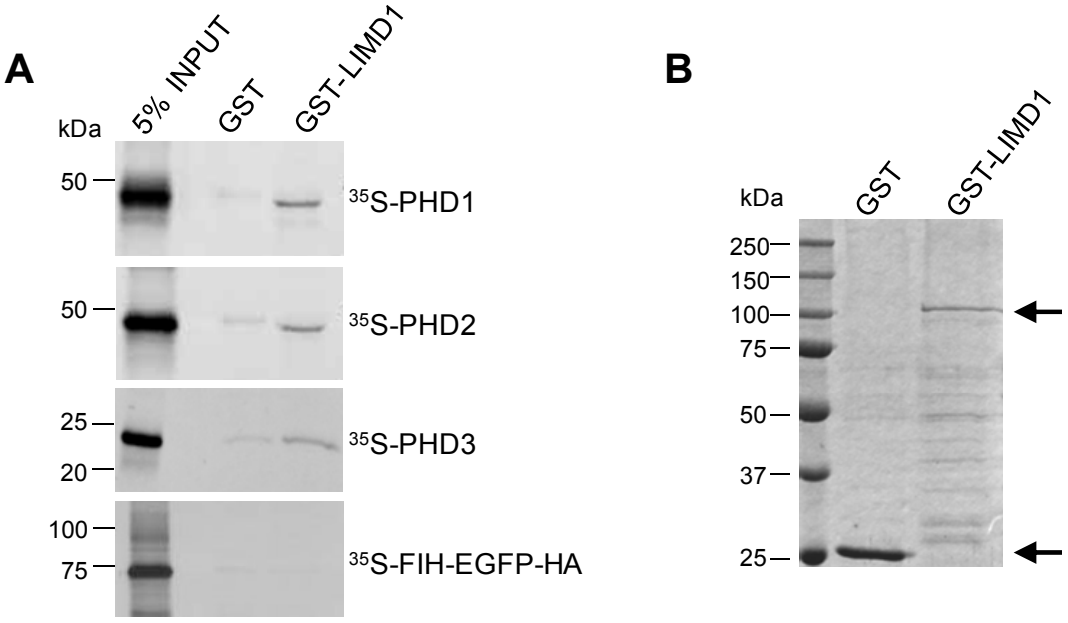

Figure 3.1.4 *LIMD1 interacts with PHD1-3 in vitro.*

Recombinant GST-LIMD1 was immobilised onto glutathione sepharose 4B and incubated with radiolabelled [^{35}S]-PHDs and EGFP-HA-tagged-FIH synthesised *in vitro* using a TNT coupled reticulocyte lysate system. **(A)** GST-LIMD1 specifically and directly binds to PHD1-3 in comparison to the GST only control, detected by autoradiography. 5% of the *in vitro* transcription and translation reaction mixture used in the assay was loaded to confirm the correct molecular weight and estimate the affinity of protein-protein interaction. FIH does not interact with GST-LIMD1 in vitro. **(B)** Representative coomassie stained acrylamide gel, demonstrating loading of GST only and GST-LIMD1 eluted from glutathione sepharose 4B.

PHD1, 2 and 3 all specifically interact with GST-LIMD1 (Figure 3.1.4). This is indicative that the interaction is *via* a direct protein-protein binding event. Whether the closely related asparaginyl hydroxylase FIH interacted with GST-LIMD1 in a similar fashion *in vitro* was further examined. *In vitro* transcribed and translated EGFP-HA-tagged-FIH did not interact with GST-LIMD1, indicating that the observed weak interaction *via* co-immunoprecipitation (Figure 3.1.1.2) may be an indirect protein interaction. This further emphasises the specificity of the direct interaction between LIMD1 with the PHDs.

3.1.5 Mapping of the LIMD1-PHD2 binding interface

The binding interface on LIMD1 within which it interacts with PHD2, the predominant physiological HIF-hydroxylase (Tuckerman et al., 2004; Appelhoff et al., 2004; Berra et al., 2003) was next examined. Constructs encoding Xpress-tagged full length LIMD1, pre-LIM and LIM domains, (Figure 3.1.5 B), were co-transfected with PHD2 to isolate the PHD2 binding region. The LIMD1 proteins were then immunoprecipitated using an Xpress antibody and binding eluates were immunoblotted for the presence of PHD2 co-immunoprecipitation (Figure 3.1.5 A).

The PHD2-LIMD1 interaction was maintained upon deletion of the LIM domains, whilst no co-immunoprecipitation of PHD2 was observed with the LIM domains alone. Therefore, PHD2 specifically interacts with the pre-LIM region of LIMD1 but not the LIM domains alone. The pre-LIM region is not highly conserved amongst other LIM proteins including those within the Zyxin family of LIM proteins. Therefore, this may represent a unique LIMD1-PHD2 binding interface.

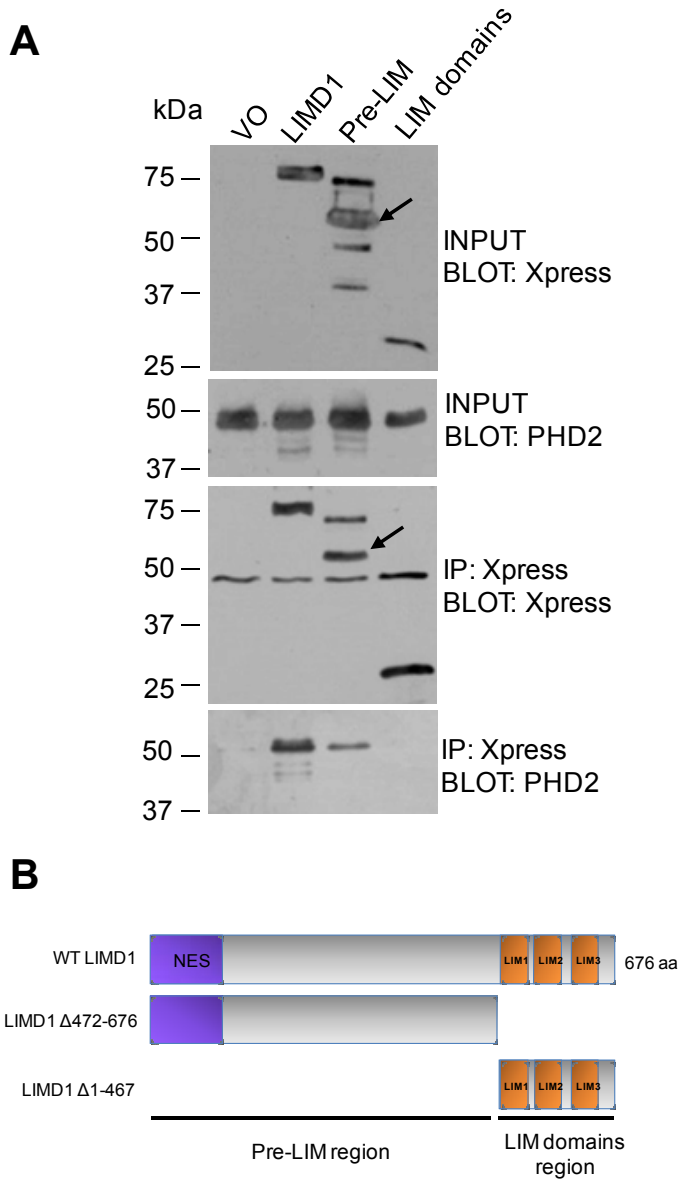

Figure 3.1.5 *LIMD1 interacts with PHD2 via the pre-LIM region.*

(A) Xpress-tagged full length LIMD1 (amino acids 1-676), pre-LIM (Δ472-676) and LIM only (Δ1-467), (illustrated schematically in **B**), were co-transfected with PHD2 into U2OS cells and immunoprecipitated using an Xpress antibody. The correct pre-LIM protein is indicated by the presence of an arrow. Pre-LIM lower molecular weight proteins may represent degradation products. The nature of the higher molecular weight proteins detected is unknown. PHD2 specifically co-immunoprecipitated with the pre-LIM (LIMD1 Δ472-676) construct but not with the LIM domains only construct (LIMD1 Δ1-467). 2% inputs indicate protein levels prior to antibody addition.

3.1.6 The Zyxin family of proteins differentially interact with the PHDs

The ability of the PHDs to interact with the closely related Zyxin LIM proteins, of which all comprise 3 C-terminal LIM domains (Figure 3.1.6.1) was next investigated. Xpress-tagged LIM proteins were co-transfected with each PHD, immunoprecipitated using anti-Xpress and then immunoblotted for the presence of PHD co-immunoprecipitation.

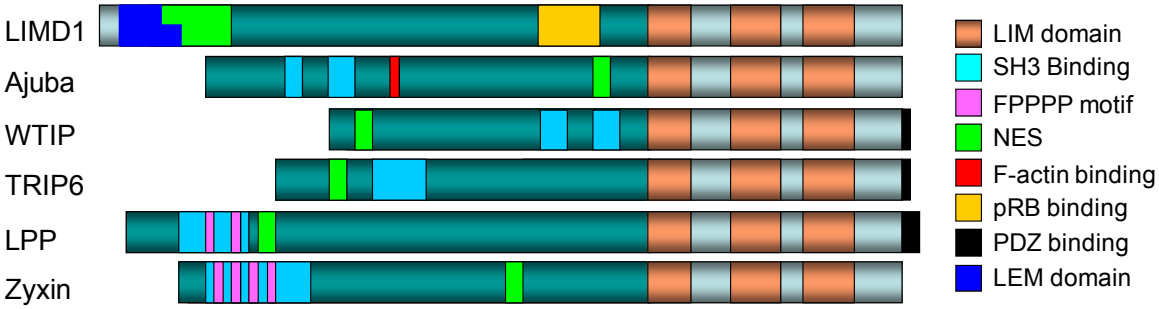

Figure 3.1.6.1 *Zyxin family of LIM proteins.*
Schematical representation of the Zyxin family of LIM proteins. The Zyxin family all comprise 3 C-terminal LIM domains, but have non-conserved pre-LIM regions containing an array of non-catalytic associated domains.

Co-IP experiments demonstrated that PHD2 only interacts with LIMD1 and not with the other Zyxin family proteins (Figure 3.1.6.2). This further emphasises the specificity of the interaction. This also corroborates the finding that PHD2 interacts with the non-conserved pre-LIM region of LIMD1 (Figure 3.1.6.2), indicating that this binding domain may be unique to LIMD1 within this family of proteins.

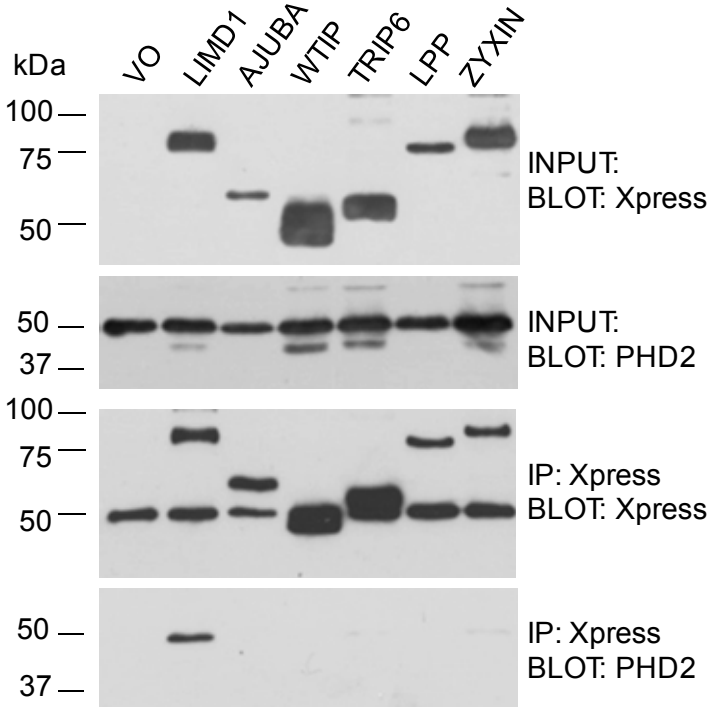

Figure 3.1.6.2 *PHD2 only interacts with LIMD1 of the Zyxin LIM proteins in vivo.*

Xpress-tagged Zyxin family LIM proteins were co-transfected with PHD2 into U2OS cells and immunoprecipitated using an Xpress antibody. PHD2 only interacted with LIMD1. 2% inputs indicate protein levels prior to antibody addition.

Whether PHD1 and PHD3 interact with multiple Zyxin proteins was next examined. PHD1 interacted with all of the LAW sub-family of Zyxin proteins (LIMD1, Ajuba and WTIP) in addition to TRIP6 (Figure 3.1.6.3). Interestingly, TRIP6 appeared to induce a modification of PHD1, resulting in a higher molecular weight form detected by the PHD1 antibody, (Figure 3.1.6.3, arrows). Furthermore, TRIP6 only interacted with this heavier PHD1 form and not the wild type protein (Figure 3.1.6.3, arrows). The nature of this modification and interaction are yet to be elucidated.

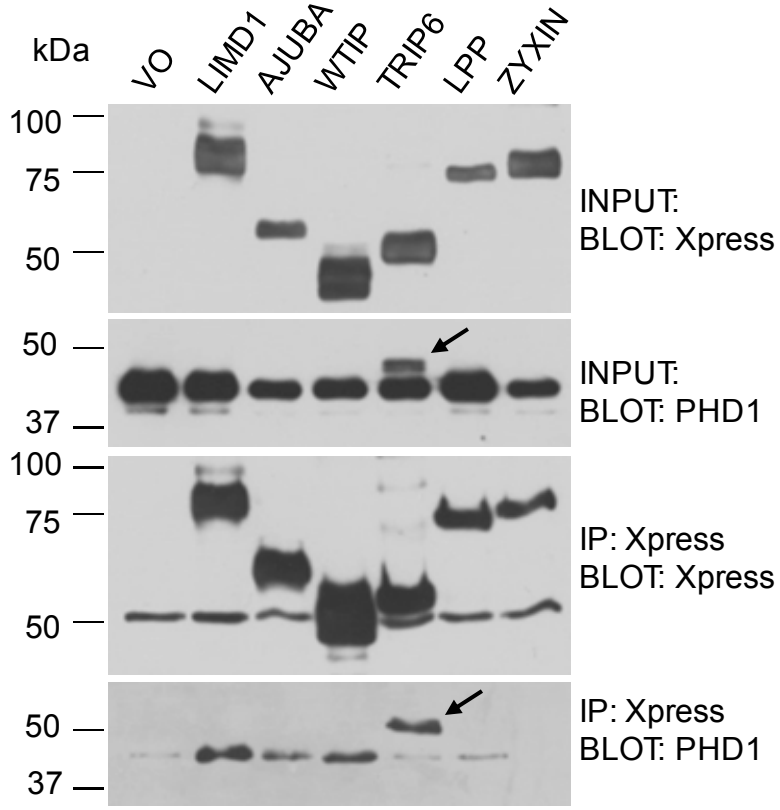

Figure 3.1.6.3 *PHD1 interacts with multiple Zyxin LIM proteins in vivo.*
Xpress-tagged Zyxin family LIM proteins were co-transfected with PHD1 into U2OS cells and immunoprecipitated using an Xpress antibody. PHD1 interacted with LIMD1, Ajuba and WTIP. TRIP6 induced a PHD1 modification, indicated by arrows, shown in the PHD1 input, and interacted with this higher molecular weight PHD1 form. 2% inputs indicate protein levels prior to antibody addition.

PHD3 also interacted with all three of the LAW proteins (LIMD1, Ajuba and WTIP) but not the other Zyxin family proteins (LPP, TRIP6 and Zyxin) (Figure 3.1.6.4). Therefore, these data indicate that the PHDs interact differentially with the LAW sub-family of proteins and therefore, presumably *via* different binding interfaces. It is possible that PHD1 and PHD3 interact with the LAW proteins *via* a conserved domain. There is a precedent for the LAW sub-family to share interacting partners *via* their highly conserved LIM domains, as all three proteins have been demonstrated to interact with a set of Snail/Slug transcriptional corepressors (introduction section 1.4) (Langer et al., 2008)

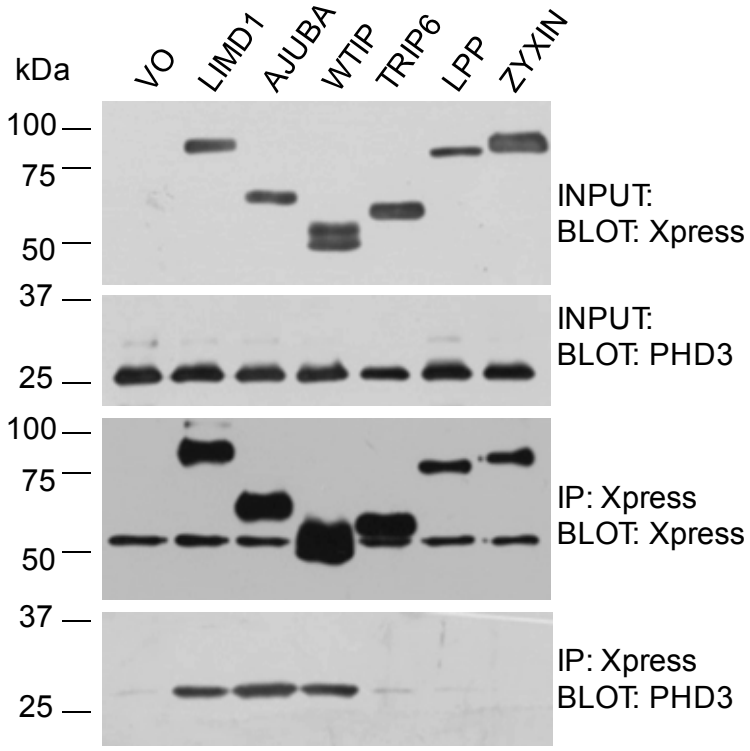

Figure 3.1.6.4 *PHD3 interacts with LIMD1, Ajuba and WTIP in vivo.*
Xpress-tagged Zyxin family LIM proteins were co-transfected into U2OS cells with PHD3 and immunoprecipitated using an Xpress antibody. PHD3 co-immunoprecipitates with all three LAW proteins but not Zyxin, LPP or TRIP6. 2% inputs indicate protein levels prior to antibody addition.

3.2 LIMD1 (and LAW) interact with VHL *in vivo*

3.2.1 LIMD1 interacts with VHL *in vivo*

As LIMD1 (and the LAW proteins) interacted with the PHD enzymes it was next examined whether LIMD1 could also interact with VHL, the recognition component of an E3 ubiquitin ligase complex responsible for HIF1α ubiquitylation in response to proline 402 and 564 hydroxylation (as described in introduction section 1.10).

Xpress-tagged LIMD1 was co-transfected with V5-tagged VHL in U2OS cells. 48 hours post-transfection, the cells were harvested in RIPA buffer and LIMD1 immunoprecipitated with a LIMD1 mAb. VHL specifically interacted with LIMD1 (Figure 3.2.1).

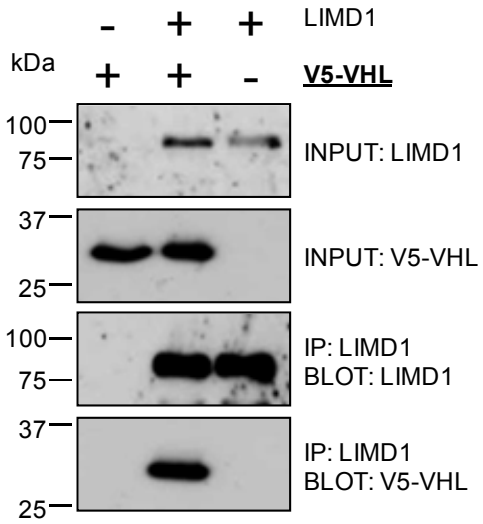

Figure 3.2.1 *LIMD1 interacts with VHL in vivo.*
Xpress-tagged LIMD1 was co-transfected with VHL in U2OS cells. LIMD1 was immunoprecipitated with a LIMD1 mAb. VHL specifically interacts with LIMD1. 2% inputs indicate protein levels prior to antibody addition.

3.2.2 Nickel-Histidine capture assays confirm LIMD1-VHL interaction

Nickel bead pulldowns were employed to confirm the interaction between LIMD1 and VHL. The amount of imidazole was again optimised to observe an optimal interaction without non-specific binding. At 2mM imidazole both endogenous (in the vector only control) and exogenous hexa-His-LIMD1 were captured by the nickel beads and therefore, VHL was pulled down in the negative vector only control (Figure 3.2.2). At 5 and 10mM imidazole, endogenous LIMD1 was not captured by the nickel beads and V5-VHL interaction was only observed upon hexa-His-LIMD1 expression. This further confirms that LIMD1 and VHL interact *in vivo*.

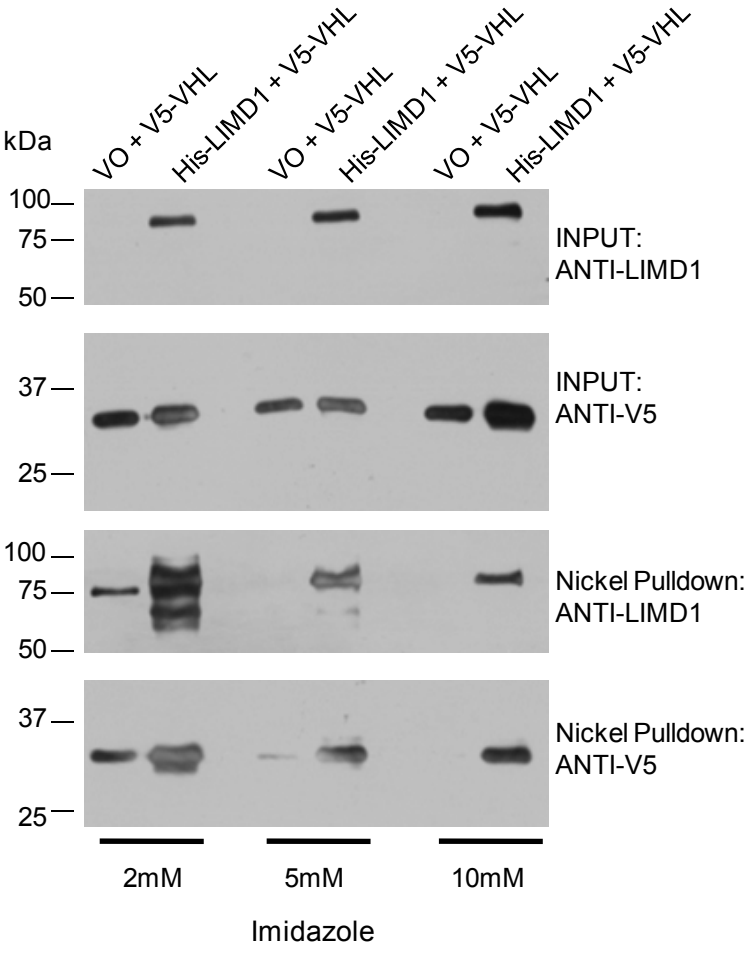

Figure 3.2.2 *VHL interacts with LIMD1 captured by nickel-histidine capture assays.*

pcDNA4-His/Max-Topo vector only and hexa-His LIMD1 were co-transfected with VHL into U2OS cells. Lysates were incubated with nickel beads in the presence of imidazole. VHL specifically interacted with hexa-His LIMD1 at 5 and 10mM imidazole concentrations. 2% inputs indicate protein levels prior to nickel bead capture.

3.2.3 Mapping of the LIMD1-VHL binding interface

The specific VHL binding region of LIMD1 was analysed by immunoprecipitating the pre-LIM and LIM only mutants in the presence of VHL (Figure 3.2.3). Deletion of the LIM domains completely ablated the interaction between LIMD1 and VHL, whilst the LIM domains alone are necessary and sufficient for the interaction (Figure 3.2.3).

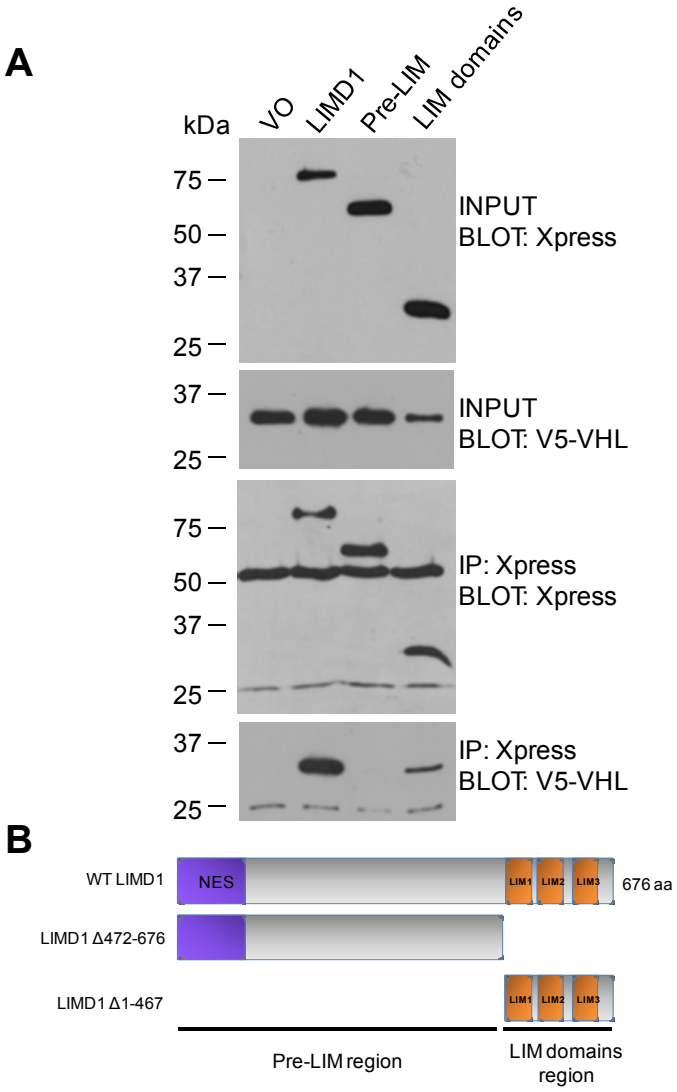

Figure 3.2.3 *LIMD1 interacts with VHL via the LIM domains.*

(A) Xpress-tagged LIMD1, pre-LIM and LIM only, (illustrated schematically in **B**), were co-transfected with VHL into U2OS cells and immunoprecipitated using an Xpress antibody. VHL specifically co-immunoprecipitated with the LIM domains alone (LIMD1 Δ1-467) construct and not to the pre-LIM region (LIMD1 Δ472-676). 2% inputs indicate protein levels prior to antibody addition.

As VHL and PHD2 interacted with LIMD1 *via* the LIM domains and pre-LIM respectively, this indicated that LIMD1 may act as a scaffold to link both enzymatic activities. LIM and pre-LIM regions in general have unique non-overlapping binding partners and therefore, commonly act as scaffolding proteins able to link distinct proteins and functions (Feng and Longmore, 2005; Kadrmas and Beckerle, 2004). Therefore, it was postulated whether LIMD1 may interact with both the PHDs and VHL, representing a novel LIMD1 mediated functional complex, bridging an association between PHD and VHL, thus enhancing their function by increasing their physical proximity. Moreover, there is a precedent for the requirement of protein scaffolds which bridge associations between HIFα and the PHDs (Baek et al., 2005), and HIFα and VHL (Jeong et al., 2002). However, no adaptor proteins have been described able to simultaneously interact with the PHDs and VHL. Whether LIMD1 is able to fulfil such a function was further examined (section 3.2.6).

3.2.4 The LAW sub-family of Zyxin proteins interact with VHL *in vivo*

As LIMD1 interacts with VHL *via* the highly conserved LIM domains region, the ability of the other LAW proteins, Ajuba and WTIP to interact with VHL was next examined. Xpress-tagged Zyxin family proteins were all co-transfected into U2OS with VHL and immunoprecipitated using an anti-Xpress mAb (Figure 3.2.4). VHL co-immunoprecipitated with all three LAW proteins, but not with LPP or Zyxin. Trip6 appeared to demonstrate a weak interaction with VHL (Figure 3.2.4).

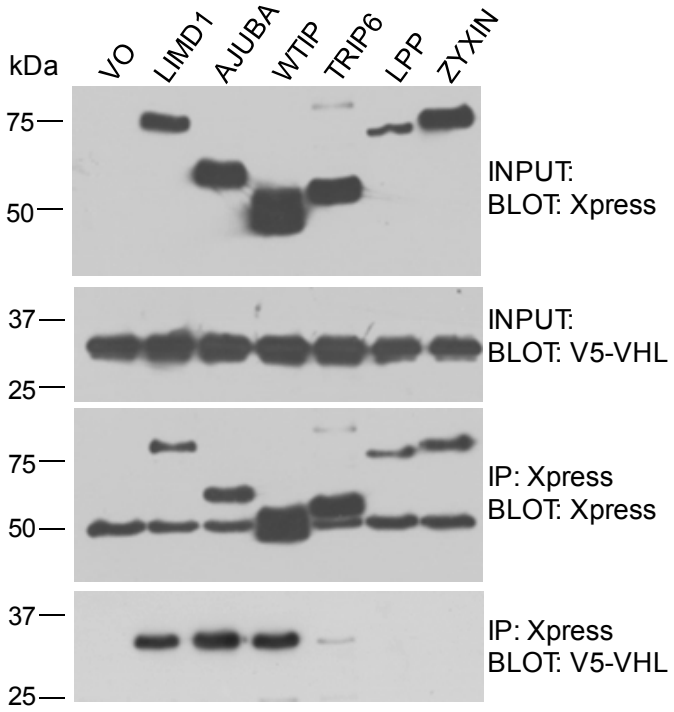

Figure 3.2.4 *VHL interacts with LIMD1, Ajuba and WTIP in vivo.*
Xpress-tagged Zyxin family LIM proteins were co-transfected into U2OS cells with PHD3 and immunoprecipitated using an anti-Xpress antibody. VHL co-immunoprecipitated with all three LAW proteins but not LPP or TRIP6. Trip6 demonstrated a weak binding affinity interaction. 2% inputs indicate protein levels prior to antibody addition.

The conserved function of the LAW proteins to interact with VHL and differentially interact with the PHDs indicates a cooperative mechanism where by the LAW proteins may link PHD/VHL enzymatic activities. TRIP6 interacted with a higher molecular weight form of PHD1 and arguably interacted to a degree with VHL but to a much lesser degree than the LAW proteins. Whether the ability of LAW to interact with the PHDs and VHL translates to a regulatory effect on HIF1 function was next examined.

3.2.5 The LIMD1-VHL interaction cannot be detected by *in vitro* binding assays.

In vitro binding assays were performed in order to evaluate whether LIMD1 interacts directly with VHL. The assay was performed as described for the PHD binding assays (section 3.1.3), immobilising GST-LIMD1 and GST only onto glutathione sepharose beads prior to incubation with radiolabelled [^{35}S]-VHL expressed *in vitro* in rabbit reticulocyte lysate (Figure 3.2.5.1).

The expression level of the radiolabelled VHL transcribed and translated *in vitro*, detected by autoradiography was markedly less than the expression detected with the PHD proteins (Figure 3.2.5.1). Increasing the quantity of plasmid DNA into the *in vitro* transcription and translation reaction did not significantly increase the levels of VHL expression. Therefore, it was not possible to evaluate whether the observed *in vivo* interaction with LIMD1 *via* co-immunoprecipitation is direct or indirect, due to the low expression level and therefore quantity of VHL in the binding assay. Proteins have been identified that have proven problematic to express *in vitro*, particularly those in excess of 100kDa or smaller than 15kDa in molecular weight. VHL isoforms are relatively small in molecular weight ranging between 18-24kDa, which may account for the low expression level as it is believed that small proteins are degraded by a ubiquitin-dependent pathway within the rabbit reticulocyte lysate. Optimisation of the potassium and magnesium

concentrations of the reaction buffer of the *in vitro* rabbit reticulocyte transcription and translation reaction has been reported to modulate *in vitro* expression levels (Craig et al., 1992) and the use of protease and proteasome inhibitors should be considered for future research.

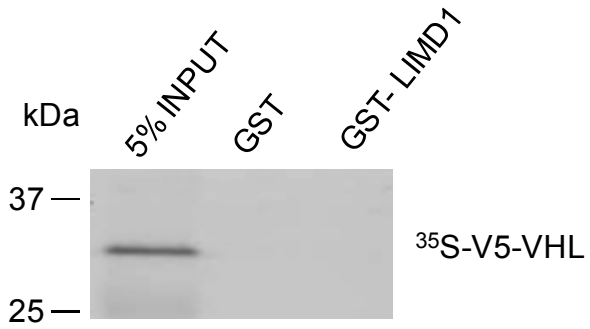

Figure 3.2.5.1 *In vitro LIMD1-VHL interaction assay.*
Recombinant GST-LIMD1 was immobilised onto glutathione sepharose 4B beads and incubated with radiolabelled [^{35}S]-VHL synthesised *in vitro* using a TNT coupled reticulocyte system. 5% of the *in vitro* transcription and translation reaction mixture used in the assay was loaded to confirm the correct molecular weight and estimate the affinity of protein-protein interaction. No VHL interaction with GST-LIMD1 can be observed by autoradiography.

VHL is the recognition component of the ubiquitin ligase complex comprising elongin B and C, Cullin2 and the ring finger protein Rbx. To identify whether Cullin2 also interacts with LIMD1 and may potentially bridge the interaction between LIMD1 and VHL, an *in vitro* GST-LIMD1 pulldown assay was performed with U2OS cell extracts ectopically expressing V5-Cullin2 alongside a positive control pulldown with V5-VHL (Figure 3.2.5.2). These assays corroborate the binding of VHL to LIMD1 but demonstrate that LIMD1 does not interact with Cullin2 and therefore, Cullin2 does not facilitate the LIMD1-VHL interaction. This suggests that association of LIMD1 with VHL may be mediated by another protein in the multi-protein complex such as the elongin proteins or may be a direct protein-protein interaction.

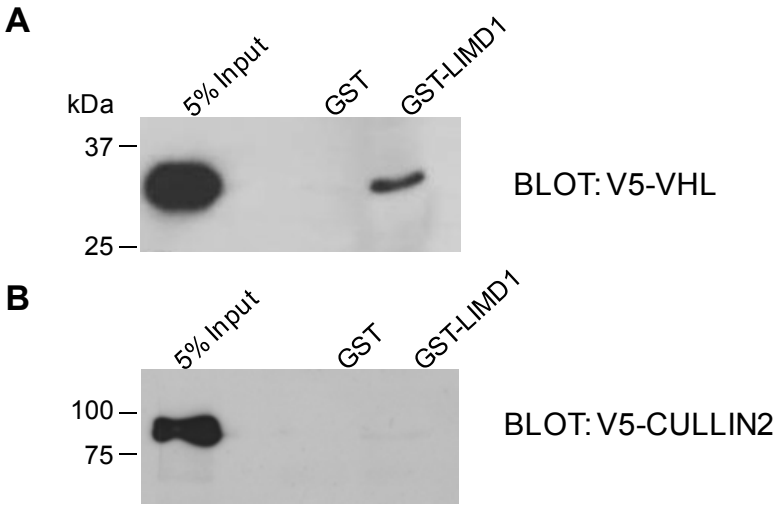

Figure 3.2.5.2 *LIMD1 does not interact with Cullin2.*

Recombinant GST-LIMD1 was immobilised onto glutathione sepharose 4B beads and incubated with U2OS extract ectopically expressing V5-tagged VHL and Cullin2. 5% of the lysate used in the assay was loaded to confirm the correct molecular weight and estimate the affinity of protein-protein interaction. Immunoblot demonstrates that VHL interacts with GST-LIMD1 in U2OS cell extracts, however this interaction is not mediated by Cullin2 as no interaction can be observed with GST-LIMD1.

3.2.6 LIMD1 simultaneously interacts with PHD2 and VHL

As LIMD1 is able to interact with both PHD2 and VHL *via* different binding interfaces it was postulated that LIMD1 may simultaneously scaffold both proteins, to increase their local concentration and therefore augment HIF1α degradation. This hypothesis was tested by co-transfecting all three proteins to see whether LIMD1 could simultaneously co-immunoprecipitate both PHD2 and VHL. This was indeed the case, LIMD1 interacted with both proteins individually and when co-transfected together, indicating an ability to simultaneously interact with PHD2 and VHL (Figure 3.2.6.1). Notably, binding of both proteins to LIMD1 does not impair the ability of either to interact with LIMD1 (Figure 3.2.6.1).

This result may have been due to LIMD1 simultaneously interacting with PHD2 and VHL (Figure 3.2.6.1 C), however it may reflect two distinct populations of LIMD1 binding PHD2 and VHL individually (Figure 3.2.6.1 D). Therefore, the ability of LIMD1 to scaffold both proteins, thus enabling an interaction between VHL and PHD2 was examined. All three proteins were co-transfected, and V5-VHL was immunoprecipitated with a V5 mAb. A barely detectable degree of interaction was observed between PHD2 and VHL in the absence of ectopic LIMD1 expression, which may have been due to the scaffolding action of endogenous LIMD1 (Figure 3.2.6.2). However, co-transfection of LIMD1, resulted in a significant increase in co-IP of PHD2 with VHL, corroborating our hypothesis that LIMD1 acts as an adaptor forming a ‘normoxic protein complex’ (normoxiplex) (Figure 3.2.6.2). To our knowledge this is the first report of a protein that can bind all three PHDs in addition to simultaneously binding PHD2 and pVHL, and is the first demonstration that these two HIF1α post-translational modifiers may exist within the same protein complex.

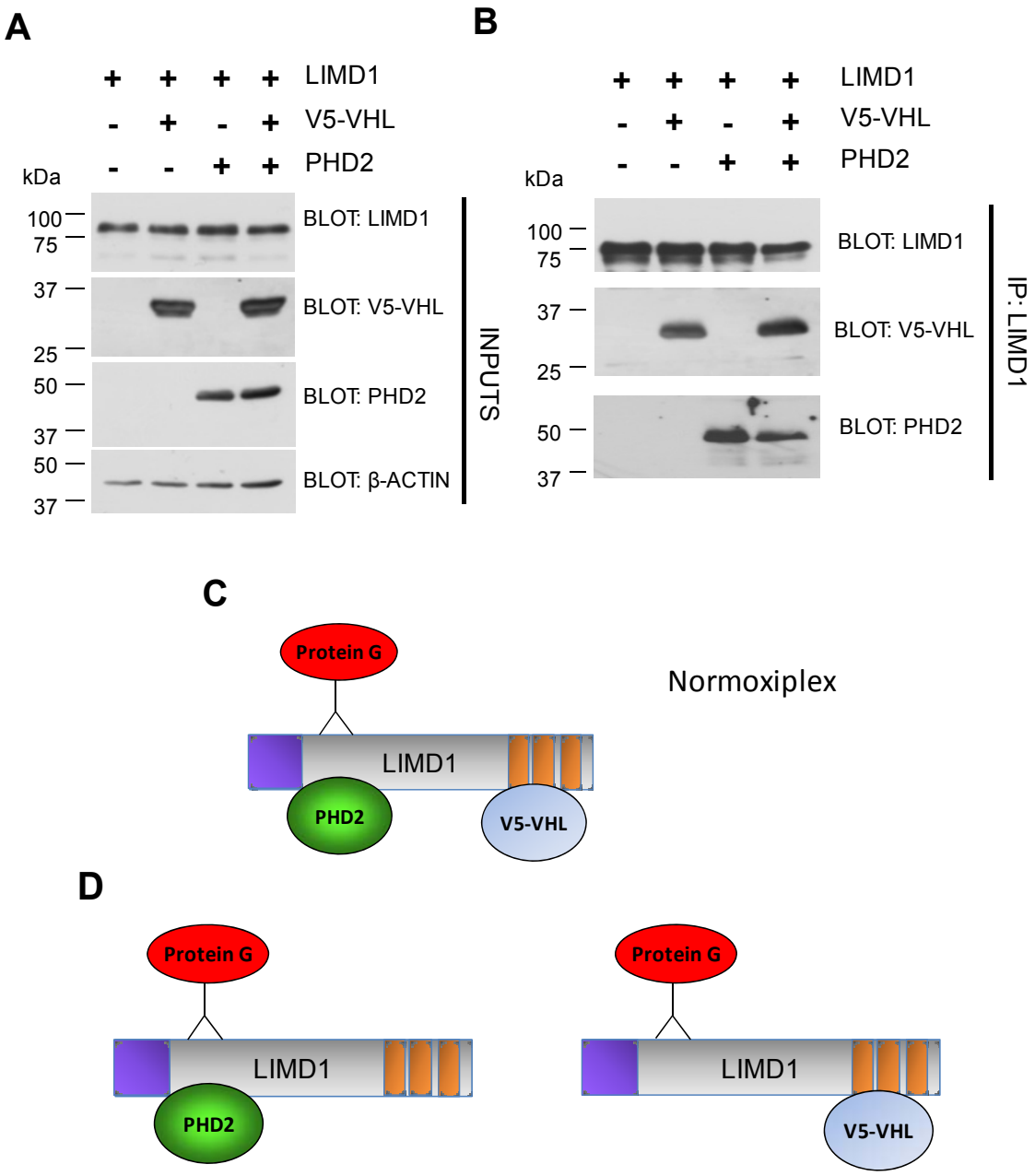

Figure 3.2.6.1 *LIMD1 interacts with PHD2 and VHL in vivo.*

Xpress-tagged LIMD1 was co-transfected into U2OS cells with V5-VHL and PHD2. LIMD1 was immunoprecipitated using a LIMD1 mAb. **(A)** 2% inputs indicate protein levels prior to antibody addition. **(B)** LIMD1 interacted with both VHL and PHD2 simultaneously. Furthermore, simultaneous binding of both proteins to LIMD1 does not impair the others ability to bind to LIMD1. **(C)** Schematic representation, indicating immunoprecipitation of LIMD1 and the simultaneous binding of PHD2 to the pre-LIM and VHL to the LIM domains. **(D)** Schema representing the possibility that distinct populations of LIMD1 individually binding PHD2 and VHL may exist.

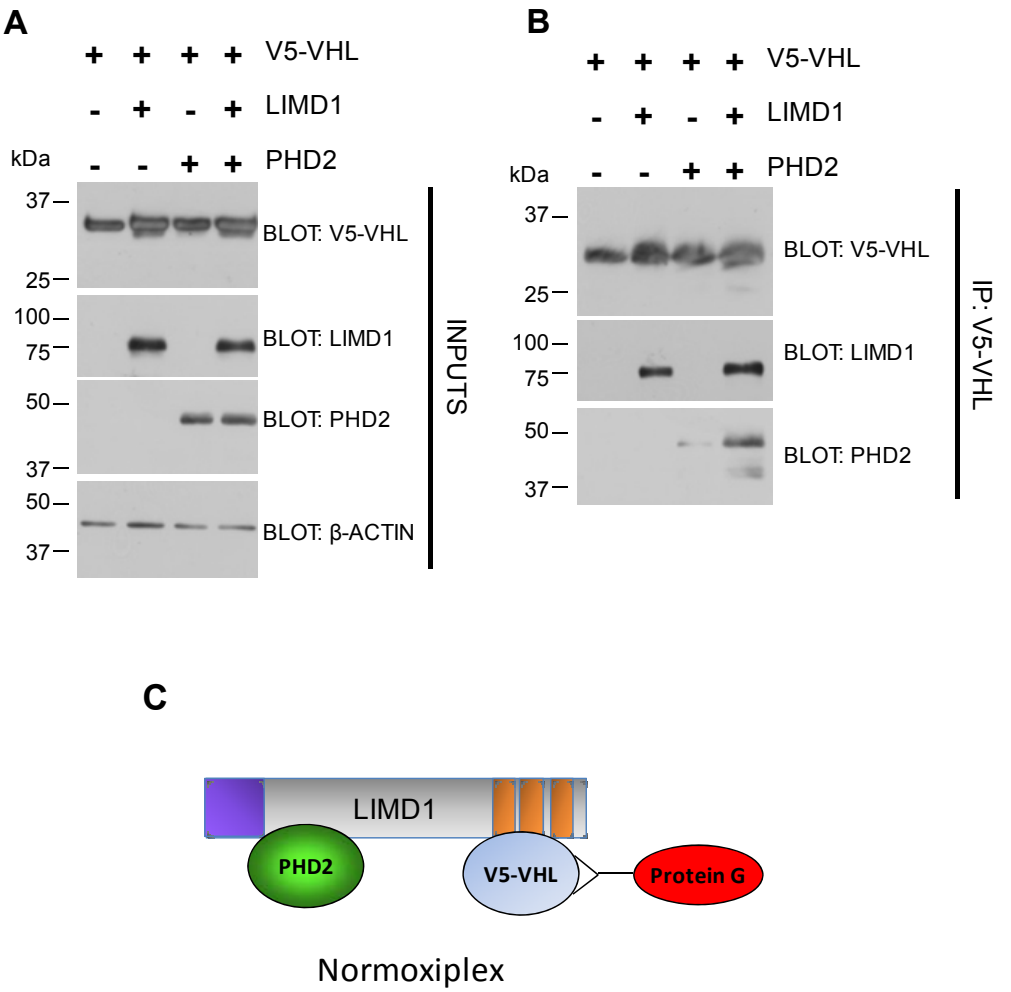

Figure 3.2.6.2 *LIMD1 acts as a scaffold, simultaneously binding PHD2 and VHL in vivo.*

V5-VHL was co-transfected with PHD2 and LIMD1. V5-VHL was immunoprecipitated using a V5 mAb. **(A)** 2% inputs indicate protein levels prior to antibody addition. **(B)** LIMD1 significantly increased the interaction between VHL and PHD2. In the absence of LIMD1 only a small degree of binding can be observed. **(C)** Schematic representation, indicating immunoprecipitation of V5-VHL, and the ability of LIMD1 to scaffold PHD2 within a protein complex.

3.3. LIMD1 does not interact with HIF1α

3.3.1 LIMD1 does not interact with HIF1α in normoxia or hypoxia

The ability of LIMD1 to simultaneously interact with PHD2 and VHL suggested that LIMD1 may form a complex with HIF1α to enhance its degradation and thus induce subsequent attenuation of HIF specific gene transcription. Therefore, whether LIMD1 was able to also interact with HIF1α was next investigated.

Firstly, *in vitro* binding assays of [^{35}S]-HIF1α with GST-LIMD1 were utilised. However, these pulldown assays did not conclusively show whether LIMD1 interacts with HIF1α, due to a high background binding of labelled HIF1α to the GST only control (Figure 3.3.1).

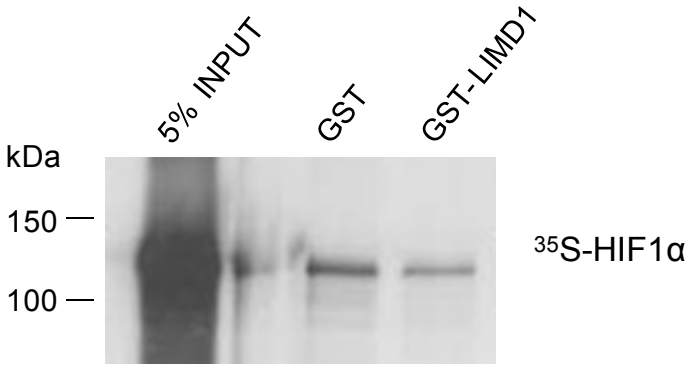

Figure 3.3.1 *In vitro GST-LIMD1 binding assays are inconclusive with regards to the LIMD1-HIF1α interaction.*
Recombinant GST-LIMD1 was immobilised onto glutathione sepharose 4B beads and incubated with radiolabelled [^{35}S]-HIF1α synthesised *in vitro* using a TNT coupled reticulocyte system. 5% of the *in vitro* transcription and translation reaction mixture used in the assay was loaded to confirm the correct molecular weight and estimate the affinity of protein-protein interaction demonstrated by autoradiography. HIF1α interacted non-specifically with the GST alone; therefore, it is inconclusive whether LIMD1 and HIF1α interact *in vitro*.

Therefore, *in vivo* co-IP experiments with ectopically expressed HIF-1α and LIMD1 were performed. Due to the instability of HIF1α in normoxia, co-IP reactions were performed with hypoxic cell lysates or normoxic cell lysates treated with proteasome inhibitor MG-132 upon lysis. Under both normoxic and hypoxic conditions, no *in vivo* interaction between HIF1α and LIMD1 was observed (Figure 3.3.1.1).

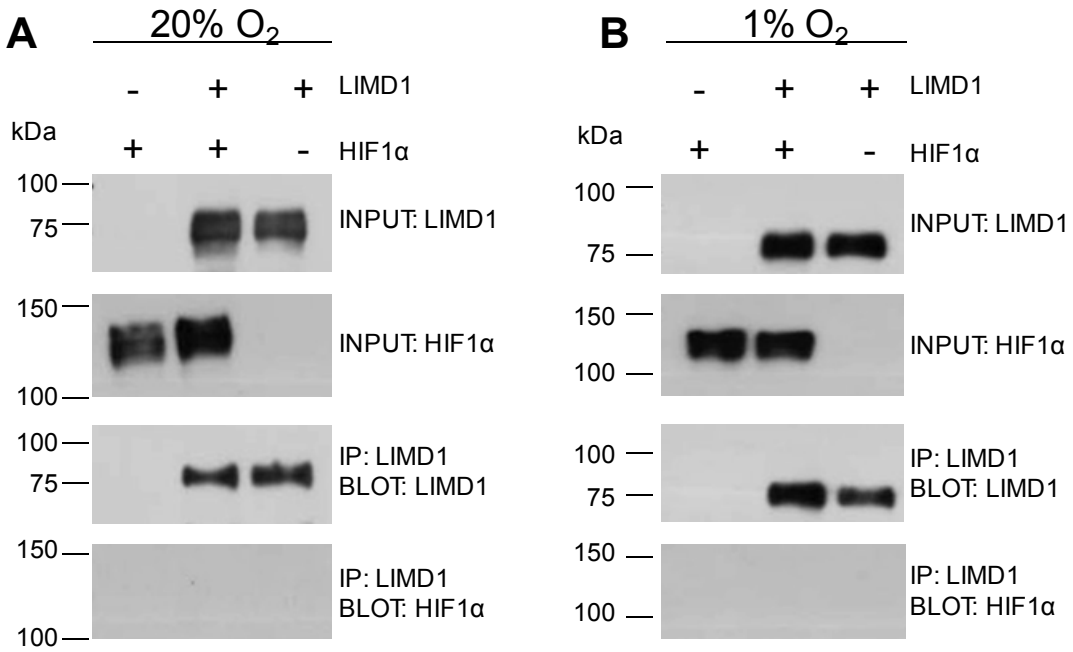

Figure 3.3.1.1 *LIMD1 does not co-immunoprecipitate with HIF1α in vivo.*
Xpress-tagged LIMD1 was co-transfected into U2OS cells with V5-HIF1α and immunoprecipitated using a LIMD1 mAb. **(A)** Cells were incubated for 16 hours at normoxia (20% O_2) or **(B)** hypoxia (1% O_2). Cells were lysed with 10μM MG-132 to prevent 26-proteasomal mediated HIF1α degradation. Lysates were incubated with antibody-protein G conjugates for 4 hours to minimise HIF1α degradation. No co-IP of LIMD1 with HIF1α in either normoxia or hypoxia could be observed. 2% inputs indicate protein levels prior to antibody addition.

3.3.2 LIMD1 does not interact with the amino, carboxyl or ODD domains of HIF1α *in vivo*

Although no co-IP could be detected between LIMD1 and full length HIF1α, it is possible that LIMD1 may interact with a concealed binding interface. Therefore, to detect if LIMD1 binds to a hidden binding domain in the full length HIF-1α protein, HIF1α mutants which dissect the proteins into three domains were used in co-IP experiments with LIMD1, immunoprecipitating LIMD1 with a LIMD1 mAb. LIMD1 was co-transfected into U2OS with the stable N-terminal domain (aa30-389), C-terminal domain (aa630-826), and the oxygen dependent degradation domain (ODD aa390-652) of which is sensitive to PHD/VHL mediated degradation (Huang et al., 1998) (Figure 3.3.2 B). 32 hours post-transfection, cells were incubated for 16 hours at 1% O_2 to accumulate the ODD domain sensitive to oxygen dependent degradation. LIMD1 did not bind any of the three domains of HIF1α (Figure 3.3.2).

This therefore, indicated that LIMD1 does not directly interact with HIF1α. However, if LIMD1 acts to scaffold PHD and VHL, increasing their efficiency in targeting HIF1α for degradation then it may be difficult to capture the transient LIMD1-PHD-VHL-HIF1α ternary complex. Although no co-IP could be observed, the protein levels of the ODD domain were markedly reduced upon co-transfection with LIMD1 (Figure 3.3.2, arrows). This indicated that LIMD1 may augment degradation of the ODD domain, fitting with the hypothesis that LIMD1 acts to bridge the hydroxylase and ubiquitylation activities. The specific effects of LIMD1 (and LAW) on the ODD domain were next examined.

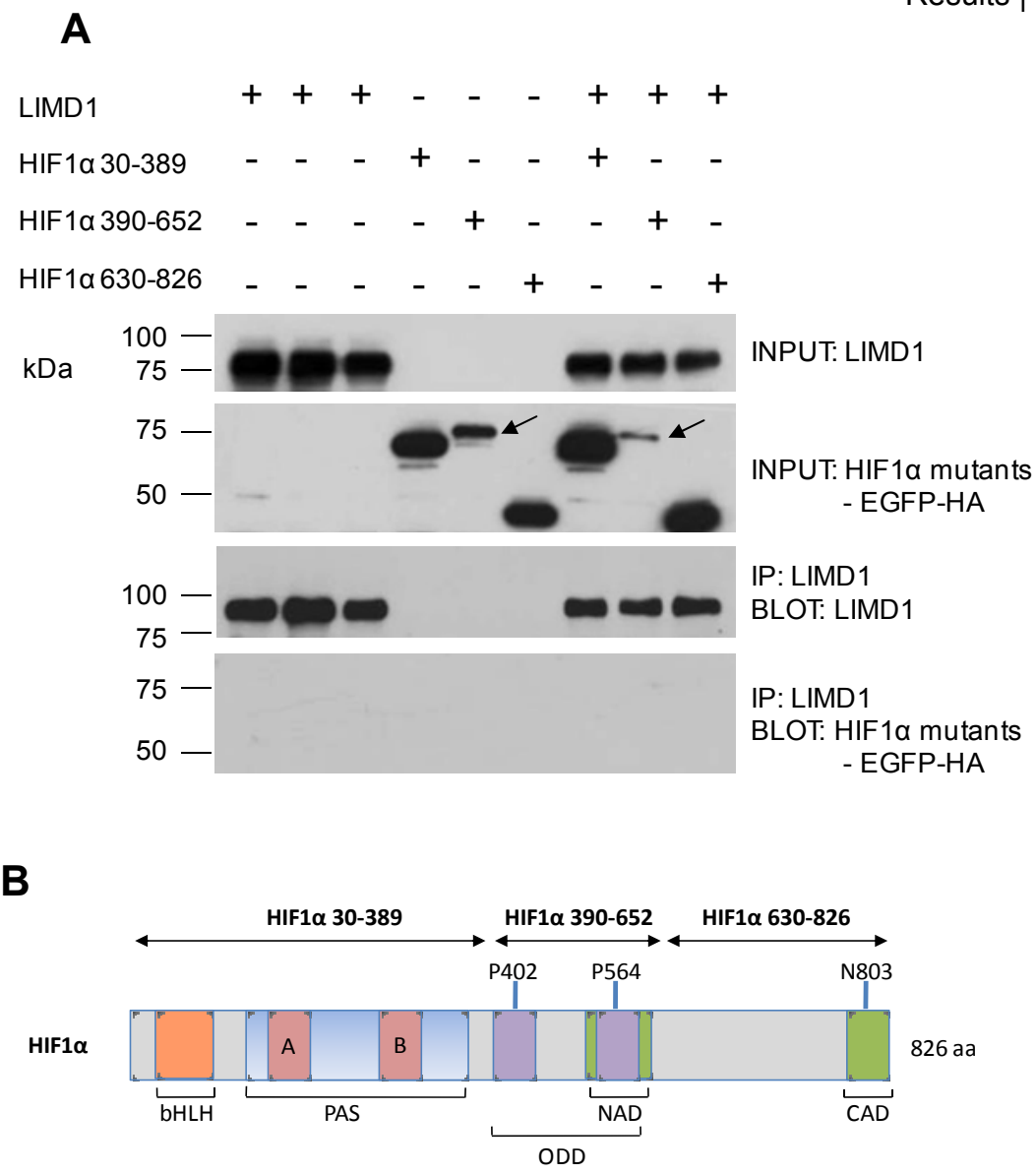

Figure 3.3.2 *LIMD1 does not co-immunoprecipitate with the amino, carboxyl or ODD domains of HIF1α in isolation.*

(A) Xpress-tagged LIMD1 was co-transfected into U2OS cells with EGFP-HA tagged HIF1α N-terminal (aa30-389), ODD (aa390-652) and C-terminal (aa630-826) domains and LIMD1 was immunoprecipitated with a mAb. To stabilise sufficient HIF1α ODD domain protein and evaluate the co-immunoprecipitated complex, cells were incubated for 16 hours at 1% O_2. Cells were lysed with 10μM MG-132 to prevent 26-proteasomal HIF1α degradation. Lysates were incubated with antibody-protein G conjugates for 4 hours to minimise HIF1α degradation. No co-IP of LIMD1 with any of the HIF1α domains was observed. However, LIMD1 expression results in reduced ODD protein levels, indicated by arrows. 2% inputs indicate protein levels prior to antibody addition. **(B)** Schematic depiction of the HIF1α domain structure.

3.4 Summary

In this chapter, the preliminary work which indicated an interaction between PHD1 and LIMD1 observed from a Y2H screen was validated. Furthermore, LIMD1 and closely related LIM proteins of the LAW subfamily differentially interact with all three of the PHDs *in vivo*. *In vitro* binding assays indicate that LIMD1 interacts with all three PHDs *via* a direct protein-protein binding event. Furthermore, VHL also interacts with the LAW proteins. Moreover, LIMD1 simultaneously interacts with PHD2 *via* its pre-LIM N-terminal region and VHL *via* its LIM domains, scaffolding the proteins within a normoxic protein complex (normoxiplex).

CHAPTER 4: RESULTS

LIMD1 induces HIF1α protein degradation

4. LIMD1 induces HIF1α protein degradation

4.1 LIMD1 induces specific degradation of the HIF1α ODD domain

Data presented in the previous chapter demonstrates that LIMD1 does not co-immunoprecipitate *in vivo* with full length HIF1α or when HIF1α is dissected into 3 domains; the N-terminal domain (aa30-389), the ODD domain (aa390-652) or the C-terminal domain (aa630-826) (Figure 3.3.2). However, upon analysis of this experiment it was observed that ectopic LIMD1 expression induced a specific reduction in ODD domain protein levels, notably the domain sensitive to O_2 dependent, PHD and pVHL mediated degradation (Huang et al., 1998). This supports the hypothesis that LIMD1 (and LAW) scaffolds PHD2 and VHL to enhance HIF1α degradation. Further experiments were performed to verify whether this effect was specific and consistent. The experiment was performed following 16 hour hypoxic (1% O_2) incubation in order to impair PHD/VHL mediated degradation of the ODD and therefore allow analysis of the effect of the LIM proteins LIMD1 and TRIP6 on ODD stability. The LIM protein TRIP6, which interacts with PHD1 but not VHL was also used to evaluate whether regulation of ODD protein levels require VHL binding/activity. LIMD1 specifically induced ODD degradation, whilst N and C-terminal domains were stable and unaffected by LIMD1 expression levels (Figure 4.1). TRIP6 did not induce ODD degradation and thus indicates that the ability to interact with both PHD and VHL proteins, rather than just PHD1, is required in order to modulate ODD stability. Therefore, this is indicative that TRIP6 does not enhance PHD1 hydroxylation of HIF1α, but may modulate a non-HIF dependent PHD1 function. One such reported example is the role of PHD1 in modulating NF-κB activity by binding and inhibiting IKKβ (Cummins et al., 2006).

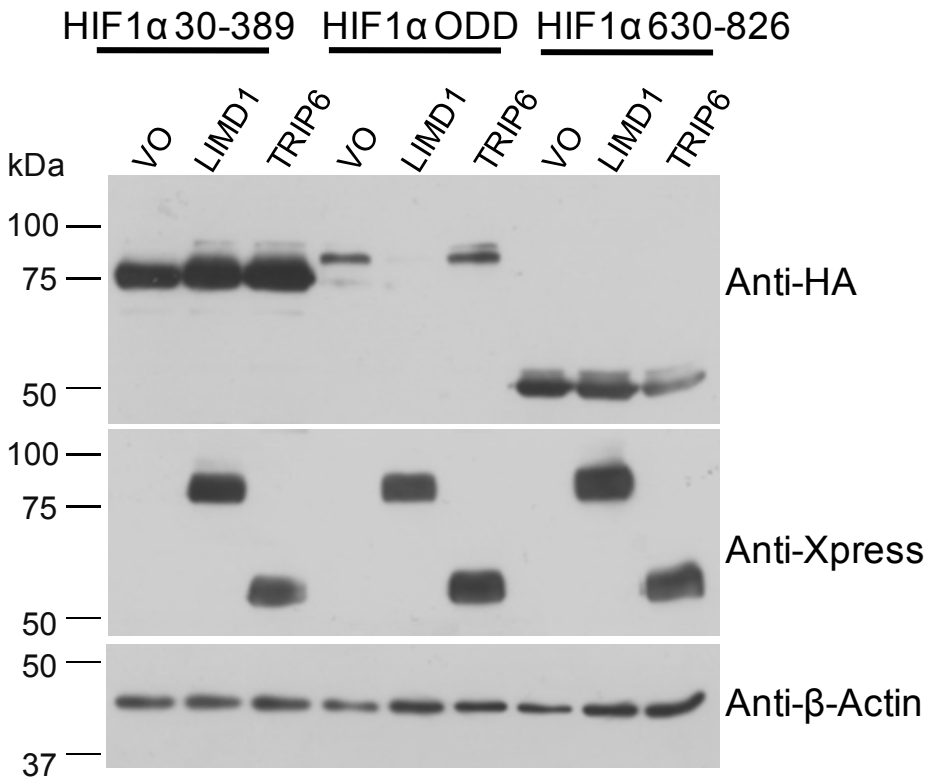

Figure 4.1 *LIMD1 expression induces a specific reduction in HIF1α ODD protein levels.*

U2OS cells were co-transfected with the HA-tagged-HIF1α ODD (aa390-652), N terminal (aa30-389) or C terminal (aa630-826) domains with the pcDNA4 His/Max vector only, Xpress-tagged LIMD1 or negative control TRIP6. 32hrs following transfection, cells were incubated at 1% O_2 for 16hrs before they were lysed with RIPA supplemented with protease, phosphatase and proteasome inhibitors (10μM MG132) and immunoblotted for protein levels. LIMD1, but not TRIP6 expression specifically reduced protein levels of the ODD but not the N or C terminal HIF1α domains. Anti-β actin immunoblot was used as a protein loading control.

4.1.1 LAW induce ODD degradation

As LIMD1 is closely related to Ajuba and WTIP, which share both structural and functional homology, the ability of the LAW proteins to induce ODD degradation was therefore next examined. Furthermore, since the LAW proteins interact with VHL and differentially bind to the PHDs it was hypothesised that all three proteins may regulate ODD protein levels.

When co-transfected with the HIF1α-ODD domain, the LAW proteins all induced specific degradation of the domain in comparison with the vector only control and negative control LIM protein TRIP6 (Figure 4.1.1 A). Furthermore, PHD2 was co-transfected with the ODD as a positive control and induced degradation of the domain to the same extent as exogenous expression of the LAW proteins. Interestingly, TRIP6 expresses as multiple higher molecular weight forms. However, the nature and specificity of these higher molecular weight forms is unknown.

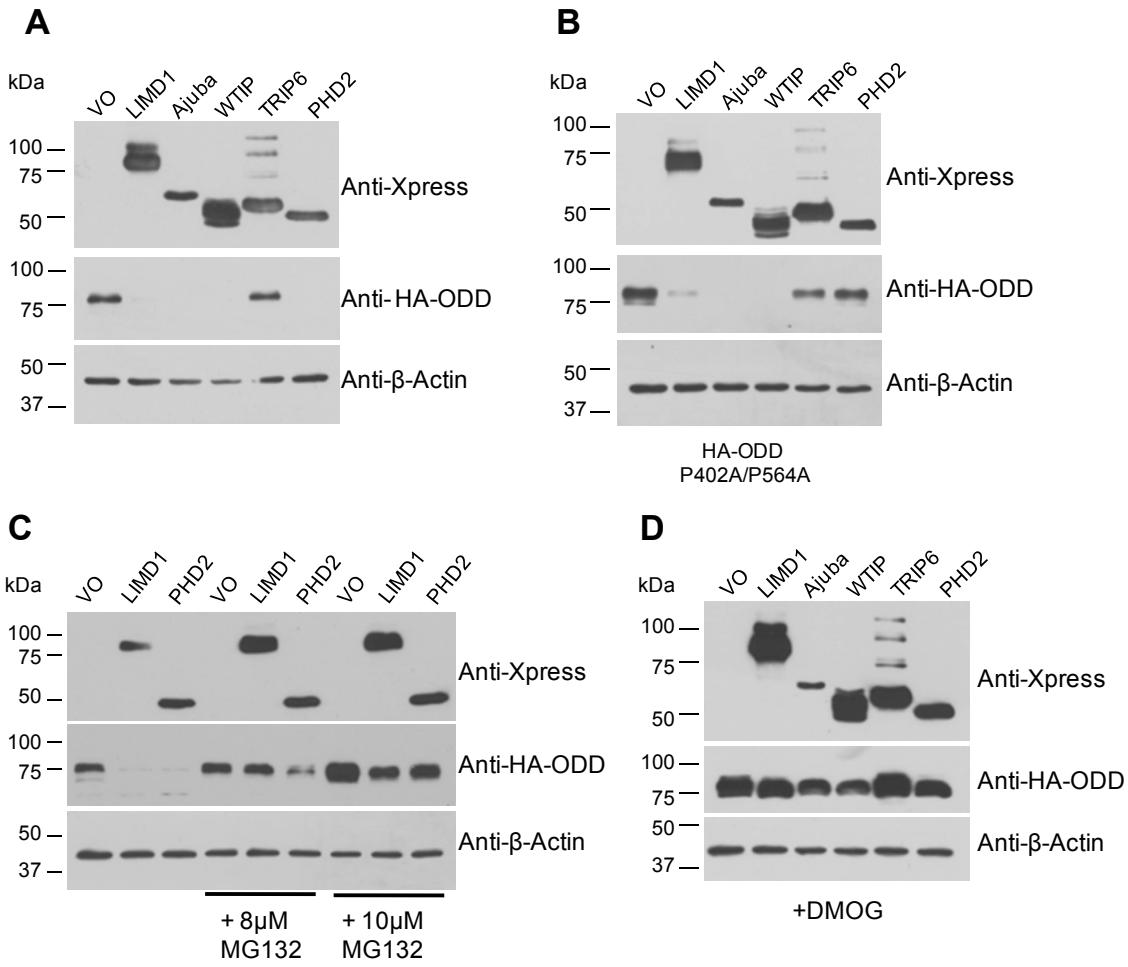

Figure 4.1.1 *LAW induce a specific reduction in HIF1α ODD protein levels, in a proteasome and prolyl hydroxylase dependent but proline 402/564 independent manner.*

(A) U2OS cells were co-transfected with the HIF1α HA-tagged-ODD (aa390-652) or HA-ODD P402A/P564A mutant **(B)**, with 250ng of Xpress vector only, Xpress-LIMD1, Ajuba, WTIP, negative control TRIP6 or positive control PHD2. 32hrs following transfection, cells were incubated at 1% O_2 (with 8 and 10 μM MG-132 **[C]** and 1mM DMOG **[D]** administration) for 16hrs before they were lysed with RIPA supplemented with protease, phosphatase and proteasome inhibitors (10μM MG132) and immunoblotted for protein levels. LIMD1, Ajuba, WTIP (LAW) and PHD2, but not TRIP6 expression specifically reduced protein levels of HIF1α ODD. **(B)** LIMD1, Ajuba and WTIP (LAW), but not TRIP6 expression specifically reduced protein levels of HIF1α ODD P402A/P564A. Xpress-PHD2 induced degradation was ablated upon P402/P564 mutation. **(C)** MG-132 inhibited both LIMD1 and PHD2's ability to induce ODD degradation. **(D)** DMOG inhibited the ability of the LAW proteins and PHD2 to induce ODD degradation. Anti-β actin immunoblot was used as a protein loading control.

4.1.2 LAW induced ODD degradation is independent of proline 402/564 hydroxylation

In keeping with the hypothesis of LAW as PHD/VHL scaffolding proteins, it was anticipated that LAW would induce ODD degradation by enhancing hydroxylation of the well characterised proline 402 and 564 residues. To address this question, an ODD construct with both critical proline 402 and 564 residues substituted to alanines (ODD P402A/P564A) was utilised. Once again, PHD2 was incorporated into the assay this time as a negative control. As PHD2 specifically targets HIF1α proline 402 and 564 for hydroxylation, PHD2 mediated ODD degradation should be attenuated upon their mutation.

Co-transfection of PHD2 with the ODD P402A/P564A mutant attenuated PHD2 induced ODD degradation. Surprisingly, LIMD1, Ajuba and WTIP still maintained the ability to induce degradation of the ODD mutant in a proline 402/564 independent manner (Figure 4.1.1 B). LIMD1 family member TRIP6 served as a negative control with no effect on either the ODD or the ODD proline mutant compared to the vector only control. This is indicative that the LAW proteins can mediate HIF1α degradation independently of proline 402/564 residues or alternatively perform multiple proline dependent and independent functions. Interestingly, a proportion of ODD P402A/P564A co-transfected with LIMD1 but not Ajuba or WTIP appeared stabilised in comparison with the wild type ODD construct. This may indicate that LIMD1 has both proline 402/564 dependent and independent functions and that the LAW proteins may regulate HIF1α *via* differential mechanisms. As LIMD1 is able to scaffold PHD2 and VHL, it may be plausible that LIMD1 alters target proline residue specificity for hydroxylation or changes the consensus sequence recognised by the PHDs. Alternatively, numerous mechanisms have been reported to regulate HIF1α independently of proline 402/564 hydroxylation including hypoxia specific sumoylation (Cheng et al., 2007), *via* the receptor of activated protein kinase C (RACK1) (Liu et al., 2007) and by GSK3 mediated phosphorylation (Flugel et al., 2007). It will be interesting to elucidate whether the LAW proteins play a role in any of these mechanisms.

4.1.3 LAW induced ODD degradation is proteasome dependent

The next question that was addressed, was whether LIMD1 mediated degradation of the ODD *via* a mechanism dependent on the 26S-proteasome, as both proteasomal (PHD-VHL) and proteasome-independent (Olmos et al., 2009) degradation mechanisms have been reported. The stability of the ODD following co-transfection with Xpress-tagged LIMD1 and positive control PHD2 was examined (as described in section 4.1.2), using the cell permeable proteasome inhibitor MG-132. MG-132 was administered to the U2OS cells 32 hours following transfection, for 16 hours, during which cells were incubated in 1% O_2.

Proteasomal inhibition attenuated LIMD1 mediated degradation of the ODD to a similar effect as positive control PHD2 (Figure 4.1.1 C). This therefore suggests that LIMD1 and potentially LAW mediate HIF1α regulation in a 26S-proteasome dependent manner, in keeping with the well characterised PHD/VHL degradation mechanism.

4.1.4 LAW induced ODD degradation is dependent on prolyl hydroxylase activity

As LAW induced degradation appeared to occur in a proline independent but proteasomal dependent manner, the dependency on hydroxylase activity was next examined. Therefore, the effect of LAW on the ODD following treatment with the competitive proly-4-hydroxylase inhibitor dimethyloxaloylglycine (DMOG) was analysed. The stability of the ODD when co-transfected with the LAW proteins was investigated in the presence of 1mM DMOG for 16 hours before lysis of cells and immunoblotting. DMOG treatment inhibited LAW and PHD2 induced ODD degradation (Figure 4.1.1.D). Therefore, LAW regulate the HIF1α ODD domain in a proteasomal, prolyl hydroxylase dependent manner but independently of proline 402 and 564 residues.

4.1.5 Mutation of LIMD1 impairs LIMD1 mediated ODD degradation

To further investigate the structure-function relationship of LIMD1 and its ability to induce ODD degradation, the effect of co-transfection of the ODD with a series of LIMD1 deletion mutants was examined (Figure 4.1.5). Deletion mutants were previously generated by QuikChange® (Stratagene, CA, USA) site directed mutagenesis by the incorporation of premature C-terminal stop codons (Figure 4.1.5 B).

Mutants were used which deleted each LIM domain of LIMD1 from the C-terminus. Deletion of the most C-terminal LIM domain (LIM 3, denoted ∆597-676) did not impair LIMD1 mediated degradation of the ODD (Figure 4.1.5 A). Interestingly, deletion of both LIM 3 and LIM 2 domains (∆535-676) did result in impaired LIMD1 function and stabilised the ODD. However, deletion of all 3 LIM domains (∆472-676) did not reproduce the same effect observed from the LIM2 and LIM3 deletion mutant as no loss of LIMD1 function was exhibited. This may suggest a mechanism whereby the LIM 2 domain is required for ODD degradation. Alternatively, this may indicate that upon deletion of the LIM 2 and LIM 3 domains, the conformation of LIMD1 may be altered to a non-physiological state that impairs normal function. Another possible explanation is that in isolation the LIM 1 domain may perform an auto-inhibitory function.

Deletion of the N-terminal pre-LIM region of LIMD1 (∆364-676 and ∆224-676) resulted in impaired ODD degradation (Figure 4.1.5 A). These data indicate that the critical region for HIF regulation may lie within amino acids 364-597, a region overlapping the LIM domains and the immediate pre-LIM region. This region could feasibly represent the PHD2 and VHL pre-LIM and LIM binding interfaces respectively. Furthermore, this region also incorporates a pre-LIM coiled-coil domain (aa444-463). Whether this coiled-coil domain is necessary for LIMD1 to induce ODD degradation function is currently unknown.

Intriguingly, expression of the three LIM domains independently, consistently demonstrated an ability to induce ODD degradation. This suggests that the interaction between LIMD1 and VHL is sufficient to induce ODD degradation. However, we currently do not know whether PHD1 or PHD3 interact with the LIM domains, which could contribute to the effect observed. Furthermore, WTIP has been recently demonstrated to homodimerise *via* interactions with its LIM domains (van Wijk et al., 2009). As the LIM domains are highly conserved between the LAW proteins, it is conceivable that the LIM domains may also homo- and/or heterodimerise with one another. Therefore, it may be possible that the LIMD1 LIM domains are able to still bridge PHD and VHL by interacting with other LAW proteins. At present the precise mechanism regulating this function is unknown.

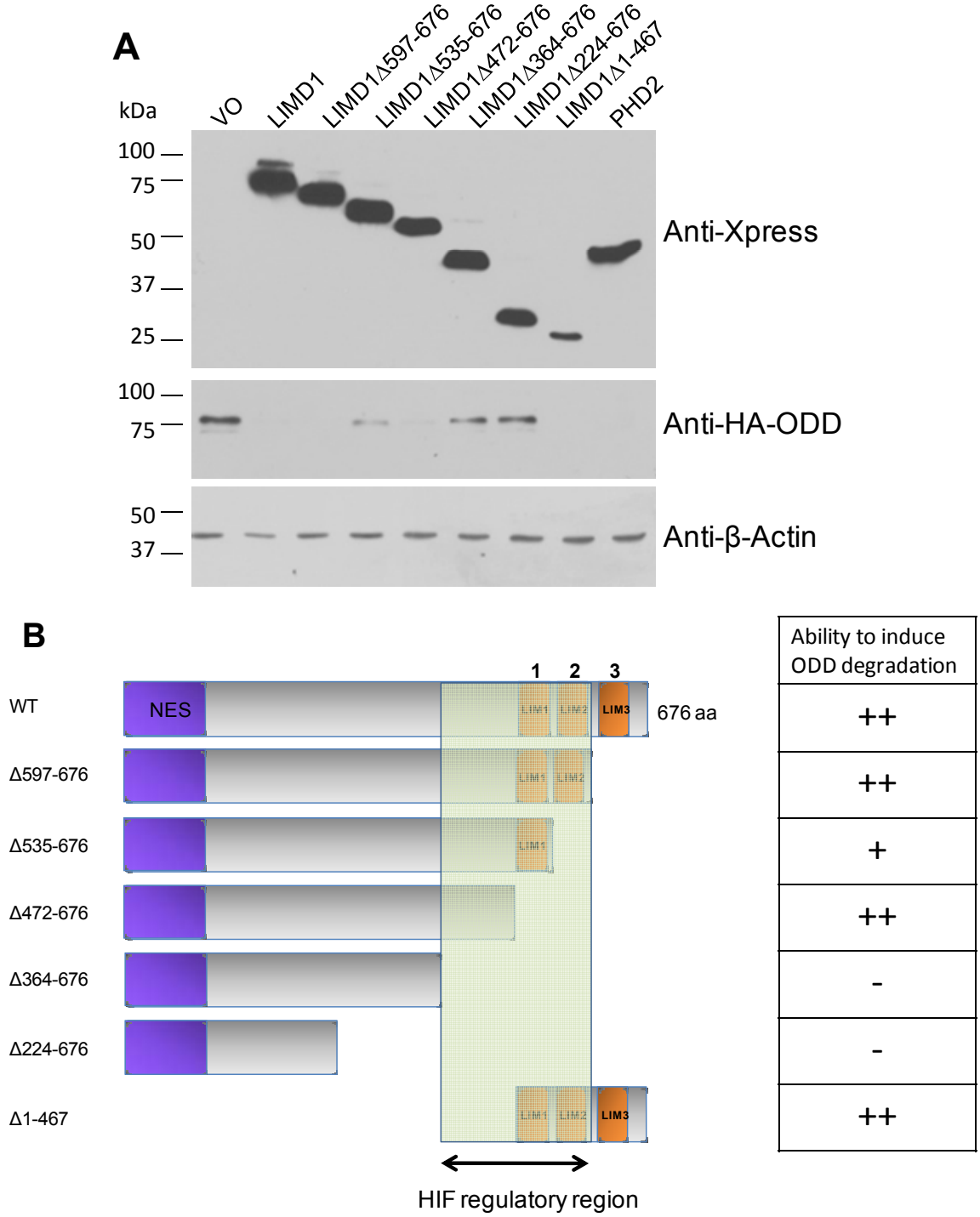

Figure 4.1.5 *LIMD1 ODD degradation is dependent upon a region encompassing amino acids 364-597.*

(A) ODD stability was examined in U2OS cells as in figure 4.1 with a series of C-terminal LIMD1 deletion mutants. Deletion of the C-terminal portion of LIMD1 from aa364-676 attenuates LIMD1's ability to induce ODD degradation. Anti-β actin immunoblot was used as a protein loading control. **(B)** Schematic representation of mutant structure and tabular representation of their ability to induce ODD degradation.

4.1.6 Depletion of endogenous LIMD1 by RNAi causes ODD protein stabilisation

Further investigation into the stability of the ODD in U2OS cell lines utilising lentiviral shRNA technology to stably deplete LIMD1 expression using RNAi was performed (materials and methods section 2.8). The HIF1α N-terminal, C-terminal and ODD domains were transiently transfected into U2OS cells stably expressing lentiviral mediated shRNA targeting sequences (scrambled control, two LIMD1 targeting shRNA and LIMD1 knock down with concurrent re-expression of an RNAi resistant rescue LIMD1 construct *via* an IRES). 32 hours following transfection, cells were incubated in 1% O_2 for 16 hours, lysed and protein levels were then analysed. Cell lines with functional LIMD1 knock down exhibited elevated ODD protein levels relative to the scramble shRNA control (Figure 4.1.6), thus exhibiting the reciprocal effect of exogenous LIMD1 expression. LIMD1 knock down and concurrent re-expression of an RNAi resistant LIMD1 construct reversed this phenotype, reducing ODD protein levels. This result indicates that the increase in ODD stability induced by RNAi mediated depletion of LIMD1 was not due to off-target effects of the shRNA. The protein levels of the N- and C-terminal domains were not significantly affected by LIMD1 down-regulation, highlighting the specificity for the ODD domain.

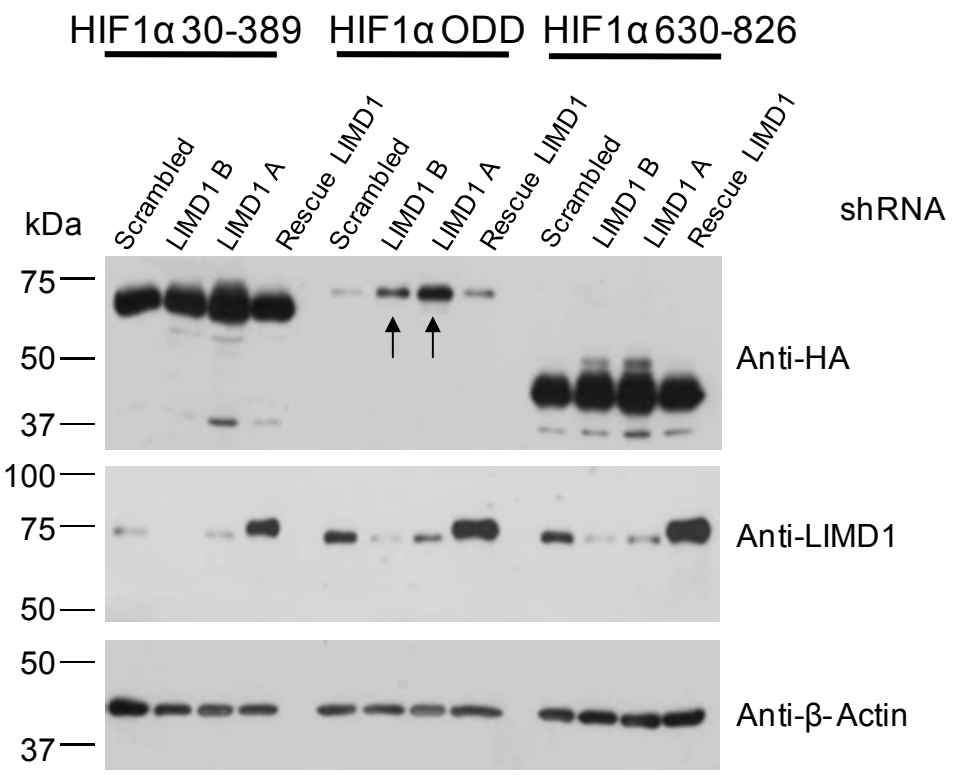

Figure 4.1.6 *LIMD1 knock down induces stabilisation of HIF1α ODD protein levels.*

U2OS cells constitutively expressing shRNA targeting LIMD1 (A:3-UTR and B: 5'), a negative control scrambled shRNA and LIMD1 shRNA with concurrent re-expression of an RNAi resistant LIMD1 expression construct, were transfected with the HIF1α HA-tagged ODD (aa390-652), N-terminal (aa30-389) or C-terminal (630-826) domains. 32hrs following transfection, cells were incubated at 1% O_2 for 16hrs before they were lysed and immunoblotted for protein levels. LIMD1 loss of function induced stabilisation of ODD protein (indicated by arrows) but not the N or C terminal HIF1α domains. Re-expression of LIMD1 attenuated ODD stabilisation. Anti-β actin immunoblot was used as a protein loading control.

4.2. LIMD1 protein levels are unaffected by hypoxia.

To evaluate whether LIMD1 protein levels were altered in hypoxia, U2OS cells were incubated at either 20% (normoxia) or 1% (hypoxia) O_2 for 16, 24 and 48 hours in duplicate, 24 hours following seeding. Cell lysates were harvested, resolved by SDS-PAGE and immunoblotted with a LIMD1 mAb to detect endogenous LIMD1 protein levels from normoxic and hypoxic cell extracts (Figure 4.2). Blots were probed with an anti-HIF1α mAb to confirm hypoxic response. No significant changes were observed in LIMD1 protein level upon hypoxic exposure, indicating that LIMD1 expression is not modulated by O_2 tension.

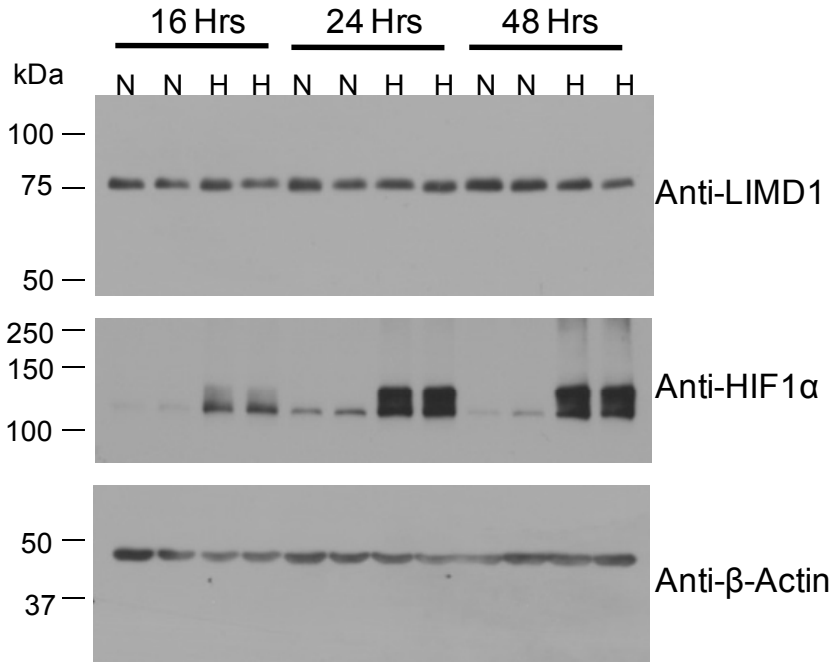

Figure 4.2 *LIMD1 protein levels are not altered by hypoxia.*
Immunoblot of duplicate U2OS cell lysates following hypoxic incubation (1% O_2, denoted as 'H') for 16, 24 and 48 hours compared to U2OS cells incubated for the same time point in normoxia (denoted 'N'). Anti-LIMD1 immunoblot shows that LIMD1 protein levels remain constant following hypoxic exposure. Anti-HIF1α immunoblot confirms hypoxic response. Anti-β Actin immunoblot was used as a protein loading control.

4.3 GFP-LIMD1 expression induces endogenous HIF1α degradation

Hypoxic incubation of U2OS cells induces endogenous HIF1α stabilisation detectable by immunofluorescence (Figure 4.3.1). It has previously been established that the function of PHD activity on HIF1α can be evaluated by visualising their effects on endogenous HIF1α expression and nuclear localisation *via* an immunofluorescence assay (Metzen et al., 2003a). Therefore, a similar assay to assess whether LIMD1's ability to simultaneously interact with the PHDs and VHL and to reduce ODD protein levels represents an ability to reduce endogenous HIF1α protein levels *in vivo* was employed. U2OS cells were transiently transfected with GFP vector only, GFP-PHD2, GFP-FIH, GFP-LIMD1 and GFP-Zyxin (Figure 4.3.2). 44 hours post-transfection cells were subjected to hypoxia (1% O_2 for 4 hours) prior to being fixed with 4% (v/v) PFA/PBS and stained for endogenous HIF1α. Exposure of U2OS cells to hypoxia induced stabilisation and localisation of HIF1α to the nucleus. Expression of GFP-LIMD1 resulted in reduced HIF1α protein levels and inhibited the nuclear accumulation of HIF1α to the same effect as GFP-PHD2 expression. However, expression of GFP vector only, FIH [which negatively regulates HIF *via* the recruitment of the p300 co-activator rather than protein stability (Lando et al., 2002)] and LIMD1 family member Zyxin had no effect on HIF1α expression level or localisation.

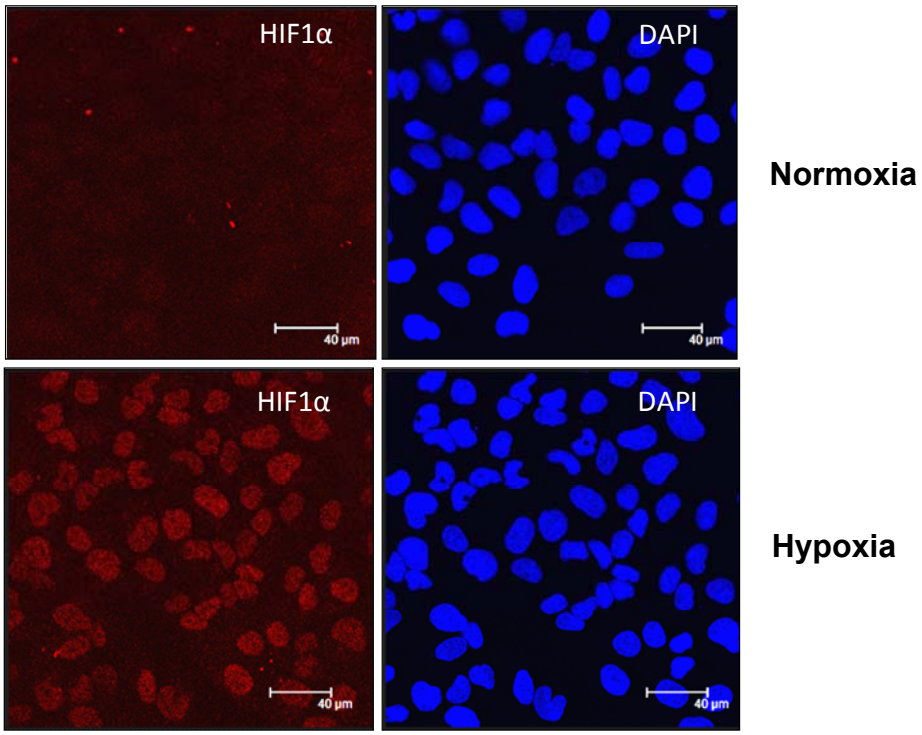

Figure 4.3.1 *Hypoxia induces nuclear accumulation and stabilisation of HIF1α.*

U2OS cells were exposed to 20% (normoxia) or 1% (hypoxia) O_2 for 4 hours. Cells were then fixed using 4% (v/v) PFA/PBS and immunostained for endogenous HIF1α and nuclear stained using DAPI. Hypoxic exposure impairs HIF1α degradation, resulting in its nuclear accumulation. (Scale = 40µm).

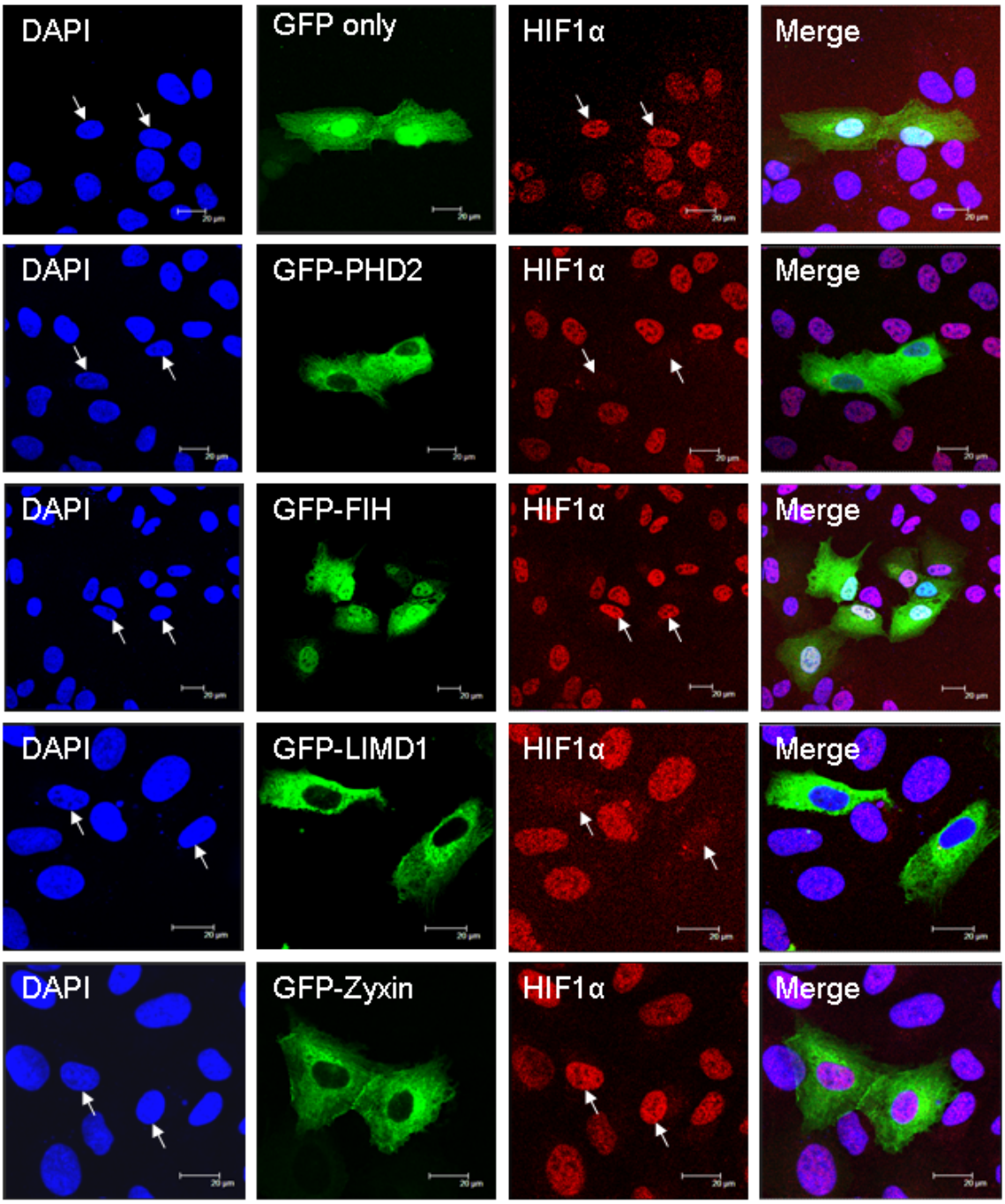

Figure 4.3.2 *LIMD1 expression inhibits the nuclear accumulation of HIF1α.*
U2OS cells were transiently transfected with GFP vector only, GFP-PHD2, GFP-FIH, GFP-LIMD1 and GFP-ZYXIN. 44hr following transfection cells were exposed to 1% O_2 for 4 hours. Cells were then fixed using 4% (v/v) PFA/PBS and immunostained for endogenous HIF1α and nuclear stained using DAPI. Expression of LIMD1 reduced HIF1α expression levels and inhibited its nuclear accumulation. (Scale = 20μm).

4.4 siRNA mediated LIMD1 knock down impairs the degradation of endogenous HIF1α

Previous data presented in this chapter demonstrates that exogenous expression of LIMD1 promotes the degradation of and inhibits the nuclear accumulation of HIF1α. Furthermore, shRNA mediated LIMD1 knock down induces stabilisation of the ODD domain. Therefore, to corroborate these findings, the effect of transient LIMD1 depletion by siRNA on full length endogenous HIF1α stability was examined. U2OS and HEK 293 cells were transfected with siRNA targeting LIMD1, PHD2 or a scrambled non-specific negative control siRNA and the lysates were then analysed by immunoblotting for endogenous HIF1α protein levels. PHD2 down regulation has been demonstrated to increase protein levels of endogenous HIF1α (Berra et al., 2003) and thus served as a positive control.

4.4.1 Optimisation of siRNA mediated LIMD1 knock down

The concentration of siRNA (Figure 4.4.1.2 and 4.4.1.3), and the degree of protease, phosphatase and proteasomal inhibition required within the lysis buffer (Figure 4.4.1.1) were all optimised respectively. LIMD1 knock down resulted in an accumulation of endogenous HIF1α, consistent across all lysis buffer optimisation conditions (Figure 4.4.1.1, arrows). RIPA supplemented with Complete Protease Inhibitor Cocktail (Roche) and Phosphatase Inhibitors (PhosSTOP, Roche) was identified as the optimal lysis condition and was maintained for further experiments utilising siRNA.

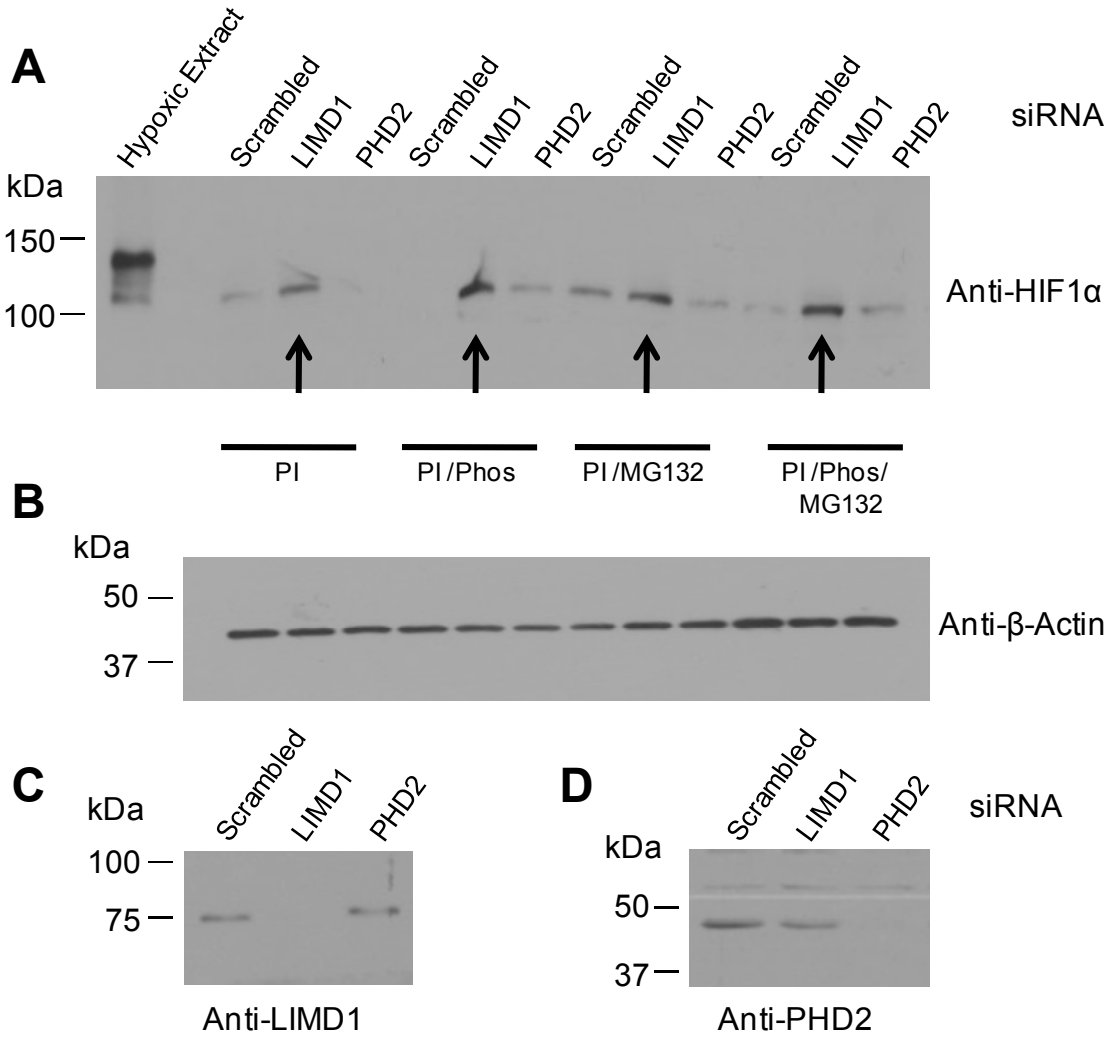

Figure 4.4.1.1 *Optimisation of siRNA mediated LIMD1 knock down.*

U2OS cells were treated with 20nM siRNA targeting LIMD1, PHD2 and a scrambled negative control. 48 hours post-transfection cells were lysed with RIPA buffer containing Complete Protease Inhibitor Cocktail (Roche), Phosphatase Inhibitors (Phos), and Proteasome Inhibitors (MG132). Lysates were then analysed by SDS-PAGE and immunoblotting. **(A)** Anti-HIF1α immunoblot. Arrows indicate increased HIF1α protein levels following LIMD1 knock down in each of the four lysis conditions. Hypoxic cell extract from U2OS cells exposed to 1% O_2 for 16 hours confirmed correct molecular weight of HIF1α detection. **(B)** Anti-β-Actin immunoblot was used as a loading control. **(C)** Representative anti-LIMD1 immunoblot indicating LIMD1 knock down. **(D)** Representative anti-PHD2 immunoblot indicating PHD2 knock down.

Down regulation of LIMD1 consistently induced an elevation in HIF1α protein levels in U2OS cells (Figure 4.4.1.2) and HEK293 cells (Figure 4.4.1.3). It was observed that administration of negative control scrambled siRNA at low concentrations (20nM) generated an increase in HIF1α protein levels in both U2OS and HEK293, which was not observed using higher siRNA concentrations (80nM). Therefore, 80nM siRNA was administered in further experiments.

Knock down of PHD2 in U2OS cells (Figure 4.4.1.2) did not stimulate the anticipated increase in HIF1α protein levels, observed in HEK293 (Figure 4.4.1.3), as previously reported by Applehoff et al using 20nM of PHD2 siRNA (Appelhoff et al., 2004). One possible reason for this may be due to HIF1 induced negative feedback. Initial PHD2 knock down may act to stabilise HIF1α protein levels, which is reported to result in increased PHD2 expression (Epstein et al., 2001; Berra et al., 2003). Therefore, HIF1α increase may result in increased PHD2 activity and subsequent HIF1α reduction. However, PHD2 protein levels at the point of lysis appeared significantly depleted in comparison with the scrambled and LIMD1 controls which suggests this theory is unlikely to account for this observed effect. Alternatively, this may reflect the contribution of PHD1 and PHD3 in U2OS cells which may provide the predominant hydroxylation activity or compensate for PHD2 loss of function. The reported induction of PHD2 expression in hypoxia was further verified in figure 4.4.1.4.

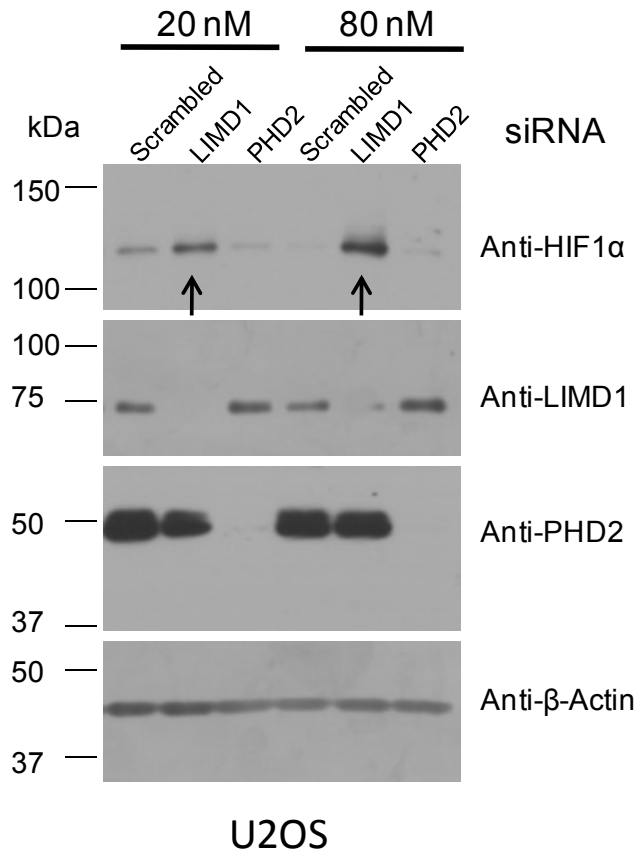

Figure 4.4.1.2 *Immunoblot analysis of siRNA mediated LIMD1 and PHD2 knock down in U2OS cells.*

U2OS cells were treated with 20 or 80nM of siRNA targeting LIMD1, PHD2 and a scrambled negative control. 48 hours post-transfection, cells were lysed with RIPA buffer containing Complete Protease Inhibitor Cocktail and Phosphatase Inhibitors. Lysates were then analysed by SDS-PAGE and immunoblotting. Arrows indicate increased HIF1α protein levels with LIMD1 knock down at both siRNA concentrations. Anti-LIMD1 and anti-PHD2 immunoblots demonstrate knock down achieved by siRNA. Anti-β-Actin immunoblot was used as a loading control.

In HEK293 cells, PHD2 knock down stimulated an increase in HIF1α protein levels following administration of siRNA at 20 and 80nM in comparison with the scrambled siRNA. The increase in HIF1α generated by LIMD1 knock down by 20nM of siRNA was less than that induced by PHD2 at the same siRNA concentration. However, at 80nM LIMD1 had as pronounced an effect on HIF1α protein levels as PHD2, emphasising the importance of the *in vivo* role of LIMD1 in HIF1α regulation (Figure 4.4.1.3).

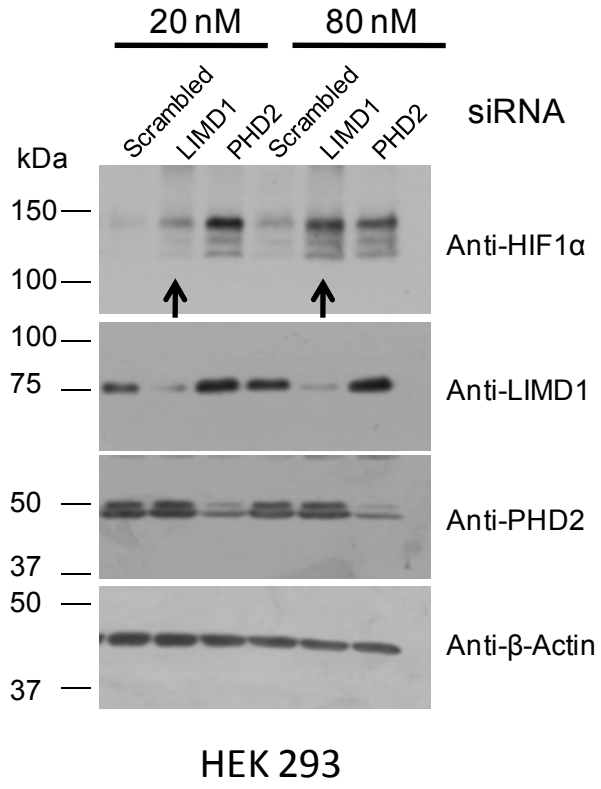

Figure 4.4.1.3 *Immunoblot analysis of siRNA mediated LIMD1 and PHD2 knock down in HEK293 cells.*

HEK293 cells were treated with 20 or 80nM of siRNA targeting LIMD1, PHD2 and a scrambled negative control. 48 hours post-transfection cells were lysed with RIPA buffer containing Complete Protease Inhibitor Cocktail and Phosphatase Inhibitors. Lysates were then analysed by SDS-PAGE and immunoblotting. Arrows indicate increased HIF1α protein levels with LIMD1 knock down at both siRNA concentrations consistent with the affect achieved by PHD2 knock down. Anti-LIMD1 and anti-PHD2 immunoblots demonstrate knock down achieved. Anti-β-Actin immunoblot was used as a loading control.

The effect of LIMD1 knock down was further examined in U2OS cells exposed to hypoxia, in order to evaluate whether LIMD1 was required to regulate HIF1α in both normoxia and hypoxia. 32 hours following siRNA administration U2OS cells were incubated at 1% O_2 or retained in normoxia for 16 hours prior to lysis and lysates were analysed by SDS-PAGE and immunoblotting. LIMD1 knock down induced an increase in HIF1α protein levels in both normoxia and hypoxia (Figure 4.4.1.4). However, stabilisation of HIF1α induced by LIMD1 knock down was markedly more pronounced in hypoxia than normoxia. Moreover, HIF1α from hypoxic cell extracts appeared to resolve as a larger molecular weight form than from normoxic cell extracts, which maybe a result of increased post-translational modification. This was also observed between HEK293 and U2OS cells, whereby HIF1α resolved as different molecular weight forms between the two cell lines in normoxia (Figure 4.4.1.2 and 4.4.1.3).

Furthermore, the effect of LIMD1 knock down on the stability of the stable O_2 independent component of the HIF heterodimer, HIF1β (ARNT) was analysed. HIF1β protein levels did not change upon LIMD1 knock down, highlighting the specificity of HIF1α stabilisation induced by LIMD1 depletion (Figure 4.4.1.4).

It has been demonstrated that PHD activity may be regulated at the level of their own stability, underpinned by the Siah ubiquitin ligases (Nakayama et al., 2004) and the peptidyl prolyl cis/trans isomerase FK506-binding protein 38 (FKBP38) (Barth et al., 2007; Barth et al., 2009). Therefore, whether the stabilisation of HIF1α protein following LIMD1 depletion arises not only due to LIMD1 scaffolding PHD and VHL activities, but also by increasing the stability of the PHDs was examined. siRNA mediated LIMD1 knock down did not effect the protein levels of the predominant prolyl hydroxylase PHD2 (Figure 4.4.1.4). However, an increase in PHD2 expression in hypoxia was observed as previously reported (Berra et al., 2003; Epstein et al., 2001).

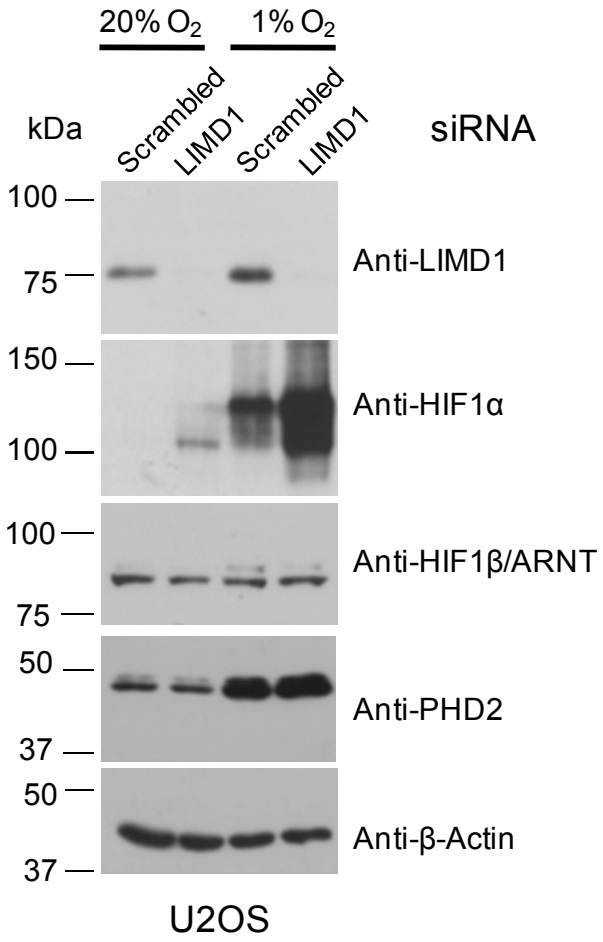

Figure 4.4.1.4 *LIMD1 knock down induces an increase in HIF1α protein levels in normoxia and hypoxia.*

U2OS cells were treated with 80nM of siRNA targeting LIMD1 and a scrambled negative control. 32 hours post-transfection, cells were incubated in normoxia or hypoxia for 16 hours prior to lysis with RIPA buffer containing Complete Protease Inhibitor Cocktail and phosphatase inhibitors. Lysates were then analysed by SDS-PAGE and immunoblotting. HIF1α protein levels increased significantly with LIMD1 knock down in both normoxia and hypoxia. Anti-LIMD1 immunoblot demonstrates knock down achieved. HIF1β and PHD2 protein levels do not change upon LIMD1 depletion in normoxia or hypoxia, emphasising the specificity for HIF1α. Anti-β-Actin immunoblot was used as a loading control.

4.4.2 Reoxygenation of cells following hypoxia reduces HIF1α protein accumulation induced by LIMD1 depletion.

Hypoxic exposure of cells treated with LIMD1 siRNA induced a marked increase in HIF1α protein levels (Figure 4.4.1.4). To confirm that this increase in HIF1α protein levels was due to the limiting O_2 tension, the effect on HIF1α protein levels upon reoxygenation of cells from hypoxia to normoxia was evaluated (Figure 4.4.2). Increasing time periods of reoxygenation from hypoxia, resulted in reduced HIF1α protein levels over time. At 30 minutes of reoxygenation in normoxia, HIF1α migrated on SDS-PAGE as the lower weight molecular form as detected in normoxic cell lysates. Thus, reoxygenation restored HIF1α protein levels in both the scrambled and LIMD1 siRNA treated cells to that observed in normoxic cell lysates. This indicates that upon limiting O_2 tensions, the function of LIMD1 may become increasingly critical, which can be recovered by increasing the oxygen tension.

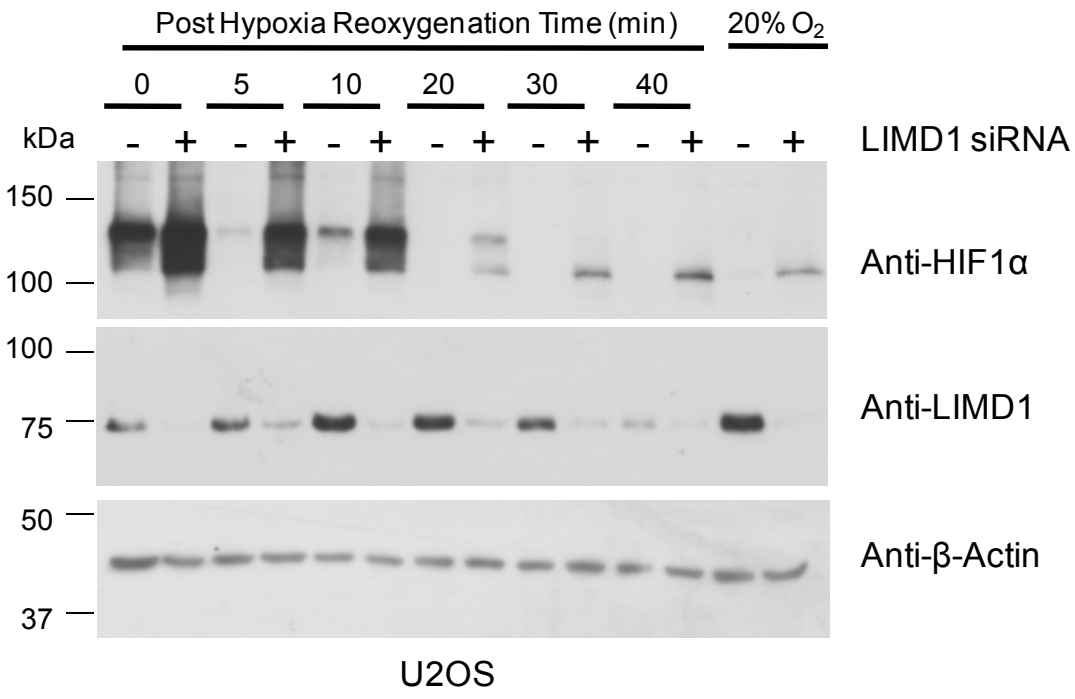

Figure 4.4.2 *Reoxygenation of cells following hypoxia reduces the levels of accumulated HIF1α protein induced by RNAi mediated LIMD1 depletion.*
U2OS cells were treated with 80nM of siRNA targeting LIMD1 (denoted '+') and a scrambled negative control (denoted '-'). 32 hours post-transfection, cells were incubated in normoxia or hypoxia for 16 hours. Hypoxic cell extracts (1%O_2) were reoxygenated in normoxia (20% O_2) for differing periods of time prior to lysis with RIPA buffer containing Complete Protease Inhibitor Cocktail and phosphatase inhibitors. Lysates were then analysed by SDS-PAGE and immunoblotting. Hypoxic HIF1α protein levels returned to those observed from normoxic cell extracts following reoxygenation in normoxia. Anti-LIMD1 immunoblot demonstrates knock down achieved. Anti-β-Actin immunoblot was used as a loading control.

4.5 Summary

LIMD1 induced degradation of the ODD domain of HIF1α, the domain sensitive to O_2 dependent PHD/VHL and proteasomal mediated degradation. The N- and C- terminal domains were not affected by ectopic LIMD1 expression. Conversely, shRNA mediated knock down of LIMD1 resulted in increased stability of the ODD domain specifically. Zyxin family member proteins Ajuba and WTIP also conserve the ability of LIMD1 to enhance ODD degradation to a similar effect as exogenous PHD2 expression. This function is dependent on prolyl hydroxylase activity and the 26S-proteasome, however is independent of proline 402 and 564 hydroxylation. LIMD1 protein levels are not modulated by hypoxia. The ability of LIMD1 to induce degradation of the ODD domain also translates to an effect on full length endogenous HIF1α. Expression of GFP-LIMD1 in U2OS cells induces degradation of endogenous HIF1α whilst LIMD1 depletion by siRNA results in accumulation of HIF1α in both U2OS and HEK 293 cells. Additionally, HIF1β protein levels and PHD2 stability was not altered by LIMD1 depletion. These findings further support the hypothesis that LIMD1 (and LAW) positively regulates PHD and VHL function to enhance the degradation of HIF1α.

CHAPTER 5: RESULTS

LIMD1 represses transcriptional activation from a Hypoxia Response Element

5. LIMD1 represses transcriptional activation from a Hypoxia Response Element

When stable HIF1α heterodimerises with HIF1β to form an active transcription factor complex, it is able to bind DNA at hypoxia response elements originally identified in the erythropoietin gene, containing a core RCGTG sequence (Semenza et al., 1994). Whether the ability of LIMD1 to specifically interact with the PHDs and VHL *in vivo*, reduce ODD protein levels and inhibit HIF1α nuclear accumulation translated to regulation of the hypoxic response using Hypoxia Response Element (HRE) -luciferase reporter system functional assays was next examined.

5.1 LIMD1 represses HRE activation in normoxia and hypoxia

To examine whether LIMD1 was able to repress HIF transcriptional activity, U2OS cells were co-transfected with 50ng of a pGL3-HRE-(firefly) luciferase construct and 5ng of pGL4-TK-*Renilla* luciferase construct. As the *Renilla* construct is constitutively expressed it was used to normalise the HRE-luciferase value, thus acting as a control for multiple steps within the assay including the transfection efficiency, lysis and the luminescence detection. The individual detection of Firefly and *Renilla* luminescence was possible due to the different individual substrate and co-factor requirements of the two enzymes. The experiment was performed in both normoxic and hypoxic conditions to evaluate whether LIMD1 performs a repressive effect independently of oxygen tension. HIF1α was ectopically expressed to induce HRE activation and co-transfected with LIMD1. 20 hours following transfection, cells were incubated for 4 hours in 1% or 20% O_2 prior to passive lysis. Firefly and *Renilla* luciferase values were then measured using a luminometer.

HRE activation was observed by ectopic HIF1α expression (32 fold induction) and by incubation in hypoxia (45 fold induction) (Figure 5.1). Ectopic expression of LIMD1 repressed HRE activation in both normoxia and hypoxia

by 54% and 44% respectively (Figure 5.1). This indicates that LIMD1 mediated regulation of HIF1 activity is maintained and not attenuated in hypoxia. As LIMD1 is believed to exhibit no intrinsic catalytic activity (Kadrmas and Beckerle, 2004) and functions independently of O_2 tension, this supports the hypothesis that LIMD1 regulates HIF1α by scaffolding the PHDs and VHL into a protein complex.

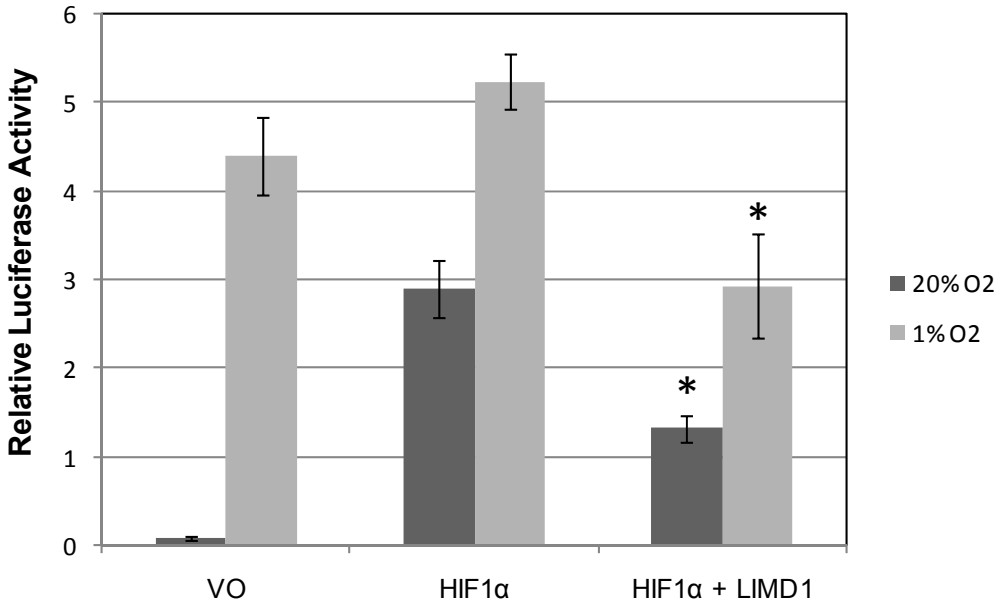

Figure 5.1 *LIMD1 represses HRE transcriptional activation in normoxia and hypoxia.*

U2OS cells were co-transfected with 50ng of pGL3-HRE-luc, 5ng of pGL4-TK-*Renilla,* 100ng of pcDNA3-HIF1α and 100ng of pcDNA4His/Max-LIMD1. Total DNA concentration was maintained by transfection of pcDNA4 vector only. 20 hours post-transfection, cells were incubated for 4 hours in 1% or 20% O_2, prior to passive lysis. Lysates were then added to firefly and *Renilla* substrate reagents and luminescence was measured. LIMD1 significantly repressed HRE activation at both 1% and 20% O_2. * p values less than 0.005.

5.1.2 LIMD1 represses HRE activation in a concentration dependent manner

To further examine the ability of LIMD1 to repress HRE activity, the concentration of ectopically expressed LIMD1 was titrated. 25, 100, 200 and 400ng of pcDNA4-LIMD1 was co-transfected with pGL3-HRE, pGL4-TK-*Renilla* and pcDNA3-HIF1α as in figure 5.1. Cells were incubated at 20% O_2. LIMD1 repressed HRE activation dependent on concentration. Transfection of 25ng of LIMD1 repressed the HRE by 23.6% which increased to a repression of 51% achieved by 400ng (Figure 5.1.2). As repression of HIF1 transcriptional activity appears to be coupled with LIMD1 expression levels, this may indicate that the reported loss of LIMD1 observed in lung (Sharp et al., 2004; Sharp et al., 2008) and head and neck carcinomas (Ghosh et al., 2008) may contribute to the increased pro-tumourigenic HIF1 target gene transcription. Experimentally, whether RNAi mediated loss of LIMD1 results in an increase in HIF1 transcriptional activity was next evaluated in figure 5.2.1.

In addition, the effect of the family member protein LPP was also examined. LPP does not interact with the PHDs or VHL. Therefore, it was anticipated that LPP would have no effect on HRE activity. This proved to be the case; LPP had no repressive affect on HRE induction at similar expression levels as LIMD1 and thus represents a good negative control for non-specific affects from ectopic over-expression (Figure 5.1.2). Conversely, LPP appears to increase activation of HRE transcription. This may represent a positive and negative regulatory system performed by the Zyxin family of proteins.

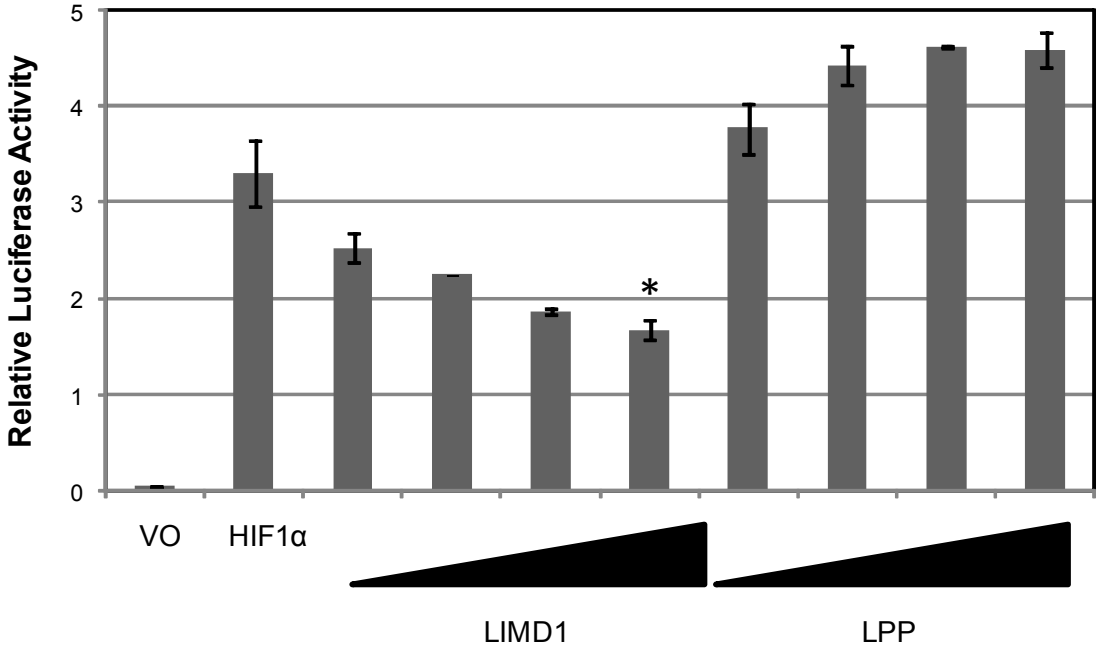

Figure 5.1.2 *LIMD1 represses HRE transcriptional activation in a concentration dependent manner.*

U2OS cells were co-transfected with 50ng of pGL3-HRE, 5ng of pGL4-TK-*Renilla,* 100ng of pcDNA3-HIF1α and titrating amounts of pcDNA4-LIMD1. Total DNA concentration was maintained by transfection of pcDNA4 vector only. 24 hours post-transfection; cells were lysed and added to firefly and *Renilla* substrate reagents and luminescence measured. LIMD1 significantly represses HRE activation in a concentration dependent manner. Family member protein LPP had no repressive effect on HRE and thus serves as a good negative control. * p value less than 0.005.

5.1.3 LIMD1 enhances PHD2 mediated repression of HRE activity

As LIMD1 interacts with the PHDs the effect of co-transfection of LIMD1 with the predominant hydroxylase PHD2 on HRE activity was examined. A sub-limiting amount of PHD2 (i.e. an amount which performs a sub-optimum repression of HRE activity, established as 1ng of pcDNA3 PHD2 per 12 well, data not shown) and LIMD1 (25ng, as identified in Figure 5.1.2) were co-transfected with HIF1α in order to assess whether LIMD1 aided PHD2 in

repressing HIF transcription. LIMD1 expression with PHD2 promoted further repression of HRE transcription by an additional 42% in comparison to when LIMD1 and PHD2 were expressed individually. Furthermore, co-transfection of LPP with PHD2 demonstrated no effect on PHD2 mediated HRE repression (Figure 5.1.3).

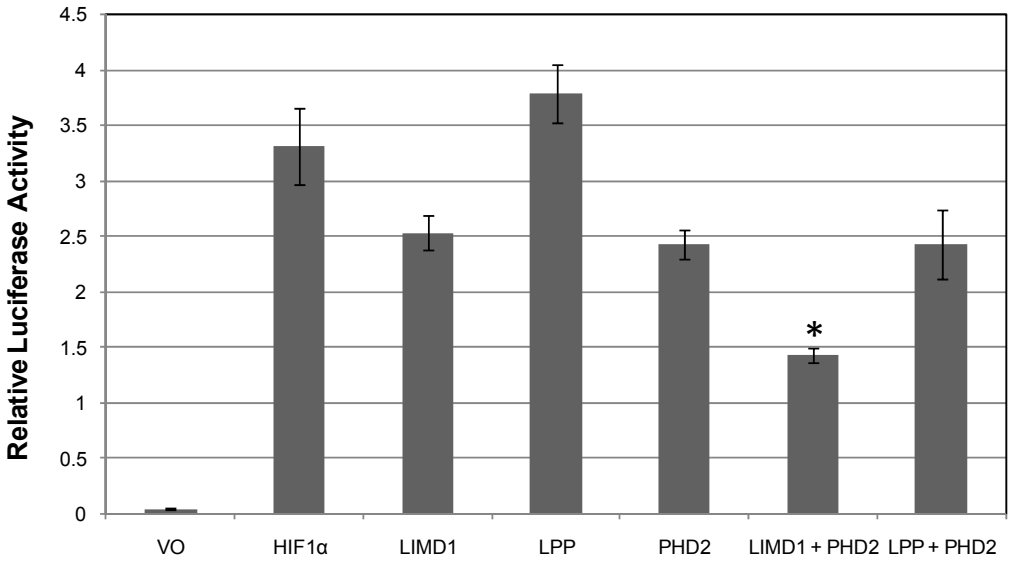

Figure 5.1.3 *LIMD1 enhances PHD2 mediated repression of HRE activity.*
U2OS cells were co-transfected with 50ng of pGL3-HRE, 5ng of pGL4-TK-*Renilla,* 100ng of pcDNA3-HIF1α and sub-limiting amounts of LIMD1 and LPP (25ng) with PHD2 (1ng). Total DNA concentration was maintained by transfection of pcDNA4 vector only. 24 hours post-transfection; cells were lysed and added to firefly and *Renilla* substrate reagents and luminescence measured. Sub-limiting co-transfection of LIMD1 with PHD2 further repressed PHD2 mediated repression of HRE activation. Co-transfection of LPP had no effect on PHD2 mediated repression of the HRE. * p value less than 0.0005.

5.1.4 LIMD1 represses HRE activation *via* a mechanism both dependent and independent of proline 402/564 residues

In section 4.1.2, data demonstrates that the ability of LIMD1 (and LAW) to induce ODD degradation may be independent of the well characterised substrates for prolyl hydroxylation P402 and P564 (Figure 4.1.1B). Therefore, whether LIMD1 may also repress HRE activation induced from the expression of full length HIF1α with these two proline residues substituted to alanines (PDM-proline double mutant) was examined. LIMD1 was co-transfected with the wild type and the HIF1α-PDM constructs and HRE-luciferase reporter assays performed as in section 5.1.

In this assay a 61% repression of HRE-luc activity was achieved by the co-transfection of LIMD1 with wild type HIF1α (Figure 5.1.4). Transfection of the HIF1α-PDM resulted in an increase in HRE activation in comparison with expression of the wild type HIF1α construct, due to the increased stability of the protein (Figure 5.1.4). However, upon co-transfection of LIMD1 with the HIF1α-PDM, 40% repression was still achieved (Figure 5.1.4). This finding is consistent with the ability of LIMD1 to maintain the degradation of the HIF1α ODD P402A/P564A mutant. Therefore, this indicates that LIMD1 can repress HIF1 transcriptional activity in the absence of these proline residues. This suggests that LIMD1 performs both proline 402/564 dependent (21%) and independent (40%) HIF1 repressive functions. As the ability to induce ODD degradation was inhibited by DMOG inhibition of 2-oxoglutarate-dependent dioxygenase (i.e. hydroxylase) activity (Figure 4.1.4), a plausible hypothesis may be that LIMD1 shifts hydroxylation to other proline residues within the ODD domain that are still able to be recognised by VHL.

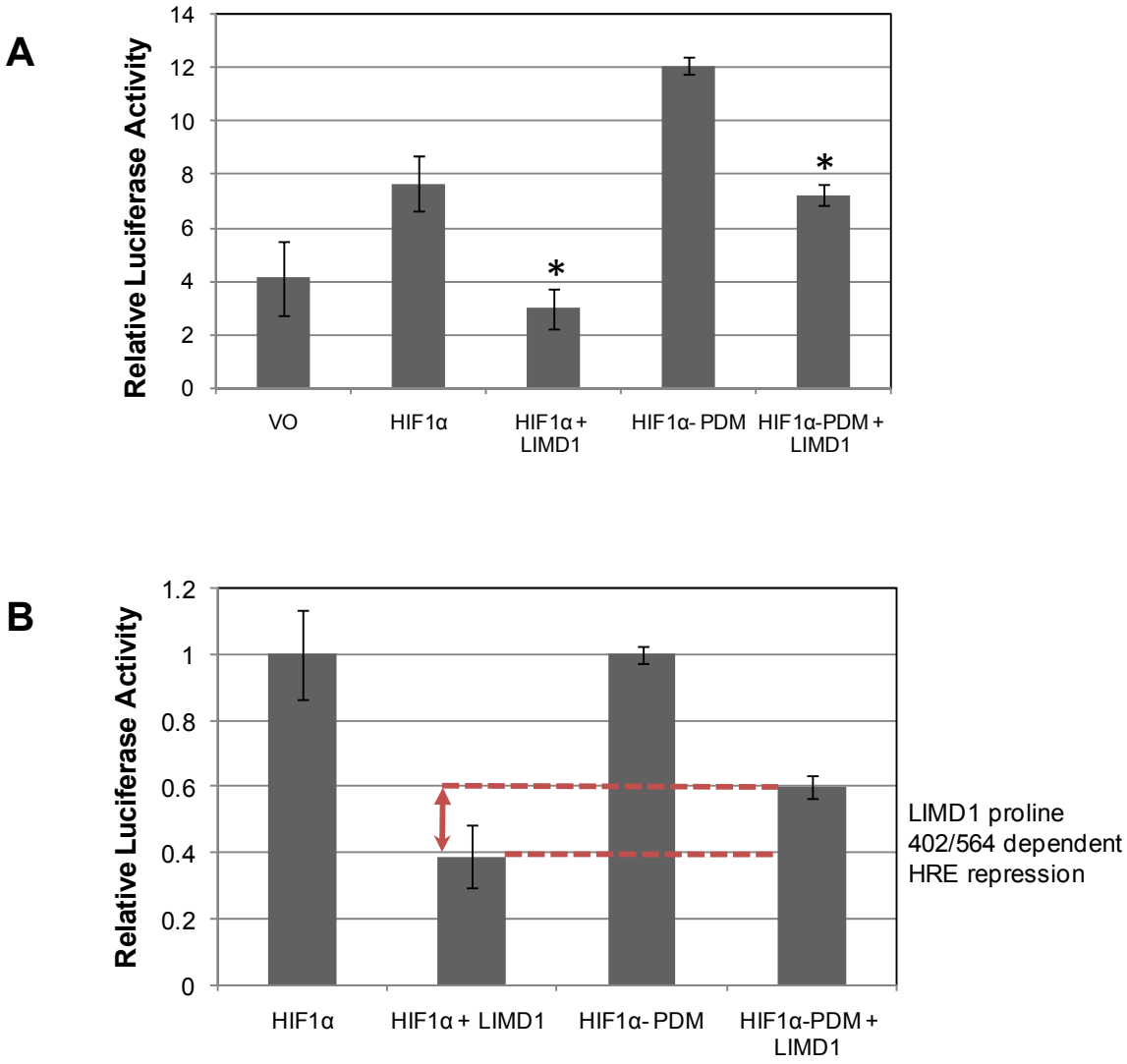

Figure 5.1.4 *LIMD1 represses HRE activity in a proline 402/564 dependent and independent manner.*

(A) U2OS cells were co-transfected with 50ng of pGL3-HRE, 5ng of pGL4-TK-*Renilla,* 100ng of pcDNA3-HIF1α or pcDNA3-HIF1α P402A/P564A (PDM-proline double mutant) and 100ng of pcDNA4-LIMD1. Total DNA concentration was maintained by transfection of pcDNA4 vector only. 24 hours post-transfection; cells were lysed and added to firefly and *Renilla* substrate reagents and luminescence measured. LIMD1 was able to repress HRE activity induced by the WT and PDM HIF1α expression. **(B)** HIF1α and HIF1α-PDM HRE-luc activation normalised to 1, in order to comparatively analyse the proline 402 and 564 dependent and independent activities of LIMD1. * p value less than 0.005.

5.2.1 Stable lentiviral mediated knock down of LIMD1 induces a de-repression of HRE activity.

To corroborate these data showing that LIMD1 represses HIF transcriptional activity, the effect of LIMD1 depletion on HRE transcription was analysed. As transient siRNA mediated LIMD1 knock down induced a stabilisation of HIF1α protein, it was anticipated that this would correlate to an increase in HRE activation. Endogenous knock down of LIMD1 was achieved in U2OS cells by stable expression of two different shRNA constructs (as described in materials and methods section 2.8 and utilised in Figure 4.1.6), confirmed by western blot (Figure 5.2.1B). Compared to cells transduced with a scrambled shRNA control, LIMD1 knock down induced a de-repression in HRE activity both in normoxic (4.3 fold increase) and hypoxic (2.3 fold increase) conditions (Figure 5.2.1A). Furthermore, of the 2 different LIMD1 targeting shRNA constructs used, one achieved a greater degree of LIMD1 depletion. This resulted in a larger increase in HRE activity, further indicating the correlation between HIF transcriptional activity and LIMD1 expression level.

To control for off-target effects of the shRNA which may contribute to the observed phenotype, an RNAi resistant LIMD1 construct was re-expressed from an IRES following shRNA depletion of endogenous LIMD1. LIMD1 re-expression reversed the observed de-repression in both normoxia and hypoxia (89.5% and 90.8% repression in comparison with the HRE-luc activation from the cells transduced with LIMD1 shRNA B in normoxia and hypoxia respectively), thus reverting the phenotype (Figure 5.2.1A). Thus, the HRE increase observed upon LIMD1 depletion is highly specific and not due to off-target effects of the shRNA. Furthermore, re-expression of the RNAi resistant LIMD1 construct which expressed LIMD1 at a higher level than endogenous LIMD1, repressed the HRE activity from the scrambled control in both normoxia and hypoxia (by 54.5% and 78.7% respectively) (Figure 5.2.1A). This corroborates the finding that ectopic LIMD1 expression represses HIF transcriptional activity (Figure 5.1 and 5.1.2). As previous data showed that LIMD1 depletion stabilises HIF1α, whilst ectopic expression of

LIMD1 reduces HIF1α protein levels, this indicates that LIMD1 modulates HRE transcriptional activity *via* regulation of HIF1α at the protein level.

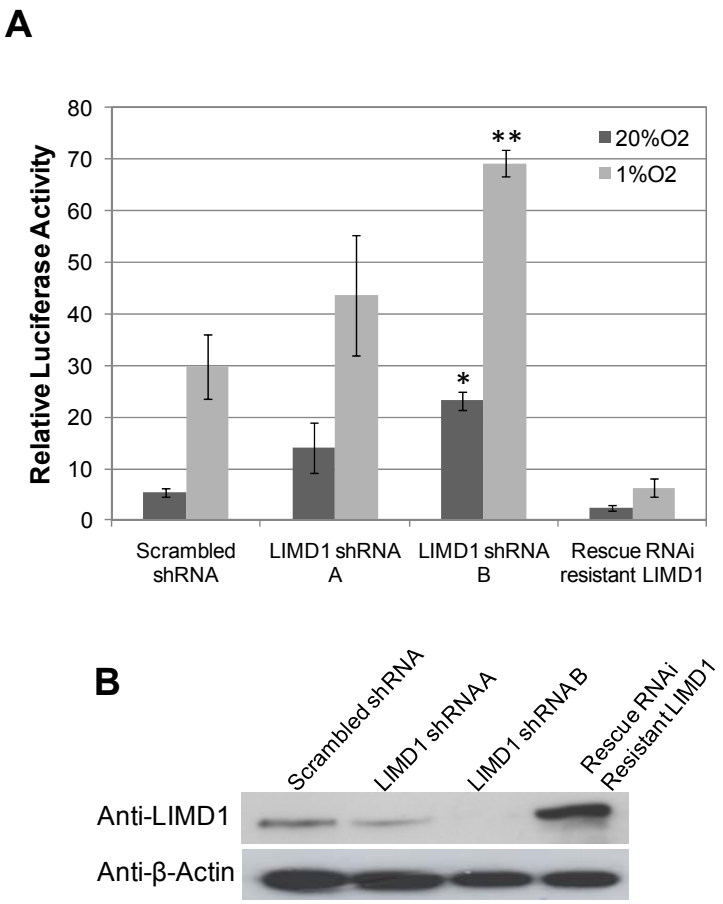

Figure 5.2.1 *shRNA mediated depletion of LIMD1 induces de-repression of HRE activity.*

(A) U2OS cells constitutively expressing shRNA targeting LIMD1 (A:3-UTR and B: 5'), a negative control scrambled shRNA and LIMD1 shRNA with concurrent re-expression of an RNAi resistant LIMD1 expression construct, were co-transfected with 50ng of pGL3-HRE and 5ng of pGL4-TK-*Renilla.* 20 hours post-transfection; cells were incubated in hypoxia or normoxia for 4 hours, lysed and added to firefly and *Renilla* substrate reagents and luminescence measured. **(B)** LIMD1 protein levels following shRNA depletion detected by immunoblot. β-actin acts as a loading control. LIMD1 knock down resulted in an increase in HRE activation in both normoxia and hypoxia, which was reverted by re-expression of an RNAi resistant LIMD1 construct. P values * less than 0.005 and ** less than 0.05.

5.2.2 LIMD1$^{-/-}$ Mouse Embryonic Fibroblasts (MEFs) exhibit elevated HRE activity in comparison to WT MEFs

To further demonstrate the ability of LIMD1 to attenuate HRE activation, the HRE activity in wild-type and *Limd1*$^{-/-}$ derived mouse embryonic fibroblasts (MEFs) was examined. *Limd1*$^{-/-}$ MEFs generated by Professor GD Longmore (Haematology division, Department of Cell Biology and Physiology, Washington University) (Feng et al., 2007) were co-transfected with pGL3-HRE-luciferase and pGL4-TK-*Renilla*. 20 hours post-transfection, the MEFS were incubated in normoxia or hypoxia for 4 hours. *Limd1*$^{-/-}$ MEFs demonstrated a small increase in HRE activity in normoxia compared to the WT MEFs. However, after 4 hours of hypoxic exposure a significant induction of HRE activation (3.2 fold) was observed in the *Limd1*$^{-/-}$ mouse embryonic fibroblasts in comparison to the wild-type MEFs (Figure 5.2.2). These data further implicate LIMD1 in the functional regulation of HIF driven HRE transcription and that the role of LIMD1 in HIF1 regulation is conserved between human and mouse.

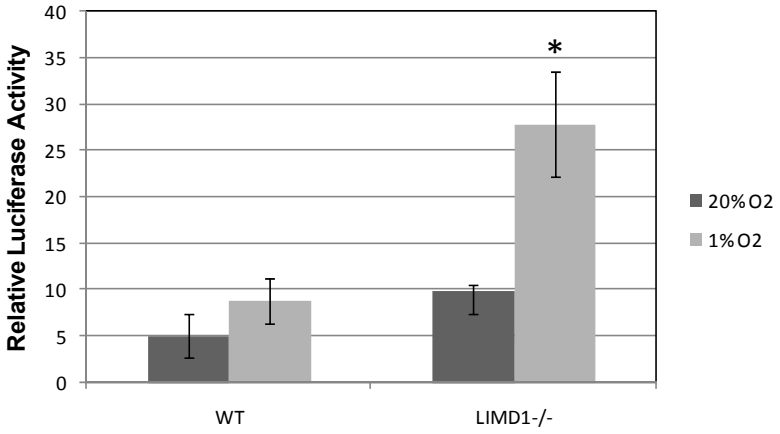

Figure 5.2.2 *Limd1*$^{-/-}$ *MEFs demonstrate elevated HRE activation in hypoxia in comparison to the wild type MEFs.*

WT and *Limd1*$^{-/-}$ MEFs were co-transfected with 50ng of pGL3-HRE and 5ng of pGL4-TK-*Renilla.* 20 hours post-transfection cells were incubated in hypoxia or normoxia, lysed and added to firefly and *Renilla* substrate reagents and luminescence measured. *Limd1*$^{-/-}$ MEFs demonstrated a significantly elevated HRE activity in hypoxia. P values * less than 0.05.

5.3 LIMD1 depletion induces an increase in endogenous HIF response gene expression

qRT-PCR was used to examine whether the role of LIMD1 in regulating HIF1α stability and HIF1 transcriptional activity resulted in an increase in downstream HIF response gene expression. mRNA levels of established HIF response genes containing functional HRE's encoding pro-apoptotic protein BNIP3 (E1B/Bcl-2 19kDa interacting protein 3) (Bruick, 2000) and vascular endothelial growth factor (VEGF) (Levy et al., 1995) were determined (in collaboration with Dr Victoria James, School of Biomedical Sciences, University of Nottingham) relative to housekeeping gene β-tubulin, following administration of scrambled and LIMD1 siRNA and following 8 hours of hypoxic incubation. The cyanine dye SYBR green, which upon binding double stranded DNA emits luminescence, was used for detection and quantification of PCR products in real time. qRT-PCR was performed to quantify the degree of LIMD1 depletion achieved by the RNAi. A significant average knock down of 91.1% and 58.5% was achieved by the LIMD1 targeting siRNA in U2OS cells, incubated in normoxia and hypoxia respectively, in comparison to the non-specific scrambled siRNA control (Figure 5.3 A). As anticipated, BNIP3 mRNA levels were elevated following 8 hours of incubation at 1% O_2 (Figure 5.3 B). Transient RNAi mediated depletion of LIMD1 resulted in a significant elevation in the endogenous transcript level of BNIP3 following 8 hours of hypoxic exposure in comparison to the scrambled siRNA control (Figure 5.3 B). However, no significant change was observed in the BNIP3 mRNA levels in normoxia. This is in keeping with the HRE activity observed from Limd1$^{-/-}$ MEFs whereby an increase was only observed upon hypoxic incubation (Figure 5.2.2).

VEGF induction by HIFs in hypoxia has been well characterised to induce key processes such as angiogenesis and neovascularisation (Fong, 2009). LIMD1 depletion induced a significant increase in normoxic VEGF transcript levels in comparison to the scrambled siRNA control (Figure 5.3 C, $p=0.03$). This preliminary data also demonstrated that there was a trend towards

significance following 8 hours hypoxic incubation, whereby, LIMD1 depletion induced an increase in VEGF mRNA levels in comparison to the scrambled control (Figure 5.3 C). Although this was a consistent finding this data was part of a larger optimisation, whereby each condition was only performed in duplicate, thus accounting for the statistical insignificance. Therefore, further work is required to provide confirmation that LIMD1 depletion results in increased VEGF transcript levels.

Furthermore, qRT-PCR analysis demonstrated that the induction of HIF1α protein was not due to an effect of LIMD1 siRNA on HIF1α mRNA levels (Figure 5.3 D). Therefore, this confirms that LIMD1 modulates HIF1α protein stability at the post-translational level rather than altering its gene expression. Therefore, this indicates that LIMD1 depletion may have a physiological effect on downstream biological processes of HIF including survival and angiogenesis.

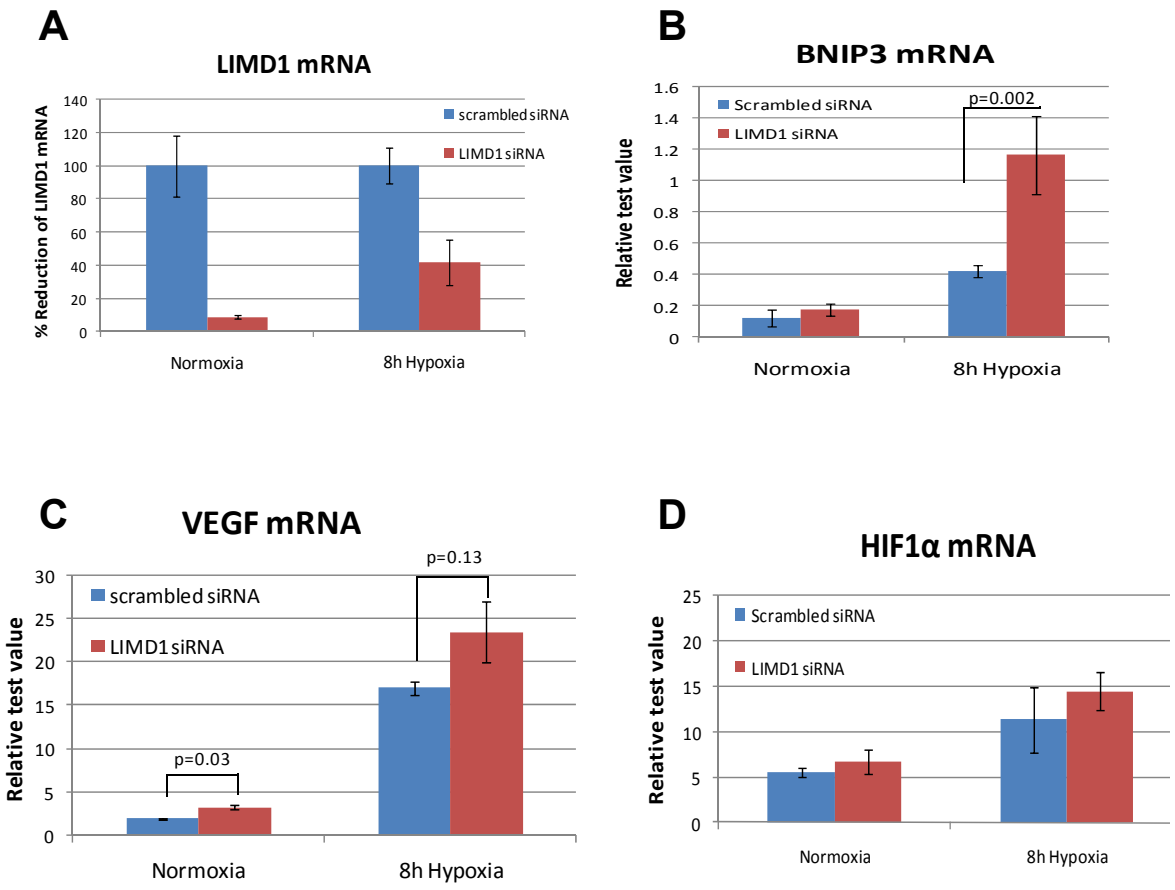

Figure 5.3 *RNAi mediated LIMD1 depletion induces an increase in BNIP3 and VEGF mRNA levels.*

U2OS cells were transfected with 80nM of scrambled control and LIMD1 siRNA. 40 hours post-transfection, cells were incubated in normoxia (20% O_2) or hypoxia (1% O_2) for 8 hours. Cells were lysed and RNA extracted using the RNAqueous micro RNA extraction kit (Ambion). qRT-PCR was performed using gene specific primers spanning an exon boundary and SYBR I green. Data was normalised to the housekeeping gene β-tubulin and analysed using the relative quantification method delta-delta Ct. **(A)** LIMD1 mRNA levels were quantified to confirm RNAi mediated depletion. LIMD1 mRNA levels were significantly reduced (in both normoxia and hypoxia) following LIMD1 siRNA transfection relative to cells transfected with the scrambled siRNA control. **(B)** LIMD1 depletion caused a significant elevation in hypoxic BNIP3 mRNA levels in comparison with the scrambled control, however no change in BNIP3 mRNA levels was observed in normoxia. **(C)** LIMD1 depletion induced an increase in both normoxic and hypoxic VEGF mRNA levels. **(D)** HIF1α mRNA levels were unaffected by LIMD1 depletion, in normoxia and hypoxia.

5.4 Summary

LIMD1 repressed transcription from a HRE-luciferase reporter, in both normoxia and hypoxia, in a concentration dependent manner. Zyxin family member protein LPP exhibited no repressive effect on HRE activation even at high concentrations. LIMD1 also enhanced PHD2 mediated repression of HRE activity upon co-expression. Substitution of the conserved PHD substrate residues P402/P564 did not completely impair LIMD1's ability to repress HIF transcriptional activity. This concurs with previous data highlighting the ability of LIMD1 to induce degradation of an ODD proline mutant. shRNA mediated LIMD1 knock down resulted in an increase in HRE activity in both normoxia and hypoxia, which could be reverted by re-expression of an RNAi resistant LIMD1 construct. Additionally, *Limd1*$^{-/-}$ MEFs exhibited a significantly increased HRE activity in comparison to WT MEFs following 4 hours of hypoxic exposure. LIMD1 mediated regulation of HRE activity also translated to an effect on the expression of HRE containing HIF response genes BNIP3 and VEGF. RNAi mediated depletion of LIMD1 resulted in an increase in the mRNA levels of both BNIP3 and VEGF following hypoxic incubation. This indicates that LIMD1has a physiological role in the regulation of HIF transcription. Furthermore, LIMD1 depletion did not alter HIF1α mRNA levels, confirming that LIMD1 modulates HIF1α by regulating its protein stability. These data indicate that LIMD1 modulates HIF transcriptional activity, presumably by scaffolding PHD and VHL activities into a protein complex.

CHAPTER 6: DISCUSSION

6. Discussion

The novel tumour suppressor protein LIMD1 was identified in 1999 from the analysis of the C3CER1 region of chromosome 3, found commonly deleted in numerous solid malignancies (Kiss et al., 1999). Although a preliminary understanding of LIMD1 has been achieved, the functions of LIMD1 are largely still unknown. One possible mechanism of LIMD1 mediated tumour suppressive activity that has been reported is by co-repression of the E2F family of transcription factors with the archetypal tumour suppressor pRB (Sharp et al., 2004). However, deletion of the pRB binding interface within LIMD1 does not completely attenuate its transcriptional repressive or tumour suppressive activity (Sharp et al., 2004). Therefore, at the beginning of this project, research focussed on unveiling novel protein-protein interactions that may underpin these pRB-independent tumour suppressive activities. A Yeast-2-hybrid screen using LIMD1 amino acids 1-363 identified prolyl hydroxylase 1 (PHD1) as a specific interacting partner. Therefore, whether LIMD1 interacts with and modulates the function of the PHDs, in order to regulate HIF1 transcription was examined.

6.1 LIMD1 and LAW differentially interact with the PHDs

In order to confirm the interaction identified in the Y2H (Figure 1.5) and control for false positive interactions, co-IP reactions were performed in U2OS cells. PHD1 is one of three isoforms, with a high degree of conserved structure and function, all of which are capable of hydroxylating HIFα subunits (Epstein et al., 2001; Bruick and McKnight, 2001). Therefore, investigations were undertaken to analyse whether LIMD1 could interact with all three PHDs. LIMD1 interacted with all three PHDs, confirmed both *in vivo* (Figure 3.1.1.2) and *in vitro* (Figure 3.1.4). PHD1 and PHD2 are highly homologous in their structure, with a shared C-terminal DBSH catalytic and oxygenase domain with an N-terminal extension (Epstein et al., 2001; Bruick and McKnight, 2001). PHD3 comprises just the C-terminal DBSH domain (as

depicted in Figure 1.14). Therefore, as LIMD1 interacts with all three PHDs this may indicate that LIMD1 interacts with the PHDs *via* their homologous C-terminal DBSH domain. To our knowledge, this is the first report of any protein (except for HIFα) that is capable of interacting with all three PHDs and therefore highlights the novelty and potential importance of this work in hypoxia biology.

Comparative analysis was then performed to identify whether the other Zyxin LIM proteins conserve the ability to interact with the PHDs. Interestingly, LIMD1, Ajuba and WTIP (LAW) displayed differential abilities to co-IP the PHDs, LIMD1 interacted with all three, whilst Ajuba and WTIP interacted with both PHD1 and PHD3 but not PHD2 (section 3.1.6). LPP and Zyxin did not interact with any of the PHDs and thus served as good negative controls highlighting the specificity of the observed interactions. Surprisingly, co-transfection of TRIP6 with PHD1 induced a modification of PHD1, resulting in the detection of a higher molecular weight form, approximately 2-3 kDa larger than the predominant PHD1 protein detected (Figure 3.1.6.3). Moreover, Xpress-TRIP6 interacted with this higher molecular weight form specifically and not the wild type form. The precise nature of this modification and whether this recruits or dictates a subsequent interaction with TRIP6 are unknown. Isolation of PHD1 by performing a large scale Xpress-TRIP6 immunoprecipitation, purification by SDS-PAGE and then analysis by liquid chromatography-tandem mass spectrometry (LC-MS/MS) may unveil whether this does represent a PHD1 post-translational modification. Increasing evidence suggests a role for PHD1 in non-HIF functions, including negative regulation of NF-κB (Cummins et al., 2006). Furthermore, PHD1 has distinct attributes in comparison to PHD2 and PHD3, including nuclear localisation (Metzen et al., 2003a), down-regulation by hypoxia (Tian et al., 2006) and the lowest reported *in vitro* hydroxylase activity for HIFα peptides (Tuckerman et al., 2004) and therefore there is a precedent that PHD1 may exhibit novel functions independent of HIF. Whether this TRIP6 induced modification represents a HIF or non-HIF function of PHD1 will be of future interest. Additionally, 14% of U2OS cells examined exhibit nuclear LIMD1

localisation (Sharp et al., 2004). Therefore, the interaction between LIMD1 and PHD1 may represent a nuclear LIMD1 function.

6.2 LIMD1 bridges the association between PHD2 and VHL

As an interaction was observed between LIMD1 and all three PHDs, research was focussed on LIMD1 and how LIMD1 may modulate PHD function. Scaffolding proteins have been described which increase the physical proximity of PHD2 and PHD3 with HIF1α (OS-9) (Baek et al., 2005), and between VHL and elongin C (SSAT2) (Baek et al., 2007a). Therefore, as LIM proteins often perform as adaptor proteins, whether LIMD1 may interact with other proteins reported to regulate HIFα in a scaffolding manner was investigated. Interestingly, all of the LAW proteins interacted with the E3 ubiquitin ligase VHL *in vivo* (Figure 3.2.4). The prolyl hydroxylation and ubiquitylation of HIFα had previously been conceived as two spatially and temporally separate processes. However, the identification of a family of proteins capable of interacting with both components prompted us to examine whether LIMD1 could simultaneously interact with both the PHDs and VHL, thus bridging an association between the post-translational modifiers. Co-IPs confirmed that LIMD1 interacted with PHD2 and VHL *via* different binding interfaces, within the pre-LIM and LIM domains respectively (Figure 3.1.5 and 3.2.3). This was in keeping with the Y2H data which first identified PHD1 as an interacting partner of the LIMD1 pre-LIM amino acids 1-363. As PHD2 and VHL were found to bind to LIMD1 *via* non-overlapping binding interfaces, this further suggested the possibility that LIMD1 may simultaneously bind to both proteins. This indeed was found to be the case as LIMD1 bound to both PHD2 and VHL simultaneously, with neither PHD2 nor VHL compromising one another's binding to LIMD1 (Figure 3.2.6.1). However, this could have reflected a population of immunoprecipitated LIMD1 interacting with PHD2 and another population of LIMD1 with VHL (Figure 3.2.6.1 D). Therefore, V5 tagged VHL was immunoprecipitated with a V5 antibody with PHD2 in the absence and presence of LIMD1, to confirm that LIMD1 simultaneously interacts with both proteins in a scaffolding

manner. LIMD1 expression facilitates an interaction between VHL and PHD2 within a protein complex denoted the normoxic protein complex ('normoxiplex'), confirming this hypothesis (Figure 3.2.6.2). To our knowledge this is the first report of an association between VHL and PHD2, unveiling an additional level of HIF regulation. Furthermore, as the LAW proteins interact differentially with the PHD proteins, and all bind VHL, presumably *via* their highly conserved LIM domains, it is plausible that they also scaffold PHD and VHL activities. The precise protein components of the normoxiplex and whether LAW share conserved binding interfaces for interacting with the PHDs and VHL within this complex need to be further investigated, which is further described in section 7.2.

6.3 LIMD1 and LAW regulate HIF1α by inducing ODD degradation

As LIMD1 was able to scaffold PHD2 and VHL, it was proposed that this would enhance their enzymatic activities and therefore, LIMD1 would promote degradation of HIF1α *via* the ODD domain sensitive to PHD/VHL mediated degradation. This was indeed the case as LIMD1 ectopic expression resulted in reduced ODD protein levels, but had no effect on the levels of the N- or C-terminal domains (Figure 4.1), consistent with the effect of LIMD1 depletion by shRNA which stabilised only the ODD domain (Figure 4.1.6). Interestingly, this was first deduced by co-IP of LIMD1 with these domains to detect an interaction. No interaction between full length HIF1α or its three domains in isolation were observed (Figures 3.3.1.1 and 3.3.2). This may be due to the pro-degradative effect of LIMD1, thus capturing a LIMD1-PHD-VHL-HIF1α ternary complex may be difficult. However, even in the presence of the proteasome inhibitor MG-132, no co-IP could be detected. This may suggest that LIMD1 scaffolds PHD and VHL which in turn interact with HIF1α, with LIMD1 more distant within a protein complex. In order to completely confirm that LIMD1 does not interact with HIF1α, a positive control for binding (VHL or PHD2) should be performed in parallel in the future.

LAW proteins Ajuba and WTIP were also demonstrated to induce a reduction in ODD protein levels, to the same effect as ectopic PHD2 expression (Figure 4.1.1 A). However, TRIP6, which interacted with PHD1 but not VHL, did not promote ODD degradation. This indicated that TRIP6 may modulate a non-HIF PHD1 function. Moreover, this may imply that VHL binding is a requirement for LAW function, supporting the hypothesis that LAW act to bridge the PHDs with VHL. The dependency on VHL was further substantiated by investigation of the effect of a series of LIMD1 deletion mutants on the stability of the ODD (Figure 4.1.5). Notably, deletion of the LIM domains, wherein the VHL binding interface lies, ablates LIMD1 induced ODD degradation. Furthermore, the LIM domains alone are sufficient to induce ODD degradation (Figure 4.1.5). The implications of this finding suggest that binding to PHD2 *via* the pre-LIM is not necessary to induce ODD degradation. However, the dependency on prolyl hydroxylase function was confirmed by treatment with the 2-oxoglutarate-dependent dioxygenase inhibitor DMOG, which inhibited LAW mediated ODD degradation (Figure 4.1.1 D). One plausible explanation to account for this finding is the possibility that LAW homo- and heterodimerise, as recently suggested with regards to WTIP (van Wijk et al., 2009). Therefore, ectopically expressed LIM domains alone may interact with VHL and endogenous LAW proteins, which in turn may interact with PHDs, thus maintaining the bridging function. Alternatively, the binding interfaces of PHD1 and PHD3 with LIMD1 have not been established. As all of the LAW proteins bind to PHD1 and PHD3, but only LIMD1 binds to PHD2, this may suggest that the binding regions differ. Therefore, it is possible that the LAW proteins interact with PHD1 and PHD3 *via* their conserved LIM domains, enabling the bridging function to be maintained.

Both proteasomal (Figure 4.1.1 C) and prolyl hydroxylase (Figure 4.1.1 D) activities were demonstrated to be required for LAW induced ODD degradation, which is in keeping with the well characterised PHD and VHL mediated HIFα regulation mechanism. However, mutation of the proline 402 and 564 residues hydroxylated by the PHDs, did not totally ablate LAW

mediated ODD degradation, although impairing the ability of PHD2 to degrade the ODD (Figure 4.1.1 B). This finding was corroborated by HRE-luciferase reporter assays, which demonstrated that LIMD1 was able to repress HRE transcriptional activation induced by a proline double mutant construct (Figure 5.1.4). Therefore, these data suggest that LAW work in a prolyl hydroxylase dependent manner independently of proline 402 and 564. However, LIMD1 only achieved a 40% repression of the HRE activity induced by the HIF1α proline double mutant, in comparison to 61% repression with wild-type HIF1α (Figure 5.1.4). Therefore, this suggests that a degree of LIMD1 induced ODD degradation is lost upon P402A/P564A substitution. Therefore, LIMD1 may perform both proline 402 and 564 dependent and independent mechanisms. One speculative hypothesis may be that LAW act to alter the specificity of the PHDs to hydroxylate different motifs within the ODD. Alternatively, LAW may recruit different post-translational modifications that still require prolyl hydroxylase function. Approaches to deduce the precise mechanism are further discussed in section 7.3.

6.4 RNAi mediated LIMD1 depletion stabilises HIF1α protein

To confirm that LIMD1 regulated endogenous HIF1α protein levels *in vivo*, the effect of LIMD1 depletion mediated by RNAi was analysed. Lentiviral mediated LIMD1 depletion by shRNA induced stabilisation of ectopically expressed ODD, which could be reverted by expression of an RNAi resistant LIMD1 construct (Figure 4.1.6). This indicated that endogenous LIMD1 expression levels were coupled with HIF1α stability. The accumulation of the ODD with LIMD1 depletion was shown to be valid, as transient siRNA mediated depletion of LIMD1 had the same effect with full length endogenous HIF1α, in both U2OS (Figure 4.4.1.2) and HEK293 (Figure 4.4.1.3) cells in normoxia. PHD2 siRNA was used as a positive control, as multiple groups have demonstrated that PHD2 depletion induces stabilisation of HIF1α. This finding was corroborated in HEK293 cells, whereby at 80nM siRNA LIMD1 had the same pronounced effect as PHD2 on HIF1α protein levels (Figure

4.4.1.3). However, in U2OS cells PHD2 depletion did not induce the anticipated accumulation of HIF1α (Figure 4.4.1.2). The precise explanation for this observation is unknown. However, this could be due to the time point of lysis post-siRNA administration. As PHD2 expression is inducible by hypoxia (Epstein et al., 2001; Berra et al., 2003), it is feasible that HIF1α accumulation as a result of PHD2 depletion led to the subsequent increase in PHD2 expression in a negative feedback manner, acting to reduce HIF1α protein levels. Therefore, at earlier time points of lysis HIF1α stabilisation may become apparent. Alternatively, this may reflect a predominant contribution by PHD1 and PHD3 in the steady state regulation of HIF1α stability in normoxia in U2OS cells. However, PHD2 ectopic expression significantly attenuates activation of a HRE reporter in U2OS, even upon transfection of a sub-limiting amount (1ng, Figure 5.1.3). This therefore, increases the likelihood of the former argument.

6.5 LIMD1 regulates HIF1 transcriptional activity

As LIMD1 ectopic expression promoted HIF1α degradation and LIMD1 depletion induced HIF1α stabilisation, it was proposed that LIMD1 expression would modulate HIF1 transcriptional ability. Therefore, a HRE-luciferase reporter was utilised to quantify HIF1 transcriptional activity with both ectopic LIMD1 expression and with LIMD1 depleted by shRNA. LIMD1 ectopic expression repressed HRE activation in a concentration dependent manner in both normoxia and hypoxia (Figure 5.1 and 5.1.2), whilst Zyxin protein LPP had no repressive effect. Arguably LPP may act to enhance HRE activity, thus indicating the possibility of a family of proteins which positively and negatively regulate HIF1. Furthermore, expression of a sub-limiting amount of LIMD1 with 1ng of PHD2 aided PHD2 mediated HRE repression by a further 42% (Figure 5.1.3). This implies that LIMD1 and PHD2 work cooperatively to negatively regulate HIF1; substantiating our hypothesis that LIMD1 acts as a scaffolding protein.

In keeping with the repressive effect on HRE activity induced by ectopic expression of LIMD1, LIMD1 depletion mediated by shRNA caused a de-repression of HRE transcriptional activation (Figure 5.2.1). Furthermore, re-expression of an RNAi resistant LIMD1 construct following endogenous LIMD1 depletion by shRNA, reverted the phenotype, repressing HRE activation (Figure 5.2.1). This highlighted that the specificity of the observed effect on HRE activity was dependent on LIMD1 protein levels and not due to off-target effects of the RNAi. *Limd1*$^{-/-}$ derived MEFs also exhibited a similar phenotype, whereby upon 4 hours of hypoxic incubation they demonstrated a marked increase in HRE activity in comparison to the wild type MEFs (Figure 5.2.2). This suggests that the role of LIMD1 is conserved between human and mouse and between multiple different cell types.

qRT-PCR was performed to examine whether LIMD1 mediated regulation of HIF transcriptional activity altered the expression level of endogenous HIF response genes (Figure 5.3). LIMD1 depletion by siRNA induced an increase in the mRNA levels of two HIF response genes containing functional HREs, BNIP3 and VEGF, following 8 hours exposure to hypoxia. This indicates that loss of LIMD1 may have a physiological role in the regulation of HIF responsive gene expression. Furthermore, HIF1α mRNA levels did not significantly change following LIMD1 depletion (Figure 5.3). This confirms that the observed increase in HIF1α protein levels following LIMD1 depletion is due to altered post-translational regulation not an increase in gene expression.

Therefore, the data presented in this thesis indicates that LIMD1 (and LAW) bridges an association between PHD2 and VHL, to enhance their enzymatic activities and augment HIF1α degradation, repressing HIF1 transcriptional activity. This data introduces a new family of hypoxic regulators and may also represent an additional novel tumour suppressive mechanism of LIMD1.

This following section contains preliminary experimental data which provides interesting scope for potential directions for future work that will improve our understanding of the role of LIMD1 and LAW in the regulation of HIF.

6.6 Confirm that LIMD1 enhances hydroxylation and ubiquitylation of HIF1α

In this thesis, it has been shown that LIMD1 (and LAW) promotes HIF1α degradation and that this is most likely achieved by bridging the association between the PHDs and VHL. Therefore, this hypothesis suggests that LIMD1 would act to promote the enzymatic activities of these two proteins. Future work is required in order to specifically confirm this hypothesis. In order to measure hydroxylation, numerous different techniques have been described including *in vitro* quantification of O_2 consumption or the CO_2 release from 2-oxoglutarate during oxidative decarboxylation [for review (Hewitson et al., 2007)]. However, a more direct approach relies on the hydroxylation dependent binding of VHL to HIF1α or a minimal peptide encompassing the conserved proline residues used in a procedure termed a VHL capture assay (Hewitson et al., 2007). This assay involves immunoprecipitating HIF1α or the ODD component of HIF1α capable of interacting with VHL following proline hydroxylation. HIF1α is then incubated with *in vitro* transcribed and translated radiolabelled [^{35}S]-VHL. The amount of [^{35}S]-VHL captured is then assessed by autoradiography and can be quantified (Marxsen et al., 2004). [^{35}S]-VHL capture by HIF1α is indicative of the degree of HIF1α hydroxylation. Therefore, whether ectopic LIMD1 expression or LIMD1 depletion by siRNA would alter the degree of VHL capture would indicate that LIMD1 modulates PHD hydroxylase activity.

Similarly, ubiquitylation can also be monitored, often by transfection of a eukaryotic expression vector encoding a tagged-ubiquitin construct. Whether LIMD1 depletion, in the presence of the proteasome inhibitor MG-132, would result in a reduction of ubiquitylated HIF1α, could be identified by immunoblotting for ubiquitin. Alternatively, to increase specificity, tagged-

ubiquitin could be isolated from these lysates treated with MG-132 by immunoprecipitation and if LIMD1 promotes HIF1α ubiquitylation then it would be anticipated that in the presence of LIMD1 more HIF1α co-IPs due to the covalent attachment to ubiquitin.

6.7 Analysis of the components of the normoxiplex and identification of protein binding interfaces

As the LAW proteins are able to differentially interact with the PHDs and VHL it was hypothesised that this may represent a normoxic protein complex which acts to enhance enzymatic activities by increasing their physical proximity. In keeping with this hypothesis, there is a precedent for the PHDs to be found within higher molecular weight complexes. This was initially identified in 2002, when Ivan et al demonstrated that HIF prolyl hydroxylase activity was observed in rabbit reticulocyte lysate elutes with an apparent molecular weight of 320-440 kDa on size exclusion columns (Ivan et al., 2002). These data were supported by research by Nakayama et al, who demonstrated that PHD2 and PHD3 were able to homodimerise, and that PHD3 can heterodimerise with PHD1 and PHD2 (Nakayama et al., 2007). Moreover, size fractionation of endogenous PHD3-containing complexes from HeLa cells were found over a range of molecular masses from 30 kDa (monomeric form) to 2000 kDa, whereby hypoxia acted to shift the distribution of PHD3 into fractions of higher molecular mass. Interestingly, PHD3 distributed in lower molecular weight complexes maintained a higher HIF hydroxylase activity, however, also maintained an interaction with the ubiquitin ligase Siah2 which targets PHD3 for degradation (Nakayama et al., 2007). Therefore, the lower molecular mass forms of PHD3 have a higher activity, but reduced stability. Interestingly, preliminary data whereby LIMD1 is co-transfected into U2OS cells with PHD2 and VHL indicates that LIMD1 expression appears to induce higher molecular weight forms which are not present upon co-transfection with the vector only control (Figure 7.2.1). VHL has been reported to be ubiquitylated by the E2-EPF (Jung et al., 2006) and

it is therefore plausible that LIMD1 promotes this process. However, LIMD1 expression does not induce degradation of VHL and therefore if this higher molecular weight form is ubiquitylated-VHL it may represent ubiquitylation as a signalling molecule. The PHD2 higher molecular weight form is of approximately 25 kDa larger than the monomeric form (Figure 6.7.1). The nature of this PHD2 form is unknown and to our knowledge no PHD2 modifications have been reported. Isolation and LC-MS/MS analysis may identify the nature of these higher molecular weight forms.

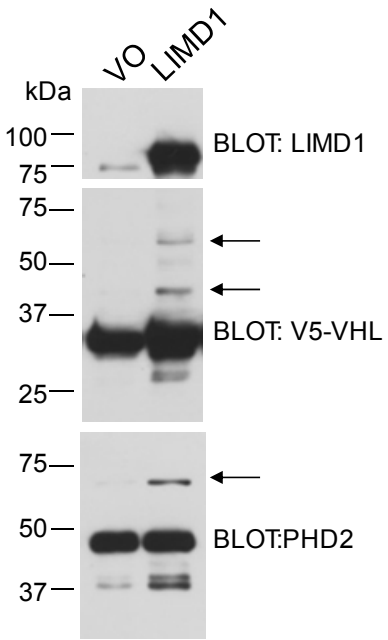

Figure 6.7.1 *LIMD1 expression induces higher molecular weight forms of PHD2 and VHL.*

pcDNA4 LIMD1 and a VO control were co-transfected into U2OS cells with PHD2 and VHL. 48 hours post-transfection cells were lysed with RIPA supplemented with protease and phosphatase inhibitors and LIMD1 was immunoprecipitated with a LIMD1 mAb. Samples were immunoblotted for LIMD1, PHD2 and V5-VHL. LIMD1 expression induces higher molecular weight forms of PHD2 and VHL indicated by arrows.

Furthermore, as previously mentioned, recent evidence also suggests that the LAW proteins are able to multimerise, as WTIP has been demonstrated to homodimerise *via* interactions between the highly conserved LIM domains (van Wijk et al., 2009). As the LIM domains are so highly conserved between the LAW proteins it is possible that the other LAW proteins both homo and heterodimerise. The differential binding of the LAW proteins with the PHDs and VHL, in addition to PHD and LAW multimerisation suggests the presence of a highly complex group of proteins, of which the precise components will require careful dissection. Numerous strategies could be performed to deduce the specific components of this protein complex, including the use of non-denaturing electrospray mass spectrometry which enables the identification of non-covalent complexes often involving mutimeric proteins. Alternatively, tandem affinity purification could be used, involving two subsequent affinity purification steps of tagged recombinant proteins to identify specific interacting partners by SDS-PAGE. In addition, size fractionation and non-denaturing native SDS-PAGE could be employed to identify whether LIMD1 is present in higher molecular weight complexes and whether these correspond to the same molecular weights as PHD3 containing complexes.

To complement these studies and determine the specific components of this LIMD1 containing protein complex, mapping of the specific protein-protein interfaces of LIMD1 with these other components will be required. There are currently 25 LIMD1 amino and carboxyl terminal expression mutants currently in use in our laboratory, in addition to a series of internal deletion mutants. Interestingly, the LAW proteins have six highly homologous motifs within their pre-LIM region, which may represent the PHD1 or PHD3 binding interfaces. These conserved regions have been deleted by site-directed mutagenesis and therefore protein interaction assays with these mutants would shed light on whether LAW interact *via* a conserved binding interface to the PHDs. Initial data using C-terminal mutants indicates the first LIM domain as the VHL interaction domain (Figure 6.7.2). However, arguably the LIMD1 mutants demonstrating a loss of VHL co-IP are immunoprecipitated less abundantly and therefore this requires confirmation. Furthermore, the lab

is in possession of eukaryotic expression vectors encoding LIMD1 with internal deletions of the three LIMD1 LIM domains (kindly donated by Professor GD Longmore, Haematology division, Department of Cell Biology and Physiology, Washington University) and therefore, mapping of the specific VHL binding interface may be confirmed. Whether these internal deletion mutants correlate with a loss of function in negatively regulating HIF transcription or ODD stability would be of great interest.

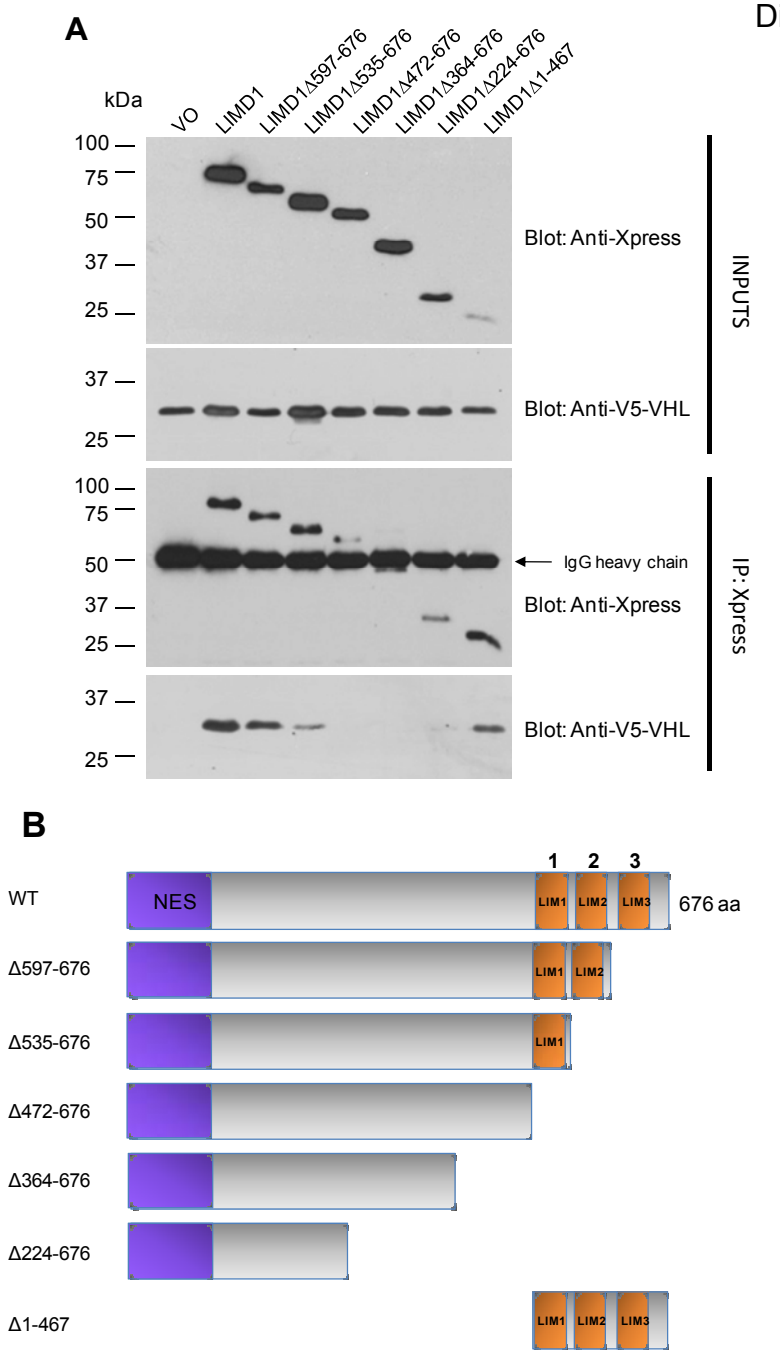

Figure 6.7.2 *LIMD1 interacts with VHL via a binding interface within the LIM 1 domain.*

(A) Xpress-LIMD1 deletion mutants and V5-VHL were co-transfected into U2OS cells. 48 hours post-transfection cells were lysed with RIPA supplemented with protease and phosphatase inhibitors and LIMD1 was immunoprecipitated with an Xpress mAb. Samples were immunoblotted for Xpress-LIMD1 and V5-VHL. IgG heavy chain is indicated by an arrow. Loss of VHL interaction occurs upon deletion of all three LIM domains, however a degree of binding remains after loss of LIM 2 and 3, indicating binding occurs *via* LIM 1. **(B)** Schematic representation of LIMD1 deletion mutants used in the co-IP.

Upon identification of the specific LIMD1 and LAW binding interfaces with the PHDs and VHL, an additional elegant approach that could be under taken would be to use the knockdown-rescue lentivirus system to remove endogenous LIMD1 (LAW) and then re-express specific deletion mutants through an IRES. This would enable the dissection of the different protein interfaces (for example LIMD1-PHD2 verses LIMD1-PHD1/3 interfaces) and subsequent effects on the ability of LIMD1 mutants to regulate HIFs and the HRE. Furthermore, definition of the specific amino acids required for simultaneous PHD2 and VHL binding and examination of how by mutating these residues LIMD1 functions in regulating the HIF activity and thus the hypoxic response pathway would be of great interest. Alongside these experiments further efforts will be required in order to define the endogenous interactions of LAW with PHD1-3 and VHL.

To further dissect which components of this protein complex LIMD1 requires in order to facilitate HIF regulation, a genetic approach could be used. Analysis of the ability of LIMD1 to regulate HIF1 following siRNA or shRNA-knockdown of specific components of the normoxiplex (PHDs and VHL) *in vivo*, would reveal the critical components of the normoxiplex required to transduce LIMD1's affects. In addition, utilisation of MEFs derived from wild-type and LIMD1$^{-/-}$ mice to functionally analyse effects of LIMD1 loss on the composition and activity of the normoxiplex would provide further insight.

An important issue to address is whether LIMD1 regulates HIF2α as well as HIF1α. Initial experiments to identify whether LIMD1 depletion by siRNA performed in U2OS, led to an accumulation of HIF2α were unsuccessful (data not shown). This may be due to the restricted tissue distribution of HIF2α in comparison to the universally expressed HIF1α, as no hypoxia induced accumulation could be detected (Tian et al., 1997). Alternatively, this could be due to the poor signal detection of the antibody used (HIF2α rabbit polyclonal, NB100-480, Novus Biologicals, Littleton, CO, USA). A concerted effort is required in order to establish whether LIMD1 is a general regulator of

HIF function. Moreover, it has been suggested that PHD3 favours hydroxylation of HIF2α over HIF1α (Appelhoff et al., 2004). As all three LAW proteins interact with PHD3 this may indicate that LIMD1 may modulate HIF2 function.

6.8 Determine the precise LIMD1 induced post-translational HIF1α modification

The ability of LIMD1 and LAW to bind with the PHDs and induce degradation of the ODD in a manner dependent on prolyl hydroxylase activity would suggest degradation is *via* P402/P564 hydroxylation. However, data presented shows that LAW induced ODD degradation can occur independently of these residues. This therefore, raises the question as to the necessity for LIMD1 to bind to the PHDs as well as VHL. Currently it is unknown how LIMD1 specifically induces post-translational modifications of HIF1α, what these modifications are and how these ultimately lead to HIF1α proteasome-dependent degradation? Therefore, systematic examination is required to identify which of the known HIFα modifications the expression of LIMD1 may induce, including hydroxylation, ubiquitylation and sumoylation. One approach would be to perform *in vitro* hydroxylation assays. These could be performed *in vivo* or *in vitro* using recombinant HIF1α ODD and ODD P402A/P564A (GST- or V5-tagged) as a substrate for prolyl hydroxylation, detected by LC-MS/MS as was used for the analysis of ankyrin hydroxylation (Coleman et al., 2007). Whether ectopic expression of LIMD1 or RNAi mediated depletion of LIMD1 modulated prolyl hydroxylation, in terms of the kinetics of the enzymatic reaction or altering the substrate proline residues would be examined. Post-translational modifications could also be examined in the context of the full length protein using full length eukaryotic expression vectors encoding V5-tagged-HIF1α and V5-HIF1α P402A/P564A. It may be plausible that only upon the deletion of these proline residues LIMD1 acts to induce an additional mechanism or alters the specificity of the PHDs to hydroxylate alternative proline residues. The ODD domain contains numerous proline residues (Figure 6.8.1), many of which share similarity to

the conserved LXXLAP hydroxylation motif. LC-MS/MS analysis may reveal whether LIMD1 is capable of altering proline hydroxylase residue specificity.

^{390}KKEPDALTLLAPAAGDTIISLDFGSNDTETDDQQLEEVPLYNDVMLP
SPNEKLQNINLAMSPLPTAETPKPLRSSADPALNQEVALKLEPNPESLE
LSFTMPQIQDQTPSPSDGSTRQSSPEPNSPSEYCFYVDSDMVNEFKLEL
VEKLFAEDTEAKNPFSTQDTDLDLEMLAPYIPMDDDFQLRSFDQLSPLE
SSSASPESASPQSTVTVFQQTQIQEPTANATTTTATTDELKTVTKDRME
DIKILIASPSPTHIHKETT^{652}

Figure 6.8.1 *HIF1α ODD domain is a proline rich sequence.*
The HIF1α ODD domain (amino acids 390-652) contains numerous proline residues (highlighted), many of which are highly similar to the well characterised proline 402 and 564 hydroxylation sites, within LXXLAP motifs (underlined).

Recent data has increasingly implicated the role of other non-prolyl hydroxylase post-translational modifications in the regulation of HIFα protein stability (Brahimi-Horn et al., 2005). One reported mechanism which occurs independently of proline 402/564 hydroxylation, but is dependent on VHL activity is sumoylation. However, there have been conflicting reports as to whether sumoylation promotes HIFα stabilisation (Carbia-Nagashima et al., 2007; Bae et al., 2004) or degradation (Cheng et al., 2007; Berta et al., 2007). Most recent publications suggest that sumoylation predominantly induces degradation. Therefore, LIMD1 in addition to PHD dependent ODD degradation may also promote HIFα sumoylation at lysine 391 and 477,

accounting for the observed proline 402/564 independent ODD degradative function. Therefore, in order to investigate this hypothesis, As-RED LIMD1 was co-transfected into U2OS cells with an EGFP-SUMO1 construct (kindly donated by Dr Simon Dawson, School of Biomedical Sciences, University of Nottingham) to examine whether a co-localisation could be observed. Preliminary data indicated that LIMD1 did indeed co-localise with EGFP-SUMO1 in bodies in the peri-nuclear region of the cytoplasm (Figure 6.8.2). However, this needs to be complemented with AsRED and EGFP vector controls and thus only provides an indication that these proteins co-localise *in vivo*.

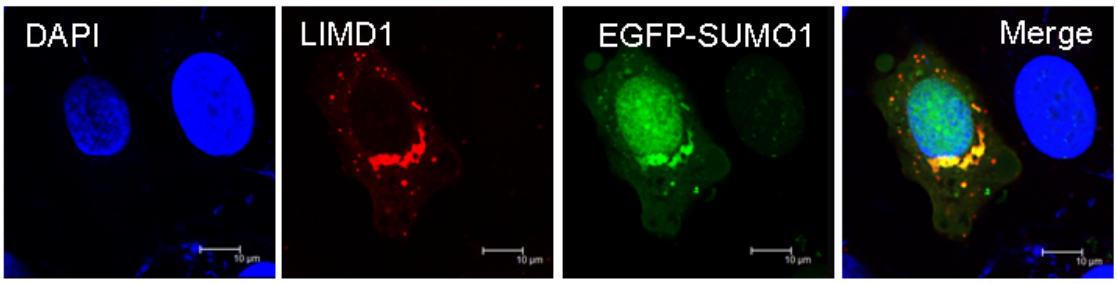

Figure 6.8.2 *LIMD1 co-localises with SUMO1 in U2OS cells in vivo.*
U2OS cells were transiently co-transfected with AsRED-LIMD1 and EGFP-SUMO1. 48 hours post-transfection cells were then fixed using 4% PFA and fluorescent fusion proteins visualised using confocal microscopy. Nuclear staining achieved using DAPI incorporated into the mounting media (Vectashield, Vector Laboratories Inc. CA, USA).

Further work is required to investigate the possibility that LIMD1 may regulate HIF by modulating sumoylation. Therefore, similarly to *in vitro* ubiquitination assays, *in vitro* sumoylation assays are required, to investigate whether ectopic expression of LIMD1 or RNAi mediated depletion alters the degree of HIFα sumoylation. To distinguish whether LIMD1 may mediate prolyl-hydroxylase independent HIFα degradation *via* sumoylation; this assay may

be repeated by the use of the hydroxylation resistant HIF1α or ODD construct (P402A/P564A).

6.9 *In vivo* analysis of the role of LIMD1 in physiological hypoxic responses

RNAi mediated LIMD1 depletion induced an increase in the endogenous mRNA levels of the HIF response genes VEGF and BNIP3. Therefore, to complement these data and confirm that the role of LIMD1 regulation has a physiological effect *in vivo*, a primary study analysing a downstream haematological parameter of HIF transcription was performed. Polycythemia or erythrocytosis (increased red blood cell numbers) has been shown to be associated with defective oxygen sensing in organs/cells producing the hypoxia response gene product erythropoietin (Semenza, 2009). Furthermore, a familial polycythemic condition has been linked to a heterozygous mutation in PHD2 that reduces hydroxylase activity (Percy et al., 2006). Moreover, conditional $Phd2^{-/-}$ or $Phd1^{-/-}$;$Phd3^{-/-}$ mice exhibit increased serum EPO levels and erythrocytosis (Takeda et al., 2008). Of the LAW proteins, only LIMD1 is significantly expressed in bone marrow cells (both haematopoietic and mesenchymal) (Luderer et al., 2008). Therefore, an initial investigation was performed to analyse whether the loss of LIMD1 contributed to a polycythemic phenotype due to aberrant HIF regulation. The hematocrit or packed cell volume is the proportion of total blood volume that is occupied by red blood cells. As red blood cell production (erythropoiesis) is regulated by the HIF response gene erythropoietin, it acts as a direct parameter for measuring the downstream physiological effect of HIF transcription. In collaboration with Professor GD Longmore (University of Washington) a pilot study was performed to evaluate whether the increased HRE activity observed in the *Limd1*$^{-/-}$ MEFs (Figure 5.2.2) translated to an increase in hematocrit in *Limd1*$^{-/-}$ mice in comparison to their WT littermate mice. Adult mice were incubated in normoxia (20% O_2) or hypoxia (10% O_2) for 16 hours before peripheral blood samples were collected *via* the inferior vena cava immediately after they were euthanized. Blood samples were

immediately mixed with EDTA and blood counts were measured using an Advia 2120 (Bayer, Pittsburgh, PA). Preliminary data indicated that *Limd1*$^{-/-}$ mice were moderately polycythemic, as the *Limd1*$^{-/-}$ mice exhibited an increased hematocrit in comparison to the WT mice following hypoxic exposure (Figure 6.9). This is in keeping with previous data which demonstrated that *Limd1*$^{-/-}$ MEFs exhibited an elevated HRE activation following hypoxic exposure (Figure 5.2.2). However, the WT mice do not exhibit an increase in hematocrit upon 16 hours hypoxic incubation which may suggest that this time period is insufficient to see the effects of erythropoietic drive. Future work, optimising this experiment over a range of time points will shed further light into the physiological consequences of LIMD1 loss. As the different PHD isoforms have been demonstrated to differentially regulate HIF1α stability in the liver and kidney and suppress erythropoiesis through distinct mechanisms (Takeda et al., 2008), the effect of LIMD1 loss may give further insights into the dichotomy of its function with the different PHD isoforms.

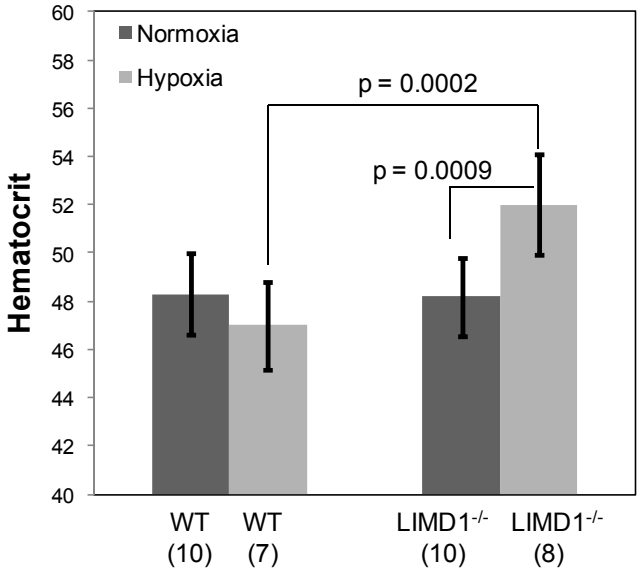

Figure 6.9 *Limd1$^{-/-}$ mice exhibit elevated hematocrit following exposure to hypoxia.*

Adult WT and *Limd1$^{-/-}$* mice (n given in bracket) were incubated at 20% and 10% O_2 for 16 hours. Peripheral blood samples were collected *via* the inferior vena cava immediately after they were euthanized. Blood samples were immediately mixed with EDTA and blood counts were measured using an Advia 2120 (Bayer, Pittsburgh, PA). *Limd1$^{-/-}$* mice incubated in 10% O_2 for 16 hours demonstrated an elevated hematocrit in comparison to the normoxic *Limd1$^{-/-}$* mice and their WT littermates.

In addition, future work incorporating a full haematological and serological analysis on these *Limd1$^{-/-}$* mice compared to WT mice as controls may be undertaken to examine *in situ* effects on hypoxic response due to *Limd1* loss. Such analysis could include complete blood count profiles of peripheral blood, serum EPO levels as well as hepatic and renal mRNA EPO levels in conjunction with red blood cell numbers (i.e., hematocrit). Flow cytometry analysis of bone marrow haematopoietic progenitors may also be performed, as polycythemia is often caused by excessive differentiation and proliferation of Ter119+ erythroid progenitors, which are known to express EPO receptors at high levels (Richmond et al., 2005).

Bone osteoblast cells express VEGF which in an autocrine manner has been shown to influence bone osteoblast differentiation and mineralization (Midy and Plouet, 1994). Interestingly, international collaborators have recently shown that Limd1 is a negative regulator of osteoblast differentiation and function (Luderer et al., 2008). Primary osteoblast precursor cells isolated from the bones of *Limd1*$^{-/-}$ mice gave rise to more osteoblast cells and exhibited increased mineralization in *ex vivo* cultures. Furthermore, they have also established immortalized osteoblast progenitor cell lines from WT and *Limd1*$^{-/-}$ mice. These cell lines behave exactly as primary cells in culture, with increased differentiation and mineralization compared to WT cells. However, the precise cellular or molecular mechanism whereby Limd1 negatively regulates osteoblastogenesis is not known. With the identification of Limd1 as a regulator of the hypoxia response this makes its role in VEGF secretion by osteoclast or osteoblast precursor cells and subsequent autocrine response to VEGF a compelling hypothesis. Future work to test this hypothesis in primary WT and *Limd1*$^{-/-}$ osteoblasts isolated from the calvarial bones of newborn mice and adult bone marrow mesenchymal progenitors is required. Analysis of secreted VEGF (ELISA) and VEGF mRNA levels (qRT-PCR) are required to establish whether Limd1 regulates osteoblastogenesis *via* VEGF. In addition, cultures of *Limd1*$^{-/-}$ progenitors will be treated with VEGF-neutralizing soluble receptor. If the absence of Limd1 leads to increased VEGF secretion and thus increased osteoblast differentiation (autocrine stimulation by VEGF) or osteoblast colony formation from mesenchymal progenitors then this treatment should inhibit these (Luderer et al., 2008).

6.10 *In vivo* analysis of the role of LIMD1 in the regulation of HIF in cancer

LIMD1 is encoded on C3CER1, a region of human chromosome 3, which harbours deletions in 83% of 576 tumours analysed (Petursdottir et al., 2004). LIMD1 has been demonstrated to be lost in human lung cancers in 75% and 79% of squamous and adenocarcinomas respectively (Sharp et al.,

2008). Furthermore, *Limd1*$^{-/-}$ mice challenged with carcinogenic urethane formed a higher incidence of tumours of increased size in comparison to their WT littermates. Solid tumours often contain hypoxic regions and both HIF1α and HIF2α are widely found over expressed in a broad range of malignancies (Talks et al., 2000). Therefore, it would be of interest to analyse whether LIMD1 loss contributes to increased HIFα levels in cancer. Immunohistochemistry of different human cancers could be used to quantify protein levels from cancer sections in order to evaluate whether LIMD1 and HIFα are inversely correlated. In particular, evaluation of lung cancer models whereby LIMD1 has been demonstrated to be down regulated and HIF1α over-expressed (Shyu et al., 2007) would be interesting. This could initially be achieved by analysis of the 48 matched lung tumour and normal samples used to evaluate LIMD1 loss and epigenetic silencing (Sharp et al., 2008). The role of LIMD1 in VHL inactive renal cell carcinomas which constitutively over-express HIF2α would also be of interest (Maxwell et al., 1999; Raval et al., 2005). Whether LIMD1 loss would further promote HIFα accumulation in VHL inactive renal cell carcinomas is arguable, depending on whether LIMD1 activity is dependent or independent of VHL activity. Furthermore, *in vivo* and *ex vivo* analysis of these renal cell carcinomas would shed further light onto the precise mechanism of LIMD1's regulation of HIF.

Another subject to address is whether and to what degree LIMD1 performs tumour suppressive activity *via* negative regulation of HIF with the PHDs in comparison to negative regulation of E2F transcription with pRB. One approach would be to perform *in vitro* experiments such as colony formation assays in both pRB$^{-/-}$ SAOS2 and VHL inactive renal cell carcinoma cell lines. In addition, following the identification of the precise PHD and VHL binding interfaces within LIMD1, colony formation assays could be performed with LIMD1 mutants with these binding regions internally deleted. This may provide an insight into whether binding to the PHDs and/or VHL is required for tumour suppressive LIMD1 function. Alternatively, LIMD1 mediated ODD degradation is attenuated by treatment of the PHD inhibitor DMOG. Therefore, to what degree LIMD1 still enables growth suppression following DMOG administration would be interesting. In combination with other *in vitro*

analysis, to dissect LIMD1's multiple different functions and to understand their physiological contribution to cancer formation would be of great interest.

There are possible therapeutic implications of the increasing evidence that LIMD1 may perform as a critical tumour suppressor. The most accessible therapeutic use is probably the loss of LIMD1 as an early onset marker for tumourigenesis. LIMD1 loss occurs early in tumour formation and therefore, LIMD1 expression could be used as a marker for early stage tumour development. Additionally, LIMD1 nuclear localisation in breast cancer correlates with good prognosis and therefore LIMD1 distribution could also be monitored (Spendlove et al., 2008). LIMD1 has been demonstrated to be regulated by epigenetic silencing. Of 48 matched lung cancer samples analysed, 26% exhibited promoter methylation, and of the tumours which showed increased methylation 86% had reduced LIMD1 expression levels determined by qRT-PCR (Sharp et al., 2008). Administration of the DNA methylation inhibitor 5-Aza-2′-deoxycytidine in the MB435 cell line which do not express LIMD1 however, contain the *LIMD1* gene, induces re-expression of LIMD1 (Sharp et al., 2008). This provides scope for the re-expression of LIMD1 in human cancers to retain tumour suppressive activity by treatment with 5-Aza-2′-deoxycytidine which has already been demonstrated to exhibit an anti-neoplastic effect on human breast carcinoma cells (Primeau et al., 2003). However, similarly to the potential inhibition of PHD activity to promote HIF activity in anaemic and ischemic disorders which may contribute to HIF induced tumour formation, the effect of LIMD1 re-expression which may promote ischemia would require careful consideration.

6.11 Regulation of LIMD1 by phosphorylation

The addition and removal of phosphate groups to proteins (phosphorylation and de-phosphorylation respectively) acts as a key molecular switch that regulates numerous cellular processes. LIMD1 is serine, threonine and tyrosine phosphorylated (Figure 6.11.1) which was confirmed by Huggins et al in 2008 (Huggins and Andrulis, 2008). Therefore, it was hypothesised that

phosphorylation status may determine LIMD1 function, thus providing a mechanism whereby functions with pRB and PHD/VHL may be distinguished. A primary investigation indicated that phospho-threonine LIMD1 interacts with PHD2 but not phospho-serine or phospho-tyrosine (Figure 6.11.2). LIMD1 interacted with PHD2 immunoprecipitated using a rabbit polyclonal antibody, thus verifying previous co-IPs whereby LIMD1 was immunoprecipitated using a LIMD1 mAb (Figure 3.1.1.2). Interestingly, immunoblotting with phospho-specific antibodies detected only the presence of phospho-threonine LIMD1 as a PHD2 interacting partner (Figure 6.11.2). This indicates that PHD2 only interacts with threonine phosphorylated (or non-phosphorylated) LIMD1. Therefore, this may suggest that the LIMD1-PHD2 interaction is dependent on phosphorylation and provides a mechanism whereby LIMD1 may interact with PHDs in response to cellular signalling cues. However, this experiment requires repetition for verification. Further research into whether alkaline phosphatase treatment impairs LIMD1-PHD binding and which kinase phosphorylates LIMD1 in response to which signalling cascades is required. It is plausible that phosphorylation status may regulate the ability of all of the LAW proteins to determine their differential interactions with PHD1, 2 and 3. Whether LIMD1 is also phosphorylated in response to hypoxia is also a consideration. The effect of RNAi mediated LIMD1 depletion resulted in a marked increase in the stability of HIF1α in hypoxia than in normoxia (Figure 4.4.1.4). As LIMD1 protein levels were not modulated by oxygen tension (Figure 4.2), phosphorylation may act in a way to enhance PHD function *via* LIMD1 and also a mechanism to distinguish LIMD1 functions. This is in keeping with the hypothesis that LIMD1 bridges PHD and VHL activities, where there may be an increased necessity for LIMD1 function in enhancing HIF1α hydroxylation, when hydroxylase activity is limited by reduced oxygen availability. Therefore, cellular signalling pathways stimulated by hypoxia may result in LIMD1 phosphorylation, augmenting the LIMD1-PHD2 interaction and thus providing a negative feedback loop to regulate HIF1 activity.

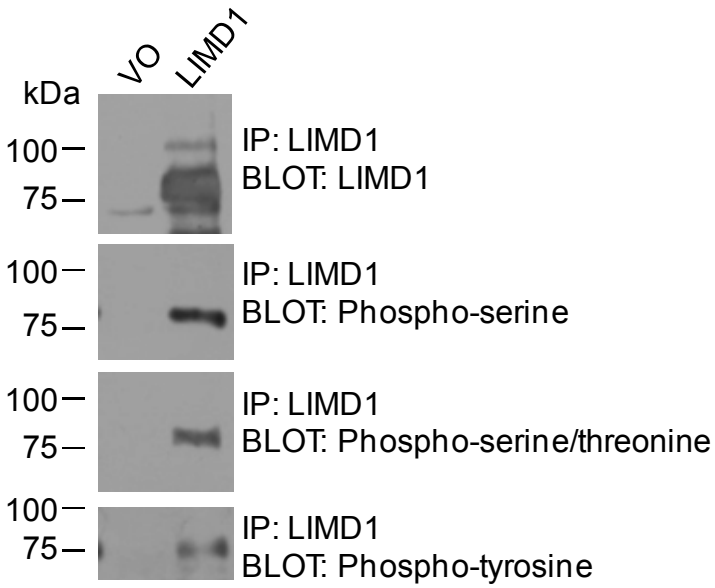

Figure 6.11.1 *LIMD1 is serine, threonine and tyrosine phosphorylated.*
Xpress-LIMD1 and vector only (VO) control were transfected into U2OS cells. 48 hours post-transfection cells were lysed with RIPA supplemented with protease and phosphatase inhibitors and LIMD1 was immunoprecipitated with a LIMD1 mAb. Samples were immunoblotted for LIMD1 IP and for phospho-serine, phospho-serine/threonine or phospho-tyrosine. Immunoblotting was performed using 5% (w/v) BSA/PBS-T rather than 5% marvel/PBS-T LIMD1, to prevent detection of phospho-casein. LIMD1 is detected by all three phospho antibodies, indicating phosphorylation.

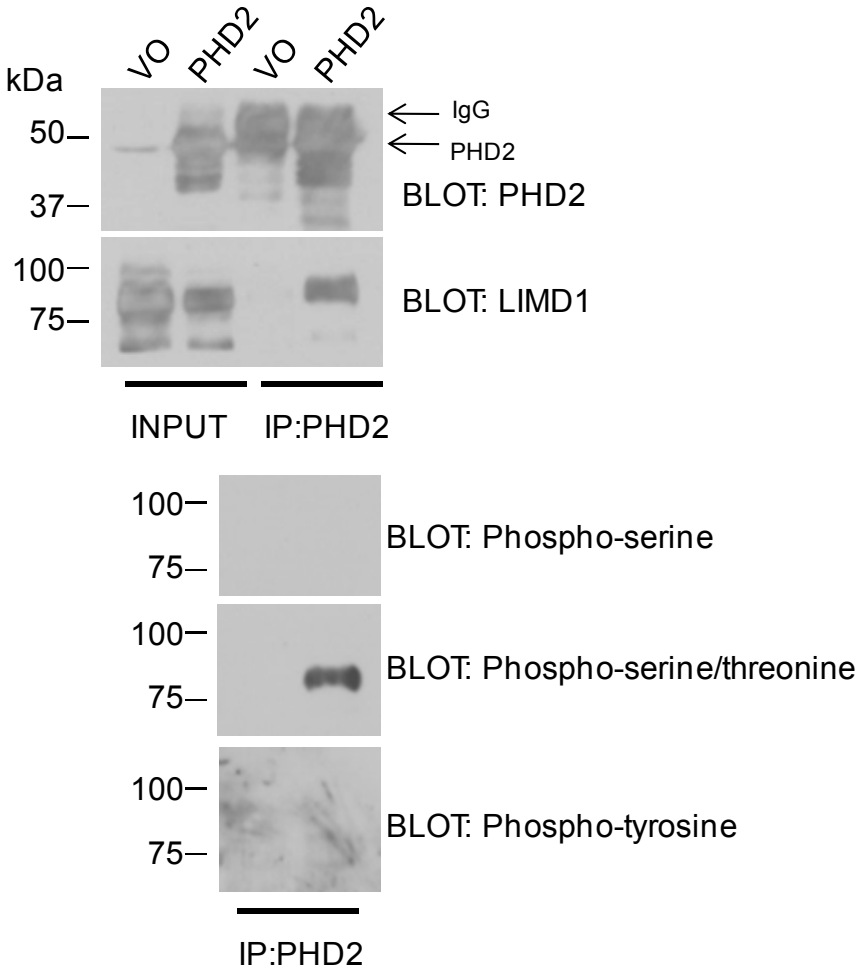

Figure 6.11.2 *PHD2 specifically interacts with phospho-threonine LIMD1.*
VO and PHD2 were co-transfected with LIMD1 into U2OS cells. 48 hours post-transfection cells were lysed with RIPA supplemented with protease and phosphatase inhibitors and PHD2 was immunoprecipitated with a polyclonal antibody. Samples were immunoblotted to detect whether LIMD1 co-IPs with PHD2 and whether specific phospho-LIMD1 forms could be detected. Immunoblotting was performed using 5% (w/v) BSA/PBS-T rather than 5% marvel/PBS-T LIMD1, to prevent detection of phospho-casein. Phospho-serine/threonine LIMD1 specifically interacts with PHD2 but not phospho-serine or phospho-tyrosine. This is therefore indicative that PHD2 specifically interacts with phospho-threonine LIMD1.

6.12 LIMD1 as a possible substrate for prolyl hydroxylation

One plausible hypothesis worth future consideration is the possibility that LIMD1 is a substrate for PHD mediated prolyl hydroxylation. The pre-LIM region of LIMD1 is highly proline rich (11.9% proline), with numerous regions with varying degrees of homology to the conserved proline hydroxylation consensus sequence 'LXXLAP' (Figure 6.12). Notably, immediately N-terminal to a pre-LIM structured coiled-coil domain there are 7 proline residues within a 21 amino acid region. It may be feasible that LIMD1 is hydroxylated, in turn inducing recruitment of VHL within the normoxic protein complex. There is a precedent for the related collagen prolyl-4-hydroxylases to hydroxylate non-collagen substrates including the human argonaute 2 protein involved in RNA-induced silencing complexes (Qi et al., 2008). However, although the ankyrin repeat domain containing proteins have been identified as FIH substrates, to date no novel non-HIF prolyl hydroxylase substrates have been confirmed (Kaelin, Jr. and Ratcliffe, 2008). To our knowledge, LIMD1 is the only protein to interact with all three PHDs except for the substrate HIFα, which may suggest that LIMD1 is a substrate.

One approach to confirm whether this is the case is to use LC-MS/MS. Recombinant LIMD1 purified *in vivo* or from an *in vitro* hydroxylation assay, could be trypsinised and then analysed for post-translational modifications including hydroxylation by LC-MS/MS. If LIMD1 was indeed a target for hydroxylation, mutagenesis of the proline substrate to analyse the functional significance of this modification would be required.

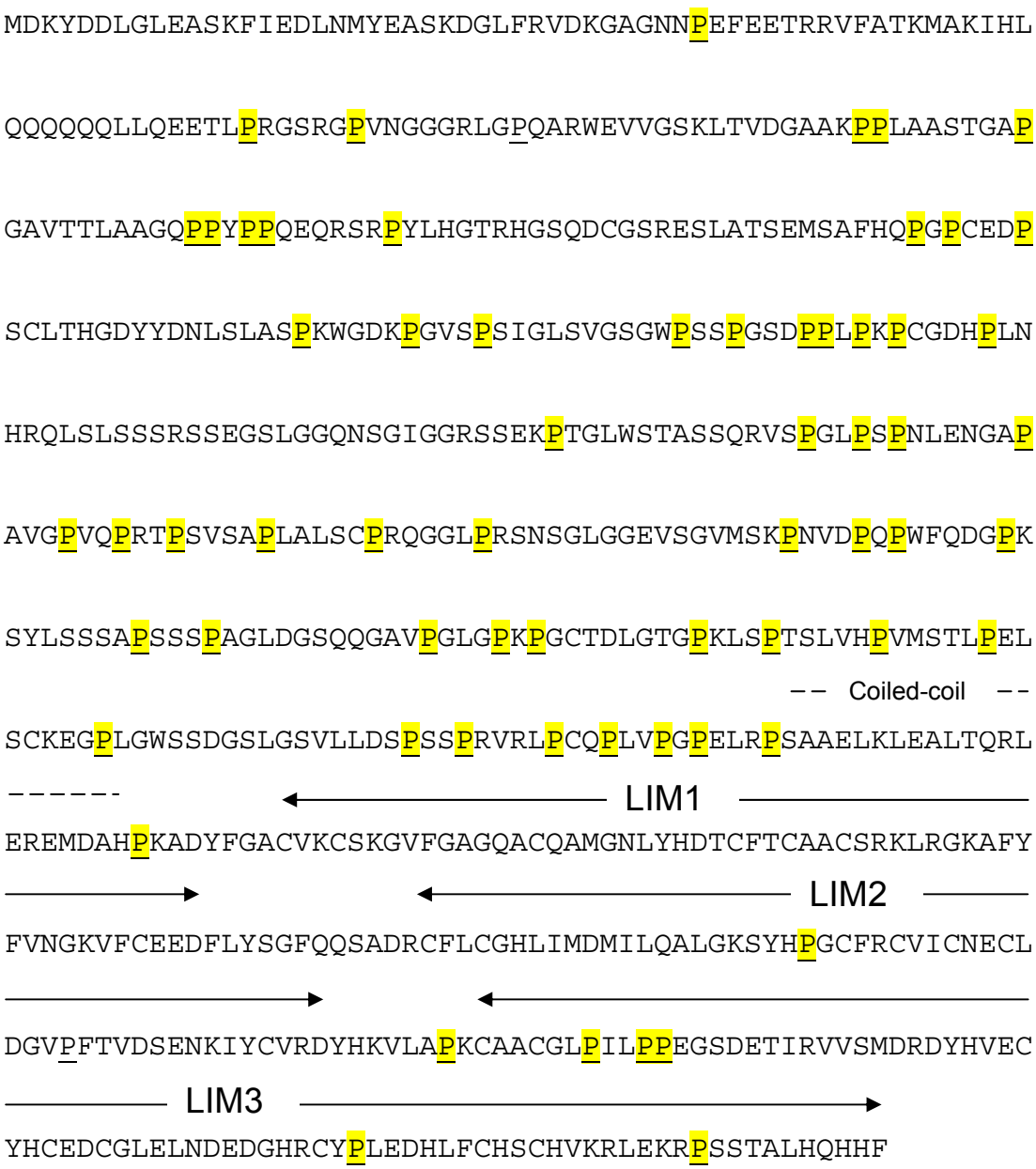

Figure 6.12 *The proline rich nature of the LIMD1 amino acid sequence.*
LIMD1 amino acid sequence, (proline residues, highlighted). LIMD1 is proline rich (9.5% proline, 11.9% proline in pre-LIM region) and therefore may be a candidate PHD substrate. LIM domains and pre-LIM coiled coil domain are designated.

6.13 Conclusion

Data presented in this thesis, demonstrate that LIMD1 and the LAW proteins represent novel proteins in the regulation of HIF function. Such is the scale and diversity of the genes responsive to the HIF transcription factors that it is becoming increasingly apparent that the regulatory networks that control their activity are similarly complex in their nature. Recent findings have described proteins that may interact with different components of the HIF regulatory system; however none to date have been demonstrated to interact with all three PHD proteins and VHL. The mode of action of LIMD1 occurs by its bridging of an association between PHD2 and VHL (shown schematically in Figure 7.8), introducing the concept that the enzymatic activities of the PHDs and VHL are exerted within a functional protein complex, rather than the current dogma whereby they are thought of as two separate subsequent processes. Furthermore, evidence for a proteasome and prolyl hydroxylase dependent, proline 402 and 564 independent mechanism has been provided. Whether LIMD1 may alter the substrate proline residues for hydroxylation or recruit additional post-translational modifiers to the normoxiplex that may act independently of these two residues, is currently unknown. Exciting current research is revealing novel functions of the PHDs, whether LAW act to influence these functions in a tissue specific, redundant or non-redundant manner is unknown, but provides a fascinating base for future research into the specific role of this newly identified family of hypoxic regulators.

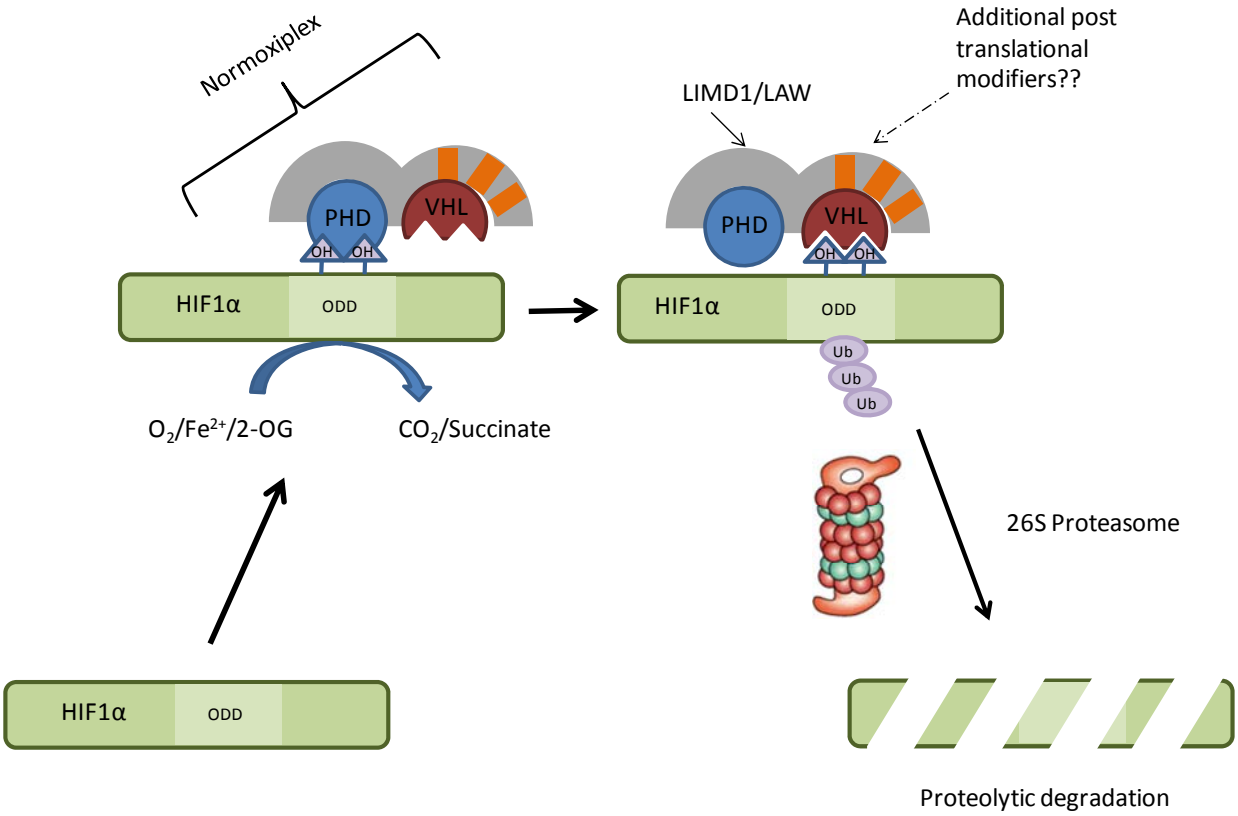

Figure 6.13 *LIMD1/LAW mediate degradation of HIF1α by bridging an association between the PHDs and VHL.*

LIMD1 interacts with PHD2 *via* its pre-LIM region and VHL *via* the LIM domains to scaffold the proteins into one protein complex. Thus, LIMD1 and LAW promote HIF1α degradation by the proteasome, by increasing the physical proximity of the enzymatic components responsible for hydroxylation and ubiquitylation. LIMD1 facilitates degradation of the ODD even upon deletion of the well characterised proline 402 and 564 residues, and therefore it is plausible that LIMD1 acts to recruit other post-translational modifiers to modulate HIFα stability. For simplicity other proteins reportedly involved in regulating HIFα stability have not been depicted in this model, including elongin B,C and Cullin2 within the VBC complex, OS-9, RACK1, SSAT1 and SSAT2, Morg-1, MUC1, MAGE-11, ARD1, HAF, Hdm2, VDU2. The interplay between LIMD1/LAW and these proteins is of future interest.

Appendix

7.1 Generation of Xpress-tagged recombinant prolyl hydroxylases

Untagged pcDNA3-PHD1, PHD2 and PHD3 constructs were kindly donated by Professor Peter Ratcliffe (Nuffield Department of Clinical Medicine, The Henry Wellcome Building for Molecular Physiology, University of Oxford). In order to comparatively analyse the PHDs with the Xpress-tagged Zyxin family proteins, PHDs were TA cloned into the pcDNA4His/Max-TOPO vector (Invitrogen) incorporating an Xpress-tag. Furthermore, for future analysis PHDs were TA cloned into pcDNA4His/Max-TOPO vector in order to sub-clone into pEGFP (EGFP tag, Clontech) and pGEX 4T-1 (GST tag, Amersham). PHD1, PHD2 and PHD3 were amplified by PCR incorporating flanking *BamH1* and *EcoR1* restriction enzyme sites for sub-cloning. In order to keep PHD coding regions in frame upon sub-cloning into pEGFP and pGEX 4T-1, separate PCR primers were designed with differing numbers of base pairs between the 5' flanking restriction site and the PHD start codon.

BamH1 and *EcoR1* sites were incorporated using the following primers:

PHD1 (pEGFP–C1+1) forward:
5'-GGGGGGATCCTGATGGACAGCCCGTGCCAGCCGCAGCCC-3'
PHD1 (pGEX 4T-1) forward:
5'-GGGGGATCCATGGACAGCCCGTGCCAGCCGCAGCCC-3'
PHD1 (pEGFP–C1+1 and pGEX 4T-1) reverse:
5'GGGGAATTCCTAGGTGGGCGTAGGCGGCTGTGATAC-3'

PHD2 (pEGFP–C1+1) forward:
5'-GGGGGGATCCTGATGGCCAATGACAGCGGCGGGCCCGGCGGGCCG-3'
PHD2 (pGEX 4T-1) forward:
5'-GGGGGATCCATGGCCAATGACAGCGGCGGGCCCGGCGGGCCG-3'
PHD2 (pEGFP–C1+1 and pGEX 4T-1) reverse:
5'-GGGGAATTCCTAGAAGACGTATTTACCGACCGAATCTGAAGG-3'

PHD3 (pEGFP–C1+1) forward:

5’-GGGGAGATCTGCATGCCCCTGGGACACATCATGAGGCTGGACCTGGAG-3’

PHD3 (pGEX 4T-1) forward:

5’-GGGAGATCTATGCCCCTGGGACACATCATGAGGCTGGACCTGGAG-3’

PHD3 (pEGFP–C1+1 and pGEX 4T-1) reverse:

5’-GGGGAATTCTCAGTCTTCAGTGAGGGCAGATTCAGTTTTCCT-3’

The PCR reactions were set up as indicated in materials and methods chapter 2.5.1. The PCR cycle for the amplification of 100ng of PHD1 and PHD3 template DNA were as follows:

Initial denaturation	5 min at 95˚c	35 Cycles
Denaturation	1 min at 95˚c	
Primer annealing	1 min at 50˚c	
DNA amplification	1 min at 72˚c	
Final extension	2 min at 72˚c	

Due to the GC rich nature of PHD2 GC melt PCR was performed (materials and methods chapter 2.5.2) using the following PCR parameters:

Initial denaturation	1 min at 95˚c	30 Cycles
Denaturation	30 sec at 94˚c	
Primer annealing	1 min at 50˚c	
DNA amplification	3 min at 68˚c	
Final extension	3 min at 68˚c	

Following the PCR reaction, PCR products were excised, solubilised and purified (section 2.4.6) and verified by agarose gel electrophoresis (Figure 7.1.1).

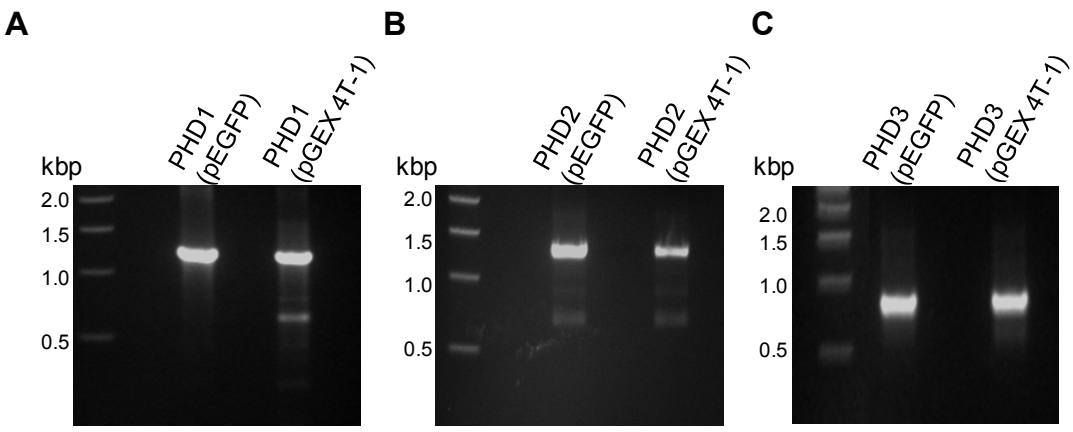

Figure 7.1.1 *PCR amplification of PHD1, PHD2 and PHD3 for TA cloning into the pCDNA4/HisMax expression vector.*

(A) Agarose (1% w/v) gel electrophoresis of PCR amplified product of PHD1 cDNA of 1220 bp. PCR performed twice incorporating restriction enzyme sites in different frames specific for sub-cloning into pEGFP-C1+1 and pGEX 4T-1. **(B)** PCR products representing PHD2 cDNA of 1280 bp and **(C)** PHD3 cDNA of 720 bp.

The PCR product was then TA cloned as described in section 2.5.3 into the pcDNA4His/Max-TOPO vector (Figure 7.1.2). The TA cloning reaction product was then transformed into competent *DH5α* and selected for growth in media containing ampicillin (section 2.3). The recombinant vectors were then mini-prep purified from the bacterial culture (section 2.4.1) and digested using *BamH1* and *EcoRI* restriction sites incorporated by PCR to verify the presence of cDNA insert (Figure 7.1.3). pcDNA4His/Max-TOPO-PHD3 contains an internal *BamHI* restriction site and was therefore cut with *BglII* which shares a compatible restriction digest site. However, this digestion resulted in generation of multiple bands, the smallest representing PHD3 cDNA. Correct incorporation of PHD3 cDNA was confirmed by sequence analysis. Sequence analysis using an Xpress forward primer (5' TATGGCTAGCATGACTGGT 3') confirmed the correct full length, in frame insertion of the PHDs in the correct 5' to 3' orientation (Figure 7.1.4).

A

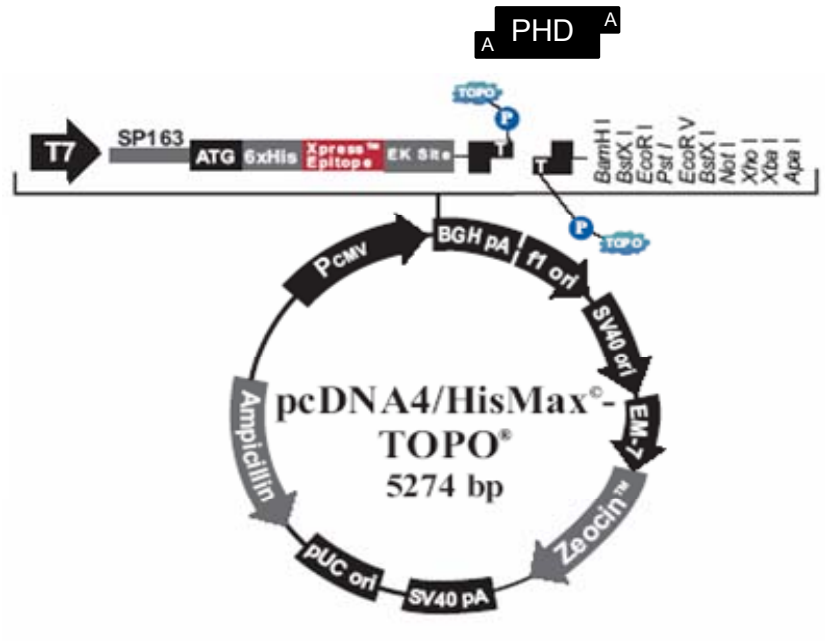

B

Figure 7.1.2 *pcDNA4His/Max-TOPO expression vector.*

(A) pcDNA4His/Max-TOPO vector map and schematic representation of the topoisomerase I mediated cloning reaction. **(B)** pcDNA4His/Max-TOPO multiple cloning site, illustrating the region of insertion of the PCR product.

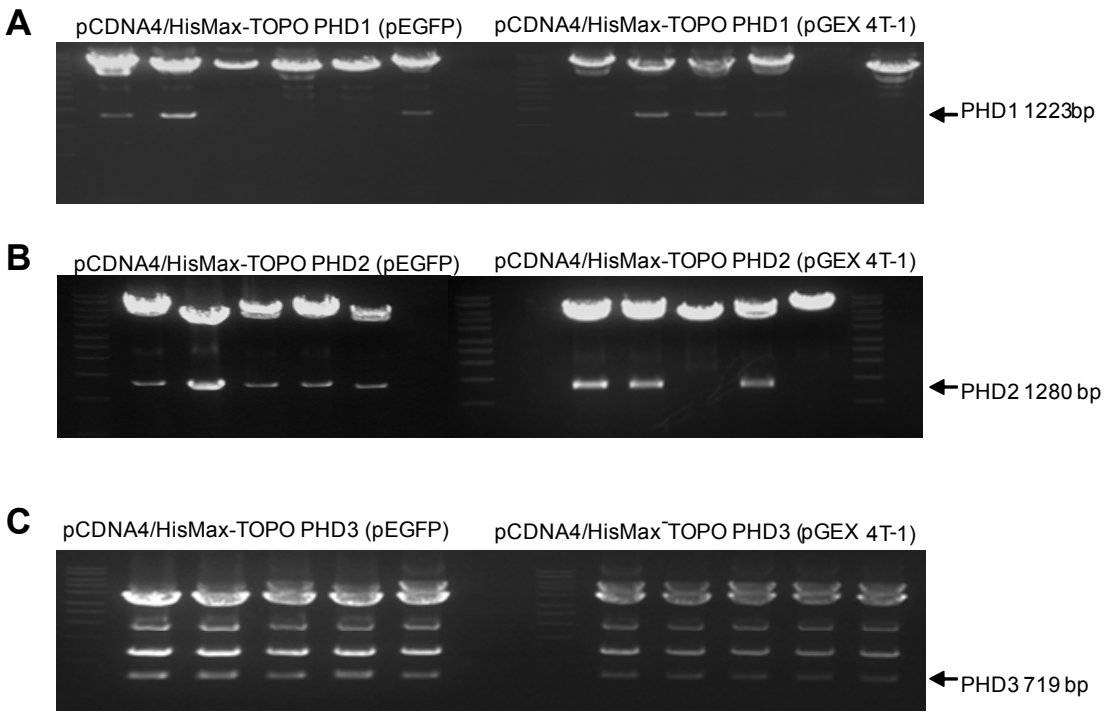

Figure 7.1.3 *Restriction digest verification of TA cloning of PHD cDNA into the pCDNA4/HisMax vector.*

pCDNA4/HisMax vectors were digested with *BamH1/EcoRI* (**[A]** PHD1 and **[B]** PHD2) and *BglII/EcoRI* (**[C]** PHD3) to confirm the presence of PHD cDNA inserted within the vector by TA cloning. PHD3 contains an internal *BamH1* restriction site. Therefore, a *BglII* site was incorporated by PCR instead, capable of ligating with a restricted *BamHI* site. However, pCDNA4/HisMax contains multiple *BglII* sites creating multiple bands upon digestion, which became problematic upon vector digest to verify PHD3 insert presence. Therefore all vectors were sequenced using a 5' pCDNA4/HisMax primer.

A: pCDNA4His/Max-PHD1 (pEGFP)

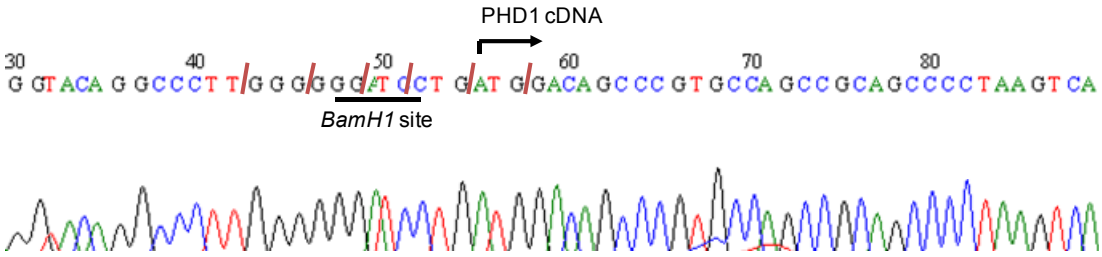

B

GGTCGGGGACTGTACGACGATGACGATAAGGTACAGGCCCTTGGGGGGATCCTGATG
GACAGCCCGTGCCAGCCGCAGCCCCTAAGTCAGGCTCTCCCTCAGTTACCAGGGTCT
TCGTCAGAGCCCTTGGAGCCTGAGCCTGGCCGGGCCAGGATGGGAGTGGAGAGTTAC
CTGCCCTGTCCCCTGCTCCCCTCCTACCACTGTCCAGGAGTGCCTAGTGAGGCCTCG
GCAGGGAGTGGGACCCCCAGAGCCACAGCCACCTCTACCACTGCCAGCCCTCTTCGG
GACGGTTTTGGCGGGCAGGATGGTGGTGAGCTGCGGCCGCTGCAGAGTGAAGGCGCT
GCAGCGCTGGTCACCAAGGGGTGCCAGCGATTGGCAGCCCAGGGCGCACGGCCTGAG
GCCCCCAAACGGAAATGGGCCGAGGATGGTGGGGATGCCCCTTCACCCAGCAAACGG
CCCTGGGCCAGGCAAGAGAACCAGGAGGCAGAGCGGGAGGGTGGCATGAGCTGCAGC
TGCAGCAGTGGCAGTGGTGAGGCCAGTGCTGGGCTGATGGAGGAGGCGCTGCCCTCT
GCGCCCGAGCGCCTGGCCCTGGACTATATCGTGCCCTGCATGCGGTACTACGGCATC
TGCGTCAAGGACAGCTTCCTGGGGGCAGCACTGGGCGGTCGCGTGCTGGCCGAGGTG
GAGGCCCTCAAACGGGGTGGGCGCCTGCGAGACGGGCAGCTAGTGAGCCAGAGGGCG
ATCCCGCCGCGCAGCATCCGTGGGGACCAGATTGCCTGGGTGGAAGGCCATGAACCA
GGCTGTCGAAGCATTGGTGCCCTCATGGCCCATGTGGACGCCGTCATCCGCCACTGC
GCAGGGCGGCTGGGCAGCTATGTCATCAACGGGCGCACCAAGGCCATGGTGGCGTGT
TACCCAGGCAACGGGCTCGGGTACGTAAGGCACGTTGACATCCCCACGGCGATGGGC
GCTGCATCAACTGTATCTATTACCTGATCAGACCTGGACGTAGTGCATGCGCTGCTG
CAGATCTCCCTGAAGGGCGACCCGTGCTAGCCACATCGAGTCCACTCAGACTGAGCT
CATTACTGACTGACCGACGAACCTCCACGAGGTTA

C: pCDNA4His/Max-PHD1 (pGEX4T-1)

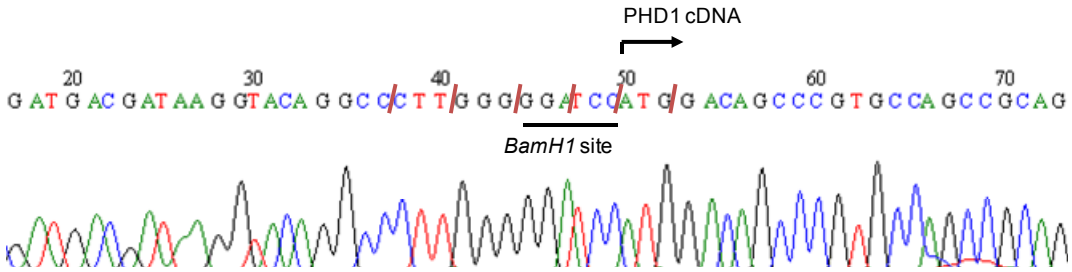

D

CTATGGTACTGTCGACGATGACGATAAGGTACAGGCCCTTGGGGGATCCATGGACAG
CCCGTGCCAGCCGCAGCCCCTAAGTCAGGCTCTCCCTCAGTTACCAGGGTCTTCGTC
AGAGCCCTTGGAGCCTGAGCCTGGCCGGGCCAGGATGGGAGTGGAGAGTTACCTGCC
CTGTCCCCTGCTCCCCTCCTACCACTGTCCAGGAGTGCCTAGTGAGGCCTCGGCAGG
GAGTGGGACCCCCAGAGCCACAGCCACCTCTACCACTGCCAGCCCTCTTCGGGACGG
TTTTGGCGGGCAGGATGGTGGTGAGCTGCGGCCGCTGCAGAGTGAAGGCGCTGCAGC
GCTGGTCACCAAGGGGTGCCAGCGATTGGCAGCCCAGGGCGCACGGCCTGAGGCCCC
CAAACGGAAATGGGCCGAGGATGGTGGGGATGCCCCTTCACCCAGCAAACGGCCCTG
GGCCAGGCAAGAGAACCAGGAGGCAGAGCGGGAGGGTGGCATGAGCTGCAGCTGCAG
CAGTGGCAGTGGTGAGGCCAGTGCTGGGCTGATGGAGGAGGCGCTGCCCTCTGCGCC
CGAGCGCCTGGCCCTGGACTATATCGTGCCCTGCATGCGGTACTACGGCATCTGCGT
CAAGGACAGCTTCCTGGGGGCAGCACTGGGCGGTCGCGTGCTGGCCGAGGTGGAGGC
CCTCAAACGGGGTGGGCGCCTGCGAGACGGGCAGCTAGTGAGCCAGAGGGCGATCCC
GCCGCGCAGCATCCGTGGGGACCAGATTGCCTGGGTGGAAGGCCATGAACCAGGCTG
TCGAAGCATTGGTGCCCTCATGGCCCATGTGGACGCCGTCATCCGCCACTGCGCAGG
GCGGCTGGGCAGCTATGTCATCAACGGGCGCACCAAGGCCATGGTGGCGTGTTACCC
AGGCAACGGGCTCGGGTACGTAAGGCACGTTGACAATCCCCACGGCGATGGGCGCTG
CATCACCTGTATCTATTACCTGAATCAGAACTGGGACGTTAAGTGCATGGCGGCCTG
CTGCAGATCTTCCTGAGGGTCGGCCCGTGGTAGCACATCGAGCCACTCTTTGACGGA
TGCTCATTTTCTGGTCTGACGCGATCCCTCCACGAGTGAGCAGCCTAATGGCACAGT
ACGCCATTCACTGTCTGGATTGAATGACAAGGACCGGTCAGCCAGCCCAATGGCACA
AG

E: pCDNA4His/Max-PHD2 (pEGFP)

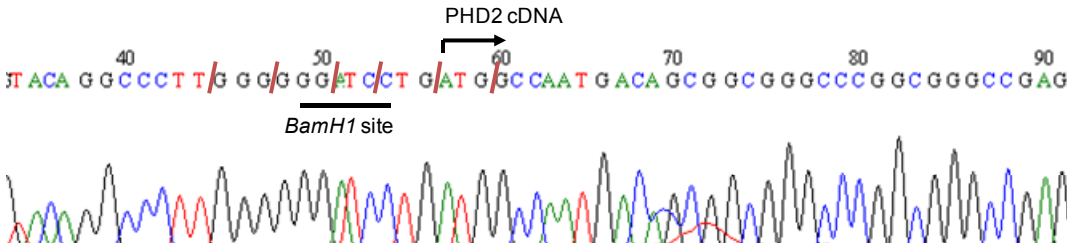

F

GGGGCGGGGGGACTGTCGACGATGACGATAAGGTACAGGCCCTTGGGGGGATCCTGA
TGGCCAATGACAGCGGCGGGCCCGGCGGGCCGAGCCCGAGCGAGCGAGACCGGCAGT
ACTGCGAGCTGTGCGGGAAGATGGAGAACCTGCTGCGCTGCAGCCGCTGCCGCAGCT
CCTTCTACTGCTGCAAGGAGCACCAGCGTCAGGACTGGAAGAAGCACAAGCTCGTGT
GCCAGGGCAGCGAGGGCGCCCTCGGCCACGGAGTGGGCCCACACCAGCATTCCGGCC
CCGCGCCGCCGGCTGCAGTGCCGCCGCCCAGGGCCGGGGCCCGGGAGCCCAGGAAGG
CAGCGGCGCGCCGGGACAACGCCTCCGGGGACGCGGCCAAGGGAAAAGTAAAGGCCA
AGCCCCCGGCCGACCCAGCGGCGGCCGCGTCGCCGTGTCGTGCGGCCGCCGGCGGCC
AGGGCTCGGCGGTGGCTGCCGAAGCCGAGCCCGGCAAGGAGGAGCCGCCGGCCCGCT
CATCGCTGTTCCAGGAGAAGGCGAACCTGTACCCCCCAAGCAACACGCCCGGGGATG
CGCTGAGCCCCGGCGGCGGCCTGCGGCCCAACGGGCAGACGAAGCCCCTGCCGGCGC
TGAAGCTGGCGCTCGAGTACATCGTGCCGTGCATGAACAAGCACGGCATCTGTGTGG
TGGACGACTTCCTCGGCAAGGAGACCGGACAGCAGATCGGCGACGAGGTGCGCGCCC
TGCACGACACCGGGAAGTTCACGGACGGGCAGCTGGTCAGCCAGAAGAATGACTCGT
CCAAGGACATCCGAGGCGATAAGATCACCTGGATCGAGGGCAAGGAGCCCGGCTGCG
AAACCATTGGGCTGCTCATGAGCAGCATGGACGACCTGATACGCCACTGTAACGGGA
AGCTGGGCAGCTACAAAATCAATGGCCGGACGAAAGCCATGGTCGCTTGTTATCCGG
CAATGGAACGGGTTATGTACGTCATGTGATATCCAATGAGATGGAAGATGTGTGACA
TGTATATATTATCTTAATAAGACTGGCATGGCAGTAGTGAGCTACCTCGATTTCAGA
AGGCAAGTCAGTGCTGACTTGAACAAATGATGACTGCGTTTTCTGGTCTGGC

G: pCDNA4His/Max-PHD2 (pGEX4T-1)

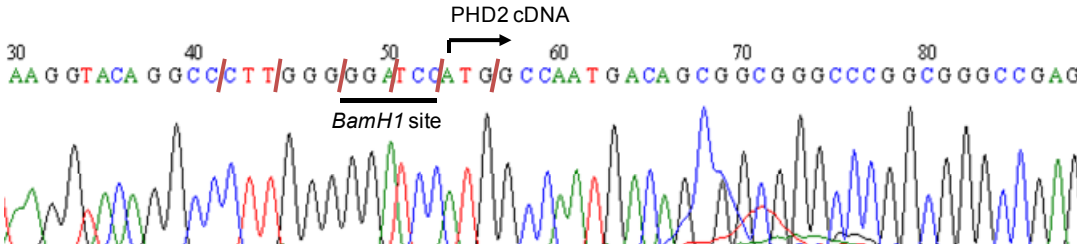

H

CTGATTGGGGACTGTACGACGATGACGATAAGGTACAGGCCCTTGGGGGATCCATGG
CCAATGACAGCGGCGGGCCCGGCGGGCCGAGCCCGAGCGAGCGAGACCGGCAGTACT
GCGAGCTGTGCGGGAAGATGGAGAACCTGCTGCGCTGCAGCCGCTGCCGCAGCTCCT
TCTACCGCTGCAAGGAGCACCAGCGTCAGGACTGGAAGAAGCACAAGCTCGTGTGCC
AGGGCAGCGAGGGCGCCCTCGGCCACGGAGTGGGCCCACACCAGCATTCCGGCCCCG
CGCCGCCGGCTGCAGTGCCGCCGCCCAGGGCCGGGGCCCGGGAGCCCGGGAAGGCAG
CGGCGCGCCGGGACAACGCCTCCGGGGACGCGGCCAAGGGAAAAGTAAAGGCCAAGC
CCCCGGCCGACCCAGCGGCGGCCGCGTCGCCGTGTCGTGCGGCCGCCGGCGGCTAGG
GCTCGGCGGTGGCTGCCGAAGCCGAGCCCGGCAAGGAGGAGCCGCCGGCCCGCTCAT
CGCTGTTCCAGGAGAAGGCGAACCTGTACCCCCCAAGCAACACGCCCGGGGATGCGC
TGAGCCCCGGCGGCGGCCTGCGGCCCAACGGGCAGACGAAGCCCCTGCCGGCGCTGA
AGCTGGCGCTCGAGTACATCGTGCCGTGCATGAACAAGCACGGCATCTGTGTGGTGG
ACGACTTCCTCGGCAAGGAGACCGGACAGCAGATCGGCGACGAGGTGCGCGCCCTGC
ACGACACCGGGAAGTTCACGGACGGGCAGCTGGTCAGCCAGAAGAGTGACTCGTCCA
AGGACATCCGAGGCGATAAGATCACCTGGATCGAGGGCAAGGAGCCCGGCTGCGAAA
CCATTGGGCTGCTCATGAGCAGCATGGACGACCTGATACGCCACTGTAACGGGAAGC
TGGGCAGCTACAAAATCAATGGCCGGACGAAAGCCATGGTCGCTTGTTATCCGGGCA
ATGGAACGGGTTATGTACGTCATGTTGATAATCCAAGTGGAGATGGAAGATGTGTGA
CATGTATATATTATCTTAATAAGACTGGGATGCCCAAGGTAAGTGGAGGTATACTTC
GAAATTTTTCAGAGCAAGCCCAGTTTGCTGACATTTGACCAAATTGATAGAACTGCT
ATTTTCTGGTCTGAACCGTCGCATCCCTCAATGAAGGTTACAACCCAGGCCAAATAT
AATTGC

I: pCDNA4His/Max-PHD3 (pEGFP)

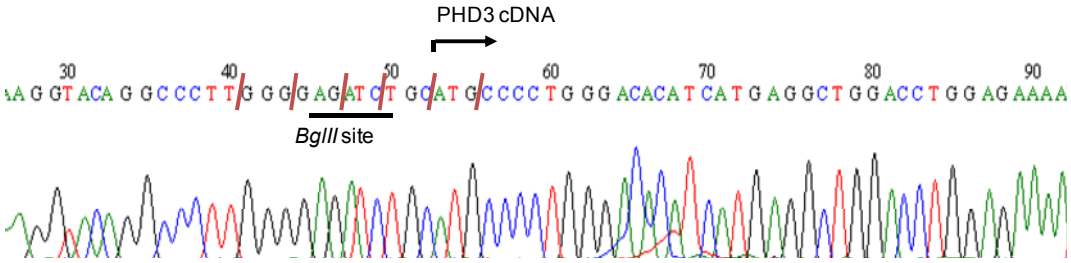

J

GGACGGGACTGTCGACGATGACGATAAGGTACAGGCCCTTGGGGAGATCTGCATGCC
CCTGGGACACATCATGAGGCTGGACCTGGAGAAAATTGCCCTGGAGTACATCGTGCC
CTGTCTGCACGAGGTGGGCTTCTGCTACCTGGACAACTTCCTGGGCGAGGTGGTGGG
CGACTGCGTCCTGGAGCGCGTCAAGCAGCTGCACTGCACCGGGGCCCTGCGGGACGG
CCAGCTGGCGGGGCCGCGCGCCGGCGTCTCCAAGCGACACCTGCGGGGCGACCAGAT
CACGTGGATCGGGGGCAACGAGGAGGGCTGCGAGGCCATCAGCTTCCTCCTGTCCCT
CATCGACAGGCTGGTCCTCTACTGCGGGAGCCGGCTGGGCAAATACTACGTCAAGGA
GAGGTCTAAGGCAATGGTGGCTTGCTATCCGGGAAATGGAACAGGTTATGTTCGCCA
CGTGGACAACCCCAACGGTGATGGTCGCTGCATCACCTGCATCTACTATCTGAACAA
GAATTGGGATGCCAAGCTACATGGTGGGATCCTGCGGATATTTCCAGAGGGGAAATC
ATTCATAGCAGATGTGGAGCCCATTTTTGACAGACTCCTGTTCTTCTGGTCAGATCG
TAGGAACCCACACGAAGTGCAGCCCTCTTACGCAACCAGATATGCTATGACTGTCTG
GTACTTTGATGCTGAAGAAAGGGCAGAAGCCAAAAAGAAATTCAGGAATTTAACTAG
GAAAACTGAATCTGCCCTCACTGAAGACTGAGAATTCCCCAAGGGCCTGTACCTAGG
ATCCAGTGTGGTGGAATTCTGCAGATATCCAGCACAGTGGCGGCCGCTCGAGTCTAG
AGGGCCCGTTTAAACCCGCTGATCAGCCTCGACTGTGCCTTCTAGTTGCCAGCCATC
TGTTGTTTGCCCCTCCCCCGTGCCTTCCTTGACCCTGGAAGGTGCCACTCCCACTGT
CCTTTCCTAATAAAATGAGGAAATTGCATCGCATTGTCTGAGTAGGTGTCATTCTTA
TTCTGGGGGGGTGGGTGGGGCAGACAGCAGGGGGAGATGGGCAGACATAGCAGCATG
CTGGGGAATGCGGTGGCTCTATGCTTCTGAGGGCGGAAGACAGCTTGGGCTCTAGGC
GATACCACTCGGCTGTAACCGGGCCAATAAAGCGTGCCGA

K: pCDNA4His/Max-PHD3 (pGEX4T-1)

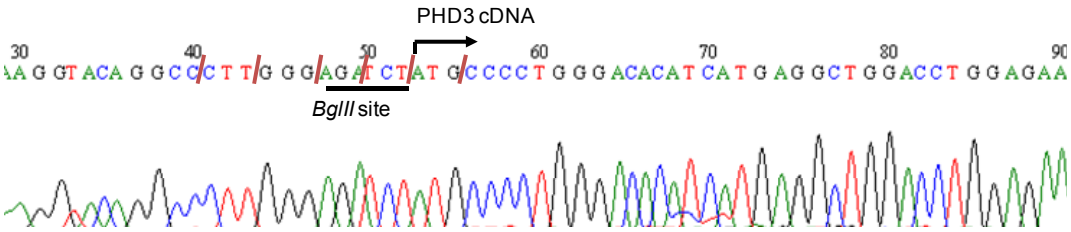

L

GGCCGGGGGACTGGTCGACGATGACGATAAGGTACAGGCCCTTGGGAGATCTATGCC
CCTGGGACACATCATGAGGCTGGACCTGGAGAAAATTGCCCTGGAGTACATCGTGCC
CTGTCTGCACGAGGTGGGCTTCTGCTACCTGGACAACTTCCTGGGCGAGGTGGTGGG
CGACTGCGTCCTGGAGCGCGTCAAGCAGCTGCACTGCACCGGGGCCCTGCGGGACGG
CCAGCTGGCGGGGCCGCGCGCCGGCGTCTCCAAGCGACACCTGCGGGGCGACCAGAT
CACGTGGATCGGGGGCAACGAGGAGGGCTGCGAGGCCATCAGCTTCCTCCTGTCCCT
CATCGACAGGCTGGTCCTCTACTGCGGGAGCCGGCTGGGCAAATACTACGTCAAGGA
GAGGTCTAAGGCAATGGTGGCTTGCTATCCGGGAAATGGAACAGGTTATGTTCGCCA
CGTGGACAACCCCAACGGTGATGGTCGCTGCATCACCTGCATCTACTATCTGAACAA
GAATTGGGATGCCAAGCTACATGGTGGGATCCTGCGGATATTTCCAGAGGGGAAATC
ATTCATAGCAGATGTGGAGCCCATTTCCCATTTTTGACAGACTCCTGTTCTTCTGGT
CAGATCGTAGGAACCCACACGAAGTGCAGCCCTCTTACGCAACCAGATATGCTATGA
CTGTCTGGTACTTTGATGCTGAAGAAAGGGCAGAAGCCAAAAAGAAATTCAGGAATT
TAACTAGGAAAACTGAATCTGCCCTCACTGAAGACTGAGAATTCCCCAAGGGCCTGT
ACCTAGGATCCAGTGTGGTGGAATTTCTGCAGATATCCAGCACAGTGGCGGCCCGCT
CGAGTCTAGAGGGCCCGTTTAAACCGCTGATCAGCCTCGACTGTGCTTCTAGTGCCA
GCCATCTGGTGGTTGCCCCTTCCCCCGTGCTTGTGACCTGAGTGCCACCTCCCACTG
TCTTTCCTATAATGAGAATGCATCGCATGCTGATAGTGTCATCATTCTGGGGTGGGT
TGCAGTACGCAAGCCCAGACTGGGAGACATGCAG

Figure 7.1.4 *Sequence analysis of pcDNA4 His/Max-PHD constructs.*
Chromatograph and sequence for pcDNA4 His/Max PHD1 for pEGFP (A and B), for pGEX 4T-1 (C and D), PHD2 for pEGFP (E and F), for pGEX 4T-1 (G and H), PHD3 for pEGFP (I and J), for pGEX 4T-1 (K and L). 5' flanking restriction site and start codon denoted.

pcDNA4His/Max-PHDs containing the correct insert cDNA verified by sequence analysis, were transfected into U2OS cells in order to confirm the correct expression. 48 hours post-transfection cells were lysed and immunoblotted to confirm that the PHDs expressed at the correct size and were detected by both the Xpress mAb and individual PHD antibodies. Un-tagged pcDNA3.1 PHDs and a pcDNA4His/Max empty vector (VO) were also transfected and immunoblotted as controls. The PHDs were all detected by both the Xpress mAb and PHD polyclonal antibody (Figure 7.1.5). The Xpress/His tag expressed in the pcDNA4His/Max vector add approximately 3.9 kDa in comparison to the un-tagged protein.

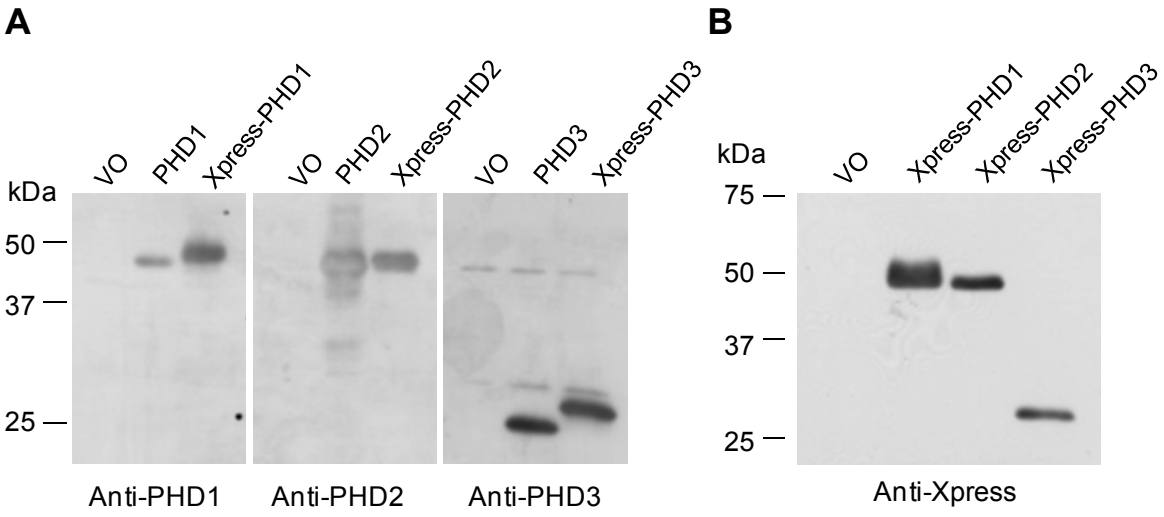

Figure 7.1.5 *Immunoblot of the Xpress-tagged PHD recombinant proteins.* pcDNA3.1-PHDs and pcDNA4His/Max-PHDs were transfected into U2OS. 48 hours post-transfection cells were lysed and immunoblotted. **(A)** pcDNA4His/Max-PHDs (Xpress-PHDs) were detected by each PHD antibody, detected as a larger molecular weight form than the un-tagged PHD protein due to the addition of the Xpress/poly-his tag. **(B)** Xpress-PHDs were also detected by the Xpress mAb at the correct size.

7.2 Sub-cloning of pcDNA4His/Max-PHDs into pEGFP–C1+1

pcDNA4His/Max-PHDs were sub-cloned into pEGFP–C1+1 in order to visualise intracellular PHD expression by fluorescence. PHD1 and PHD2 cDNA were excised from pcDNA4His/Max using *BamHI* and *EcoRI* restriction sites incorporated 5' and 3' of the cDNA during PCR amplification. PHD3 cDNA was excised from pcDNA4His/Max using *BglII* and *EcoRI* sites. BglII was chosen as PHD3 has an intrinsic *BamHI* site. However, *BglII* and *BamHI* digestions are compatible for ligation. pEGFP-C1+1 was linearised by digestion with *BglII* and *EcoRI*. Linearised cDNA fragments were solubilised, purified and eluted and the complementary pEGFP-C1+1 and PHD restriction fragments were ligated overnight at 16˚c. Ligates were transformed into competent *DH5α* and selected for kanamycin resistance. Validation of PHD integration within pEGFP-C1+1 was performed by *BglII* and *EcoRI* digestion of PHD3 and *BsrGI* and *EcoRI* digestion of PHD1 and PHD2, as the *BamHI-BglII* ligation forms a site unable to restrict by each of the restriction enzymes that created the original restriction digest (Figure 7.2.1). pEGFP-C1+1-PHDs were transfected into U2OS cells, which were lysed 48 hours later and immunoblotted with anti-GFP and anti-PHD antibodies to confirm the correct expression of the recombinant protein (Figure 7.2.2). pEGFP-C1+1-PHD2 was utilised in figure 4.3.2, whereby it was detected in the cytoplasm [as previously reported (Metzen et al., 2003a)] by laser scanning confocal microscopy.

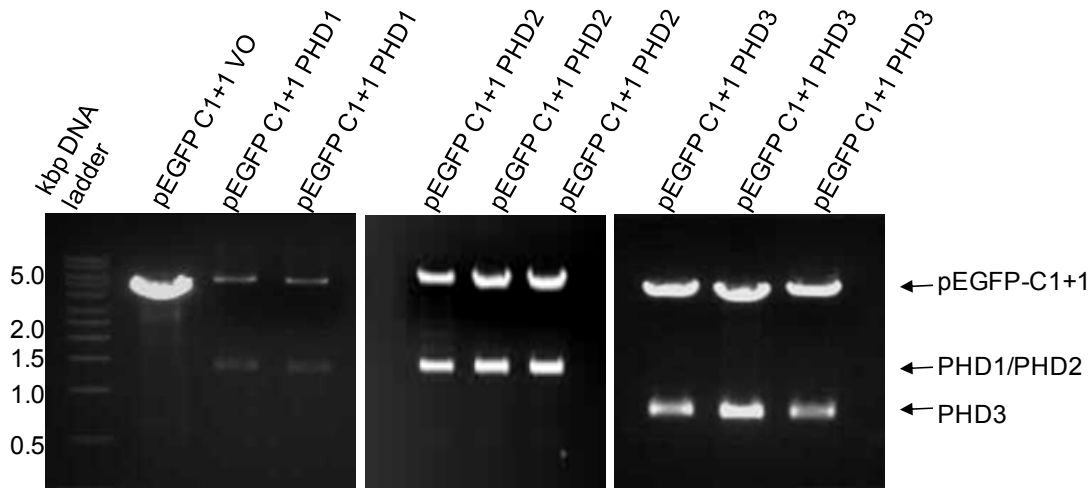

Figure 7.2.1 *Restriction digest verification of correct insertion of PHD cDNA into pEGFP-C1+1 vector.*

Agarose (1% w/v) gel electrophoresis of *BglII/BsrGI* and *EcoRI* digestion of pEGFP-C1+1-PHD constructs. Digest confirms cDNA presence of the correct size (PHD1 1220bp, PHD2 1280bp and PHD3 720bp) and the correct sized pEGFP-C1+1 vector backbone (4700bp).

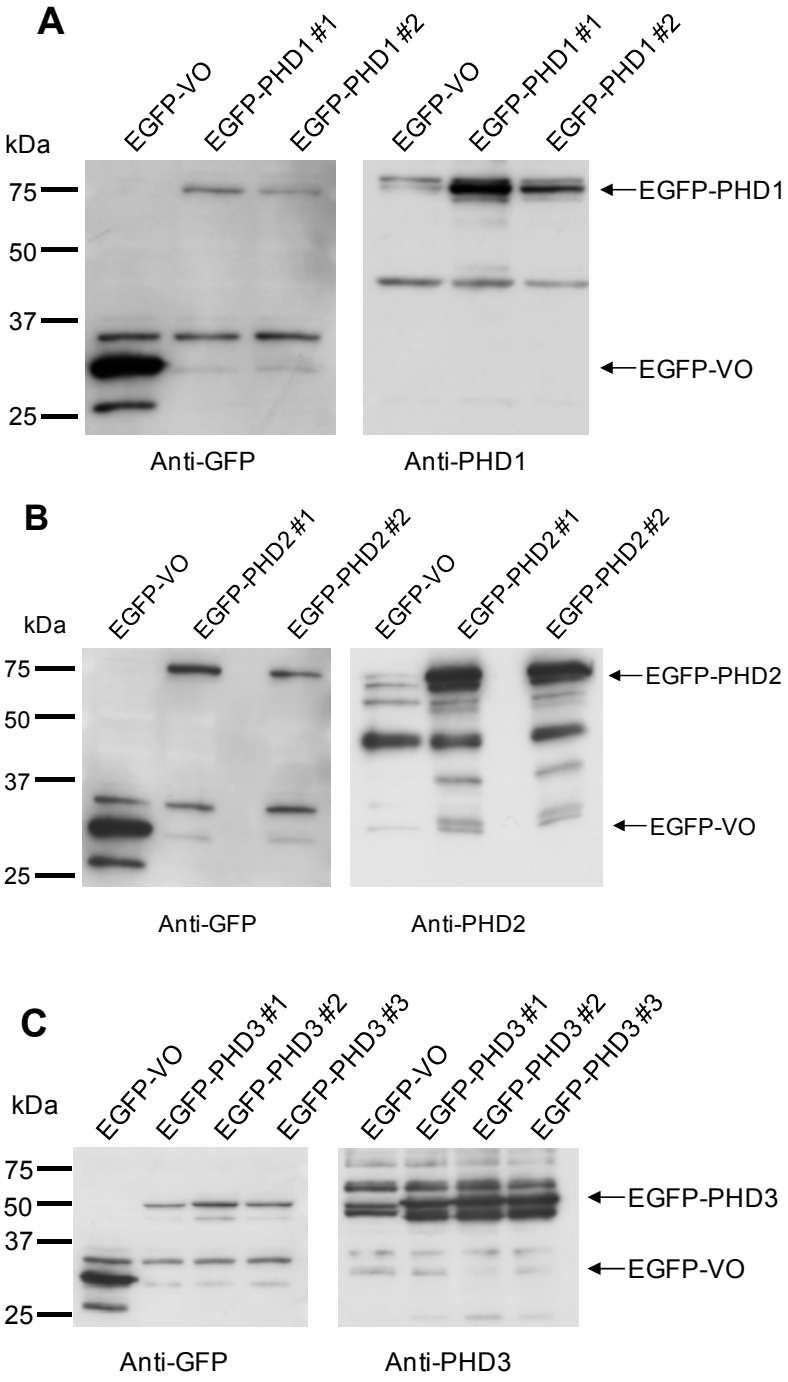

Figure 7.2.2 *Immunoblot of the pEGFP-PHD recombinant proteins.*

pEGFP-PHDs and the pEGFP–C1+1 vector only control were transfected into U2OS. 48 hours post-transfection cells were lysed and immunoblotted. EGFP-PHDs were detected by each PHD antibody **(A)** EGFP-PHD1, **(B)** EGFP-PHD2, **(C)** EGFP-PHD3) and the GFP antibody. Recombinant proteins express at the correct molecular weight (PHD1 45kDa, PHD2 46kDa and PHD3 28kDa in addition to the molecular weight of the EGFP (27 kDa) tag. As the proteins are recognised by both EGFP and PHD antibodies this confirms that they express as an intact recombinant fusion protein.

7.3 Sub-cloning of pcDNA4His/Max-LIMD1 into pEGFP–C1+1

In order to visualise the intracellular localisation of LIMD1 in U2OS cells LIMD1 was sub-cloned from the pCDNA4HisMax vector into a pEGFP-C1+1 vector, enabling expression of an EGFP-LIMD1 fusion protein. LIMD1 was excised from the pCDNA4His/Max vector *via* flanking *EcoRI* and *SalI* restriction enzyme sites, previously incorporated by PCR. The pEGFP-C1+1 vector was linearised at *EcoRI* and *SalI* sites in order to enable LIMD1 integration (Figure 7.3.1). *EcoRI* and *SalI* restriction of the pCDNA4HisMax vector results in the production of 3 digest products (Figure 8.3.1 A, arrows), due to the presence of a *SalI* restriction site in the vector. The middle of the 3 DNA fragments is the LIMD1 cDNA digest product of 2031bp. The linearised pEGFP–C1+1 and LIMD1 cDNA were excised from the agarose gel, purified and then resolved by agarose gel electrophoresis to verify the isolation of the desired restriction fragments (Figure 7.3.1B). The restricted LIMD1 fragments and the linearised pEGFP-C1+1 were then ligated into the complementary sequences generated by the *EcoRI*/*SalI* restriction using DNA ligase. Ligation reactions were then transformed and positive kanamycin colonies picked. Plasmid DNA was then re-digested with *EcoRI*/*SalI* to confirm correct ligation and presence of LIMD1 cDNA (Figure 7.3.1C). Sequence analysis using a 5' GFP primer (5' AGCAAAGACCCCAACGAGAAG 3') was performed to validate the correct size of the inserted LIMD1 fragment, the correct fusion and to confirm the methionine start codon (ATG) was in frame for correct expression (Figure 7.3.1D).

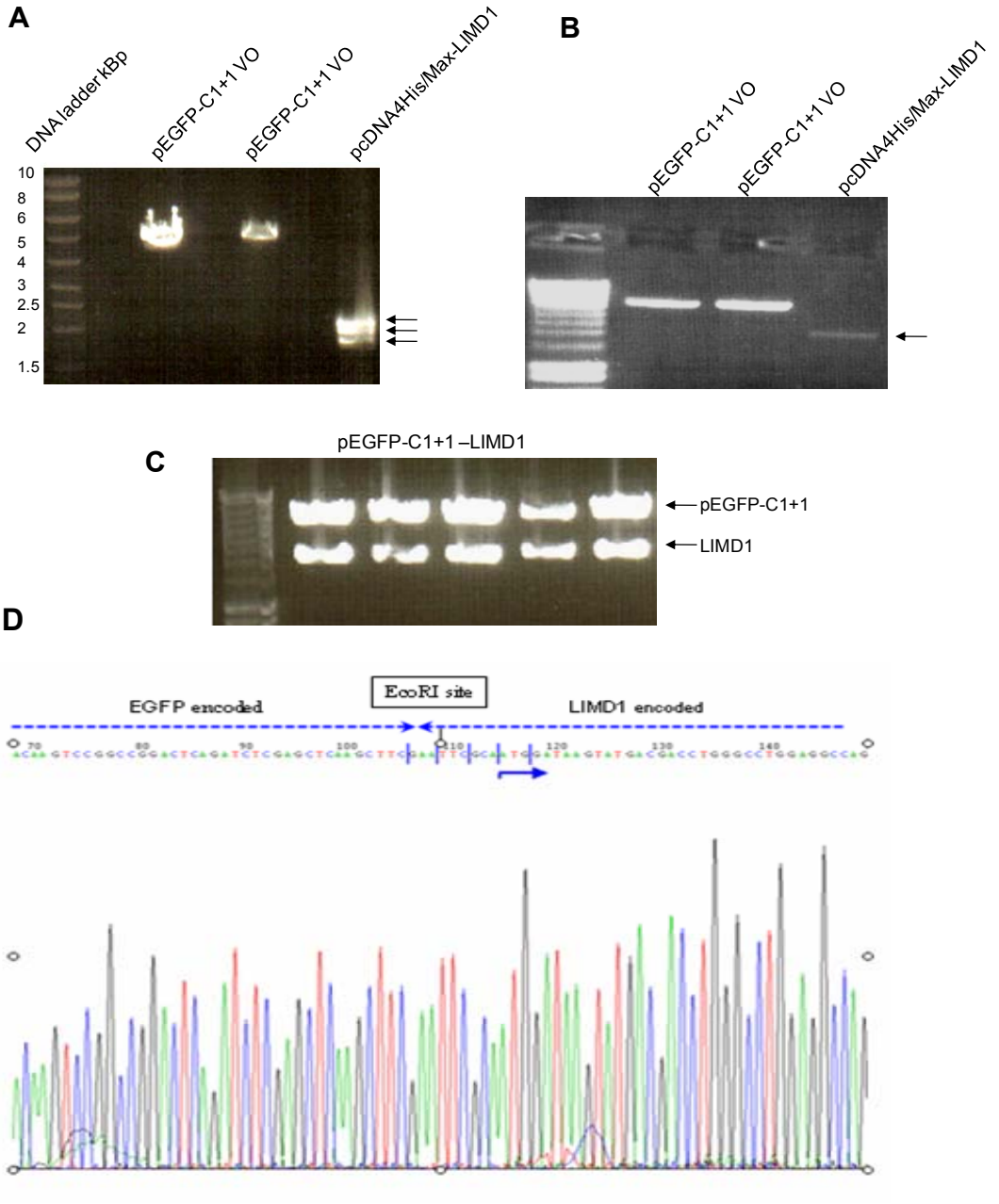

Figure 7.3.1 *Sub-cloning of LIMD1 into the pEGFP C1+1 vector.*

(A) Agarose (1%) gel electrophoresis of *EcoRI*/*SalI* restriction digests of the pEGFP-C1+1 vector only fragment and pCDNA4/HisMax-LIMD1 digest products. *EcoRI/SalI* digestion of the pCDNA4/HisMax vector results in the production of multiple digest products (indicated by arrows), due to an internal *SalI* site. LIMD1 cDNA (2031bp) resolves as the middle band. **(B)** pEGFP vector only and LIMD1 cDNA linearised digest fragments were excised, purified and verified by agarose (1%) gel electrophoresis. Correct vector-insert in frame fusion sequence, size and nature of the recombinant were established *via* sequence analysis *via* a primer designed to anneal to a region of the pEGFP gene sequence upstream of the desired fusion region **(D)** and by *EcoRI*/*SalI* digestion **(C)**.

pEGFP-C1+1-LIMD1 was transfected into U2OS and immunoblotted with LIMD1 mAb and the GFP rabbit polyclonal antibody, in order to confirm the correct expression of the fusion protein (Figure 7.3.2). The immunoblots confirm the correct identity of the expressed fusion protein detectable by both anti-GFP and anti-LIMD1. The anti-LIMD1 immunoblot also identifies endogenous LIMD1 of an approximate molecular weight of 72kDa. Furthermore, the anti-GFP immunoblot detects the molecular weight of EGFP as 27kDa. Therefore as the pEGFP-LIMD1 WT fusion migrated to approximately 100kDa, this indicates the correct expression of the fusion protein. pEGFP-LIMD1 was utilised in figure 4.3.2, detected by laser scanning confocal microscopy.

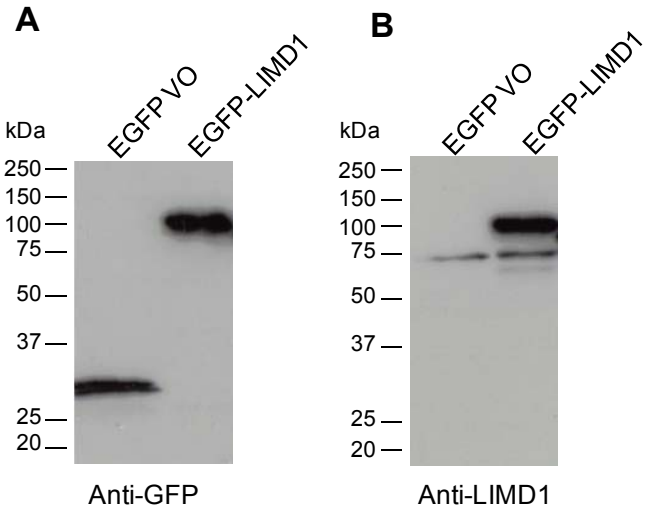

Figure 7.3.2 *Immunoblot of the EGFP-LIMD1 fusion protein.*
(A) Immunoblot of EGFP VO and EGFP-LIMD1 expressed in U2OS cells. Anti-GFP immunoblot detects both the EGFP vector only and the EGFP-LIMD1 fusion, at approximately 100kDa, the correct fusion protein molecular weight (LIMD1 72kDa and EGFP 27kDa). **(B)** This fusion protein is also detected by immunoblot with a LIMD1 mAb at the same molecular weight. Endogenous LIMD1 can also be detected at 72kDa.

7.4 Primary Antibodies

Antigen	Concentration used for Immunoblotting	Host Species	Molecular Weight (kDa)	Company	Catalogue Number
LIMD1	1:500	Mouse	72	N/A	N/A
HIF1α	1:500	Mouse	120	BD Transduction Laboratories™	610959
HIF1β	1:500	Rabbit	116	Cell Signalling	#3718S
PHD1	1:1500	Rabbit	45-50	Abcam	AB5156
PHD2	1:1500	Rabbit	46	Abcam	AB4561
PHD3	1:3000	Rabbit	27	Novus Biologicals	NB100-303A2
VHL	1:400	Mouse	21-30	BD	536347
β-Actin	1:10000	Mouse	42	Sigma-Aldrich	A1978
GFP	1:5000	Rabbit	27	Abcam	AB290
V5	1:2000	Mouse	N/A	Ab-Serotec	
Xpress	1:5000	Mouse	N/A	Invitrogen	46-0528
HA	1:1000	Rabbit	N/A	Sigma-Aldrich	H6908
P-Ser	1:250	Mouse	N/A	BD	612546
P-Ser/Thr	1:250	Mouse	N/A	BD	612548
P-Tyr	1:1000	Mouse	N/A	Sigma-Aldrich	P5872

7.5 Secondary Antibodies

Antigen	Concentration	Host	Company	Catalogue Number
Mouse	1:5000	Goat	DAKO	P0447
Rabbit	1:5000	Goat	DAKO	P0448
Alexafluor Rabbit 568	1:1000	Goat	Invitrogen	A11036
Alexafluor Mouse 568	1:1000	Goat	Invitrogen	A11004
Alexafluor Rabbit 488	1:1000	Goat	Invitrogen	A11008
Alexafluor Mouse 488	1:1000	Goat	Invitrogen	A11001
Alexafluor Mouse 350	1:1000	Goat	Invitrogen	A11045

7.6 Vectors

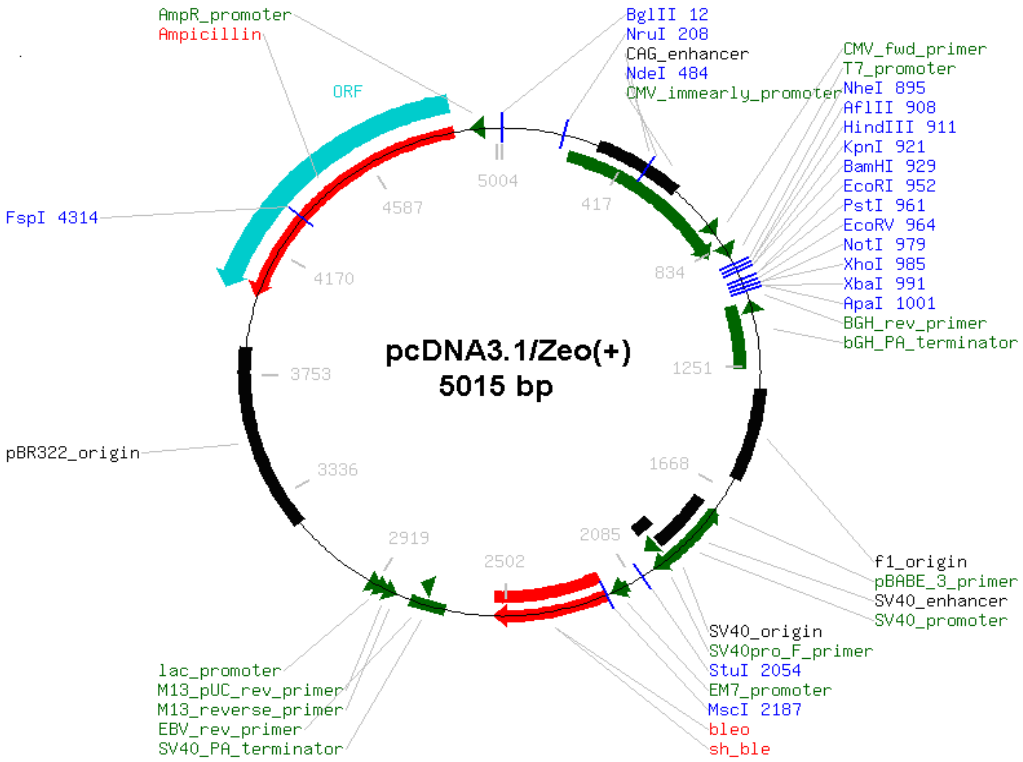

Vector Type:	Mammalian
Viral/Non-viral:	Nonviral
Stable/Transient:	Transient
Constitutive/Inducible:	Constitutive
Promoter:	CMV
Expression Level:	High
Backbone Size (bp):	5015
Sequencing Primer:	T7 Fwd
Sequencing Primer Sequence:	5'd[TAATACGACTCACTATAGGG]3'
Tag:	V5 tag[GGTAAGCCTATCCCTAACCCTCT CCTCGGTCTCGATTCTAGC] inserted within *NheI* and *KpnI* RE sites within the MCS
Bacteria Resistance:	Ampicillin
Mammalian Selection:	Zeocin

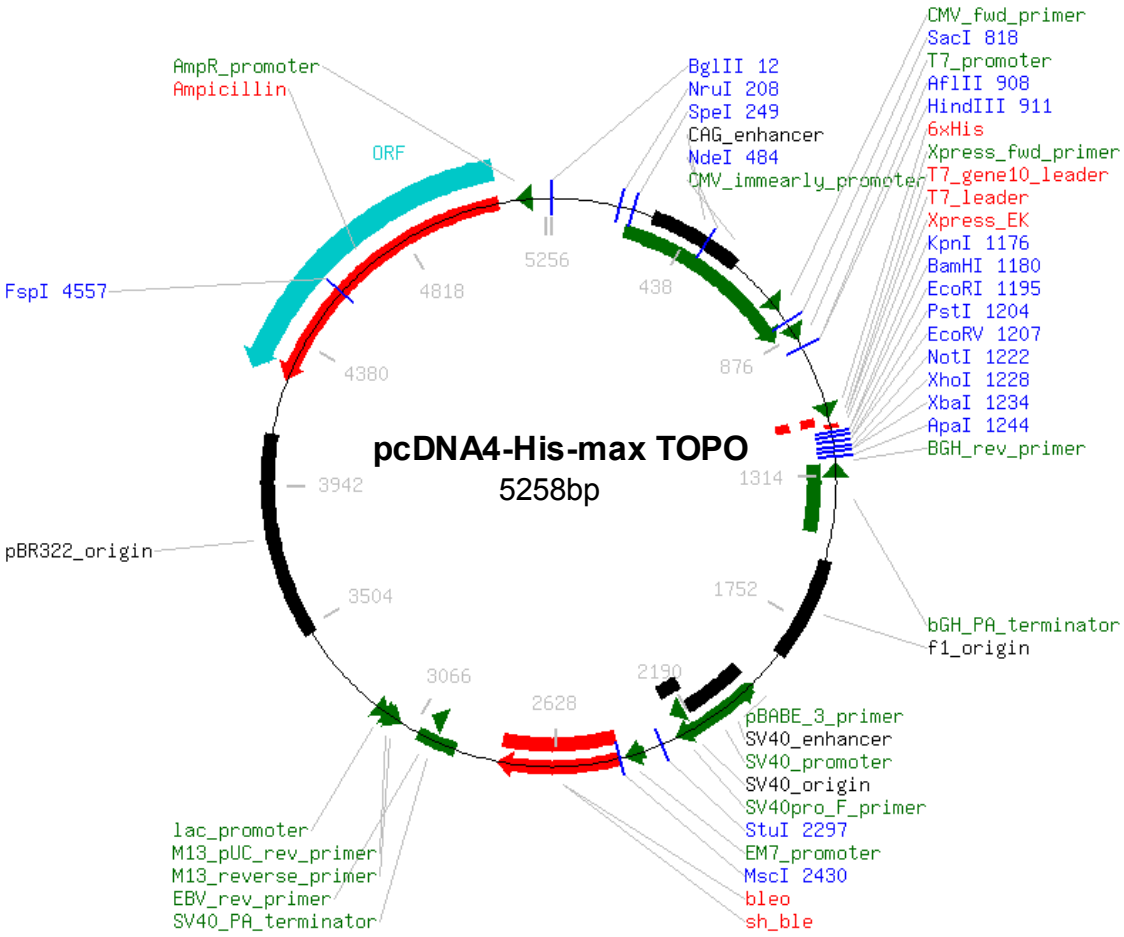

Vendor: Invitrogen

Vector Type: Mammalian

Viral/Non-viral: Nonviral

Stable/Transient: Transient

Constitutive/Inducible: Constitutive

Promoter: CMV

Expression Level: High

Backbone Size (bp): 5258

Sequencing Primer: T7 Fwd

Sequencing Primer Sequence: 5'd[TAATACGACTCACTATAGGG]3'

Tag: 6X His, Xpress

Bacteria Resistance: Ampicillin

Mammalian Selection: Zeocin

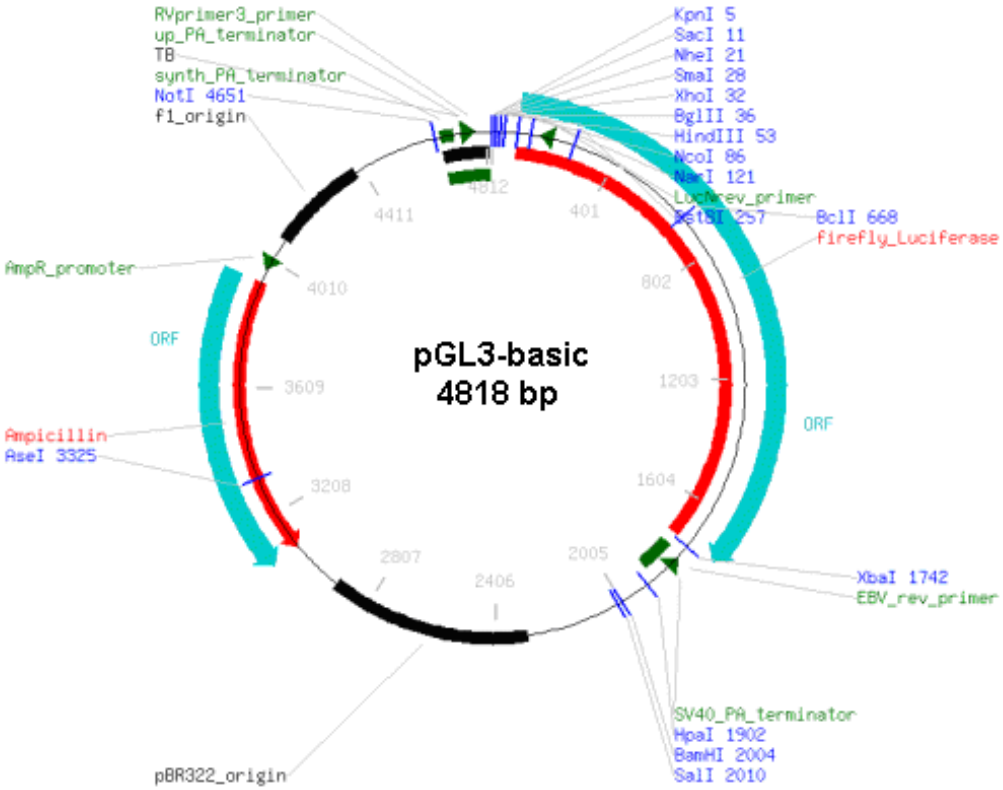

Vendor: Promega

Vector Type: Mammalian

Viral/Non-viral: Nonviral

Backbone Size (bp): 4818

Sequencing Primer: RVprimer3

Sequencing Primer Sequence: CTAGCAAAATAGGCTGTCCC

Bacteria Resistance: Ampicillin

Catalogue number: E1751

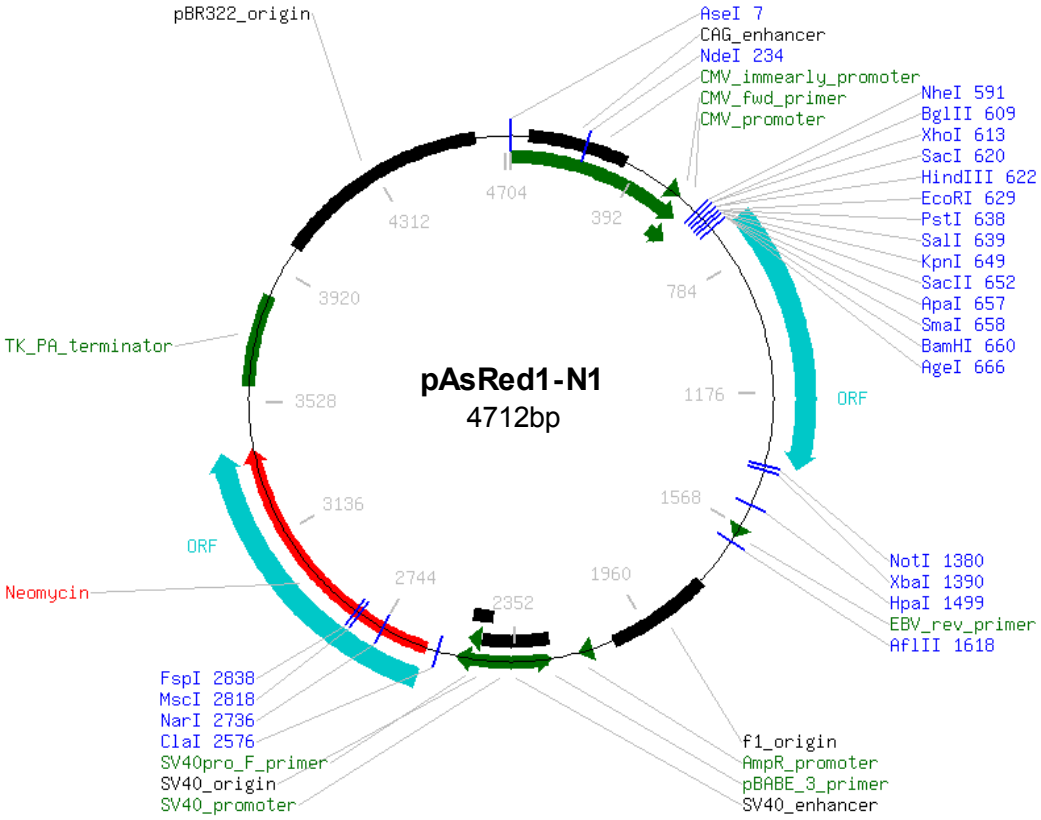

Vendor: Clontech

Vector Type: Mammalian

Viral/Non-viral: Nonviral

Stable/Transient: Stable (transfected)

Constitutive/Inducible: Constitutive

Promoter: CMV

Backbone Size (bp): 4700

Tag: AsRed1 (Cterm)

Bacteria Resistance: Kanamycin

Mammalian Selection: Neomycin

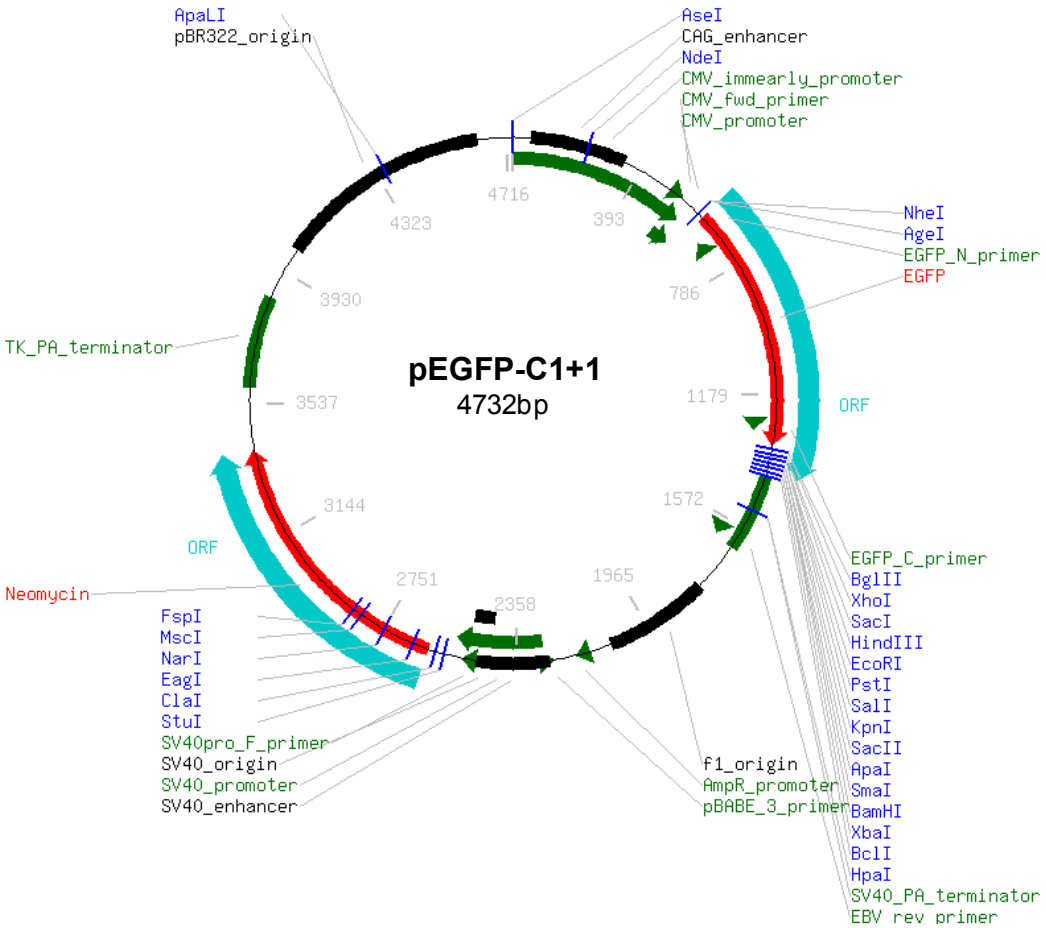

Vendor: Clontech

Vector Type: Mammalian

Viral/Non-viral: Nonviral

Stable/Transient: Stable (transfected)

Constitutive/Inducible: Constitutive

Promoter: CMV

Backbone Size (bp): 4700

Sequencing Primer: EGFP-C

Sequencing Primer Sequence: 5'd[CATGGTCCTGCTGGAGTTCGTG]

Tag: EGFP (Nterm)

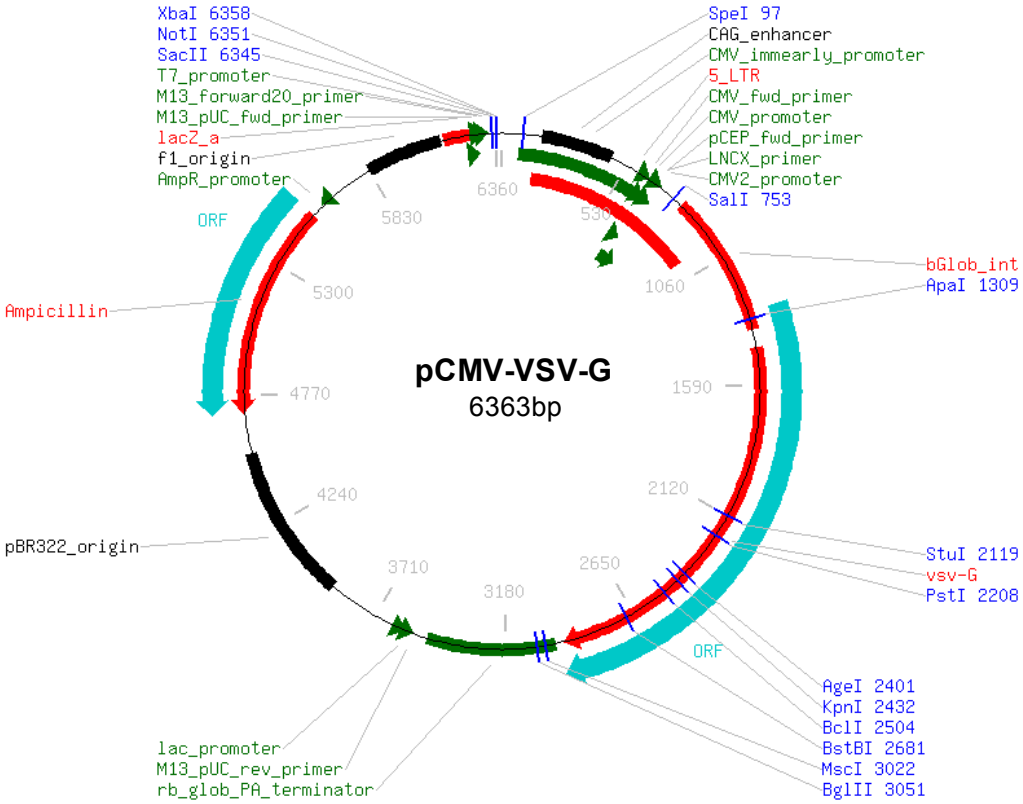

Lenti-viral Plasmid:	Envelop Construct
Insert size (bp):	Unknown
Vector backbone:	N/A
Type of vector:	Mammalian expression
Backbone size (bp):	6363
5' Sequencing primer:	T7
Bacteria resistance:	Ampicillin
High or low copy:	High Copy
Grow in standard E. coli @ 37C:	Yes
Plasmid Provided In:	DH5a

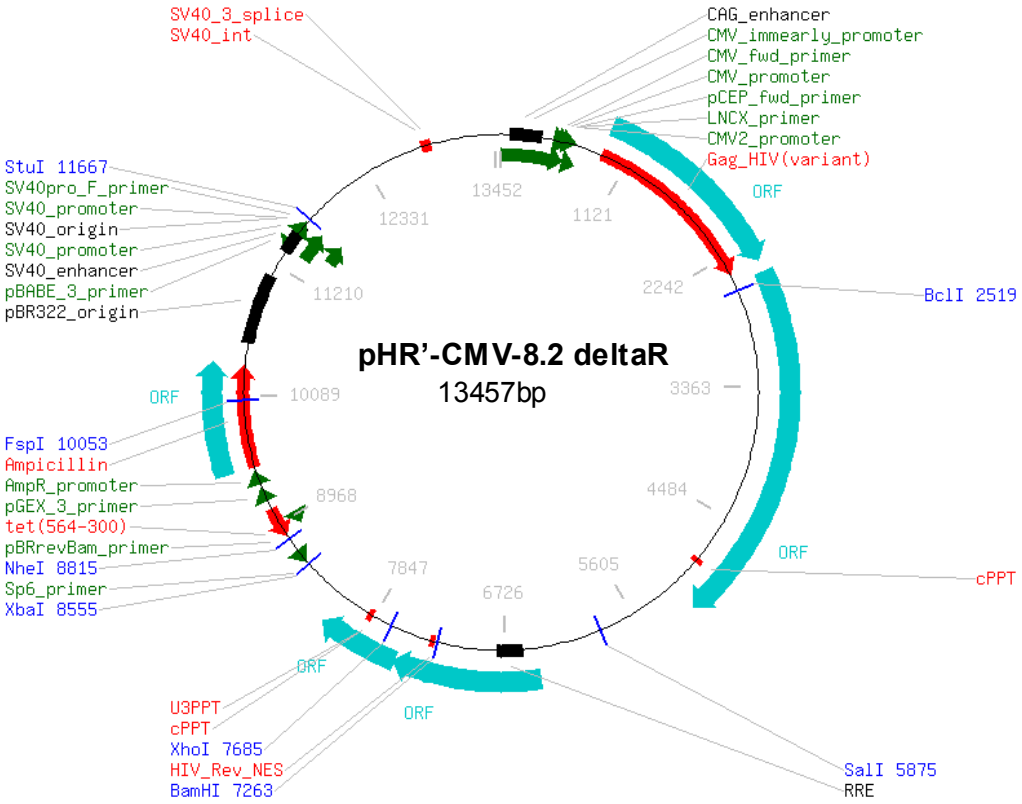

Lenti-viral Plasmid:	Packaging Construct
Insert size (bp):	Unknown
Vector backbone:	N/A
Type of vector:	Mammalian expression,Lentiviral
Backbone size (bp):	Unknown
5' Sequencing primer:	CMV Forward
Bacteria resistance:	Ampicillin
High or low copy:	High Copy
Grow in standard E. coli @ 37C:	Yes
Plasmid Provided In:	DH5a

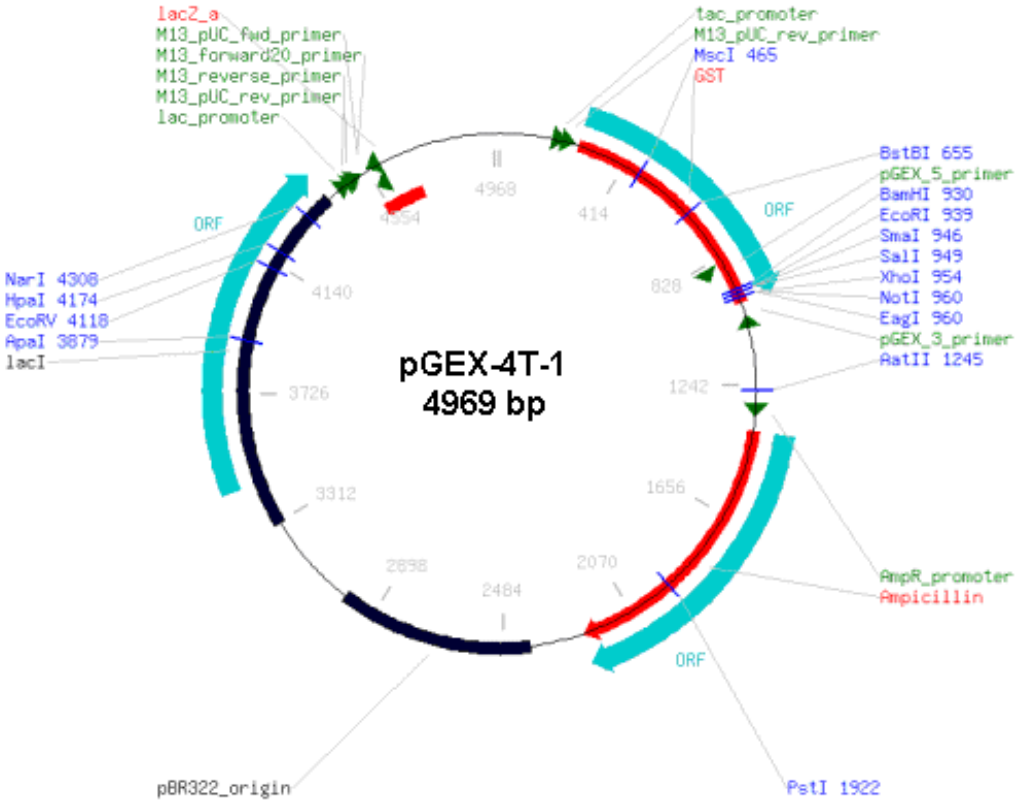

Vendor: Amersham

Vector Type: Bacterial

Viral/Non-viral: Nonviral

Stable/Transient: Transient

Constitutive/Inducible: Constitutive

Promoter: Tac

Expression Level: High (Activate with IPTG)

Backbone Size (bp): 4900

Sequencing Primer: pGEX Fwd

Sequencing Primer Sequence: 5'd[GGGCTGGCAAGCCACGTTTGGTG]3'

Tag: GST (Nterm)

Bacteria Resistance: Ampicillin

pcDNA3.1 V5-VHL

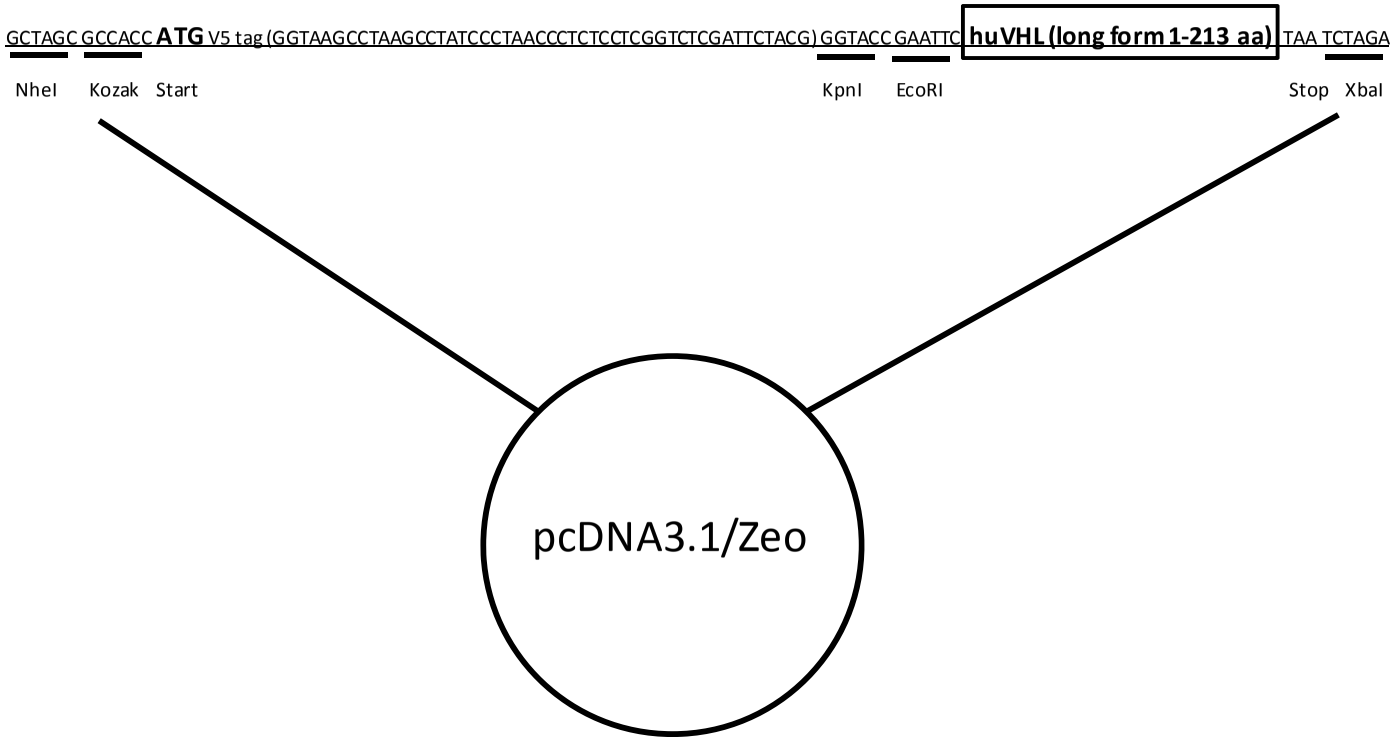

pcDNA3.1 HIF1α WT, HIF1α P402A/P564A

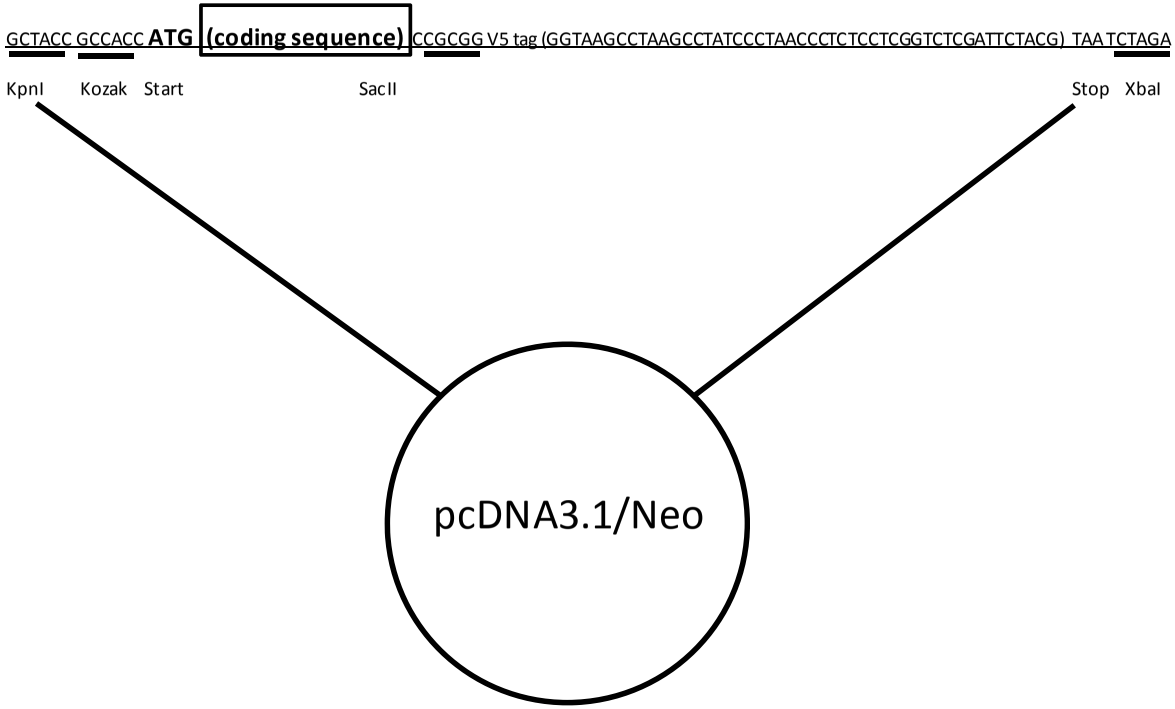

pcDNA3.1 HIF1α 30-389, HIF1α 390-652, HIF1α 630-826, FIH

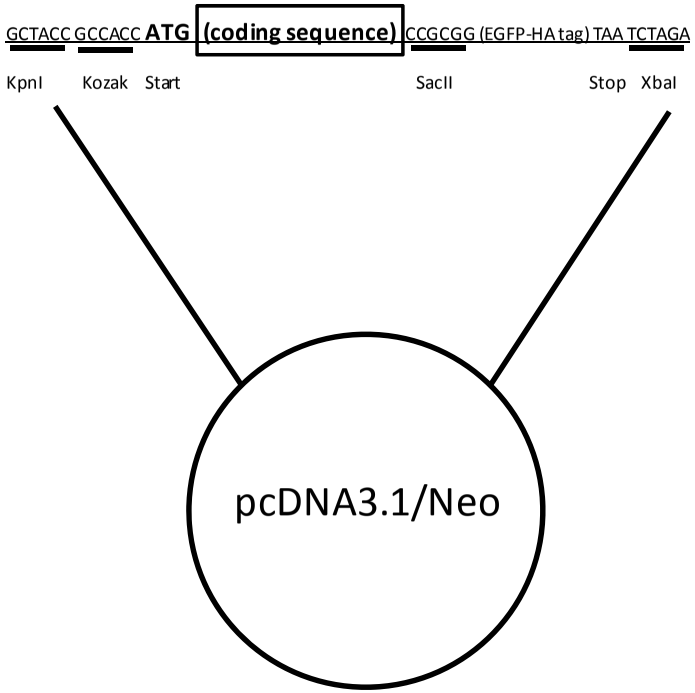

pcDNA4/HisMax TOPO PHD1/PHD2 (for insertion into pEGFP-c1+1)

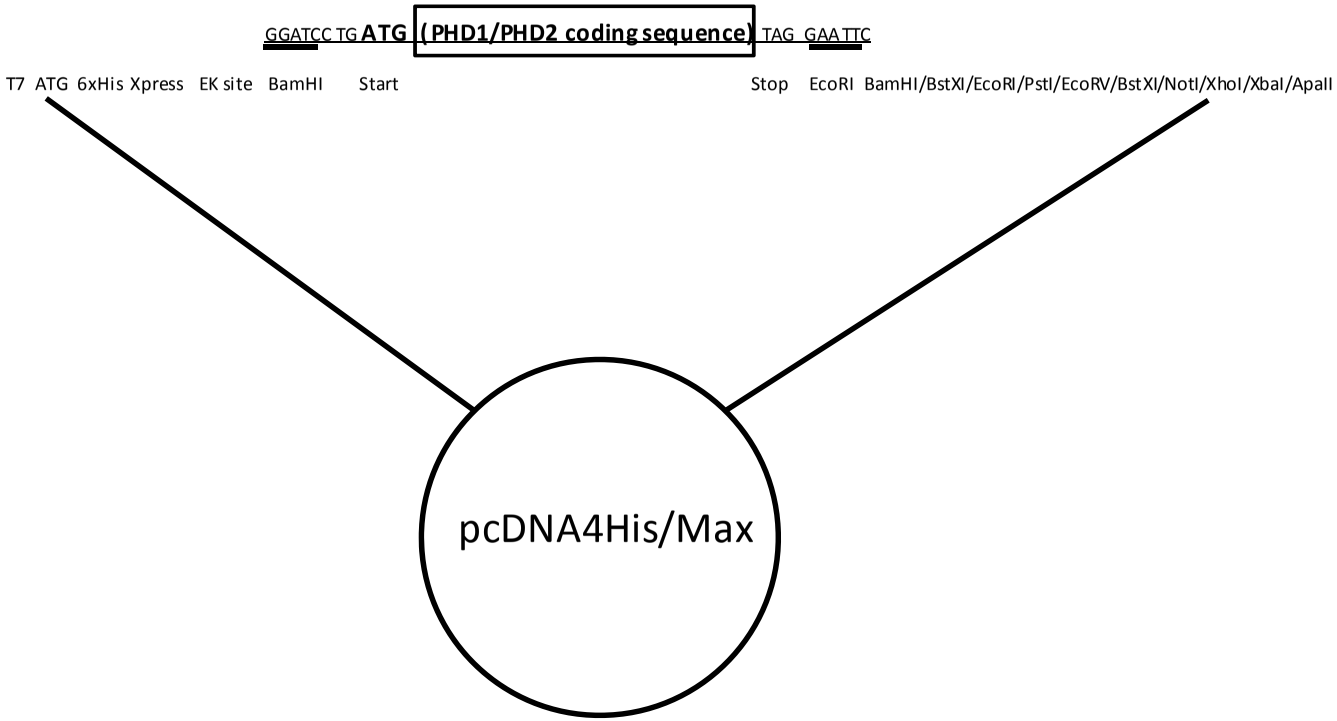

pcDNA4/HisMaxTOPO PHD1/PHD2 (for insertion into pGEX4T-1)

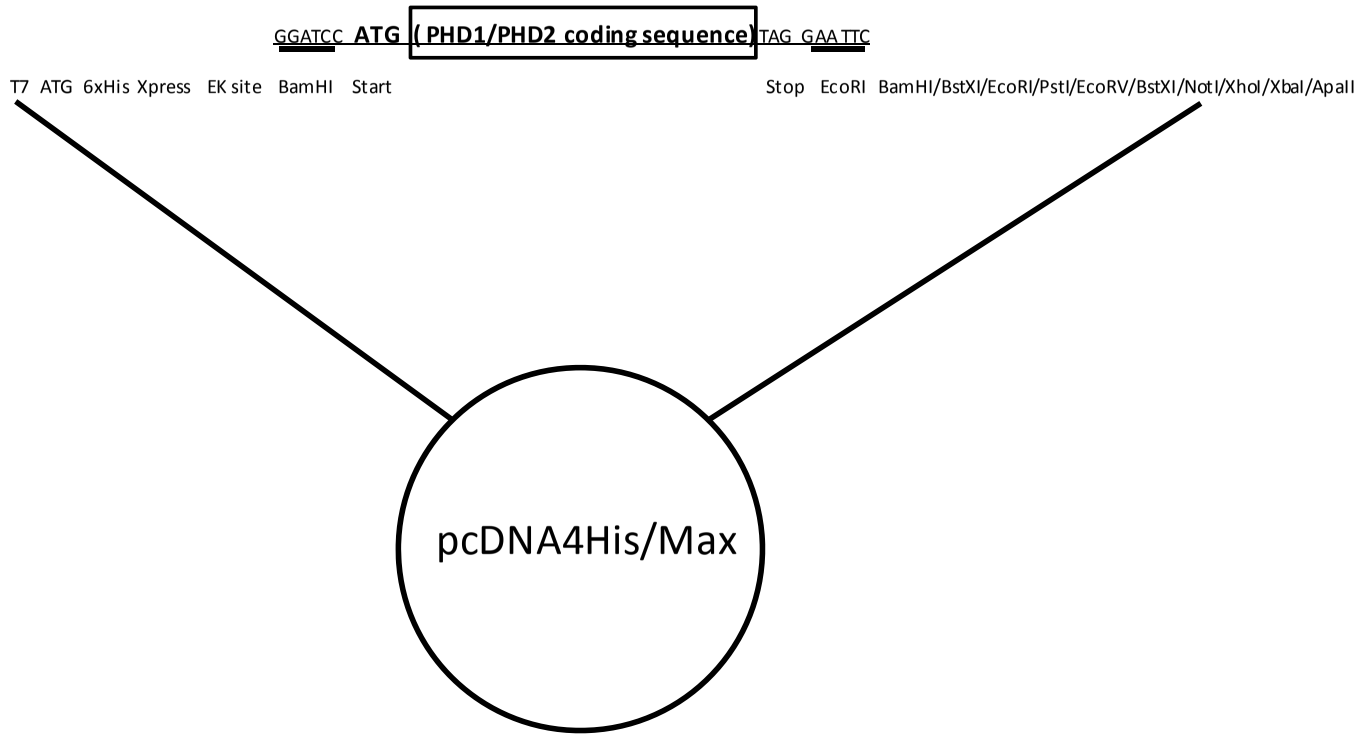

pcDNA4/HisMaxTOPO PHD3 (for insertion into pEGFP-c1+1)

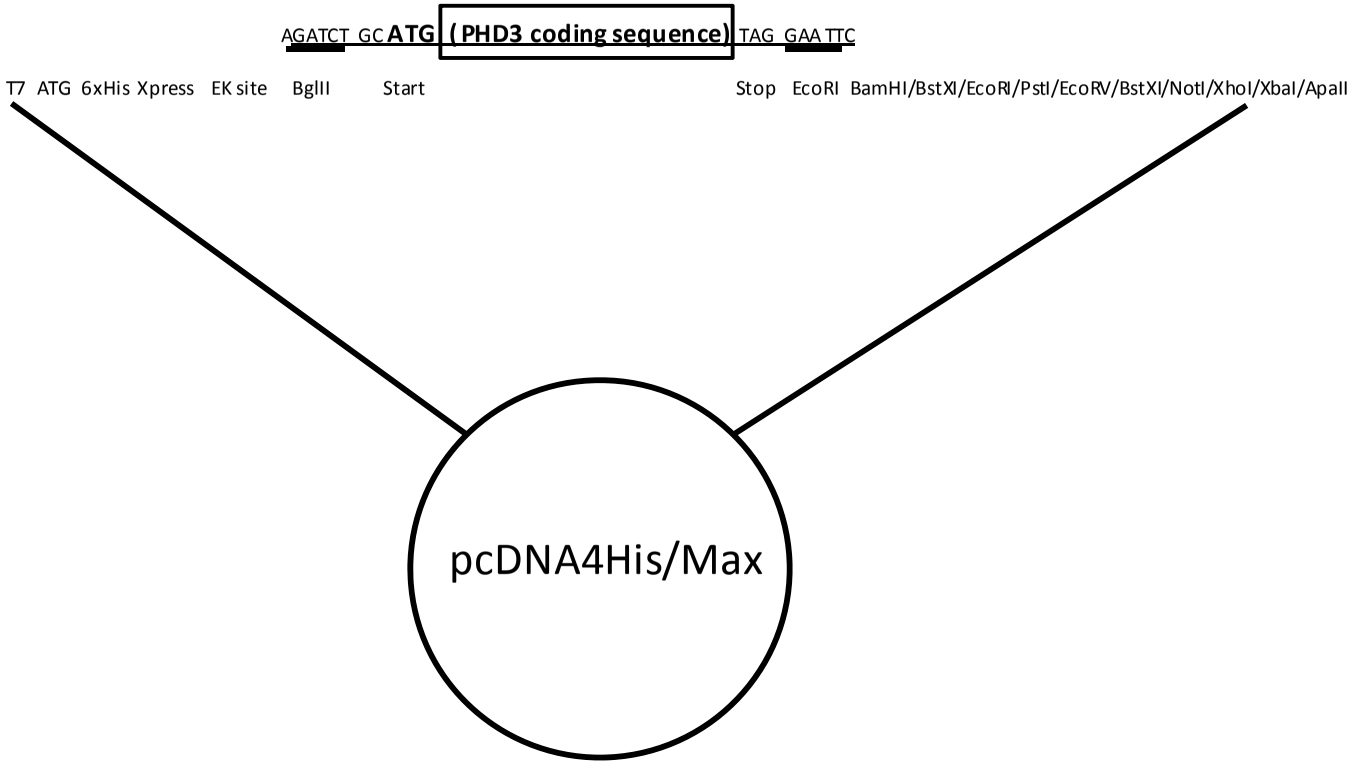

N.B BglII and BamHI are compatible cleavage sites for ligation.

pcDNA4/HisMax TOPO PHD3 (for insertion into pGEX4T-1)

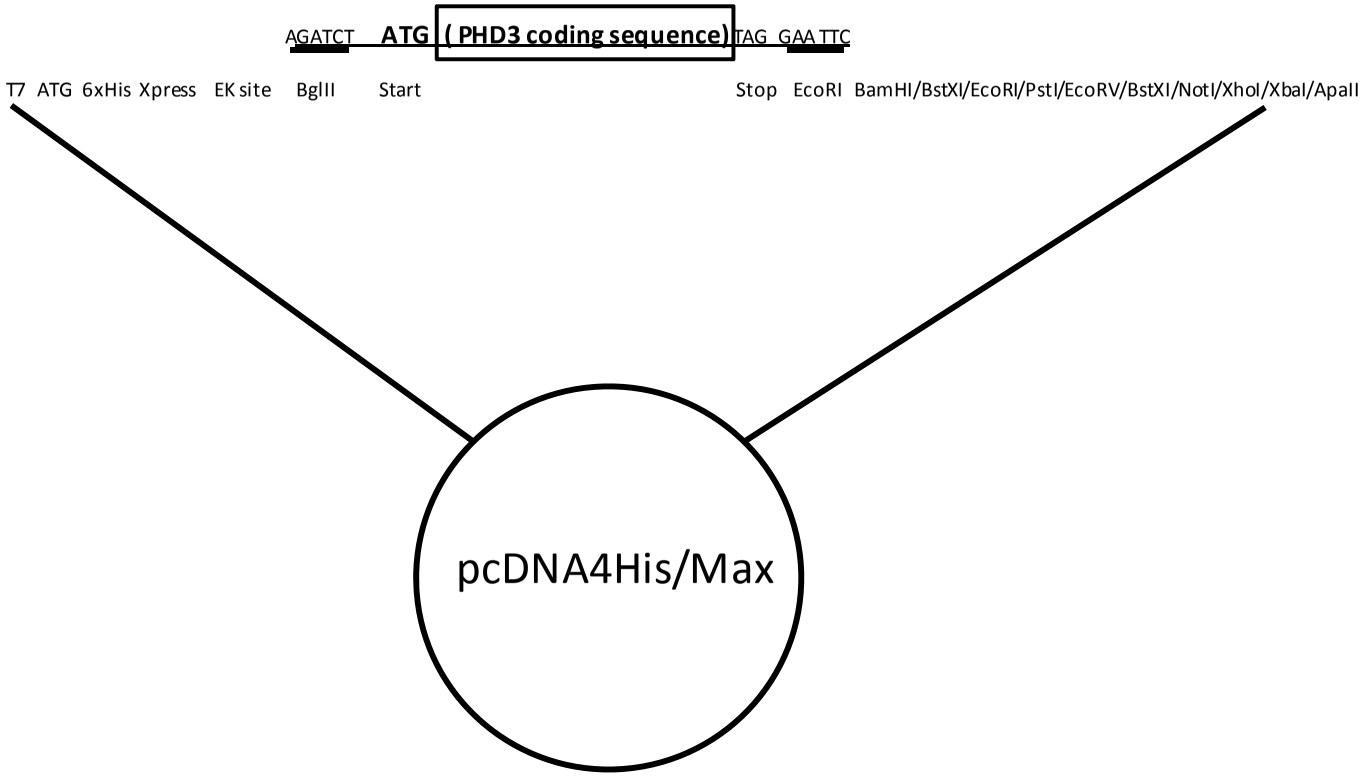

N.B BglII and BamHI are compatible cleavage sites for ligation.

Further acknowledgments for the donation of the following plasmids:

Dr Thilo Hagen, Department of Biochemistry, National University of Singapore:

pcDNA3.1 V5-VHL
pcDNA3.1 V5-HIF1α
pcDNA3.1 V5-HIF1α-P402A/P564A
pcDNA3.1 HA-HIF1α-30-389
pcDNA3.1 HA-HIF1α-390-652/ P402A,P564A
pcDNA3.1 HA-HIF1α-630-826
pcDNA3.1 V5-CUL2
pcDNA3.1 EGFP-HA-FIH
pGL3-HRE

Professor Peter Ratcliffe, Nuffield Department of Clinical Medicine, The Henry Wellcome Building for Molecular Physiology, University of Oxford:

pcDNA3.1 PHD1
pcDNA3.1 PHD2
pcDNA3.1 PHD3

Professor Greg Longmore, Haematology division, Department of Cell Biology and Physiology, Washington University:

Lentiviral plasmids: pCMV-VSVG, pHR ∆8.2, pFLRu-Scrambled/LIMD1 shRNA

Dr Simon Dawson, School of Biomedical Sciences, University of Nottingham:

pEGFP-SUMO1

Reference List

Ader,I., Brizuela,L., Bouquerel,P., Malavaud,B., and Cuvillier,O. (2008). Sphingosine kinase 1: a new modulator of hypoxia inducible factor 1alpha during hypoxia in human cancer cells. Cancer Res. *68*, 8635-8642.

Amir,S., Wang,R., Simons,J.W., and Mabjeesh,N.J. (2009). SEPT9_v1 up-regulates hypoxia-inducible factor 1 by preventing its RACK1-mediated degradation. J. Biol. Chem. *284*, 11142-11151.

Andre,H. and Pereira,T.S. (2008). Identification of an alternative mechanism of degradation of the hypoxia-inducible factor-1alpha. J. Biol. Chem. *283*, 29375-29384.

Appelhoff,R.J., Tian,Y.M., Raval,R.R., Turley,H., Harris,A.L., Pugh,C.W., Ratcliffe,P.J., and Gleadle,J.M. (2004). Differential function of the prolyl hydroxylases PHD1, PHD2, and PHD3 in the regulation of hypoxia-inducible factor. J. Biol. Chem. *279*, 38458-38465.

Aprelikova,O., Pandolfi,S., Tackett,S., Ferreira,M., Salnikow,K., Ward,Y., Risinger,J.I., Barrett,J.C., and Niederhuber,J. (2009). Melanoma antigen-11 inhibits the hypoxia-inducible factor prolyl hydroxylase 2 and activates hypoxic response. Cancer Res. *69*, 616-624.

Arabi,A., Wu,S., Ridderstrale,K., Bierhoff,H., Shiue,C., Fatyol,K., Fahlen,S., Hydbring,P., Soderberg,O., Grummt,I., Larsson,L.G., and Wright,A.P. (2005). c-Myc associates with ribosomal DNA and activates RNA polymerase I transcription. Nat. Cell Biol. *7*, 303-310.

Aragones,J., Schneider,M., van,G.K., Fraisl,P., Dresselaers,T., Mazzone,M., Dirkx,R., Zacchigna,S., Lemieux,H., Jeoung,N.H., Lambrechts,D., Bishop,T., Lafuste,P., Diez-Juan,A., Harten,S.K., Van,N.P., De,B.K., Willam,C., Tjwa,M., Grosfeld,A., Navet,R., Moons,L., Vandendriessche,T., Deroose,C., Wijeyekoon,B., Nuyts,J., Jordan,B., Silasi-Mansat,R., Lupu,F., Dewerchin,M., Pugh,C., Salmon,P., Mortelmans,L., Gallez,B., Gorus,F., Buyse,J., Sluse,F., Harris,R.A., Gnaiger,E., Hespel,P., Van,H.P., Schuit,F., Van,V.P., Ratcliffe,P., Baes,M., Maxwell,P., and Carmeliet,P. (2008). Deficiency or inhibition of oxygen sensor Phd1 induces hypoxia tolerance by reprogramming basal metabolism. Nat. Genet. *40*, 170-180.

Arany,Z., Huang,L.E., Eckner,R., Bhattacharya,S., Jiang,C., Goldberg,M.A., Bunn,H.F., and Livingston,D.M. (1996). An essential role for p300/CBP in the cellular response to hypoxia. Proc. Natl. Acad. Sci. U. S. A *93*, 12969-12973.

Arnesen,T., Kong,X., Evjenth,R., Gromyko,D., Varhaug,J.E., Lin,Z., Sang,N., Caro,J., and Lillehaug,J.R. (2005). Interaction between HIF-1 alpha (ODD) and hARD1 does not induce acetylation and destabilization of HIF-1 alpha. FEBS Lett. *579*, 6428-6432.

Ayyanathan,K., Peng,H., Hou,Z., Fredericks,W.J., Goyal,R.K., Langer,E.M., Longmore,G.D., and Rauscher,F.J., III (2007). The Ajuba LIM domain protein is a corepressor for SNAG domain mediated repression and participates in nucleocytoplasmic Shuttling. Cancer Res. *67*, 9097-9106.

Bae,S.H., Jeong,J.W., Park,J.A., Kim,S.H., Bae,M.K., Choi,S.J., and Kim,K.W. (2004). Sumoylation increases HIF-1alpha stability and its transcriptional activity
24. Biochem. Biophys. Res. Commun. *324*, 394-400.

Baek,J.H., Liu,Y.V., McDonald,K.R., Wesley,J.B., Hubbi,M.E., Byun,H., and Semenza,G.L. (2007a). Spermidine/spermine-N1-acetyltransferase 2 is an essential component of the ubiquitin ligase complex that regulates hypoxia-inducible factor 1alpha. J. Biol. Chem. *282*, 23572-23580.

Baek,J.H., Liu,Y.V., McDonald,K.R., Wesley,J.B., Zhang,H., and Semenza,G.L. (2007b). Spermidine/spermine N(1)-acetyltransferase-1 binds to hypoxia-inducible factor-1alpha (HIF-1alpha) and RACK1 and promotes ubiquitination and degradation of HIF-1alpha. J. Biol. Chem. *282*, 33358-33366.

Baek,J.H., Mahon,P.C., Oh,J., Kelly,B., Krishnamachary,B., Pearson,M., Chan,D.A., Giaccia,A.J., and Semenza,G.L. (2005). OS-9 interacts with hypoxia-inducible factor 1alpha and prolyl hydroxylases to promote oxygen-dependent degradation of HIF-1alpha. Mol. Cell *17*, 503-512.

Barth,S., Edlich,F., Berchner-Pfannschmidt,U., Gneuss,S., Jahreis,G., Hasgall,P.A., Fandrey,J., Wenger,R.H., and Camenisch,G. (2009). HIF prolyl-4-hydroxylase PHD2 protein abundance depends on integral membrane-anchoring of FKBP38. J. Biol. Chem.

Barth,S., Nesper,J., Hasgall,P.A., Wirthner,R., Nytko,K.J., Edlich,F., Katschinski,D.M., Stiehl,D.P., Wenger,R.H., and Camenisch,G. (2007). The peptidyl prolyl cis/trans isomerase FKBP38 determines hypoxia-inducible transcription factor prolyl-4-hydroxylase PHD2 protein stability. Mol. Cell Biol. *27*, 3758-3768.

Beck,I., Ramirez,S., Weinmann,R., and Caro,J. (1991). Enhancer element at the 3'-flanking region controls transcriptional response to hypoxia in the human erythropoietin gene. J. Biol. Chem. *266*, 15563-15566.

Berchner-Pfannschmidt,U., Tug,S., Trinidad,B., Oehme,F., Yamac,H., Wotzlaw,C., Flamme,I., and Fandrey,J. (2008). Nuclear oxygen sensing: induction of endogenous prolyl-hydroxylase 2 activity by hypoxia and nitric oxide. J. Biol. Chem. *283*, 31745-31753.

Berra,E., Benizri,E., Ginouves,A., Volmat,V., Roux,D., and Pouyssegur,J. (2003). HIF prolyl-hydroxylase 2 is the key oxygen sensor setting low steady-state levels of HIF-1alpha in normoxia. EMBO J. *22*, 4082-4090.

Berta,M.A., Mazure,N., Hattab,M., Pouyssegur,J., and Brahimi-Horn,M.C. (2007). SUMOylation of hypoxia-inducible factor-1alpha reduces its transcriptional activity
2. Biochem. Biophys. Res. Commun. *360*, 646-652.

Bertout,J.A., Patel,S.A., and Simon,M.C. (2008). The impact of O2 availability on human cancer. Nat. Rev. Cancer *8*, 967-975.

Bilton,R., Mazure,N., Trottier,E., Hattab,M., Dery,M.A., Richard,D.E., Pouyssegur,J., and Brahimi-Horn,M.C. (2005). Arrest-defective-1 protein, an acetyltransferase, does not alter stability of hypoxia-inducible factor (HIF)-1alpha and is not induced by hypoxia or HIF. J. Biol. Chem. *280*, 31132-31140.

Bishop,T., Gallagher,D., Pascual,A., Lygate,C.A., de Bono,J.P., Nicholls,L.G., Ortega-Saenz,P., Oster,H., Wijeyekoon,B., Sutherland,A.I., Grosfeld,A., Aragones,J., Schneider,M., van,G.K., Teixeira,D., Diez-Juan,A., Lopez-Barneo,J., Channon,K.M., Maxwell,P.H., Pugh,C.W., Davies,A.M., Carmeliet,P., and Ratcliffe,P.J. (2008). Abnormal sympathoadrenal development and systemic hypotension in PHD3-/- mice. Mol. Cell Biol. *28*, 3386-3400.

Bracken,C.P., Fedele,A.O., Linke,S., Balrak,W., Lisy,K., Whitelaw,M.L., and Peet,D.J. (2006). Cell-specific regulation of hypoxia-inducible factor (HIF)-1alpha and HIF-2alpha stabilization and transactivation in a graded oxygen environment. J. Biol. Chem. *281*, 22575-22585.

Brahimi-Horn,C., Mazure,N., and Pouyssegur,J. (2005). Signalling via the hypoxia-inducible factor-1alpha requires multiple posttranslational modifications. Cell Signal. *17*, 1-9.

Brugarolas,J., Lei,K., Hurley,R.L., Manning,B.D., Reiling,J.H., Hafen,E., Witters,L.A., Ellisen,L.W., and Kaelin,W.G., Jr. (2004). Regulation of mTOR function in response to hypoxia by REDD1 and the TSC1/TSC2 tumor suppressor complex. Genes Dev. *18*, 2893-2904.

Bruick,R.K. (2000). Expression of the gene encoding the proapoptotic Nip3 protein is induced by hypoxia. Proc. Natl. Acad. Sci. U. S. A *97*, 9082-9087.

Bruick,R.K. and McKnight,S.L. (2001). A conserved family of prolyl-4-hydroxylases that modify HIF. Science *294*, 1337-1340.

Carbia-Nagashima,A., Gerez,J., Perez-Castro,C., Paez-Pereda,M., Silberstein,S., Stalla,G.K., Holsboer,F., and Arzt,E. (2007). RSUME, a small RWD-containing protein, enhances SUMO conjugation and stabilizes HIF-1alpha during hypoxia
1. Cell *131*, 309-323.

Carmeliet,P. and Jain,R.K. (2000). Angiogenesis in cancer and other diseases. Nature *407*, 249-257.

Cattaruzza,M., Lattrich,C., and Hecker,M. (2004). Focal adhesion protein zyxin is a mechanosensitive modulator of gene expression in vascular smooth muscle cells. Hypertension *43*, 726-730.

Chan,D.A., Sutphin,P.D., Denko,N.C., and Giaccia,A.J. (2002). Role of prolyl hydroxylation in oncogenically stabilized hypoxia-inducible factor-1alpha. J. Biol. Chem. *277*, 40112-40117.

Chan,D.A., Sutphin,P.D., Yen,S.E., and Giaccia,A.J. (2005). Coordinate regulation of the oxygen-dependent degradation domains of hypoxia-inducible factor 1 alpha. Mol. Cell Biol. *25*, 6415-6426.

Chandel,N.S., Maltepe,E., Goldwasser,E., Mathieu,C.E., Simon,M.C., and Schumacker,P.T. (1998). Mitochondrial reactive oxygen species trigger hypoxia-induced transcription. Proc. Natl. Acad. Sci. U. S. A *95*, 11715-11720.

Chandel,N.S., McClintock,D.S., Feliciano,C.E., Wood,T.M., Melendez,J.A., Rodriguez,A.M., and Schumacker,P.T. (2000). Reactive oxygen species generated at mitochondrial complex III stabilize hypoxia-inducible factor-1alpha during hypoxia: a mechanism of O2 sensing. J. Biol. Chem. *275*, 25130-25138.

Cheng,J., Kang,X., Zhang,S., and Yeh,E.T. (2007). SUMO-specific protease 1 is essential for stabilization of HIF1alpha during hypoxia. Cell *131*, 584-595.

Choi,K.O., Lee,T., Lee,N., Kim,J.H., Yang,E.G., Yoon,J.M., Kim,J.H., Lee,T.G., and Park,H. (2005). Inhibition of the catalytic activity of hypoxia-inducible factor-1alpha-prolyl-hydroxylase 2 by a MYND-type zinc finger. Mol. Pharmacol. *68*, 1803-1809.

Cockman,M.E., Lancaster,D.E., Stolze,I.P., Hewitson,K.S., McDonough,M.A., Coleman,M.L., Coles,C.H., Yu,X., Hay,R.T., Ley,S.C., Pugh,C.W., Oldham,N.J., Masson,N., Schofield,C.J., and Ratcliffe,P.J. (2006). Posttranslational hydroxylation of ankyrin repeats in IkappaB proteins by the hypoxia-inducible factor (HIF) asparaginyl hydroxylase, factor inhibiting HIF (FIH). Proc. Natl. Acad. Sci. U. S. A *103*, 14767-14772.

Cockman,M.E., Masson,N., Mole,D.R., Jaakkola,P., Chang,G.W., Clifford,S.C., Maher,E.R., Pugh,C.W., Ratcliffe,P.J., and Maxwell,P.H. (2000). Hypoxia inducible factor-alpha binding and ubiquitylation by the von Hippel-Lindau tumor suppressor protein. J. Biol. Chem. *275*, 25733-25741.

Cockman,M.E., Webb,J.D., Kramer,H.B., Kessler,B.M., and Ratcliffe,P.J. (2009). Proteomics-based identification of novel factor inhibiting hypoxia-inducible factor (FIH) substrates indicates widespread asparaginyl hydroxylation of ankyrin repeat domain-containing proteins. Mol. Cell Proteomics. *8*, 535-546.

Coleman,M.L., McDonough,M.A., Hewitson,K.S., Coles,C., Mecinovic,J., Edelmann,M., Cook,K.M., Cockman,M.E., Lancaster,D.E., Kessler,B.M.,

Oldham,N.J., Ratcliffe,P.J., and Schofield,C.J. (2007). Asparaginyl hydroxylation of the notch ankyrin repeat domain by factor inhibiting hypoxia inducible factor. J. Biol. Chem.

Craig,D., Howell,M.T., Gibbs,C.L., Hunt,T., and Jackson,R.J. (1992). Plasmid cDNA-directed protein synthesis in a coupled eukaryotic in vitro transcription-translation system. Nucleic Acids Res. *20*, 4987-4995.

Crawford,A.W., Michelsen,J.W., and Beckerle,M.C. (1992). An interaction between zyxin and alpha-actinin. J. Cell Biol. *116*, 1381-1393.

Cummins,E.P., Berra,E., Comerford,K.M., Ginouves,A., Fitzgerald,K.T., Seeballuck,F., Godson,C., Nielsen,J.E., Moynagh,P., Pouyssegur,J., and Taylor,C.T. (2006). Prolyl hydroxylase-1 negatively regulates IkappaB kinase-beta, giving insight into hypoxia-induced NFkappaB activity. Proc. Natl. Acad. Sci. U. S. A *103*, 18154-18159.

Dalgard,C.L., Lu,H., Mohyeldin,A., and Verma,A. (2004). Endogenous 2-oxoacids differentially regulate expression of oxygen sensors. Biochem. J. *380*, 419-424.

Dames,S.A., Martinez-Yamout,M., De Guzman,R.N., Dyson,H.J., and Wright,P.E. (2002). Structural basis for Hif-1 alpha /CBP recognition in the cellular hypoxic response. Proc. Natl. Acad. Sci. U. S. A *99*, 5271-5276.

Dawid,I.B., Breen,J.J., and Toyama,R. (1998). LIM domains: multiple roles as adapters and functional modifiers in protein interactions. Trends Genet. *14*, 156-162.

Duan,D.R., Pause,A., Burgess,W.H., Aso,T., Chen,D.Y., Garrett,K.P., Conaway,R.C., Conaway,J.W., Linehan,W.M., and Klausner,R.D. (1995). Inhibition of transcription elongation by the VHL tumor suppressor protein. Science *269*, 1402-1406.

Ebert,B.L., Firth,J.D., and Ratcliffe,P.J. (1995). Hypoxia and mitochondrial inhibitors regulate expression of glucose transporter-1 via distinct Cis-acting sequences. J. Biol. Chem. *270*, 29083-29089.

Ehrismann,D., Flashman,E., Genn,D.N., Mathioudakis,N., Hewitson,K.S., Ratcliffe,P.J., and Schofield,C.J. (2007). Studies on the activity of the hypoxia-inducible-factor hydroxylases using an oxygen consumption assay. Biochem. J. *401*, 227-234.

Elkins,J.M., Hewitson,K.S., McNeill,L.A., Seibel,J.F., Schlemminger,I., Pugh,C.W., Ratcliffe,P.J., and Schofield,C.J. (2003). Structure of factor-inhibiting hypoxia-inducible factor (HIF) reveals mechanism of oxidative modification of HIF-1 alpha. J. Biol. Chem. *278*, 1802-1806.

Ema,M., Hirota,K., Mimura,J., Abe,H., Yodoi,J., Sogawa,K., Poellinger,L., and Fujii-Kuriyama,Y. (1999). Molecular mechanisms of transcription activation by HLF and HIF1alpha in response to hypoxia: their stabilization

and redox signal-induced interaction with CBP/p300. EMBO J. *18*, 1905-1914.

Ema,M., Taya,S., Yokotani,N., Sogawa,K., Matsuda,Y., and Fujii-Kuriyama,Y. (1997). A novel bHLH-PAS factor with close sequence similarity to hypoxia-inducible factor 1alpha regulates the VEGF expression and is potentially involved in lung and vascular development. Proc. Natl. Acad. Sci. U. S. A *94*, 4273-4278.

Epstein,A.C., Gleadle,J.M., McNeill,L.A., Hewitson,K.S., O'Rourke,J., Mole,D.R., Mukherji,M., Metzen,E., Wilson,M.I., Dhanda,A., Tian,Y.M., Masson,N., Hamilton,D.L., Jaakkola,P., Barstead,R., Hodgkin,J., Maxwell,P.H., Pugh,C.W., Schofield,C.J., and Ratcliffe,P.J. (2001). C. elegans EGL-9 and mammalian homologs define a family of dioxygenases that regulate HIF by prolyl hydroxylation. Cell *107*, 43-54.

Erez,N., Stambolsky,P., Shats,I., Milyavsky,M., Kachko,T., and Rotter,V. (2004). Hypoxia-dependent regulation of PHD1: cloning and characterization of the human PHD1/EGLN2 gene promoter. FEBS Lett. *567*, 311-315.

Erler,J.T., Bennewith,K.L., Nicolau,M., Dornhofer,N., Kong,C., Le,Q.T., Chi,J.T., Jeffrey,S.S., and Giaccia,A.J. (2006). Lysyl oxidase is essential for hypoxia-induced metastasis. Nature *440*, 1222-1226.

Esteban,M.A. and Maxwell,P.H. (2005). HIF, a missing link between metabolism and cancer. Nat. Med. *11*, 1047-1048.

Evans,A.J., Russell,R.C., Roche,O., Burry,T.N., Fish,J.E., Chow,V.W., Kim,W.Y., Saravanan,A., Maynard,M.A., Gervais,M.L., Sufan,R.I., Roberts,A.M., Wilson,L.A., Betten,M., Vandewalle,C., Berx,G., Marsden,P.A., Irwin,M.S., Teh,B.T., Jewett,M.A., and Ohh,M. (2007). VHL promotes E2 box-dependent E-cadherin transcription by HIF-mediated regulation of SIP1 and snail. Mol. Cell Biol. *27*, 157-169.

Feng,Y. and Longmore,G.D. (2005). The LIM protein Ajuba influences interleukin-1-induced NF-kappaB activation by affecting the assembly and activity of the protein kinase Czeta/p62/TRAF6 signaling complex. Mol. Cell Biol. *25*, 4010-4022.

Feng,Y., Zhao,H., Luderer,H.F., Epple,H., Faccio,R., Ross,F.P., Teitelbaum,S.L., and Longmore,G.D. (2007). The LIM protein, Limd1, regulates AP-1 activation through an interaction with Traf6 to influence osteoclast development. J. Biol. Chem. *282*, 39-48.

Ferrara,N., Gerber,H.P., and LeCouter,J. (2003). The biology of VEGF and its receptors. Nat. Med. *9*, 669-676.

Flamme,I., Frohlich,T., von,R.M., Kappel,A., Damert,A., and Risau,W. (1997). HRF, a putative basic helix-loop-helix-PAS-domain transcription factor is closely related to hypoxia-inducible factor-1 alpha and developmentally expressed in blood vessels. Mech. Dev. *63*, 51-60.

Flashman,E., Bagg,E.A., Chowdhury,R., Mecinovic,J., Loenarz,C., McDonough,M.A., Hewitson,K.S., and Schofield,C.J. (2008). Kinetic rationale for selectivity toward N- and C-terminal oxygen-dependent degradation domain substrates mediated by a loop region of hypoxia-inducible factor prolyl hydroxylases. J. Biol. Chem. *283*, 3808-3815.

Flugel,D., Gorlach,A., Michiels,C., and Kietzmann,T. (2007). Glycogen synthase kinase 3 phosphorylates hypoxia-inducible factor 1alpha and mediates its destabilization in a VHL-independent manner. Mol. Cell Biol. *27*, 3253-3265.

Fong,G.H. (2009). Regulation of angiogenesis by oxygen sensing mechanisms. J. Mol. Med. *87*, 549-560.

Fradelizi,J., Noireaux,V., Plastino,J., Menichi,B., Louvard,D., Sykes,C., Golsteyn,R.M., and Friederich,E. (2001). ActA and human zyxin harbour Arp2/3-independent actin-polymerization activity. Nat. Cell Biol. *3*, 699-707.

Freedman,S.J., Sun,Z.Y., Poy,F., Kung,A.L., Livingston,D.M., Wagner,G., and Eck,M.J. (2002). Structural basis for recruitment of CBP/p300 by hypoxia-inducible factor-1 alpha. Proc. Natl. Acad. Sci. U. S. A *99*, 5367-5372.

Freyd,G., Kim,S.K., and Horvitz,H.R. (1990). Novel cysteine-rich motif and homeodomain in the product of the Caenorhabditis elegans cell lineage gene lin-11. Nature *344*, 876-879.

Fu,J., Menzies,K., Freeman,R.S., and Taubman,M.B. (2007). EGLN3 prolyl hydroxylase regulates skeletal muscle differentiation and myogenin protein stability. J. Biol. Chem. *282*, 12410-12418.

Fukuba,H., Takahashi,T., Jin,H.G., Kohriyama,T., and Matsumoto,M. (2008). Abundance of aspargynyl-hydroxylase FIH is regulated by Siah-1 under normoxic conditions. Neurosci. Lett. *433*, 209-214.

Fukuba,H., Yamashita,H., Nagano,Y., Jin,H.G., Hiji,M., Ohtsuki,T., Takahashi,T., Kohriyama,T., and Matsumoto,M. (2007). Siah-1 facilitates ubiquitination and degradation of factor inhibiting HIF-1alpha (FIH). Biochem. Biophys. Res. Commun. *353*, 324-329.

Gerald,D., Berra,E., Frapart,Y.M., Chan,D.A., Giaccia,A.J., Mansuy,D., Pouyssegur,J., Yaniv,M., and Mechta-Grigoriou,F. (2004). JunD reduces tumor angiogenesis by protecting cells from oxidative stress. Cell *118*, 781-794.

Ghosh,S., Ghosh,A., Maiti,G.P., Alam,N., Roy,A., Roy,B., Roychoudhury,S., and Panda,C.K. (2008). Alterations of 3p21.31 tumor suppressor genes in head and neck squamous cell carcinoma: Correlation with progression and prognosis. Int. J. Cancer *123*, 2594-2604.

Gnarra,J.R., Tory,K., Weng,Y., Schmidt,L., Wei,M.H., Li,H., Latif,F., Liu,S., Chen,F., Duh,F.M., and . (1994). Mutations of the VHL tumour suppressor gene in renal carcinoma. Nat. Genet. *7*, 85-90.

Goldberg,M.A., Dunning,S.P., and Bunn,H.F. (1988). Regulation of the erythropoietin gene: evidence that the oxygen sensor is a heme protein. Science *242*, 1412-1415.

Gordan,J.D., Bertout,J.A., Hu,C.J., Diehl,J.A., and Simon,M.C. (2007). HIF-2alpha promotes hypoxic cell proliferation by enhancing c-myc transcriptional activity. Cancer Cell *11*, 335-347.

Gothie,E., Richard,D.E., Berra,E., Pages,G., and Pouyssegur,J. (2000). Identification of alternative spliced variants of human hypoxia-inducible factor-1alpha. J. Biol. Chem. *275*, 6922-6927.

Goyal,R.K., Lin,P., Kanungo,J., Payne,A.S., Muslin,A.J., and Longmore,G.D. (1999). Ajuba, a novel LIM protein, interacts with Grb2, augments mitogen-activated protein kinase activity in fibroblasts, and promotes meiotic maturation of Xenopus oocytes in a Grb2- and Ras-dependent manner. Mol. Cell Biol. *19*, 4379-4389.

Graeber,T.G., Osmanian,C., Jacks,T., Housman,D.E., Koch,C.J., Lowe,S.W., and Giaccia,A.J. (1996). Hypoxia-mediated selection of cells with diminished apoptotic potential in solid tumours. Nature *379*, 88-91.

Graven,K.K., Yu,Q., Pan,D., Roncarati,J.S., and Farber,H.W. (1999). Identification of an oxygen responsive enhancer element in the glyceraldehyde-3-phosphate dehydrogenase gene. Biochim. Biophys. Acta *1447*, 208-218.

Gray,M.J., Zhang,J., Ellis,L.M., Semenza,G.L., Evans,D.B., Watowich,S.S., and Gallick,G.E. (2005). HIF-1alpha, STAT3, CBP/p300 and Ref-1/APE are components of a transcriptional complex that regulates Src-dependent hypoxia-induced expression of VEGF in pancreatic and prostate carcinomas. Oncogene *24*, 3110-3120.

Gu,Y.Z., Moran,S.M., Hogenesch,J.B., Wartman,L., and Bradfield,C.A. (1998). Molecular characterization and chromosomal localization of a third alpha-class hypoxia inducible factor subunit, HIF3alpha. Gene Expr. *7*, 205-213.

Guertin,D.A. and Sabatini,D.M. (2005). An expanding role for mTOR in cancer. Trends Mol. Med. *11*, 353-361.

Hagen,T., Taylor,C.T., Lam,F., and Moncada,S. (2003). Redistribution of intracellular oxygen in hypoxia by nitric oxide: effect on HIF1alpha. Science *302*, 1975-1978.

Hanahan,D. and Weinberg,R.A. (2000). The hallmarks of cancer. Cell *100*, 57-70.

Hankinson,O. (1995). The aryl hydrocarbon receptor complex. Annu. Rev. Pharmacol. Toxicol. *35*, 307-340.

Hardy,A.P., Prokes,I., Kelly,L., Campbell,I.D., and Schofield,C.J. (2009). Asparaginyl beta-hydroxylation of proteins containing ankyrin repeat domains influences their stability and function. J. Mol. Biol. *392*, 994-1006.

Heacock,C.S. and Sutherland,R.M. (1990). Enhanced synthesis of stress proteins caused by hypoxia and relation to altered cell growth and metabolism. Br. J. Cancer *62*, 217-225.

Hegg,E.L. and Que,L., Jr. (1997). The 2-His-1-carboxylate facial triad--an emerging structural motif in mononuclear non-heme iron(II) enzymes. Eur. J. Biochem. *250*, 625-629.

Hellstrom,M., Phng,L.K., and Gerhardt,H. (2007). VEGF and Notch signaling: the yin and yang of angiogenic sprouting. Cell Adh. Migr. *1*, 133-136.

Hewitson,K.S., McNeill,L.A., Riordan,M.V., Tian,Y.M., Bullock,A.N., Welford,R.W., Elkins,J.M., Oldham,N.J., Bhattacharya,S., Gleadle,J.M., Ratcliffe,P.J., Pugh,C.W., and Schofield,C.J. (2002). Hypoxia-inducible factor (HIF) asparagine hydroxylase is identical to factor inhibiting HIF (FIH) and is related to the cupin structural family. J. Biol. Chem. *277*, 26351-26355.

Hewitson,K.S., Schofield,C.J., and Ratcliffe,P.J. (2007). Hypoxia-inducible factor prolyl-hydroxylase: purification and assays of PHD2. Methods Enzymol. *435*, 25-42.

Hirsila,M., Koivunen,P., Gunzler,V., Kivirikko,K.I., and Myllyharju,J. (2003). Characterization of the human prolyl 4-hydroxylases that modify the hypoxia-inducible factor. J. Biol. Chem. *278*, 30772-30780.

Hogenesch,J.B., Chan,W.K., Jackiw,V.H., Brown,R.C., Gu,Y.Z., Pray-Grant,M., Perdew,G.H., and Bradfield,C.A. (1997). Characterization of a subset of the basic-helix-loop-helix-PAS superfamily that interacts with components of the dioxin signaling pathway. J. Biol. Chem. *272*, 8581-8593.

Hon,W.C., Wilson,M.I., Harlos,K., Claridge,T.D., Schofield,C.J., Pugh,C.W., Maxwell,P.H., Ratcliffe,P.J., Stuart,D.I., and Jones,E.Y. (2002). Structural basis for the recognition of hydroxyproline in HIF-1 alpha by pVHL. Nature *417*, 975-978.

Hopfer,U., Hopfer,H., Jablonski,K., Stahl,R.A., and Wolf,G. (2006). The novel WD-repeat protein Morg1 acts as a molecular scaffold for hypoxia-inducible factor prolyl hydroxylase 3 (PHD3). J. Biol. Chem. *281*, 8645-8655.

Hou,Z., Peng,H., Ayyanathan,K., Yan,K.P., Langer,E.M., Longmore,G.D., and Rauscher,F.J., III (2008). The LIM protein AJUBA recruits protein arginine methyltransferase 5 to mediate SNAIL-dependent transcriptional repression. Mol. Cell Biol. *28*, 3198-3207.

Huang,L.E., Arany,Z., Livingston,D.M., and Bunn,H.F. (1996). Activation of hypoxia-inducible transcription factor depends primarily upon redox-sensitive stabilization of its alpha subunit. J. Biol. Chem. *271*, 32253-32259.

Huang,L.E., Gu,J., Schau,M., and Bunn,H.F. (1998). Regulation of hypoxia-inducible factor 1alpha is mediated by an O2-dependent degradation domain via the ubiquitin-proteasome pathway. Proc. Natl. Acad. Sci. U. S. A *95*, 7987-7992.

Huggins,C.J. and Andrulis,I.L. (2008). Cell cycle regulated phosphorylation of LIMD1 in cell lines and expression in human breast cancers. Cancer Lett. *267*, 55-66.

Iliopoulos,O., Kibel,A., Gray,S., and Kaelin,W.G., Jr. (1995). Tumour suppression by the human von Hippel-Lindau gene product. Nat. Med. *1*, 822-826.

Iliopoulos,O., Ohh,M., and Kaelin,W.G., Jr. (1998). pVHL19 is a biologically active product of the von Hippel-Lindau gene arising from internal translation initiation. Proc. Natl. Acad. Sci. U. S. A *95*, 11661-11666.

Imreh,S., Kost-Alimova,M., Kholodnyuk,I., Yang,Y., Szeles,A., Kiss,H., Liu,Y., Foster,K., Zabarovsky,E., Stanbridge,E., and Klein,G. (1997). Differential elimination of 3p and retention of 3q segments in human/mouse microcell hybrids during tumor growth. Genes Chromosomes. Cancer *20*, 224-233.

Isaacs,J.S., Jung,Y.J., Mole,D.R., Lee,S., Torres-Cabala,C., Chung,Y.L., Merino,M., Trepel,J., Zbar,B., Toro,J., Ratcliffe,P.J., Linehan,W.M., and Neckers,L. (2005). HIF overexpression correlates with biallelic loss of fumarate hydratase in renal cancer: novel role of fumarate in regulation of HIF stability. Cancer Cell *8*, 143-153.

Ivan,M., Haberberger,T., Gervasi,D.C., Michelson,K.S., Gunzler,V., Kondo,K., Yang,H., Sorokina,I., Conaway,R.C., Conaway,J.W., and Kaelin,W.G., Jr. (2002). Biochemical purification and pharmacological inhibition of a mammalian prolyl hydroxylase acting on hypoxia-inducible factor. Proc. Natl. Acad. Sci. U. S. A *99*, 13459-13464.

Ivan,M., Kondo,K., Yang,H., Kim,W., Valiando,J., Ohh,M., Salic,A., Asara,J.M., Lane,W.S., and Kaelin,W.G., Jr. (2001). HIFalpha targeted for VHL-mediated destruction by proline hydroxylation: implications for O2 sensing. Science *292*, 464-468.

Jaakkola,P., Mole,D.R., Tian,Y.M., Wilson,M.I., Gielbert,J., Gaskell,S.J., Kriegsheim,A., Hebestreit,H.F., Mukherji,M., Schofield,C.J., Maxwell,P.H., Pugh,C.W., and Ratcliffe,P.J. (2001). Targeting of HIF-alpha to the von Hippel-Lindau ubiquitylation complex by O2-regulated prolyl hydroxylation. Science *292*, 468-472.

Jain,R.K. (2005). Normalization of tumor vasculature: an emerging concept in antiangiogenic therapy. Science *307*, 58-62.

Jain,S., Maltepe,E., Lu,M.M., Simon,C., and Bradfield,C.A. (1998). Expression of ARNT, ARNT2, HIF1 alpha, HIF2 alpha and Ah receptor mRNAs in the developing mouse. Mech. Dev. *73*, 117-123.

Jeong,J.W., Bae,M.K., Ahn,M.Y., Kim,S.H., Sohn,T.K., Bae,M.H., Yoo,M.A., Song,E.J., Lee,K.J., and Kim,K.W. (2002). Regulation and destabilization of HIF-1alpha by ARD1-mediated acetylation. Cell *111*, 709-720.

Jiang,B.H., Rue,E., Wang,G.L., Roe,R., and Semenza,G.L. (1996). Dimerization, DNA binding, and transactivation properties of hypoxia-inducible factor 1. J. Biol. Chem. *271*, 17771-17778.

Jiang,B.H., Zheng,J.Z., Leung,S.W., Roe,R., and Semenza,G.L. (1997). Transactivation and inhibitory domains of hypoxia-inducible factor 1alpha. Modulation of transcriptional activity by oxygen tension. J. Biol. Chem. *272*, 19253-19260.

Jung,C.R., Hwang,K.S., Yoo,J., Cho,W.K., Kim,J.M., Kim,W.H., and Im,D.S. (2006). E2-EPF UCP targets pVHL for degradation and associates with tumor growth and metastasis. Nat. Med. *12*, 809-816.

Jung,J.E., Kim,H.S., Lee,C.S., Shin,Y.J., Kim,Y.N., Kang,G.H., Kim,T.Y., Juhnn,Y.S., Kim,S.J., Park,J.W., Ye,S.K., and Chung,M.H. (2008). STAT3 inhibits the degradation of HIF-1alpha by pVHL-mediated ubiquitination. Exp. Mol. Med. *40*, 479-485.

Kadrmas,J.L. and Beckerle,M.C. (2004). The LIM domain: from the cytoskeleton to the nucleus. Nat. Rev. Mol. Cell Biol. *5*, 920-931.

Kaelin,W.G., Jr. (2002). Molecular basis of the VHL hereditary cancer syndrome. Nat. Rev. Cancer *2*, 673-682.

Kaelin,W.G., Jr. (2007). The von hippel-lindau tumor suppressor protein: an update. Methods Enzymol. *435*, 371-383.

Kaelin,W.G., Jr. and Ratcliffe,P.J. (2008). Oxygen sensing by metazoans: the central role of the HIF hydroxylase pathway. Mol. Cell *30*, 393-402.

Kallio,P.J., Okamoto,K., O'Brien,S., Carrero,P., Makino,Y., Tanaka,H., and Poellinger,L. (1998). Signal transduction in hypoxic cells: inducible nuclear translocation and recruitment of the CBP/p300 coactivator by the hypoxia-inducible factor-1 alpha. Embo Journal *17*, 6573-6586.

Kallio,P.J., Pongratz,I., Gradin,K., McGuire,J., and Poellinger,L. (1997). Activation of hypoxia-inducible factor 1alpha: posttranscriptional regulation and conformational change by recruitment of the Arnt transcription factor. Proc. Natl. Acad. Sci. U. S. A *94*, 5667-5672.

Kamura,T., Koepp,D.M., Conrad,M.N., Skowyra,D., Moreland,R.J., Iliopoulos,O., Lane,W.S., Kaelin,W.G., Jr., Elledge,S.J., Conaway,R.C., Harper,J.W., and Conaway,J.W. (1999). Rbx1, a component of the VHL tumor suppressor complex and SCF ubiquitin ligase. Science *284*, 657-661.

Kanungo,J., Pratt,S.J., Marie,H., and Longmore,G.D. (2000). Ajuba, a cytosolic LIM protein, shuttles into the nucleus and affects embryonal cell proliferation and fate decisions. Mol. Biol. Cell *11*, 3299-3313.

Karlsson,O., Thor,S., Norberg,T., Ohlsson,H., and Edlund,T. (1990). Insulin gene enhancer binding protein Isl-1 is a member of a novel class of proteins containing both a homeo- and a Cys-His domain. Nature *344*, 879-882.

Kawanami,D., Mahabeleshwar,G.H., Lin,Z., Atkins,G.B., Hamik,A., Haldar,S.M., Maemura,K., Lamanna,J.C., and Jain,M.K. (2009). Kruppel-like Factor 2 Inhibits Hypoxia-inducible Factor 1{alpha} Expression and Function in the Endothelium. J. Biol. Chem. *284*, 20522-20530.

Kelly,L., McDonough,M.A., Coleman,M.L., Ratcliffe,P.J., and Schofield,C.J. (2009). Asparagine beta-hydroxylation stabilizes the ankyrin repeat domain fold. Mol. Biosyst. *5*, 52-58.

Kibel,A., Iliopoulos,O., DeCaprio,J.A., and Kaelin,W.G., Jr. (1995). Binding of the von Hippel-Lindau tumor suppressor protein to Elongin B and C. Science *269*, 1444-1446.

Kim,J.W., Tchernyshyov,I., Semenza,G.L., and Dang,C.V. (2006). HIF-1-mediated expression of pyruvate dehydrogenase kinase: a metabolic switch required for cellular adaptation to hypoxia. Cell Metab *3*, 177-185.

Kiss,H., Kedra,D., Yang,Y., Kost-Alimova,M., Kiss,C., O'Brien,K.P., Fransson,I., Klein,G., Imreh,S., and Dumanski,J.P. (1999). A novel gene containing LIM domains (LIMD1) is located within the common eliminated region 1 (C3CER1) in 3p21.3. Hum. Genet. *105*, 552-559.

Kivirikko,K.I. and Myllyharju,J. (1998). Prolyl 4-hydroxylases and their protein disulfide isomerase subunit. Matrix Biol. *16*, 357-368.

Kivirikko,K.I. and Pihlajaniemi,T. (1998). Collagen hydroxylases and the protein disulfide isomerase subunit of prolyl 4-hydroxylases. Adv. Enzymol. Relat Areas Mol. Biol. *72*, 325-398.

Knauth,K., Bex,C., Jemth,P., and Buchberger,A. (2006). Renal cell carcinoma risk in type 2 von Hippel-Lindau disease correlates with defects in pVHL stability and HIF-1alpha interactions. Oncogene *25*, 370-377.

Knowles,H.J., Raval,R.R., Harris,A.L., and Ratcliffe,P.J. (2003). Effect of ascorbate on the activity of hypoxia-inducible factor in cancer cells. Cancer Res. *63*, 1764-1768.

Koditz,J., Nesper,J., Wottawa,M., Stiehl,D.P., Camenisch,G., Franke,C., Myllyharju,J., Wenger,R.H., and Katschinski,D.M. (2007). Oxygen-dependent ATF-4 stability is mediated by the PHD3 oxygen sensor. Blood *110*, 3610-3617.

Koh,M.Y., Darnay,B.G., and Powis,G. (2008). Hypoxia-associated factor, a novel E3-ubiquitin ligase, binds and ubiquitinates hypoxia-inducible factor

1alpha, leading to its oxygen-independent degradation. Mol. Cell Biol. *28*, 7081-7095.

Koivunen,P., Hirsila,M., Gunzler,V., Kivirikko,K.I., and Myllyharju,J. (2004). Catalytic properties of the asparaginyl hydroxylase (FIH) in the oxygen sensing pathway are distinct from those of its prolyl 4-hydroxylases. J. Biol. Chem. *279*, 9899-9904.

Koivunen,P., Hirsila,M., Kivirikko,K.I., and Myllyharju,J. (2006). The length of peptide substrates has a marked effect on hydroxylation by the hypoxia-inducible factor prolyl 4-hydroxylases. J. Biol. Chem. *281*, 28712-28720.

Koivunen,P., Hirsila,M., Remes,A.M., Hassinen,I.E., Kivirikko,K.I., and Myllyharju,J. (2007). Inhibition of hypoxia-inducible factor (HIF) hydroxylases by citric acid cycle intermediates - Possible links between cell metabolism and stabilization of HIF. Journal of Biological Chemistry *282*, 4524-4532.

Kourembanas,S., Hannan,R.L., and Faller,D.V. (1990). Oxygen tension regulates the expression of the platelet-derived growth factor-B chain gene in human endothelial cells. J. Clin. Invest *86*, 670-674.

Kreidberg,J.A., Sariola,H., Loring,J.M., Maeda,M., Pelletier,J., Housman,D., and Jaenisch,R. (1993). WT-1 is required for early kidney development. Cell *74*, 679-691.

Landazuri,M.O., Vara-Vega,A., Viton,M., Cuevas,Y., and del,P.L. (2006). Analysis of HIF-prolyl hydroxylases binding to substrates. Biochem. Biophys. Res. Commun. *351*, 313-320.

Lando,D., Peet,D.J., Gorman,J.J., Whelan,D.A., Whitelaw,M.L., and Bruick,R.K. (2002). FIH-1 is an asparaginyl hydroxylase enzyme that regulates the transcriptional activity of hypoxia-inducible factor. Genes Dev. *16*, 1466-1471.

Langer,E.M., Feng,Y., Zhaoyuan,H., Rauscher,F.J., III, Kroll,K.L., and Longmore,G.D. (2008). Ajuba LIM proteins are snail/slug corepressors required for neural crest development in Xenopus. Dev. Cell *14*, 424-436.

Le,N.T. and Richardson,D.R. (2002). The role of iron in cell cycle progression and the proliferation of neoplastic cells. Biochim. Biophys. Acta *1603*, 31-46.

Lee,S., Nakamura,E., Yang,H., Wei,W., Linggi,M.S., Sajan,M.P., Farese,R.V., Freeman,R.S., Carter,B.D., Kaelin,W.G., Jr., and Schlisio,S. (2005). Neuronal apoptosis linked to EglN3 prolyl hydroxylase and familial pheochromocytoma genes: developmental culling and cancer. Cancer Cell *8*, 155-167.

Levy,A.P., Levy,N.S., Wegner,S., and Goldberg,M.A. (1995). Transcriptional regulation of the rat vascular endothelial growth factor gene by hypoxia. J. Biol. Chem. *270*, 13333-13340.

Li,B., Zhuang,L., Reinhard,M., and Trueb,B. (2003). The lipoma preferred partner LPP interacts with alpha-actinin. J. Cell Sci. *116*, 1359-1366.

Li,Z., Na,X., Wang,D., Schoen,S.R., Messing,E.M., and Wu,G. (2002a). Ubiquitination of a novel deubiquitinating enzyme requires direct binding to von Hippel-Lindau tumor suppressor protein. J. Biol. Chem. *277*, 4656-4662.

Li,Z., Wang,D., Messing,E.M., and Wu,G. (2005). VHL protein-interacting deubiquitinating enzyme 2 deubiquitinates and stabilizes HIF-1alpha. EMBO Rep. *6*, 373-378.

Li,Z., Wang,D., Na,X., Schoen,S.R., Messing,E.M., and Wu,G. (2002b). Identification of a deubiquitinating enzyme subfamily as substrates of the von Hippel-Lindau tumor suppressor. Biochem. Biophys. Res. Commun. *294*, 700-709.

Lieb,M.E., Menzies,K., Moschella,M.C., Ni,R., and Taubman,M.B. (2002). Mammalian EGLN genes have distinct patterns of mRNA expression and regulation. Biochem. Cell Biol. *80*, 421-426.

Lisy,K. and Peet,D.J. (2008). Turn me on: regulating HIF transcriptional activity. Cell Death. Differ. *15*, 642-649.

Liu,Y.V., Baek,J.H., Zhang,H., Diez,R., Cole,R.N., and Semenza,G.L. (2007). RACK1 competes with HSP90 for binding to HIF-1alpha and is required for O(2)-independent and HSP90 inhibitor-induced degradation of HIF-1alpha. Mol. Cell *25*, 207-217.

Lonergan,K.M., Iliopoulos,O., Ohh,M., Kamura,T., Conaway,R.C., Conaway,J.W., and Kaelin,W.G., Jr. (1998). Regulation of hypoxia-inducible mRNAs by the von Hippel-Lindau tumor suppressor protein requires binding to complexes containing elongins B/C and Cul2. Mol. Cell Biol. *18*, 732-741.

Luderer,H.F., Bai,S., and Longmore,G.D. (2008). The LIM protein LIMD1 influences osteoblast differentiation and function. Exp. Cell Res. *314*, 2884-2894.

MacKenzie,E.D., Selak,M.A., Tennant,D.A., Payne,L.J., Crosby,S., Frederiksen,C.M., Watson,D.G., and Gottlieb,E. (2007). Cell-permeating alpha-ketoglutarate derivatives alleviate pseudohypoxia in succinate dehydrogenase-deficient cells. Mol. Cell Biol. *27*, 3282-3289.

Mahon,P.C., Hirota,K., and Semenza,G.L. (2001). FIH-1: a novel protein that interacts with HIF-1alpha and VHL to mediate repression of HIF-1 transcriptional activity. Genes Dev. *15*, 2675-2686.

Maisonpierre,P.C., Suri,C., Jones,P.F., Bartunkova,S., Wiegand,S.J., Radziejewski,C., Compton,D., McClain,J., Aldrich,T.H., Papadopoulos,N., Daly,T.J., Davis,S., Sato,T.N., and Yancopoulos,G.D. (1997). Angiopoietin-2, a natural antagonist for Tie2 that disrupts in vivo angiogenesis. Science *277*, 55-60.

Makino,Y., Cao,R., Svensson,K., Bertilsson,G., Asman,M., Tanaka,H., Cao,Y., Berkenstam,A., and Poellinger,L. (2001). Inhibitory PAS domain protein is a negative regulator of hypoxia-inducible gene expression. Nature *414*, 550-554.

Marie,H., Pratt,S.J., Betson,M., Epple,H., Kittler,J.T., Meek,L., Moss,S.J., Troyanovsky,S., Attwell,D., Longmore,G.D., and Braga,V.M. (2003). The LIM protein Ajuba is recruited to cadherin-dependent cell junctions through an association with alpha-catenin. J. Biol. Chem. *278*, 1220-1228.

Marxsen,J.H., Stengel,P., Doege,K., Heikkinen,P., Jokilehto,T., Wagner,T., Jelkmann,W., Jaakkola,P., and Metzen,E. (2004). Hypoxia-inducible factor-1 (HIF-1) promotes its degradation by induction of HIF-alpha-prolyl-4-hydroxylases. Biochem. J. *381*, 761-767.

Masson,N., Appelhoff,R.J., Tuckerman,J.R., Tian,Y.M., Demol,H., Puype,M., Vandekerckhove,J., Ratcliffe,P.J., and Pugh,C.W. (2004). The HIF prolyl hydroxylase PHD3 is a potential substrate of the TRiC chaperonin. FEBS Lett. *570*, 166-170.

Masson,N., Willam,C., Maxwell,P.H., Pugh,C.W., and Ratcliffe,P.J. (2001). Independent function of two destruction domains in hypoxia-inducible factor-alpha chains activated by prolyl hydroxylation. EMBO J. *20*, 5197-5206.

Mateo,J., Garcia-Lecea,M., Cadenas,S., Hernandez,C., and Moncada,S. (2003). Regulation of hypoxia-inducible factor-1alpha by nitric oxide through mitochondria-dependent and -independent pathways. Biochem. J. *376*, 537-544.

Maxwell,P.H., Wiesener,M.S., Chang,G.W., Clifford,S.C., Vaux,E.C., Cockman,M.E., Wykoff,C.C., Pugh,C.W., Maher,E.R., and Ratcliffe,P.J. (1999). The tumour suppressor protein VHL targets hypoxia-inducible factors for oxygen-dependent proteolysis. Nature *399*, 271-275.

Mazzone,M., Dettori,D., Leite de,O.R., Loges,S., Schmidt,T., Jonckx,B., Tian,Y.M., Lanahan,A.A., Pollard,P., Ruiz de,A.C., De,S.F., Vinckier,S., Aragones,J., Debackere,K., Luttun,A., Wyns,S., Jordan,B., Pisacane,A., Gallez,B., Lampugnani,M.G., Dejana,E., Simons,M., Ratcliffe,P., Maxwell,P., and Carmeliet,P. (2009). Heterozygous deficiency of PHD2 restores tumor oxygenation and inhibits metastasis via endothelial normalization. Cell *136*, 839-851.

McDonough,M.A., Li,V., Flashman,E., Chowdhury,R., Mohr,C., Lienard,B.M., Zondlo,J., Oldham,N.J., Clifton,I.J., Lewis,J., McNeill,L.A., Kurzeja,R.J., Hewitson,K.S., Yang,E., Jordan,S., Syed,R.S., and Schofield,C.J. (2006). Cellular oxygen sensing: Crystal structure of hypoxia-inducible factor prolyl hydroxylase (PHD2). Proc. Natl. Acad. Sci. U. S. A *103*, 9814-9819.

McNeill,L.A., Hewitson,K.S., Claridge,T.D., Seibel,J.F., Horsfall,L.E., and Schofield,C.J. (2002). Hypoxia-inducible factor asparaginyl hydroxylase (FIH-

1) catalyses hydroxylation at the beta-carbon of asparagine-803. Biochem. J. *367*, 571-575.

Metzen,E., Berchner-Pfannschmidt,U., Stengel,P., Marxsen,J.H., Stolze,I., Klinger,M., Huang,W.Q., Wotzlaw,C., Hellwig-Burgel,T., Jelkmann,W., Acker,H., and Fandrey,J. (2003a). Intracellular localisation of human HIF-1 alpha hydroxylases: implications for oxygen sensing. J. Cell Sci. *116*, 1319-1326.

Metzen,E., Zhou,J., Jelkmann,W., Fandrey,J., and Brune,B. (2003b). Nitric oxide impairs normoxic degradation of HIF-1alpha by inhibition of prolyl hydroxylases. Mol. Biol. Cell *14*, 3470-3481.

Michelsen,J.W., Schmeichel,K.L., Beckerle,M.C., and Winge,D.R. (1993). The LIM motif defines a specific zinc-binding protein domain. Proc. Natl. Acad. Sci. U. S. A *90*, 4404-4408.

Midy,V. and Plouet,J. (1994). Vasculotropin/vascular endothelial growth factor induces differentiation in cultured osteoblasts
2. Biochem. Biophys. Res. Commun. *199*, 380-386.

Mikami,Y., Hisatsune,A., Tashiro,T., Isohama,Y., and Katsuki,H. (2009). Hypoxia enhances MUC1 expression in a lung adenocarcinoma cell line. Biochem. Biophys. Res. Commun. *379*, 1060-1065.

Milkiewicz,M., Pugh,C.W., and Egginton,S. (2004). Inhibition of endogenous HIF inactivation induces angiogenesis in ischaemic skeletal muscles of mice. J. Physiol *560*, 21-26.

Min,J.H., Yang,H., Ivan,M., Gertler,F., Kaelin,W.G., Jr., and Pavletich,N.P. (2002). Structure of an HIF-1alpha -pVHL complex: hydroxyproline recognition in signaling. Science *296*, 1886-1889.

Minamishima,Y.A., Moslehi,J., Bardeesy,N., Cullen,D., Bronson,R.T., and Kaelin,W.G., Jr. (2008). Somatic inactivation of the PHD2 prolyl hydroxylase causes polycythemia and congestive heart failure. Blood *111*, 3236-3244.

Montoya-Durango,D.E., Velu,C.S., Kazanjian,A., Rojas,M.E., Jay,C.M., Longmore,G.D., and Grimes,H.L. (2008). Ajuba functions as a histone deacetylase-dependent co-repressor for autoregulation of the growth factor-independent-1 transcription factor. J. Biol. Chem. *283*, 32056-32065.

Muller,J.M., Metzger,E., Greschik,H., Bosserhoff,A.K., Mercep,L., Buettner,R., and Schule,R. (2002). The transcriptional coactivator FHL2 transmits Rho signals from the cell membrane into the nucleus. EMBO J. *21*, 736-748.

Muller,S., Hoege,C., Pyrowolakis,G., and Jentsch,S. (2001). SUMO, ubiquitin's mysterious cousin
30. Nat. Rev. Mol. Cell Biol. *2*, 202-210.

Nakayama,K., Frew,I.J., Hagensen,M., Skals,M., Habelhah,H., Bhoumik,A., Kadoya,T., Erdjument-Bromage,H., Tempst,P., Frappell,P.B., Bowtell,D.D., and Ronai,Z. (2004). Siah2 regulates stability of prolyl-hydroxylases, controls HIF1alpha abundance, and modulates physiological responses to hypoxia. Cell *117*, 941-952.

Nakayama,K., Gazdoiu,S., Abraham,R., Pan,Z.Q., and Ronai,Z. (2007). Hypoxia-induced assembly of prolyl hydroxylase PHD3 into complexes: implications for its activity and susceptibility for degradation by the E3 ligase Siah2. Biochemical Journal *401*, 217-226.

Nix,D.A., Fradelizi,J., Bockholt,S., Menichi,B., Louvard,D., Friederich,E., and Beckerle,M.C. (2001). Targeting of zyxin to sites of actin membrane interaction and to the nucleus. J. Biol. Chem. *276*, 34759-34767.

O'Rourke,J.F., Tian,Y.M., Ratcliffe,P.J., and Pugh,C.W. (1999). Oxygen-regulated and transactivating domains in endothelial PAS protein 1: comparison with hypoxia-inducible factor-1alpha. J. Biol. Chem. *274*, 2060-2071.

Oh,H., Takagi,H., Suzuma,K., Otani,A., Matsumura,M., and Honda,Y. (1999). Hypoxia and vascular endothelial growth factor selectively up-regulate angiopoietin-2 in bovine microvascular endothelial cells. J. Biol. Chem. *274*, 15732-15739.

Ohh,M., Park,C.W., Ivan,M., Hoffman,M.A., Kim,T.Y., Huang,L.E., Pavletich,N., Chau,V., and Kaelin,W.G. (2000). Ubiquitination of hypoxia-inducible factor requires direct binding to the beta-domain of the von Hippel-Lindau protein. Nat. Cell Biol. *2*, 423-427.

Olmos,G., Arenas,M.I., Bienes,R., Calzada,M.J., Aragones,J., Garcia-Bermejo,M.L., Landazuri,M.O., and Lucio-Cazana,J. (2009). 15-Deoxy-Delta(12,14)-prostaglandin-J(2) reveals a new pVHL-independent, lysosomal-dependent mechanism of HIF-1alpha degradation. Cell Mol. Life Sci. *66*, 2167-2180.

Ozer,A., Wu,L.C., and Bruick,R.K. (2005). The candidate tumor suppressor ING4 represses activation of the hypoxia inducible factor (HIF). Proc. Natl. Acad. Sci. U. S. A *102*, 7481-7486.

Page,E.L., Chan,D.A., Giaccia,A.J., Levine,M., and Richard,D.E. (2008). Hypoxia-inducible factor-1alpha stabilization in nonhypoxic conditions: role of oxidation and intracellular ascorbate depletion. Mol. Biol. Cell *19*, 86-94.

Pause,A., Lee,S., Worrell,R.A., Chen,D.Y., Burgess,W.H., Linehan,W.M., and Klausner,R.D. (1997). The von Hippel-Lindau tumor-suppressor gene product forms a stable complex with human CUL-2, a member of the Cdc53 family of proteins. Proc. Natl. Acad. Sci. U. S. A *94*, 2156-2161.

Pawson,T. and Nash,P. (2003). Assembly of cell regulatory systems through protein interaction domains. Science *300*, 445-452.

Pennacchietti,S., Michieli,P., Galluzzo,M., Mazzone,M., Giordano,S., and Comoglio,P.M. (2003). Hypoxia promotes invasive growth by transcriptional activation of the met protooncogene. Cancer Cell *3*, 347-361.

Percy,M.J., Zhao,Q., Flores,A., Harrison,C., Lappin,T.R., Maxwell,P.H., McMullin,M.F., and Lee,F.S. (2006). A family with erythrocytosis establishes a role for prolyl hydroxylase domain protein 2 in oxygen homeostasis. Proc. Natl. Acad. Sci. U. S. A *103*, 654-659.

Petit,M.M., Fradelizi,J., Golsteyn,R.M., Ayoubi,T.A., Menichi,B., Louvard,D., Van de Ven,W.J., and Friederich,E. (2000). LPP, an actin cytoskeleton protein related to zyxin, harbors a nuclear export signal and transcriptional activation capacity. Mol. Biol. Cell *11*, 117-129.

Petit,M.M., Mols,R., Schoenmakers,E.F., Mandahl,N., and Van de Ven,W.J. (1996). LPP, the preferred fusion partner gene of HMGIC in lipomas, is a novel member of the LIM protein gene family. Genomics *36*, 118-129.

Petursdottir,T.E., Thorsteinsdottir,U., Jonasson,J.G., Moller,P.H., Huiping,C., Bjornsson,J., Egilsson,V., Imreh,S., and Ingvarsson,S. (2004). Interstitial deletions including chromosome 3 common eliminated region 1 (C3CER1) prevail in human solid tumors from 10 different tissues. Genes Chromosomes. Cancer *41*, 232-242.

Pollard,P.J., Briere,J.J., Alam,N.A., Barwell,J., Barclay,E., Wortham,N.C., Hunt,T., Mitchell,M., Olpin,S., Moat,S.J., Hargreaves,I.P., Heales,S.J., Chung,Y.L., Griffiths,J.R., Dalgleish,A., McGrath,J.A., Gleeson,M.J., Hodgson,S.V., Poulsom,R., Rustin,P., and Tomlinson,I.P. (2005). Accumulation of Krebs cycle intermediates and over-expression of HIF1alpha in tumours which result from germline FH and SDH mutations. Hum. Mol. Genet. *14*, 2231-2239.

Pollenz,R.S., Sattler,C.A., and Poland,A. (1994). The Aryl-Hydrocarbon Receptor and Aryl-Hydrocarbon Receptor Nuclear Translocator Protein Show Distinct Subcellular Localizations in Hepa 1C1C7 Cells by Immunofluorescence Microscopy. Molecular Pharmacology *45*, 428-438.

Pouyssegur,J., Dayan,F., and Mazure,N.M. (2006). Hypoxia signalling in cancer and approaches to enforce tumour regression. Nature *441*, 437-443.

Pratt,S.J., Epple,H., Ward,M., Feng,Y., Braga,V.M., and Longmore,G.D. (2005). The LIM protein Ajuba influences p130Cas localization and Rac1 activity during cell migration. J. Cell Biol. *168*, 813-824.

Primeau,M., Gagnon,J., and Momparler,R.L. (2003). Synergistic antineoplastic action of DNA methylation inhibitor 5-AZA-2'-deoxycytidine and histone deacetylase inhibitor depsipeptide on human breast carcinoma cells. Int. J. Cancer *103*, 177-184.

Pugh,C.W., O'Rourke,J.F., Nagao,M., Gleadle,J.M., and Ratcliffe,P.J. (1997). Activation of hypoxia-inducible factor-1; definition of regulatory domains within the alpha subunit. J. Biol. Chem. *272*, 11205-11214.

Pugh,C.W., Tan,C.C., Jones,R.W., and Ratcliffe,P.J. (1991). Functional analysis of an oxygen-regulated transcriptional enhancer lying 3' to the mouse erythropoietin gene. Proc. Natl. Acad. Sci. U. S. A *88*, 10553-10557.

Qi,H.H., Ongusaha,P.P., Myllyharju,J., Cheng,D., Pakkanen,O., Shi,Y., Lee,S.W., Peng,J., and Shi,Y. (2008). Prolyl 4-hydroxylation regulates Argonaute 2 stability. Nature *455*, 421-424.

Rankin,E.B. and Giaccia,A.J. (2008). The role of hypoxia-inducible factors in tumorigenesis. Cell Death. Differ. *15*, 678-685.

Rantanen,K., Pursiheimo,J., Hogel,H., Himanen,V., Metzen,E., and Jaakkola,P.M. (2008). Prolyl hydroxylase PHD3 activates oxygen-dependent protein aggregation. Mol. Biol. Cell *19*, 2231-2240.

Raval,R.R., Lau,K.W., Tran,M.G., Sowter,H.M., Mandriota,S.J., Li,J.L., Pugh,C.W., Maxwell,P.H., Harris,A.L., and Ratcliffe,P.J. (2005). Contrasting properties of hypoxia-inducible factor 1 (HIF-1) and HIF-2 in von Hippel-Lindau-associated renal cell carcinoma. Mol. Cell Biol. *25*, 5675-5686.

Ravi,R., Mookerjee,B., Bhujwalla,Z.M., Sutter,C.H., Artemov,D., Zeng,Q., Dillehay,L.E., Madan,A., Semenza,G.L., and Bedi,A. (2000). Regulation of tumor angiogenesis by p53-induced degradation of hypoxia-inducible factor 1alpha. Genes Dev. *14*, 34-44.

Reinhard,M., Zumbrunn,J., Jaquemar,D., Kuhn,M., Walter,U., and Trueb,B. (1999). An alpha-actinin binding site of zyxin is essential for subcellular zyxin localization and alpha-actinin recruitment. J. Biol. Chem. *274*, 13410-13418.

Renfranz,P.J. and Beckerle,M.C. (2002). Doing (F/L)PPPPs: EVH1 domains and their proline-rich partners in cell polarity and migration. Curr. Opin. Cell Biol. *14*, 88-103.

Richmond,T.D., Chohan,M., and Barber,D.L. (2005). Turning cells red: signal transduction mediated by erythropoietin
1. Trends Cell Biol. *15*, 146-155.

Rico,M., Mukherjee,A., Konieczkowski,M., Bruggeman,L.A., Miller,R.T., Khan,S., Schelling,J.R., and Sedor,J.R. (2005). WT1-interacting protein and ZO-1 translocate into podocyte nuclei after puromycin aminonucleoside treatment. Am. J. Physiol Renal Physiol *289*, F431-F441.

Roof,D.J., Hayes,A., Adamian,M., Chishti,A.H., and Li,T. (1997). Molecular characterization of abLIM, a novel actin-binding and double zinc finger protein. J. Cell Biol. *138*, 575-588.

Salceda,S. and Caro,J. (1997). Hypoxia-inducible factor 1alpha (HIF-1alpha) protein is rapidly degraded by the ubiquitin-proteasome system under

normoxic conditions. Its stabilization by hypoxia depends on redox-induced changes. J. Biol. Chem. *272*, 22642-22647.

Sanchez,M., Galy,B., Muckenthaler,M.U., and Hentze,M.W. (2007). Iron-regulatory proteins limit hypoxia-inducible factor-2alpha expression in iron deficiency. Nat. Struct. Mol. Biol. *14*, 420-426.

Schioppa,T., Uranchimeg,B., Saccani,A., Biswas,S.K., Doni,A., Rapisarda,A., Bernasconi,S., Saccani,S., Nebuloni,M., Vago,L., Mantovani,A., Melillo,G., and Sica,A. (2003). Regulation of the chemokine receptor CXCR4 by hypoxia. J. Exp. Med. *198*, 1391-1402.

Schmeichel,K.L. and Beckerle,M.C. (1994). The LIM domain is a modular protein-binding interface. Cell *79*, 211-219.

Schofield,C.J. and Ratcliffe,P.J. (2004). Oxygen sensing by HIF hydroxylases. Nat. Rev. Mol. Cell Biol. *5*, 343-354.

Schofield,C.J. and Zhang,Z. (1999). Structural and mechanistic studies on 2-oxoglutarate-dependent oxygenases and related enzymes. Curr. Opin. Struct. Biol. *9*, 722-731.

Schuster,S.J., Badiavas,E.V., Costa-Giomi,P., Weinmann,R., Erslev,A.J., and Caro,J. (1989). Stimulation of erythropoietin gene transcription during hypoxia and cobalt exposure. Blood *73*, 13-16.

Sciandra,J.J., Subjeck,J.R., and Hughes,C.S. (1984). Induction of glucose-regulated proteins during anaerobic exposure and of heat-shock proteins after reoxygenation. Proc. Natl. Acad. Sci. U. S. A *81*, 4843-4847.

Selak,M.A., Armour,S.M., MacKenzie,E.D., Boulahbel,H., Watson,D.G., Mansfield,K.D., Pan,Y., Simon,M.C., Thompson,C.B., and Gottlieb,E. (2005). Succinate links TCA cycle dysfunction to oncogenesis by inhibiting HIF-alpha prolyl hydroxylase. Cancer Cell *7*, 77-85.

Semenza,G.L. (2007). HIF-1 mediates the Warburg effect in clear cell renal carcinoma. J. Bioenerg. Biomembr. *39*, 231-234.

Semenza,G.L. (2009). Involvement of oxygen-sensing pathways in physiologic and pathologic erythropoiesis. Blood *114*, 2015-2019.

Semenza,G.L., Nejfelt,M.K., Chi,S.M., and Antonarakis,S.E. (1991). Hypoxia-inducible nuclear factors bind to an enhancer element located 3' to the human erythropoietin gene. Proc. Natl. Acad. Sci. U. S. A *88*, 5680-5684.

Semenza,G.L., Roth,P.H., Fang,H.M., and Wang,G.L. (1994). Transcriptional regulation of genes encoding glycolytic enzymes by hypoxia-inducible factor 1. J. Biol. Chem. *269*, 23757-23763.

Semenza,G.L. and Wang,G.L. (1992). A nuclear factor induced by hypoxia via de novo protein synthesis binds to the human erythropoietin gene

enhancer at a site required for transcriptional activation. Mol. Cell Biol. *12*, 5447-5454.

Shao,R., Zhang,F.P., Tian,F., Anders,F.P., Wang,X., Sjoland,H., and Billig,H. (2004). Increase of SUMO-1 expression in response to hypoxia: direct interaction with HIF-1alpha in adult mouse brain and heart in vivo 67. FEBS Lett. *569*, 293-300.

Sharp,T.V., Al-Attar,A., Foxler,D.E., Ding,L., de,A., V, Zhang,Y., Nijmeh,H.S., Webb,T.M., Nicholson,A.G., Zhang,Q., Kraja,A., Spendlove,I., Osborne,J., Mardis,E., and Longmore,G.D. (2008). The chromosome 3p21.3-encoded gene, LIMD1, is a critical tumor suppressor involved in human lung cancer development. Proc. Natl. Acad. Sci. U. S. A *105*, 19932-19937.

Sharp,T.V., Munoz,F., Bourboulia,D., Presneau,N., Darai,E., Wang,H.W., Cannon,M., Butcher,D.N., Nicholson,A.G., Klein,G., Imreh,S., and Boshoff,C. (2004). LIM domains-containing protein 1 (LIMD1), a tumor suppressor encoded at chromosome 3p21.3, binds pRB and represses E2F-driven transcription. Proc. Natl. Acad. Sci. U. S. A *101*, 16531-16536.

Sherr,C.J. (2004). Principles of tumor suppression. Cell *116*, 235-246.

Shyu,K.G., Hsu,F.L., Wang,M.J., Wang,B.W., and Lin,S. (2007). Hypoxia-inducible factor 1alpha regulates lung adenocarcinoma cell invasion. Exp. Cell Res. *313*, 1181-1191.

Simon,M.C. and Keith,B. (2008). The role of oxygen availability in embryonic development and stem cell function. Nat. Rev. Mol. Cell Biol. *9*, 285-296.

Sowter,H.M., Raval,R.R., Moore,J.W., Ratcliffe,P.J., and Harris,A.L. (2003). Predominant role of hypoxia-inducible transcription factor (Hif)-1alpha versus Hif-2alpha in regulation of the transcriptional response to hypoxia. Cancer Res. *63*, 6130-6134.

Spendlove,I., Al-Attar,A., Watherstone,O., Webb,T.M., Ellis,I.O., Longmore,G.D., and Sharp,T.V. (2008). Differential subcellular localisation of the tumour suppressor protein LIMD1 in breast cancer correlates with patient survival. Int. J. Cancer.

Sprenger,S.H., Gijtenbeek,J.M., Wesseling,P., Sciot,R., van,C.F., Lammens,M., and Jeuken,J.W. (2001). Characteristic chromosomal aberrations in sporadic cerebellar hemangioblastomas revealed by comparative genomic hybridization. J. Neurooncol. *52*, 241-247.

Srichai,M.B., Konieczkowski,M., Padiyar,A., Konieczkowski,D.J., Mukherjee,A., Hayden,P.S., Kamat,S., El-Meanawy,M.A., Khan,S., Mundel,P., Lee,S.B., Bruggeman,L.A., Schelling,J.R., and Sedor,J.R. (2004). A WT1 co-regulator controls podocyte phenotype by shuttling between adhesion structures and nucleus. J. Biol. Chem. *279*, 14398-14408.

Stebbins,C.E., Kaelin,W.G., Jr., and Pavletich,N.P. (1999). Structure of the VHL-ElonginC-ElonginB complex: implications for VHL tumor suppressor function. Science *284*, 455-461.

Steinhoff,A., Pientka,F.K., Mockel,S., Kettelhake,A., Hartmann,E., Kohler,M., and Depping,R. (2009). Cellular oxygen sensing: Importins and exportins are mediators of intracellular localisation of prolyl-4-hydroxylases PHD1 and PHD2. Biochem. Biophys. Res. Commun. *387*, 705-711.

Takeda,K., Aguila,H.L., Parikh,N.S., Li,X., Lamothe,K., Duan,L.J., Takeda,H., Lee,F.S., and Fong,G.H. (2008). Regulation of adult erythropoiesis by prolyl hydroxylase domain proteins. Blood *111*, 3229-3235.

Takeda,K., Cowan,A., and Fong,G.H. (2007). Essential role for prolyl hydroxylase domain protein 2 in oxygen homeostasis of the adult vascular system. Circulation *116*, 774-781.

Takeda,K. and Fong,G.H. (2007). Prolyl hydroxylase domain 2 protein suppresses hypoxia-induced endothelial cell proliferation. Hypertension *49*, 178-184.

Takeda,K., Ho,V.C., Takeda,H., Duan,L.J., Nagy,A., and Fong,G.H. (2006). Placental but not heart defects are associated with elevated hypoxia-inducible factor alpha levels in mice lacking prolyl hydroxylase domain protein 2. Mol. Cell Biol. *26*, 8336-8346.

Talks,K.L., Turley,H., Gatter,K.C., Maxwell,P.H., Pugh,C.W., Ratcliffe,P.J., and Harris,A.L. (2000). The expression and distribution of the hypoxia-inducible factors HIF-1alpha and HIF-2alpha in normal human tissues, cancers, and tumor-associated macrophages. Am. J. Pathol. *157*, 411-421.

Thiery,J.P. and Sleeman,J.P. (2006). Complex networks orchestrate epithelial-mesenchymal transitions. Nat. Rev. Mol. Cell Biol. *7*, 131-142.

THOMLINSON,R.H. and GRAY,L.H. (1955). The histological structure of some human lung cancers and the possible implications for radiotherapy. Br. J. Cancer *9*, 539-549.

Tian,H., McKnight,S.L., and Russell,D.W. (1997). Endothelial PAS domain protein 1 (EPAS1), a transcription factor selectively expressed in endothelial cells. Genes Dev. *11*, 72-82.

Tian,Y.M., Mole,D.R., Ratcliffe,P.J., and Gleadle,J.M. (2006). Characterization of different isoforms of the HIF prolyl hydroxylase PHD1 generated by alternative initiation. Biochem. J. *397*, 179-186.

To,K.K. and Huang,L.E. (2005). Suppression of hypoxia-inducible factor 1alpha (HIF-1alpha) transcriptional activity by the HIF prolyl hydroxylase EGLN1. J. Biol. Chem. *280*, 38102-38107.

Tu,Y., Wu,S., Shi,X., Chen,K., and Wu,C. (2003). Migfilin and Mig-2 link focal adhesions to filamin and the actin cytoskeleton and function in cell shape modulation. Cell *113*, 37-47.

Tuckerman,J.R., Zhao,Y., Hewitson,K.S., Tian,Y.M., Pugh,C.W., Ratcliffe,P.J., and Mole,D.R. (2004). Determination and comparison of specific activity of the HIF-prolyl hydroxylases. FEBS Lett. *576*, 145-150.

Valegard,K., van Scheltinga,A.C., Lloyd,M.D., Hara,T., Ramaswamy,S., Perrakis,A., Thompson,A., Lee,H.J., Baldwin,J.E., Schofield,C.J., Hajdu,J., and Andersson,I. (1998). Structure of a cephalosporin synthase. Nature *394*, 805-809.

van Wijk,N.V., Witte,F., Feike,A.C., Schambony,A., Birchmeier,W., Mundlos,S., and Stricker,S. (2009). The LIM domain protein Wtip interacts with the receptor tyrosine kinase Ror2 and inhibits canonical Wnt signalling. Biochem. Biophys. Res. Commun.

Villar,D., Vara-Vega,A., Landazuri,M.O., and del,P.L. (2007). Identification of a region on hypoxia-inducible-factor prolyl 4-hydroxylases that determines their specificity for the oxygen degradation domains. Biochem. J. *408*, 231-240.

Wagner,K.D., Wagner,N., Wellmann,S., Schley,G., Bondke,A., Theres,H., and Scholz,H. (2003). Oxygen-regulated expression of the Wilms' tumor suppressor Wt1 involves hypoxia-inducible factor-1 (HIF-1). FASEB J. *17*, 1364-1366.

Wang,G.L., Jiang,B.H., Rue,E.A., and Semenza,G.L. (1995). Hypoxia-inducible factor 1 is a basic-helix-loop-helix-PAS heterodimer regulated by cellular O2 tension. Proc. Natl. Acad. Sci. U. S. A *92*, 5510-5514.

Wang,G.L. and Semenza,G.L. (1993a). Characterization of hypoxia-inducible factor 1 and regulation of DNA binding activity by hypoxia. J. Biol. Chem. *268*, 21513-21518.

Wang,G.L. and Semenza,G.L. (1993b). Desferrioxamine induces erythropoietin gene expression and hypoxia-inducible factor 1 DNA-binding activity: implications for models of hypoxia signal transduction. Blood *82*, 3610-3615.

Wang,G.L. and Semenza,G.L. (1993c). General involvement of hypoxia-inducible factor 1 in transcriptional response to hypoxia. Proc. Natl. Acad. Sci. U. S. A *90*, 4304-4308.

Wang,G.L. and Semenza,G.L. (1995). Purification and characterization of hypoxia-inducible factor 1. J. Biol. Chem. *270*, 1230-1237.

Wang,Y. and Gilmore,T.D. (2003). Zyxin and paxillin proteins: focal adhesion plaque LIM domain proteins go nuclear. Biochim. Biophys. Acta *1593*, 115-120.

WARBURG,O. (1956). On the origin of cancer cells. Science *123*, 309-314.

Way,J.C. and Chalfie,M. (1988). mec-3, a homeobox-containing gene that specifies differentiation of the touch receptor neurons in C. elegans. Cell *54*, 5-16.

Wenger,R.H., Kvietikova,I., Rolfs,A., Gassmann,M., and Marti,H.H. (1997). Hypoxia-inducible factor-1 alpha is regulated at the post-mRNA level. Kidney Int. *51*, 560-563.

Wiesener,M.S., Jurgensen,J.S., Rosenberger,C., Scholze,C.K., Horstrup,J.H., Warnecke,C., Mandriota,S., Bechmann,I., Frei,U.A., Pugh,C.W., Ratcliffe,P.J., Bachmann,S., Maxwell,P.H., and Eckardt,K.U. (2003). Widespread hypoxia-inducible expression of HIF-2alpha in distinct cell populations of different organs. FASEB J. *17*, 271-273.

Wilkins,S.E., Hyvarinen,J., Chicher,J., Gorman,J.J., Peet,D.J., Bilton,R.L., and Koivunen,P. (2009). Differences in hydroxylation and binding of Notch and HIF-1alpha demonstrate substrate selectivity for factor inhibiting HIF-1 (FIH-1). Int. J. Biochem. Cell Biol. *41*, 1563-1571.

Wistuba,I.I., Berry,J., Behrens,C., Maitra,A., Shivapurkar,N., Milchgrub,S., Mackay,B., Minna,J.D., and Gazdar,A.F. (2000). Molecular changes in the bronchial epithelium of patients with small cell lung cancer. Clin. Cancer Res. *6*, 2604-2610.

Yamamoto,Y. and Gaynor,R.B. (2004). IkappaB kinases: key regulators of the NF-kappaB pathway. Trends Biochem. Sci. *29*, 72-79.

Yancopoulos,G.D., Davis,S., Gale,N.W., Rudge,J.S., Wiegand,S.J., and Holash,J. (2000). Vascular-specific growth factors and blood vessel formation. Nature *407*, 242-248.

Yang,Q.C., Zeng,B.F., Dong,Y., Shi,Z.M., Jiang,Z.M., and Huang,J. (2007). Overexpression of hypoxia-inducible factor-1alpha in human osteosarcoma: correlation with clinicopathological parameters and survival outcome. Jpn. J. Clin. Oncol. *37*, 127-134.

Yasumoto,K., Kowata,Y., Yoshida,A., Torii,S., and Sogawa,K. (2009). Role of the intracellular localization of HIF-prolyl hydroxylases. Biochim. Biophys. Acta *1793*, 792-797.

Yee,K.M., Spivak-Kroizman,T.R., and Powis,G. (2008). HIF-1 regulation: not so easy come, easy go. Trends Biochem. Sci. *33*, 526-534.

Yi,J. and Beckerle,M.C. (1998). The human TRIP6 gene encodes a LIM domain protein and maps to chromosome 7q22, a region associated with tumorigenesis. Genomics *49*, 314-316.

Yin,L., Kharbanda,S., and Kufe,D. (2007). Mucin 1 oncoprotein blocks hypoxia-inducible factor 1alpha activation in a survival response to hypoxia. J. Biol. Chem. *282*, 257-266.

Yu,B., Miao,Z.H., Jiang,Y., Li,M.H., Yang,N., Li,T., and Ding,J. (2009). c-Jun Protects Hypoxia-Inducible Factor-1{alpha} from Degradation via Its Oxygen-Dependent Degradation Domain in a Nontranscriptional Manner. Cancer Res.

Yu,F., White,S.B., Zhao,Q., and Lee,F.S. (2001). HIF-1alpha binding to VHL is regulated by stimulus-sensitive proline hydroxylation. Proc. Natl. Acad. Sci. U. S. A *98*, 9630-9635.

Zhang,H., Gao,P., Fukuda,R., Kumar,G., Krishnamachary,B., Zeller,K.I., Dang,C.V., and Semenza,G.L. (2007). HIF-1 inhibits mitochondrial biogenesis and cellular respiration in VHL-deficient renal cell carcinoma by repression of C-MYC activity. Cancer Cell *11*, 407-420.

Zheng,Q. and Zhao,Y. (2007). The diverse biofunctions of LIM domain proteins: determined by subcellular localization and protein-protein interaction. Biol. Cell *99*, 489-502.

Zheng,X., Linke,S., Dias,J.M., Zheng,X., Gradin,K., Wallis,T.P., Hamilton,B.R., Gustafsson,M., Ruas,J.L., Wilkins,S., Bilton,R.L., Brismar,K., Whitelaw,M.L., Pereira,T., Gorman,J.J., Ericson,J., Peet,D.J., Lendahl,U., and Poellinger,L. (2008). Interaction with factor inhibiting HIF-1 defines an additional mode of cross-coupling between the Notch and hypoxia signaling pathways. Proc. Natl. Acad. Sci. U. S. A *105*, 3368-3373.